Uncertainty in Hydrodynamic Model Test Experiments of Wave Energy Converters

Jarrah Orphin
Bachelor of Engineering (Ocean Engineering) (Honours)
National Centre for Maritime Engineering and Hydrodynamics
Australian Maritime College, University of Tasmania

Submitted in partial fulfilment of the requirements
for the Degree of Doctor of Philosophy

Supervisors:
Professor Irene Penesis
Dr Jean-Roch Nader

September 2020

Link to thesis document: https://cloudstor.aarnet.edu.au/plus/f/4947725154

Declarations

I declare that this thesis contains no material which has been accepted for a degree or diploma by the University or any other institution, except by way of background information and duly acknowledged in the thesis, and that, to the best of my knowledge and belief, this thesis contains no material previously published or written by another person, except where due acknowledgement is made in the text of the thesis.

Signed: ______________ Date: 20 September 2020

Jarrah Orphin

Statement of Co-Authorship

The following people and institutions contributed to the peer-reviewed publication of work undertaken as part of this thesis:

Candidate	Jarrah Orphin	University of Tasmania
Author 1	Professor Irene Penesis	University of Tasmania
Author 2	Dr Jean-Roch Nader	University of Tasmania
Author 3	Damon Howe	University of Tasmania

Contribution of work by co-authors for each paper:

Paper 1: Informed Chapters 3 to 5, located in Appendix D.

J. Orphin, J.-R. Nader, I. Penesis, and D. Howe. "Experimental Uncertainty Analysis of an OWC Wave Energy Converter". In: *European Wave and Tidal Energy Conference* (2017).

Conceived experiment design: Candidate, Author 1, Author 2, Author 3

Performed experiments: Candidate, Author 3

Data analysis: Candidate, Author 1, Author 2

Manuscript preparation: Candidate, Author 1, Author 2, Author 3

Paper 2: Informed Chapters 3 to 5, located in Appendix E.

J. Orphin, I. Penesis, and J.-R. Nader. "Uncertainty analysis for a wave energy converter: the Monte Carlo method". In: *Asian Wave and Tidal Energy Conference* (2018).

Conceived experiment design: Candidate, Author 1, Author 2

Performed experiments: Candidate

Data analysis: Candidate, Author 1, Author 2

Manuscript preparation: Candidate, Author 1, Author 2

We, the undersigned, endorse the above stated contribution of work undertaken for each of the published peer-reviewed manuscripts contributing to this thesis:

Signed: ______________ Date: 20 September 2020

Jarrah Orphin – Candidate
National Centre for Maritime Engineering and Hydrodynamics
Australian Maritime College, University of Tasmania

Signed: ______________ Date: 2 October 2020

Professor Irene Penesis – Primary Supervisor
National Centre for Maritime Engineering and Hydrodynamics
Australian Maritime College, University of Tasmania

Signed: ______________ Date: 2 October 2020

Dr Jean-Roch Nader – Co-Supervisor
National Centre for Maritime Engineering and Hydrodynamics
Australian Maritime College, University of Tasmania

Signed: ______________ Date: 2 October 2020

Dr Vikram Garaniya – Acting Director
National Centre for Maritime Engineering and Hydrodynamics
Australian Maritime College, University of Tasmania

"*When dealing with water, first experiment then use judgement.*"

– Leonardo da Vinci

"*If you're certain, you're certainly wrong.*"

– Bertrand Russell

"*We absolutely must leave room for doubt or there is no progress and no learning...People search for certainty. But there is no certainty.*"

– Richard Feynman

"*The edge of the sea is a strange and beautiful place.*"

– Rachel Carson

Abstract

Renewable energy is key to solving the great challenges of climate change, energy security, and pollution. Ocean wave energy is a nascent renewable energy with a vast technical potential, but a relatively high Levelised Cost of Energy (LCOE) due to limited commercial Wave Energy Converter (WEC) technologies. This suggests that WEC development methods and guidelines are still maturing. For early-stage WEC development, which requires hydrodynamic model test experiments, a recognised gap is experimental uncertainty. This gap is striking because uncertainty can significantly influence experimental results. Despite extensive knowledge on experimental uncertainty in similar fields such as shipping and marine structures, applying this knowledge in WEC experiments is inadequate and carries risk because WECs uniquely maximise motions, use a Power Take-Off (PTO) system, and often have complex geometry and moorings that influence motions – all of which can introduce significant experimental uncertainty in the results of power performance and hydrodynamic loads.

To better understand the causes and effects of uncertainty in hydrodynamic model test experiments of WECs, we reviewed technical guidelines and literature to identify major uncertainties needing investigation, then conducted a series of model test experiments designed to investigate these uncertainties. This research presents an overview of and experimental investigations into uncertainty in hydrodynamic model test experiments of WECs, focusing on a Oscillating Water Column (OWC) WEC. The set of experiments, representative of Technology Readiness Levels 1-4, assess power performance and hydrodynamic loads in regular and irregular waves. The case study OWC WEC is based on Australian company Wave Swell Energy's (WSE) Uniwave technology, a bottom-fixed device with a unidirectional airflow PTO.

Through reviewing the literature of WEC model test guidelines, advances, and uncertainties, we found that despite substantial progress in developing best practices, they remain dispersed across many documents, are inconsistent in some parameters and procedures, and have gaps or are inadequate in several areas. WEC-specific guidance was found to be lacking in: the modelling of moorings, PTOs, and arrays and clusters; identifying and modelling survival conditions; installation and tow-out tests; specific tests for calibrating and validating numerical models; methods for extrapolating model-scale results; full-scale validation; and,

most important to this research, understanding of and methods to account for measurement uncertainty, scale effects, and laboratory effects.

Hence, these uncertainties became the focus of subsequent experimental investigations: (1) a 1:30 scale model test of the OWC WEC in the Australian Maritime College (AMC) Model Test Basin, which, building on knowledge obtained from experimental work, was conducted to better understand measurement uncertainty and develop new WEC-specific uncertainty analysis (UA) methods; (2) a series of model tests at three scales (1:40, 1:30, 1:20) of the OWC WEC in the AMC MTB, conducted to identify, quantify, and evaluate parameters causing scale effects; and (3) reproducing this model test at 1:30 scale in a similar shallow water wave basin, the Queen's University Belfast Coastal Wave Basin, to identify, quantify, and evaluate parameters causing laboratory effects.

In experiment (1), we develop a comprehensive UA methodology and apply it to the OWC WEC experiment, demonstrating how and when UA can be used throughout an experimental program. In doing so, we outline UA principles, identify parameters causing measurement uncertainty, and develop new WEC-specific methods for General Uncertainty Analysis (GUA), evaluating Type A and Type B uncertainty, and the Monte Carlo Method (MCM) to propagate uncertainty. We found that GUA is indispensable in experimental planning and design because it assures relevant and high-quality results are obtained, that a new Type A uncertainty evaluation method reduces the number of required repeat runs thereby saving time and cost, and that the MCM effectively and efficiently propagates uncertainty for the complex OWC WEC experiment. We also give detailed examples of evaluating Type B uncertainties. Results from the experiment show the expanded uncertainty averaged $\pm 16\%$ for capture width ratio (C_W) and $\pm 6\%$ for loads, with Type B uncertainty tending to be slightly larger than Type A uncertainty, and uncertainty in irregular wave results slightly smaller than regular waves. Key causes of uncertainty in C_W were measurements used to derive the lower level measurands of incident wave power and OWC power, and the PTO modelling. We conclude that UA is required in WEC model tests because it assures and quantifies the quality of experimental results. Specific recommendations are also offered to update guidelines on UA for WECs.

Importantly, experiment (1) generated the knowledge required to determine whether experimental results across model scales in experiment (2) or between laboratories in experiment (3) agreed or disagreed. In (2), we found moderate to major differences on average in power and loads results across scales (10-30%+). Significant scale effects in the results were evaluated to be mainly caused by deviating nonlinear incident wave profiles and deviating quadratic PTO damping due to maintaining the similitude condition of orifice-OWC chamber ratio. In (3), we found moderate to major differences on average in power results between laboratories. Significant laboratory effects in the results were evaluated to be mainly caused by differences in the test environment (wavemaker and nonlinear wave transformations), the model (deployment position and the PTO influenced by different test environment ambient conditions), and instrumentation (loads measurements). Other instrumentation, water properties, air compressibility, and human factors were evaluated to have a negligible to minor contribution to the differences in results in both (2) and (3). These results clearly showed that, despite conducting the model test experiments to a high standard according to international guidelines, model scale and the laboratory can significantly influence experimental results. Therefore, scale and laboratory effects cannot be neglected when carrying out these experiments.

The primary conclusion from this research is that experimental uncertainty is an inseparable part of and can significantly influence the results of hydrodynamic model test experiments of WECs. Therefore, stakeholders in early-stage WEC development should be aware of this; should invest resources, time, and money into accounting for newly identified parameters causing measurement uncertainty, scale effects, and laboratory effects; and should consider implementing the outcomes of this research into future guidelines on WEC model tests. This research contributes to the efforts in developing an international standardised set of robust, consistent, and validated guidelines on WEC development, needed to assure the reliability of model test results, reduce technical and financial risks, enable better data-driven decisions, and ultimately reduce wave energy's LCOE.

Acknowledgements

I am indebted and grateful to the many generous and conscientious individuals who have supported me along the winding path that is PhD research. First, I express my deep gratitude to my first-rate supervisors, Prof. Irene Penesis and Dr Jean-Roch Nader, who inspired me to pursue a PhD, and later offered more than a few alluring topics. The total sum of their unerring support, active patience, immense knowledge, and timely guidance, has made this project a profoundly enriching and rewarding experience. Our fruitful discussions in meetings or over lunch (or dinner, with wine) sparked insights in my mind that undoubtedly improved the execution and outcomes of this work in significant ways. It has been a pleasure and a privilege.

I thank the technical staff at the AMC who imparted their outstanding knowledge, skills, advice, enthusiasm, and humour when helping with my experiments. Thank you: Assoc. Prof. Gregor Macfarlane, for the generous laboratory time and guidance; Liam Honeychurch, for the unmatched craftsmanship and help transporting models; Tim Lilienthal, Kirk Meyer, and Michael Underhill for technical support throughout my experiments; and Dr Alan Fleming, for exposing me to the wonders of wave energy and being a continual valued source of theoretical and practical knowledge. Thank you also to Michael Woodward for help with uncertainty analysis.

I also thank all my peers for their help in my experiments, analysis, writing, or encouragement. Special thanks to Damon Howe, Dong Wook Hwang, Constantin Scherelis, Christelle Auguste, Samuel Smith, Brian Winship, Dr Arno Dubois, Dr Thomas Mitchell Ferguson, Dr Philip Marsh, Dr Fletcher Thompson, Eric Gubesch, Nazanin Ansarifard, Dr Ahmed Elhanafi, Dr Maia Osborn, Reuben Kent, and James Keane.

A big thank you to the Wave Swell Energy team who let us use their auspicious wave energy technology, Uniwave®, for this research. I hope this research has in some way contributed to the commercialisation of the technology and I am looking forward to seeing it deliver wave energy generated electricity into King Island's microgrid in Tasmania, Australia.

I express my deep gratitude to the researchers at Queen's University Belfast (QUB), and for the financial support provided by IMarEST's Laurie Prandolini Research Fellowship, who made our ambitions for interlaboratory experiments possible. I am deeply indebted to QUB researchers Dr Louise Kregting, Dr Pal Schmitt, Dr Paul Lamont-Kane and other technical staff, and Greg Hellessey and others involved at IMarEST. At QUB, the warm hospitality, generous resources and time for setting up and carrying out the experiments, and countless other things made the venture thoroughly enjoyable and worthwhile. A special acknowledgement to Pal who spent some late nights with me in the lab, and to Pal and Cicilia for welcoming me into their home for a week or two after unfortunate delays in the experiment.

Finally, my family deserve a special acknowledgement. The odds of being born into such a beautiful family, in a quaint coastal community endowed with world-class waves, are vanishingly small. I am extraordinarily lucky – lucky to have been given opportunity after opportunity to learn, adventure, and play. My family have instilled a deep sense of awe and wonder of the natural world, and given guidance on being a being in it. My parents are an infinite source of wisdom, support, love, and encouragement to pursue that which piques my interests. My brother has influenced me countless ways, all of which have helped me to become who and what I am. I also thank Devon Bunce for supporting me in the final few months of writing this thesis, in the strange and uncertain times of Coronavirus (COVID-19).

Thank you.

Table of Contents

List of Tables

List of Figures

Nomenclature

Symbol	**Description**	**Units**
$\bar{q}$	Mean	-
η_{inc}	Incident wave elevation	m
η_{owc}	Wave elevation inside the OWC	m
γ	JONSWAP parameter	-
γ_p	Polytropic expansion index for air	-
$\hat{y_j}$	Fitted value to calibration curve	-
λ	Full scale to model scale ratio	-
$\lambda_{40,30,20}$	Scale ratio for 1:40, 1:30, 1:20 model scales, respectively	-
E	Effect (Table 4.3)	-
Lh	Likelihood (Table 4.3)	-
L	Likely (Table 4.3)	-
M	Minor (Table 4.3)	-
M	Number of Monte Carlo simulations	-
N	Negligible (Table 4.3)	-
P	Possible (Table 4.3)	-
S	Significant (Table 4.3)	-
U	Unlikely (Table 4.3)	-
μ	Shallow water parameter	m/m

Ω	Compression number	-
ω	Angular wave frequency	rad/s
ρ_a	Density of air	kg/m^3
ρ_w	Density of fresh water	kg/m^3
A_0	Orifice cross-sectional area	m^2
A_d	OWC cross-sectional area	m^2
A_P	Wave peak amplitude	m
A_T	Wave trough amplitude	m
$A_{\eta_{owc}}$	Amplitude of η_{owc}	m
B	Characteristic dimension of WEC	m
c	Wave celerity	m/s
C_d	Orifice discharge coefficient	-
c_g	Group velocity	m/s
$C_h(\omega)$	Correction factor that modifies irregular wave power from deep water to finite water	-
C_W	Capture width ratio	-
D	Depth	m
D_0	Orifice diameter	m
D_c	Diameter of OWC chamber	m
E_{AMC}	Experiment at Australian Maritime College (AMC)	-
E_{QUB}	Experiment at Queen's University Belfast (AMC)	-
F'	Force coefficient (Table 4.1)	N/N
$F'^{+}_{x,z}$	Force coefficient in positive x- and z-axis direction	N/N
$F'^{-}_{x,4}$	Force coefficient of average of four highest waves in an irregular timeseries in negative x-axis direction	N/N
$F'^{-}_{x,s}$	Significant force coefficient in negative x-axis direction	N/N

$F'^{-}_{x,z}$	Force coefficient in negative x- and z-axis direction	N/N
$F'^{-}_{z,4}$	Force coefficient of average of four highest waves in an irregular timeseries in negative z-axis direction	N/N
$F'^{-}_{z,s}$	Significant force coefficient in negative z-axis direction	N/N
F_x	Surge force	N
F_y	Sway force	N
F_z	Heave force	N
Fe	Froude Number (Table 4.1)	-
g	Acceleration due to gravity	m/s^2
H	Wave height	m
h	Water depth	m
H'	Wave height-water depth ratio (Table 4.1)	m/m
H'_{m0}	Dimensionless significant wave height (spectral) (Table 4.1)	m/m
H_s	Significant wave height (time domain)	m
$H_{\eta_{AF}}$	Amplification factor (Table 4.1)	m/m
H_{m0}	Significant wave height (spectral)	m
j	Iteration of Monte Carlo simulation	-
K	Relationship between p' and OWC chamber air flow velocity $\bar{v}$	Pa/m^2/s^2
k	Wave number (general)	m^{-1}
k_0	Wave number (deep water)	m^{-1}
k_c	Coverage interval	-
K_n	Keulegan-Carpenter number	-
k_ph	Peak wavenumber	m^{-1}
kh	Wavelength-water depth ratio (Table 4.1)	m/m
L	Length	m

L_m	Length parameter of model	m
L_p	Length parameter of prototype	m
M	Number of calibration points	-
M'	Moment coefficient (Table 4.1)	N-m/N-m
M'^{+}_{y}	Moment coefficient in positive rotation about y-axis	N/N
$M'^{-}_{y,4}$	Force coefficient of average of four highest waves in an irregular timeseries in negative rotation about y-axis	N/N
$M'^{-}_{y,s}$	Significant moment coefficient in negative rotation about y-axis	N/N
M'^{-}_{y}	Moment coefficient in negative rotation about y-axis	N/N
m_n	Spectral moments	-
M_x	Roll moment	N-m
M_y	Pitch moment	N-m
M_z	Yaw moment	N-m
N	Number of input quantities	-
n	Independent observations (repeats)	-
P	Mean power absorbed by WEC	W
p	Air pressure	Pa
p'	Dimensionless pressure (Table 4.1)	Pa/Pa
P'_W	Dimensionless wave power (Table 4.1)	$\frac{\mathrm{W/m}}{\mathrm{W/m}}$
p_0	Atmospheric pressure	Pa
$P_{W_{irr}}$	Wave power in irregular waves per unit length	W/m
$P_{W_{reg}}$	Wave power in regular waves per unit length	W/m
q	Air flow rate	$\mathrm{m^3/s}$
q_k	Independent observations	-
$q_{\eta_{owc}}$	Air volume displace by the OWC internal free surface	$\mathrm{m^3/s}$

q_{C_d}	Air flow rate derived from C_d	m^3/s
Re_h	Reynolds Number (hydrodynamic) (Table 4.1)	-
Re_o	Reynolds Number (orifice) (Table 4.1)	-
S	Steepness parameter	m/m
s	Wave steepness (Table 4.1)	m/m
$s(\bar{q})$	Standard deviation of the mean	-
$S(\omega)$	Power spectral density function	m^2/Hz
S_c	OWC waterplane cross-sectional area	m^2
T	Wave period	s
t	Tonne	kg
T_e	Energy period	s
T_p	Peak period	s
T_z	Zero up-crossing period	s
T_{m01}	Mean wave period	s
U	Expanded uncertainty	
$u_A(x_i)$	Type A standard uncertainty	-
$u_B(x_i)$	Type B standard uncertainty	-
$u_c(y)$	Combined standard uncertainty	-
$u_G(X_i)$	General standard uncertainty	-
U_o	Air flow velocity through orifice	m/s
U_s	Ursell Number	m^3/m^3
U_v	Characteristic velocity	m/s
W	Width	m
X_i	Input quantities	-
x_i	Input quantities (estimate)	-

Y	Measurand	-
y	Measurand (estimate)	-
y_j	Calibrated data point	-

Chapter 1

Thesis Introduction

How we get and use energy in the rest of the twenty-first century could be fundamentally different to how we got and used energy in the past few centuries. Why? Because carbon-releasing human activities, most significantly the use of fossil-fuel energy, have caused global impacts on natural and human systems. For example, global warming and climate change [1], millions of air-pollution deaths [2], and more frequent and severe extreme weather events costing billions [3]. In response to these ominous trends the world is entering a new era of energy, one in which fossil fuels are being displaced by renewable energy from wind, water, and sunlight [4, 5].

An immense water-based renewable energy is ocean wave energy, estimated to have a technical potential approximately equal to the world's energy consumption [6, 7]. This potential has inspired thousands of ideas and technologies to convert wave energy into a useful form, but converged techno-economic solutions await. Wave energy is therefore a nascent, though relatively immature industry, still with limited full-scale knowledge and experience of techno-economic Wave Energy Converter (WEC) technologies, still in the research, development and demonstration phase with many early-stage WECs, and still with a relatively high Leveilised Cost of Energy (LCOE) [8]. So, technically possible, yes. Economic, not yet.

Techno-economic solutions for demanding applications, such as space flight, can however be engineered through a proven methodology based on the Technology Readiness Levels (TRLs) [9]. The wave energy industry has adopted and adapted the TRLs for WEC development [10, 11]. In early-stage development, TRLs 1-5 are divided into several stages coupled to hydrodynamic model test experiments of WECs. Experimental data obtained in each stage are used to validate WEC prototype performance against numerical and wave-to-wire models, and extrapolated to predict the WEC's full-scale performance. Developers then use these findings to underpin further investment to support large scale open water tests. Hence, high-quality experimental data is critical. Obtaining such data requires the model test best practices – parameters and procedures recommended by technical guidelines – to be accurate and robust.

Over the past two decades several projects and organisations have developed technical guidelines on WEC model test experiments [12, 13, 14, 15, 16, 11, 10]. Despite substantial progress, evident by recent international publications [11, 10], the guidelines are still undergoing active development to refine the best practices and address gaps, through technical investigations and integrating full-scale knowledge feedback loops. In particular, the International Towing Tank Conference (ITTC) Specialist Committee on Hydrodynamic Modelling of Marine Renewable Energy Devices (SC-HMMRED) are continuing to develop their set of technical guidelines for WECs [11, 17]. Based on a review of hydrodynamic modelling of marine renewable energy devices [18] and technical reports to the ITTC [19, 20], terms of reference have been assigned to SC-HMMRED to further develop the guidelines, especially in the area of experimental uncertainty. The tasks include: (1) to review and update the current guideline on WEC model test experiments [11], (2) to better understand modelling uncertainties and develop the guideline on uncertainty analysis [17], and (3) to initiate a 'round robin' test campaign to investigate laboratory effects/bias [20].

What are the current best practices? What are the causes and effects of experimental uncertainty? Which parameters cause the most uncertainty? How to deal with experimental uncertainty? These are the questions that arose from the tasks above and directed this PhD research project. The following sections describe the specific problem this research aims to address, the research objectives and design, novelty, and thesis outline.

1.1 Problem definition

Uncertainty is an inseparable and important part of experimental hydrodynamics, and there are three main sources of experimental uncertainty. First, measurement is imperfect [21]. This uncertainty is known as *measurement uncertainty*, and it is accounted for through uncertainty analysis. Second, hydrodynamic similitude is seldom achieved in practice due to physical and practical constraints, resulting in deviations between model and prototype behaviour [22, 23]. This uncertainty is known as *scale effects.* Third, the wave basin laboratory itself can cause uncertainty due to, for example, unrealistic wave simulation, wave reflections from boundaries and models, or varied configurations, dimensions, experimental procedures, or ambient conditions [22]. This uncertainty is known as *laboratory effects.*

WECs are likely sensitive to all three of these main sources of experimental uncertainty. The following points highlight how scale effects, laboratory effects, and measurement uncertainty are problematic in WEC model tests, and why they are important to understand.

Consider this: (1) WECs maximise the motions of a working surface that captures wave energy (a *captor*); (2) WECs use a PTO to convert captor motions into useful energy; (3)

WECs often have dynamic moorings that interact with WEC motions, loads, and power; and (4) WECs often operate in intermediate to shallow waters that are characterised by an interplay of nonlinear processes. In other words, nonlinear waves induce nonlinear motions of the captor, WEC body, and mooring, which all interact with a nonlinear PTO. Such nonlinearities, as well PTO modelling constraints, are likely scale-dependent. Moreover, limited knowledge of scale effects, especially between the laboratory and open water, makes it difficult to avoid, compensate, or correct for scale effects [24, 23].

Furthermore, if the same WEC model test was carried out in multiple similar wave basins, would the results be consistent? At present the wave energy field does not have an answer. Indeed, no such studies have been published (to our knowledge). Laboratory series investigations carried out in related maritime fields show laboratory influences on model test results can be significant [25, 26, 27]. This suggests it is important to understand how laboratory parameters and uncertainties influence WEC model test results.

Finally, WECs present new modelling and measurement challenges due to their unique characteristics discussed above: large and nonlinear motions, PTOs, dynamic moorings, and their interactions. Thus, it is no trivial task to design dynamically similar WEC models and measure motions, power, and loads. Modelling the PTO is a known major uncertainty source [11]. Measurement challenges include the requirement to measure WEC body and captor motions without influencing motions, and implementing instrumentation that can sufficiently resolve the motions in time and space, across the entire working surface. In addition, it is often necessary to derive key quantities from measurements, such as the kinematics of the PTO. Such derivations can introduce considerable measurement uncertainty.

The common denominator here is that these uncertainties – scale effects, laboratory effects, and measurement uncertainty – influence all the ways in which experimental data are used. Data are used to predict larger or full-scale prototype power performance and survivability, directly in design, to validate and calibrate numerical models, or to secure continued and new investment. Thus, if experimental uncertainty is unknown, poorly understood, or of a significant magnitude, WEC development could be seriously impacted, thereby increasing technical and financial risks. Surprisingly, given the deep and diverse reliance on experimental data, few studies have focused on the issue of uncertainty in hydrodynamic model test experiments of WECs [18]. This represents a significant gap in the knowledge required to develop techno-economic WECs.

This context points to the challenges of developing a standardised set of best practice guidelines for WEC model tests. As said, two international committees have recently published guidelines that help researchers, developers, and hydrodynamic testing laboratories perform model tests of WECs. However, the issues described above suggest guidance is limited in these areas. Experimental investigations – such as the present work – and knowledge feedbacks are therefore needed in these areas to refine, validate, and update best practices for future versions of the guidelines.

1.2 Research objectives and design

The aim of this PhD research is to extend the knowledge of and develop methods to account for uncertainty in hydrodynamic model test experiments of WECs, focusing on a realistic Oscillating Water Column (OWC) WEC as a case study. Two questions directed the research to achieve this aim:

1. What are the best practices in hydrodynamic model test experiments of wave energy converters?

2. What are the causes and effects of experimental uncertainty in hydrodynamic model test experiments of OWC wave energy converters?

We designed two phases to answer the research questions:

1. A literature review carried out to answer research question (1). The review focuses on guidelines developed specifically for WEC model test experiments, as well as reviewing uncertainties in model tests to understand how, or the degree to which, the guides and recent advances address these uncertainties. This initial research phase informed the next phase, specifically by identifying the major experimental uncertainties needing further technical investigation and also identifying the best practices required to conduct high-quality experiments according to the international guidelines.

2. A technical research phase consisting of several experimental investigations carried out to answer research question (2). These investigations focus on the identified experimental uncertainties of measurement uncertainty, scale effects, and laboratory effects. A realistic OWC WEC was used as the case study for these experiments. The OWC WEC was selected amongst other the main WEC types of oscillating bodies and overtopping devices because it has been subject to arguably the most research, development and demonstration (RD&D). Its advantages include: several prototypes have delivered power into the grid [28, 29, 30]; a versatile concept that can be configured many ways, such as breakwater-integrated [31, 32], onshore fixed [30], nearshore bottom-fixed [33], or offshore stationary–floating [34]; relatively high wave-to-wire efficiency [35]; and no moving parts underwater. §§ 1.2.2 and 1.2.3 describe the case study OWC WEC and the scope, assumptions, and limitations of the experiments.

The experiments carried out in the technical research phase identified, generally, the causes and effects of experimental uncertainty. However, to objectively answer research question (2) with regards to scale and laboratory effects it was necessary to formulate a hypothesis: *If a hydrodynamic model test experiment of an OWC WEC is carried out at different scales or in different laboratories the experimental results will differ by an amount larger than the measurement uncertainty.* The experiments we designed to answer research question (2) were designed to ensure they would, among broader aims, test this hypothesis. Specific aspects of the experiments that test the hypothesis are as follows:

1. A 1:30 scale model test experiment of the case study OWC WEC focusing on understanding and applying uncertainty analysis. This, as well as a synthesis of previous experimental work, would generate the knowledge needed to quantify uncertainty in experimental results. Such uncertainty bounds provide the means to determine whether results obtained between model scales in the same laboratory, or between a reproduced experiment in different laboratories, differ by an amount larger than the measurement uncertainty.

2. A systematic series of model test experiments at three scales (1:40, 1:30, 1:20) of the case study OWC WEC. These experiments would generate sufficient data needed to determine whether experimental results differ between scales, with the previously developed uncertainty analysis methods applied to determine whether by an amount larger than the uncertainty.

3. Reproducing this model test at 1:30 and 1:20 scale in similar wave basin laboratory. This experiment would generate sufficient data needed to determine whether experimental results differ between laboratories, again with the uncertainty analysis providing the means to determine whether by an amount larger than the uncertainty.

The following subsections present the rationale for and details of the research design.

1.2.1 Experimental modelling

Developing WEC technology requires several hydrodynamic modelling techniques consisting of mathematical (analytical/numerical) and experimental models. Although the interdependence among these techniques increasingly strengthens, experimental modelling is still considered the roots and trunk from which validated mathematical modelling branches out into a wider domain of investigation [36]. Experimental modelling in hydrodynamic wave basins therefore remains a central tool [18] to progress WECs from proof-of-concept through the Technology Readiness Levels (TRLs) [11]. Like all modelling, however, it has advantages and disadvantages, uncertainties and limitations.

At a technical level, physical models used in hydrodynamic experimentation have two central advantages. First, physical models are a convenient means of predicting full-scale performance because they integrate the appropriate equations governing wave-WEC interactions, without the simplifying assumptions that must be made for analytical or numerical models. Second, small-scale models permit easier data collection under controlled conditions at a reduced cost, time and risk, thus enabling concentrated learning and optimisation, whereas field data collection is far more expensive and difficult, and at the mercy of the uncontrollable vicissitudes of ocean conditions [22]. The key disadvantages are measurement uncertainty, scale effects, and laboratory effects, as described above.

Regarding the design of the experimental investigations, various parameters were assessed to ensure the obtained data would be sufficiently detailed to identify and quantify the important uncertainty sources, yet sufficiently broad to evaluate the set of identified parameters and their relative contribution to the overall experimental uncertainty. Given any WEC design must integrate the competing design criteria of optimal power in average waves (operational) and survival in extreme waves (survival), the two key model parameters we considered were power absorbed by the OWC, and hydrodynamic wave loads imposed on the OWC body. In terms of the environmental parameters, following the relevant guidance [11, 10], we considered regular waves and long-crested irregular waves, covering an appropriate range of wave heights, periods, and sea states. The "appropriate range" here was based on a site-specific wave climate study. The site is at King Island off the coast of Tasmania, Australia. The rationale here is that we decided to use as the subject of this research an OWC WEC technology being developed commercially. Australian company Wave Swell Energy (WSE) [37] is developing the technology, and they are due to deploy a prototype at King Island in 2020-2021. The following section extends the rationale of the case study approach and describes the details of the technology.

Details of the model and environmental parameters, as well as the data analysis techniques and experimental instrumentation, are introduced in Chapters 3 to 5. It is important to emphasise that the model test experiments were carried out to a high standard according to international guidelines [11, 10].

1.2.2 Case study WEC technology

The decision to use a realistic OWC WEC rather than a generalised concept was based on the attempt to reveal the real-world challenges of hydrodynamic model tests with a technology that is being developed commercially, and has strong techno-economic potential. Further, generalised OWCs have been subject to many studies so the workings and drawbacks by now are sufficiently well known [28]. In contrast, we are not aware of any publicly available studies using an OWC WEC being developed commercially to investigate the modelling issues surrounding these often more complex systems.

The WSE Uniwave technology is based on the established concept of the OWC WEC (Fig. 1.1). The working principle of an OWC is similar to that of a blowhole in a cliff. It has a partially submerged hollow chamber with a small opening at the top and a large opening underwater. The chamber entraps air, and this air is forced out and in of the small opening as the inner water level rises and falls causing air pressure fluctuations when waves pass. The kinetic energy in the air flowing through the small opening is converted into mechanical energy via an air turbine-generator, and electricity is transferred onshore.

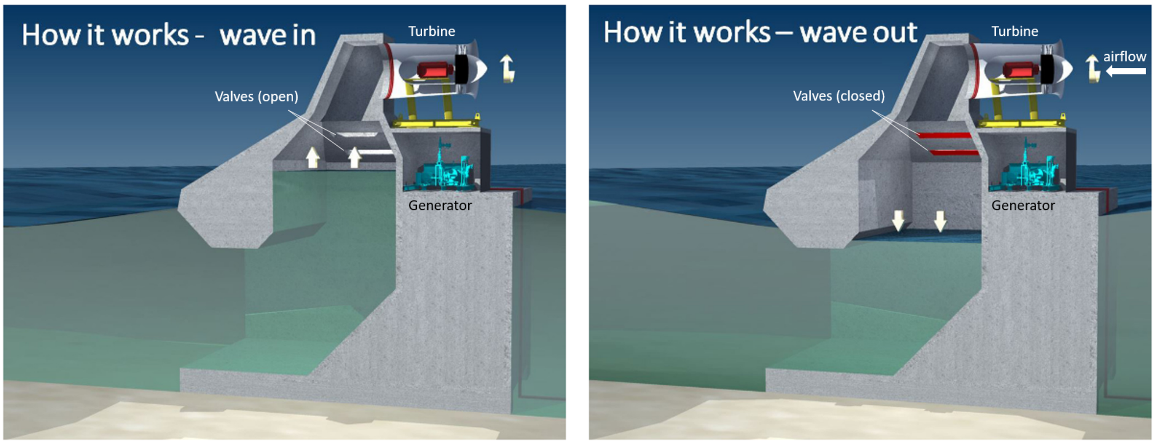

Figure 1.1: Working Principle of the Wave Swell Energy bottom-standing Oscillating Water Column Wave Energy Converter, the case study technology used as the subject of this research.

The OWC WEC considered in this study, however, differs from conventional bidirectional flow OWCs by way of using valves to create unidirectional air flow. The energy conversion process is as follows. When the inner free surface rises in the chamber, air escapes through the passive valves, causing slightly positive chamber pressure; when the inner free surface falls, the valves close, forcing air to flow through the air turbine only, causing dramatic negative chamber pressure. Even though air is directed through the air turbine for only half the wave cycle, almost all of the energy from the entire wave cycle (subtracting conventional turbulent and frictional losses) is available for absorption, because potential energy is temporarily stored in the heave of the water column when it rises in the chamber (see [33] for more details).

As mentioned, details of the physical model of this described OWC technology are given in Chapters 3 to 5.

1.2.3 Assumptions and limitations

The fundamental assumption in hydrodynamic modelling is hydrodynamic similitude – a condition in which the geometry, kinematics (motions), and dynamics (forces) are identical between the model and prototype. This, however, cannot be achieved in practice, so practical similitude is the aim, where the dominant force ratios are scaled (using Froude scaling for WECs) and the others (e.g., viscosity forces) assumed negligible. Another key assumption relates to the case study approach, where for the experimental investigations we are using an OWC WEC technology being developed commercially by Wave Swell Energy. For any case study approach there is an inherent assumption that the specific outcomes are applicable within a broader, more general context. This assumption means that the knowledge generated around uncertainty in hydrodynamic model test experiments of the WSE OWC WEC is applicable to other types of OWC WECs, and applicable to other types of WECs in a more general sense. Such generalisations, however, must be carefully interpreted when applying the knowledge in a broader context.

There are several limitations of the research regarding the experimental investigations. The limitations include: the number of model scales limited to three for the experimental investigations into scale effects (Chapter 4); the number of laboratories limited to two for the experimental investigations into laboratory effects (Chapter 5); limited model and environmental conditions, such as PTO damping settings and model angles, and wave types and water depths; neglecting to model air compressibility in the OWC WEC; limited survival wave tests; and the sole focus on experiments, neglecting numerical modelling. Each chapter elaborates on these limitations, and Chapter 6 explicitly discusses them at a higher level.

1.3 Novelty

This research addresses the major sources of experimental uncertainty in hydrodynamic model test experiments of WECs. In doing so it makes several novel contributions to the wave energy field, as follows.

The first is a pioneering experimental-based approach aiming to enhance the understanding and uses of uncertainty analysis in WEC model test experiments. While there have been previous studies on uncertainty in WEC experiments [38, 39], which investigated measurement uncertainty related to arrays tests, and by the authors [40, 41], which investigate measurement uncertainty and uncertainty analysis related to OWC WEC experiments, the present work differs from these by taking a broader approach. Within the context of WEC experiments, it outlines uncertainty analysis principles, identifies parameters causing measurement uncertainty, and develops WEC-specific uncertainty analysis methods not yet recommended in relevant guidelines (e.g., [42, 17]). These aims are achieved through and presented in a comprehensive uncertainty analysis applied to a model test of the WSE OWC described above. Thus, the technical outcome of this work is a practical, yet comprehensive, guide to applying the many uses of uncertainty analysis in a WEC experiment, which is a demonstrable extension of both previous uncertainty-focused studies and said guidance.

The second contribution is an experimental investigation into scale effects of OWC WECs, with the WSE OWC as the case study, consisting of a series of model tests at three scales (1:40, 1:30, 1:20). While there is substantial literature on some aspects of scale effects of OWC WECs, almost all of it focuses on how the scale effect of air compressibility impacts power performance in generic designs, with one study looking at how scale influences the hydrodynamic loads on a generic OWC WEC (see the literature review and discussion in Chapter 4). The present research takes a different, broader approach. It focuses on identifying, quantifying, and evaluating other kinds of scale effects arising in model tests of a realistic OWC WEC under commercial development, such as scale effects on power performance and hydrodynamic loads due to nonlinear waves, nonlinear motions, and a nonlinear PTO. No other such model test experiments at three scales have been published in the wave energy field, so this represents a seminal attempt.

The third contribution is an experimental investigation into laboratory effects of OWC WECs, with the WSE OWC as the case study, consisting of a reproduced model test at 1:30 scale in two similar wave basin laboratories. Other maritime fields have undertaken 'round robin' campaigns of hydrodynamic model tests to identify, quantify, and evaluate parameters causing laboratory effects, which lead to differences in results from similar test laboratories (see the literature review and discussion in Chapter 5). A striking finding that emerges from this literature is the apparent significant influence the laboratory (towing tanks, flumes, or wave basins) can have on experimental results. This finding highlights the importance of (1) identifying, quantifying, and evaluating all possible laboratory parameters that may impact results and (2) to develop guidelines with standardised procedures that account for the known influences of the laboratory on results. Recognising this, a 'round robin' campaign was attempted for wave energy, but it was abandoned [43]. Therefore, this PhD research presents for the first time a reproduced WEC model test experiment in two wave basin laboratories, including inter-laboratory comparisons of results.

1.4 Thesis outline

Chapter 1 provides and introduction to the thesis. It sets out the context and motivation for the research, briefly describes previous work relevant to the study, and defines research questions and the research design used to answer these. It also outlines the structure of the thesis and points to the outcomes.

Chapter 2 is the main literature review of this research. It focuses on WEC model test guidelines, advances, and uncertainties, aiming to answer research question (1): *What are the best practices in hydrodynamic model test experiments of wave energy converters?* In doing so, it describes the best practices and identifies guidance limitations and gaps. The following chapters address the identified limitations and gaps associated with experimental uncertainty.

Chapter 3 presents a comprehensive uncertainty analysis methodology, applied to the 1:30 scale model test conducted in the Australian Maritime College (AMC) Model Test Basin (MTB). This chapter presents the methodology of the uncertainty analyses applied to the subsequent experiments to determine whether the results across scales and between laboratories agree or disagree. It is one line of investigation of research question (2): *What are the causes and effects of experimental uncertainty in hydrodynamic model tests of OWC WECs*?

Chapter 4 reports an experimental investigation into scale effects of the OWC WEC, consisting of three model scales tested in the AMC MTB. It reports results and uncertainty of power performance and hydrodynamic loads in regular and irregular waves. The analysis identifies key parameters causing scale effects, and quantifies and evaluates the degree to which the scale-dependent parameters influenced the results and uncertainty. This chapter is another line of investigation of research question (2).

Chapter 5 reports an experimental investigation into laboratory effects of the OWC WEC, consisting of interlaboratory comparisons of the 1:30 scale model test that was reproduced in a similar laboratory, the Queens University Belfast (QUB) Coastal Wave Basin. It reports results and uncertainty of power performance in regular and irregular waves. The analysis identifies key parameters causing laboratory effects, and quantifies and evaluates the degree to which the laboratory-dependent parameters influenced the results and uncertainty. This chapter is third line of investigation of research question (2).

Chapter 6 concludes the thesis by providing a summary of the main findings, discussing their relevance at higher level of abstraction. It also concludes on the findings, highlights implications for the wave energy model test community and more broadly, and provides recommendations for future research and guideline development.

Chapter 2

Wave Energy Converter Model Test Experiments: Review of Guidelines, Advances and Uncertainties

Hydrodynamic model test experiments are central to developing wave energy converters. However, guidelines and methods for conducting these experiments are still maturing. This chapter reviews WEC model test guidelines, advances, and uncertainties to identify and describe the current best practices and evaluate their coverage, consensus, and gaps. The chapter also establishes the context and rationale for the subsequent experimental investigations, and generates the knowledge required to carry out these experiments to a high quality.

2.1 Introduction

Wave Energy Converters (WECs) are complex machines that must produce power economically and survive storms reliably. The challenges in meeting these disparate demands have been stubbornly persistent: despite a vast technical potential and about two decades of intense research, development and demonstration of hundreds of prototypes, the wave energy industry still lacks WECs that can produce a competitive Levelised Cost of Energy (LCOE) [8], and only a fraction of a percent of renewable energy feeding into electricity grids around the world comes from wave energy [44]. Therefore, while wave energy is a nascent industry it is also still immature. It follows that the methods and guidelines used to test and develop WECs are similarly immature [45]. Methods and guidelines are undergoing active development through technical investigations, refining existing and introducing new experimental and numerical modelling techniques, and integrating knowledge feedback loops extracted from advances in technologies and prototype demonstrations. Such active technology and guideline development in a burgeoning industry suggests the guidelines and related literature need regular review, to identify the current best practices, recent advances, and outstanding issues needing further investigation.

Several projects and organisations have produced technical guidelines on early-stage WEC development [12, 13, 14, 15, 16, 46, 10], and other publications provide additional guidance [47, 48]. Given WECs are complex machines operating in demanding marine environments, the wave energy industry has adopted and adapted a proven technology development methodology, the Technology Readiness Levels (TRLs), established by industries with similarly challenging demands, such as space flight [49, 9]. The TRLs mitigate technical and financial risks as a technology is progressed from a basic concept (TRL 1) to a full-scale commercial product (TRL 9). In the wave energy context, TRLs 1-5 require a series of hydrodynamic model test experiments, and technical guidelines recommend the best practices – the parameters, procedures, and high-level requirements – for carrying out these model tests. Data obtained in these experimental tests are used to validate WEC prototype performance against numerical and wave-to-wire models, and extrapolated to predict the WEC's full-scale performance. Developers then use these findings to underpin further investment to support large scale open water tests. Thus, high-quality experimental data is critical, and obtaining such data requires the guidelines to be accurate and robust, coherent and consistent, and frequently updated as methods are advanced and issues resolved.

A relatively recent study reviewed guidelines and key studies on hydrodynamic modelling of marine renewable energy devices, identifying issues in the physical modelling of these devices, including WECs [18]. Outstanding issues were found to be modelling Power Take-Off (PTO) systems and the uncertainty in performance prediction from model test results. This review was produced by the International Towing Tank Conference (ITTC) Specialist Committee on Hydrodynamic Modelling of Marine Renewable Energy Devices (SC-HMMRED), who are developing two guidelines for WEC model tests (7.5-02-07-03.7 [11] and 7.5-02-07-03.12 [17]). More recently, as part of the MaRINET 2 project [16], a broader review was carried out on marine renewable energy standards and guidelines, to summarise them, and to highlight gaps or areas for further development [50]. The gap analysis revealed several lacking areas and challenges: modelling PTOs and extrapolating power-related results; designing and modelling moorings; working toward a coherent set of guidelines/standards used by all test facilities; and guidance on how to transition between TRL stages and deal with scaling from the controlled laboratory to the uncontrolled marine environment. Moreover, through a questionnaire it was found that developers, researchers, and facility managers use a wide range of different guidelines and standards for WEC model tests.

This chapter builds on these works by a carrying out a more focused, comprehensive review of guidelines on WEC model test experiments, including recent advances and, most important to this PhD research, experimental uncertainty. There are two aims. The first is to answer, *What are the best practices in hydrodynamic model test experiments of WECs?* To answer this question, we focus on identifying the parameters, procedures, and high-level requirements of WEC model tests, and key areas in which there are unresolved issued to be investigated. An important area revealed is experimental uncertainty. So, not only does this review identify what is required and how to carry out a WEC model test, but also helps formulate the technical research question of this PhD study, on what are the causes and effects of experiment uncertainty in WEC model tests, and informs the various experimental investigations undertaken to answer this question (presented in Chapters 3 to 5).

The second aim, which is broader, is to reduce experimental uncertainty in a more general sense by providing a comprehensive overview of WEC model tests to such stakeholders as developers, researchers, students, facility managers, and investors. This reference may be used to understand the overall aspects of model tests, what the general considerations are, what the relevant parameters and procedures are, which high-level requirements need to be addressed and when, which uncertainties are most important and means to address them, and whether there are recent advances which might help solve specific problems in physical modelling applications.

2.2 Why model test?

It is first necessary to provide the rationale for model tests in WEC development and describe the role they play. To begin, some definitions and context. A WEC converts energy in ocean waves into a useful form, for example, electricity, desalinated water, or hydrogen. It does this using a working surface (a *captor* that interacts directly with waves) coupled to a PTO system including a generator and other power electronics. The many ways in which wave energy can be harnessed – up/down, back/forth, in/out, circular – has yielded a remarkably branched tree of WEC designs, with thousands of concepts and many hundreds of prototypes deployed or under development [8]. Several classifications of WECs exist, some based on working principle, size, and location [51, 52], others on three levels: working principle, PTO subsystem, mooring and control subsystems [53].

In terms of requirements of WECs, five high-level requirements have been identified: power performance, the wave-to-wire efficiency; survivability, the ability to survive design life storms; reliability and maintainability, with low failure rates and ease of access; scalability, the potential for enlarged dimensions and arrays; and environmental benefit, with acceptable or positive impact [47].

At a more technical level, the following circumstances characterise WEC development: diverse spectrum of concepts with no evidence of technology convergence; demanding consenting and environmental impact assessment requirements; strongly reduced market opportunity at reduced scales (unit and array); limited transferability of experience, design, production, and operation of seemingly related mature industries; expensive, delayed, and difficult offshore access for repair and maintenance, prohibiting high failure rates from the onset of commercial operations; system design loads are one to two orders of magnitude higher than high-power operational loads; global average incident energy flux density is on the order of 10- to 30-kW/m wave crest width; reciprocating irregular, multidirectional wave load characteristics [54].

At a hydrodynamic level, a WEC interacts with its environment in complex, interdependent ways, a hydrodynamic interplay of wave-captor-PTO-mooring interactions. For most WECs most of these interactions and components are nonlinear – nonlinear incident waves, nonlinear fluid-structure interactions such as viscous effects, and nonlinear PTO systems [55]. These nonlinearities, which arise from high velocities, amplitudes, and forces, place exacting demands on mathematical/numerical modelling [55]. Moreover, the ability to simulate WEC behaviour in storms, in which occur one to two orders of magnitude higher velocities, amplitudes, and forces than normal operation, raises questions about the accuracy of modelling such phenomena [36]. Finally, [36] argued that even the most widely used numerical models lack rigorous and critical empirical validation, though efforts in this area have since begun [56].

The above context highlights key requirements, circumstances, and challenges in developing techno-economic WECs. The confluence of these factors points to the need for continued, perhaps increased [54], reliance on physical/experimental modelling in the form of hydrodynamic model test experiments in wave basin laboratories; it evidently paid off for the offshore oil and gas industry. Besides, physical models as validation and design tool is central to the TRL methodology adopted by the wave energy community (§ 2.3.1.1). Like all models, however, physical models have advantages and disadvantages (Table 2.1).

Having set out the rationale for and context of model test experiments in WEC development, now to the specific aim: to obtain high-quality data in a controlled environment to analyse and estimate prototype performance [59]. The specific objectives of a model test varies depending on the development stage, detailed in the following section (§ 2.3).

Hence, while the role of model test experiments will likely change as numerical models become more accurate, computationally efficient, and user-friendly, the role of model test experiments in WEC development, especially at early-stage, will likely remain as important in the next decade as at present.

Table 2.1 Advantages, disadvantages, requirements, and challenges of WEC model test experiments.

Model test...	**Details**
Advantages	· Integrated governing physics · Reduced cost, time, and complexity of data collection in a controlled, repeatable environment compared to ocean/sea tests · Obtain empirical coefficients [57] · Visual, qualitative feedback of overall processes improves understanding of the system [22] · Helps de-risk technology development [54, 10] · Quantify performance variables of system and subsystems · Simulate strongly nonlinear or unpredicted phenomena [58, 57] · Validate and calibrate numerical models [13, 14, 11, 10] · Investigate deployment methodologies [11, 57] · Secure continued and future investment [10]
Disadvantages	· Scale effects, arising from the inability to scale all physical quantities in correct relationship with each other (Chapter 4) · Laboratory effects, arising from the inability to simulate realistic processes due to laboratory limitations and influences, and possible inconsistent results between laboratories (Chapter 5) · Measurement uncertainty, arising from random and systematic uncertainties in experiments (Chapter 3) [21, 11] · Often more expensive than numerical models.
Challenges [11]	· Simulate and measure complex kinematics and dynamics, material properties and fluid-structure interactions · Novel concepts · Simulate WECs with large dimensions (transverse or longitudinal) · Simulate PTO system, potentially requiring large-scale models with corresponding large waves · Multiple WECs in an array, requiring large basins for reliable results

2.3 General considerations, uncertainties, and advances

This section summarises WEC model test experiments in terms of the general considerations and common practices, uncertainties and advances. Implicit in these are the detailed requirements of WEC model tests. Subsequently, § 2.4 identifies and evaluates the high-level requirements.

Experimental test programs comprise diverse activities that can be grouped numerous ways — and have in the wave energy field, with many publications all proffering different headings and sections, subheadings and subsections, and so on [12, 13, 14, 15, 16, 11, 10, 48, 50]. This review proffers yet another structure but one consisting of general experimental phases: Plan, Design, Construct, Debug, Execute, Analyse, and Report (as in [60]). To that end we synthesise related materials from said guidance publications and relevant studies into these phases. The review excludes guidelines and standards developed for other maritime industries; sometimes, however, such publications are referenced in the primary references and so they are implicitly included in these cases.

2.3.1 Plan and design

The aim of experiments and tests is to obtain the maximum quantity of high-quality information in the shortest time at minimum cost [42]. This aim guides the iterative planning and design process to ensure maximum return on invested time, effort, and money. When planning and designing a test, the key considerations are test objectives and means to achieve them. Questions are useful here: *why is the test program is being carried out*? and, then, *how to carry it out*? In answering the *why* question users define objectives and expected outcomes. This initial planning leads to the *how* question whereby users decide on a suitable model scale, consider model and environmental parameters, measurements and uncertainties, and design the technical components to be used to achieve the test goals. These activities fall within the Plan and Design phases. The following subsections describe, in roughly chronological order, the main aspects to be considered when planning and designing a test.

2.3.1.1 Technology development stages

Early-stage WEC development generally requires three stages of hydrodynamic model tests generally increasing in model scale, scope, and representation of the prototype (Table 2.2). Objectives of each stage are linked to TRL descriptors adapted for WEC technology [13, 14]. Progressing to the next stage requires users to satisfy their pre-defined objectives through a stage gate review. This review may be both technical and economic, based on performance and qualitative results, comparison with the design statement defined at the beginning of the test program, and an independent design review. This staged approach thus reduces risk, technical and financial, as the technology progresses from model to prototype to product in a safe, timely, and cost-effective manner, with reduced life-cycle costs, and results that are defensible to expert reviewers [49].

2.3.1.2 Selecting model scale and test facility

Selecting model scale and the test facility is an interdependent, iterative process that requires users to consider, often compromise between, numerous parameters and constraints. The main parameters, summarised below, are WEC similitudes, development stage and test goals, subsystems and components, and test facility configuration and capabilities.

Model-prototype similarity, whereby the physical model behaves identically to its prototype, is always the aim. This aim, however, is seldom achieved in practice, so scaling compensations are required [23]. At least four aspects govern model-prototype similarity: WEC body geometry, waves, their interaction, and the PTO interaction with both. That is,

Table 2.2 Staged development structure for early-stage, pre-prototype WEC development.

Stage/ TRL	Objectives	Scale	Parameters
1/1	Prove concept	1:25-100	*Model*: idealised, easy to modify; simplified PTO mechanism; generic mooring.
1/2	Validate performance		*Environment*: flume or basin; generic regular and irregular waves.
1/3	Optimise performance		*Metrics*: RAOs/timeseries of dominant DoF motions, loads, power.
2/4	Validate design	1:10-25	*Model*: realistic, quasi-dynamic similitude; realistic PTO simulator, control option; realistic mooring, geometric and structural similitude. *Environment*: basin; site-specific wave climate, inc. extreme waves. *Metrics*: RAOs/timeseries of motions, loads, power; operational and survival conditions.
3/5-6	Validate subsystems	1:2-5	*Model*: realistic, dynamic similitude; advanced PTO simulator, control; actual mooring, geometric/structural similitude. *Environment*: sheltered test site; uncontrolled conditons. *Metrics*: RAOs/timeseries of motions, loads, power; PTO efficiency and control; deployment; environmental impact; O&M procedures; costs; corrosion; fatigue; component reliability.

similitude in geometry, kinematics, and dynamics of wave-WEC interactions (for prescriptive similitude guidance see [22, 57, 13, 10, 22]). Froude (waves and WEC body) and Cauchy (structural) similarity criteria are generally used for WECs where inertia forces dominate; some cases may require Reynolds scaling if viscous forces dominate. A larger model scale is generally preferred to a smaller one as it reduces scale effects and improves prototype simulation [61]. Thus model scale generally increases with development stage.

WEC subsystems can also govern model scale selection. PTO scaling is a key recognised challenge in WEC model tests, as Froude scaling does not readily apply [11, 47, 61]. As a result, it is often impractical to down-scale prototype PTOs; instead, a simplified damper mechanism or similar [62] is used to represent the dynamic-kinematic (e.g., force-velocity, pressure-flow) characteristics of absorbed power. Similarly, moorings may govern model scale if the mooring strongly influences WEC motions and thus power performance and survival responses [63, 11], or mooring lines have to be truncated leading to inconsistently scale water depth [64]. Survival tests typically require accurate simulation of the moorings as they will likely impact WEC motions and loads. Mooring design and scaling for model tests may be guided by other offshore structures [65] or numericals tools [66]. Other subsystems such as PTO control [47] or practical constraints such as model construction [50] may also play a dominant role in scale selection.

Arrays and clusters tests present substantial challenges for model tests which implicates scaling considerations [39, 38, 67, 68], especially when large footprint moorings will be deployed [11].

Another factor is the test facility configurations and capabilities. First to consider is the range of suitable facilities. These include, in approximate order of their use in relation to the development stage: wave flumes or towing tanks, for 2D tests in long-crested waves; wave basins, for 2D or 3D tests in long- and short-crested waves; or wave flumes or basins with wave and current flow capabilities [13, 14, 15, 16, 11, 10]. Having in mind the test goals and a reasonable estimate of model scale or, more likely, a range of suitable scales, users select a test facility that suits the goals and scale (for any development stage multiple facilities can be used). Numerous facility parameters require consideration: size, with boundaries and water depth [64] being important; wave/current/wind generation and absorption capabilities; model building and installation, instrumentation, and data acquisition capabilities; fixing points and footprint for moorings; and availability of technical support to assist and advise the test program [42, 11, 10].

In wave basins the maximum wave height a wavemaker can generate often sets an upper limit to model scale. An array of other laboratory limitations might affect scale selection. Flume and towing tank limitations include long-crested waves only (2D), high aspect ratio affecting moorings, and the model will be necessarily close to wave-reflecting side walls causing blockage effects [69, 48]. Wave basin limitations include reflections, settling time and sample length, and facility specific performance in environment simulation [42]. Specific aspects of wave generation and absorption, and basin and flume flow were recently reviewed [48].

Table 2.3 summarises scale related issues drawn from established publications [22, 57] and recent studies. Users must be aware of and approximate scale effects where possible when they select model scale.

Finally, it can be difficult to assess both power performance and survivability at one scale, due to wavemaker limitations in generating extreme waves. If survival tests are a key objective, careful consideration is needed to ensure the scale is appropriate for the test facility capabilities in terms of wavemaking and moorings [11].

2.3.1.3 Test plan

A test plan describes the objectives, resources, and processes for a model test; it is a strategy that ensures the high-level requirements are met. The main aspects are the design statement and test matrix, informed by uncertainty analysis and Design of Experiment.

Table 2.3 Summary of possible scale effects in WEC model tests, including issues and advances. Table continues with mode-specific scale effects on next page.

Scale effect	**Description, issues, and/or advances**
Hydrodynamics	
Wave reflection	Wave reflections from boundaries or models may be different to prototype. Smooth-wall reflections tend to be relatively smaller in models due to relatively greater surface roughness. Boundary reflections should be minimised with absorbers [22]. Relevant for breakwater integrated WECs [32].
Wave transmission	Transmission through a WEC, or an array of WECs, may be relatively less in models due to relatively larger frictional losses [22], problematic to quantifying 'q-factor' [70, 71] or coastal dynamics in array studies [72]. Methods exist to acccount for wave transmission scale effects in rubble mound breakwaters [22].
Viscosity, friction	Viscous effects (e.g. vortex shedding) may be disproportionally significant in small models, producing conservative results [13]. Wave attenuation from seabed/bottom friction may be important for long towing tanks. Surface roughness may require consideration at small scales. Notable studies on viscous scale effects in model tests include: floating structures [73], point-absorbing WECs [74, 75, 76], Oscillating Wave Surge Converters [77, 78, 79, 80, 81].
Nonlinear waves	Shallow water and extreme waves are often highly nonlinear, with large velocities, amplitudes, and forces, and such phenomena do not scale well with fluid-structure interactions [22, 82]
Wave breaking	Entrained air bubbles in breaking waves tend to be relatively larger in models due to surface tension. Also, air entrainment depth is larger in the model [22]. While the process of energy dissipation will be in similitude due to the momentum theorem [83], WECs may suffer from reduced hydrodynamic efficiency due to nonlinear wave breaking sub-process of turbulent, vortical and interfacial energy transfer [84].
Water density	Fresh water in laboratories causes discrepancy in buoyancy and mass distributions, pressures, and forces due to different density to seawater [22]. Hydrodynamic forces are 2.5% larger in seawater, and buoyancy may change significantly [10].
Water depth	Incorrect depth scaling for WECs in intermediate depth can lead to considerable errors in wave parameters, including +/-30\% error for wavelength/steepness and +/-20\% for group velocity and power [64]. Design diagrams developed in this work quantify and visualise these errors to aid experimental design, uncertainty analysis, and correlation of model test results with prototype data.

Table 2.3 ...continued

Scale effect	Description, issues, and/or advances
Model	
Friction	Forces required to overcome Coulomb friction are relatively larger in models, so must be considered where two solid bodies are in contact [22]. Problematic for PTO simulators such as mechanical breaks, air dampers, oil-filled dashpots, which suffer from static friction, non-physical hysteretic effects, and temperature dependency [85]. Another issue is scaling bearing surfaces in PTOs, where losses are not correctly scaled; addressed by a friction analysis to improve power predictions [10].
PTO limitations	PTO simulators may not implement prototype limitations such as maximum forces or slew rates from the generator [10].
Air compressibility	Hydrodynamic/aerodynamic scaling is inconsistent due to air compressibility [86]. This affects WECs with wave-to-pneumatic energy conversion; it has been well-studied for OWC WECs [87]. To correctly model air compressibility, required in later stages, Froude/hydrodynamic similitude should be met for the part of the WEC subject to wave loads, but not for the air chamber size or turbine simulator. For the air chamber, this in practice requires an air reservoir or scaling the air chamber by the length scale λ squared (λ^2) not λ^3 , i.e., a relatively larger chamber [88, 89].
Power scaling	Froude criterion for power is $\lambda^{3.5}$, indicating the disparity between geometry and power. An example of this significance: a 1:30 scale model of a 1 MW prototype absorbs only 7 W, requiring mW range measurements. Question about the accuracy of extrapolating model watts to prototype megawatts have been raised [13].
Material properties	Inconsistent scale ratios of materials, for example flexible membranes [90], dielectric elastomers [91], or mooring lines [82] presents problems for model tests.

A design statement typically consists of specified test goals, technical drawings of the WEC at model- and full-scale including moorings, approximate descriptions of hydrodynamic behaviour of the WEC, and a mathematical model if developed. Later stages have increasingly exacting design statement demands. Increasingly detailed descriptions are required of the physical model subsystems in terms of design and construction, environmental parameters such as site-specific wave resource information, PTO control strategies, operation and maintenance procedures, and survival and failure modes [10].

A test matrix typically consist of the scope and sequence of environmental and model conditions to be run – the data to be collected in which order. This process requires a sound knowledge of waves and WEC responses, i.e., wave-WEC interactions. Such knowledge may be acquired from notable works [92, 93, 8, 47, 48]. The main wave parameters are wave height, period, and direction. However, descriptions of these parameters differ significantly depending on whether the waves are regular, or long- or short-crested irregular. General guidance [94, 95] and WEC-specific guidance [13, 96, 97, 98] is available to aid the understanding, analysis, and usage of wave parameters in model tests.

Regular waves and long-crested irregular waves are used at the concept and design validation stages and for comparative studies. Regular and irregular wave tests typically produce capture width ratio Response Amplitude Operators (RAOs) and transfer functions. Irregular wave tests also produce the power matrix from which an estimate of annual energy production can be made [99]. Added to the test matrix at later stages are more realistic waves, short-crested irregular sea states described by the directional wave spectral density function [11]. Such multidirectional spectra tests produce a more accurate power matrix. Alternatively, measured wave spectra from the intended deployment site can be used to yield better performance estimates. When WEC performance can be compromised by multidirectionality (e.g., bimodal spectra with two peaks [100]), testing in sea states with multiple wave systems is recommended [11].

The specific parameters and number of regular wave periods/heights and irregular wave sea states to be run depends on the test stage and objectives. Section § 2.4 outlines the wave conditions for such requirements.

Users should also be aware of the challenges and uncertainties in assessing WEC performance under realistic ocean environments, and recent advances in this area [20, 101]. Issues have been raised over assessing WEC power performance using two parameters only (significant wave height H_s, energy/peak period T_e/T_p) [102, 103, 104, 105, 106, 107, 100, 108, 109, 110]. Additional parameters – such as spectral distributions with multimodal peaks, and directional spreading – may be required to accurately assess WEC performance, both at the time-scales of sea state and long-term power predictions. Other limitations include: resolution of sea states, linear interpolation between elements of the matrix, standard spectral shapes, constant bin size, more dimensions relevant (direction, water level), and limited data sets. An alternative to avoid the challenges of WEC performance assessment under irregular waves is using simpler polychromatic waves, composed of a smaller number of combined regular wave components [111].

There are also issues with predicting WEC loads and motions in extreme waves for survival tests. Reviews of numerical and experimental methods for survival tests [112, 113] suggest guidance from offshore structures or shipping is generally useful but limited due to WECs maximising motions while other ocean structures minimise motions. Also, it is not always the largest wave that causes the extreme response and load, rather a series of waves [105], implicating the use of focused/transient waves [11].

In terms of model conditions, some common parameters include: model heading, for direction dependent WECs; geometry changes, for parametric performance assessments in early stages; PTO settings, where for passive PTO simulators a series of fixed-step PTO characteristics can be modelled, with a recommended damping range from zero (disconnected/open-system) to infinity (fixed/closed-system) with better resolution around optimal damping; and mooring configuration changes.

It is no trivial task to fully integrate the above technical aspects in a way that maximises the likelihood of a high-quality experiment, completed on time, to budget. Uncertainty analysis can help. Uncertainty analysis is the analysis of uncertainties in an experiment to assure and quantify the quality of results. It can be applied here, at the pre-test stage, to evaluate the relative importance of overall (general) uncertainties in parameters, to inform decisions on various approaches, instruments, apparatus, and overall measurement procedures that might best answer questions or attain the objectives. This is called General Uncertainty Analysis (GUA). While it is not yet covered in WEC-specific guidance, Chapter 3 provides a comprehensive description and application of GUA in a case study WEC model test.

Finally, having identified the test plan and test matrix, Design of Experiment methods may then be used to optimise the test procedure [42].

2.3.1.4 Measurements, instrumentation, and uncertainty

There are many possible measurements, and instruments to do the measuring, in a typical WEC model test. Typical measured quantities, measurement procedure, and related instrumentation are as follows:

Wave elevation. Local and flanking to the model, as well as far up-wave and down-wave as appropriate. Also position inside models such as OWCs to measure the internal free surface. Instruments are typically surface piercing twin wire probes (resistive or capacitive), or non-intrusive methods (optics, acoustics, radars, imaging methods, combined laser-scanner and video hybrid system) [96, 63, 114].

Detailed fluid flow. Detailed investigation of fluid flow around and inside devices, OWCs for example, using Particle Imaging Velocimetry (PIV) [115, 116, 117].

Motions/kinematics. Measured to determine RAOs and the kinematic quantity of the captor for deriving WEC power. Quantities and instruments include: all degrees of freedom of a body or captor, using optic-based Qualysis, accelerometers, or wire potentiometers; overtopping rates for overtopping devices; fluid flow/velocity using flowmeters (e.g. pitot tubes, thermal-mass, differential-pressure), Hot-Wire and Hot-Film Anemometers, or Acoustic Doppler velocimeters [48].

Loads/dynamics. Measured to determine structural loads, the dynamic quantity of the captor for deriving WEC power, and mooring loads. Quantities and instruments include: force transducers for mechanical PTOs, in-line loadcells for mooring lines, and multi-component force balances for fixed WECs; pressure transducers for pneumatic/hydraulic PTOs and wave forces imposed on surfaces; dynamometers or similar to measure torque for rotational-based PTOs.

Data acquisition hardware/software varies widely for different tests and different WECs. Some common parameters and requirements are as follows: *analog signal*, where a sensor is required for each physical quantity being measured, with key parameters including type of sensor, range, calibration, accuracy, resolution, weight/dimensions, waterproof protection; *signal conditioning*, where signals should be acquired as raw as possible, avoiding aliasing; *signal conversion*, requiring a multiplexer to acquire as many signals as needed, data synchronisation using a common trigger, and an analogue to digital converter; *sample rate*, which needs to be sufficiently high to avoid aliasing, and especially high if investigating extreme, fast events such as wave slamming; *signal length*, requiring 30-100 wave periods for regular waves per period/height, and for irregular waves 20-30 minutes full-scale for operational sea states, and three hours for survival sea states; *measurement quality*, where later stages require more accurate instrumentation to obtain better measurement quality. Further information on practical considerations for data acquisition and storage is given in [42, 5].

Regarding measurement uncertainty, the above section introduced the notion of using GUA before a test to help plan and design high-level parts of it. Here, uncertainty analysis can be used to evaluate uncertainties at a detailed level, considering the uncertainty associated with parameters as separate components. This is called Detailed Uncertainty Analysis (DUA). It is used, for example, to guide decisions on choosing appropriate instruments (as those above) according to a desired uncertainty budget; to guide changes in the test program; to inform calibration procedures; and once data are collected, quantify their quality [60]. We introduce the basic principles here, at this pre-test stage, because the sooner users are aware of the importance and uses of uncertainty analysis, the sooner they can put them into practice to design, construct, debug, execute, analyse and report high-quality model tests. Uncertainty analysis has three main stages and several steps, composed of the basic principles [21, 118, 17].

1. *Formulate:*

   (a) Define the measurand: $Y = f\left(X_1, X_2, \ldots, X_N\right)$, where Y is the output quantity (the measurand) which depends on input quantities $X_1, X_2, \ldots, X_N$ (e.g., measurements and constants);

   (b) Identify uncertainty sources: assemble a list of uncertainty sources – instruments, environmental factors, assumptions, etc. – to be evaluated;

(c) Evaluate standard uncertainty: the X_i is a function of two uncertainty components, Type A and Type B. Evaluating Type A standard uncertainty requires the statistical analysis of series of observations, i.e. the standard deviation of the probability density function (PDF) produced by repeated observations. Type B standard uncertainty, also characterised by PDFs, is evaluated by means other than the statistical analysis of series of observations, for example, from instrument calibrations, manufacturer's specifications, or uncertainties taken from handbooks. Thus, on the basis of available knowledge PDFs – Gaussian (normal), rectangular (uniform), etc. – to the X_i. Assign instead a joint PDF to those X_i that are not independent.

2. *Propagate*: determine combined uncertainty: propagate the PDFs for the X_i (Type A and B) through the model to obtain the PDF for Y. Uncertainty propagation thus determines the combinatorial effect of X_i uncertainties on the uncertainty of Y.

3. *Summarise:* use the PDF for Y to obtain: (a) an estimate (the mean) of Y; (b) the standard deviation of Y, taken as the general uncertainty $u_c(y)$ associated with Y; and (c) a coverage interval k containing Y with a specified probability, which gives the expanded general uncertainty $U = ku_c(Y)$

Noted, some of the principles described as follows are put into practice once the test begins and in post-test analysis. It is obvious from above that Type A uncertainty evaluation in the Formulate stage can only be performed once data is collected in the test, which § 2.3.3 describes below. Additionally, this three-stage uncertainty analysis structure can also be used for GUA, but is not yet covered in guidance (Chapter 3 addresses this).

2.3.1.5 Physical model design and construction

In early-stage tests model designs should allow for quick and easy modifications, either to expand the number or nature of parameters under investigation or to allow for variations in case of unexpected results. Moving parts and appendages require careful design, ensuring minimal friction and appropriate dynamics. Especially at smaller scales, static and dynamic friction is a dominant source of uncertainty. To minimise scale effects due to viscous effects, designs should avoid sharp edges and narrow channels.

Similarly, articulated and flexible models require careful design; for articulated models it is important to achieve correct mass properties for each moving segment as well as for the model as a whole; for flexible models it is important to scale the material properties correctly to reproduce elastic behaviour at scale. It might also be important to consider the mass properties and size of instrumentation, as it can influence model properties, especially for floating and articulated WECs.

Model construction methods and materials vary widely, depending on the desired fidelity and scale of testing. Models are rarely constructed from prototype materials. Instead, common practice is to use light alloys, marine plywood, fibreglass, epoxy, and plastics. Acrylics such as Perspex are practical as they are close to neutrally buoyant, and transparent which allows visual feedback of flow behaviour inside WECs, for example in the chamber of an OWC [13]. This qualitative feedback, or in some applications quantitative [117, 115], can stimulate intuitive discovery and inform optimisation.

To design and construct a model PTO system is no trivial task. Often, prototype PTO characteristics are unknown and cannot readily be down-scaled in any case. More, there is the issue of a large disparity in power similitude. Thus it is common practice to use PTO simulators. Depending on the WEC working principle, such simulators may be either mechanical-, pneumatic-, or hydraulic-based. Fixed step passive damping mechanisms of some description are mainly used in early stages. For example, orifice plates or fabric mesh for OWCs [35, 28, 119], damping brakes or linear generators for point-absorbers, and bilge pumps or flowmeters for overtopping device [48].

More sophisticated PTO simulators are required in later stages, perhaps with actively controlled damping using electronics. For example, actively controlled actuators [85]. Such active control allows for open-loop tests for system identification and to investigate control strategies to optimise power performance and survive extreme events. Care, however, should be taken to ensure the active control strategies do not result in energy input to the system. Other challenges of active systems include weight of system, water-proofing, and impact of cabling on floating models.

Whatever means is used to simulate the PTO, it should dampen energy at a known relation to the captor dynamics. It is also beneficial to carry out appropriate tests of the damping system prior to installing it in the model, to characterise the relationship between damping force and velocity. This process allows to estimate the quantitative magnitude of damping at different settings, and to confirm the repeatability of damping settings.

As ever, care should be taken to minimise static/dynamic mechanical friction, for example, hydraulic seals. Active PTO simulators may be capable of eliminating friction with an appropriate control strategy. Other challenges include achieving desired ranges of travel of dampers, especially when using linear dampers or angular systems, and non-linear friction behaviour, especially where coefficients of static and dynamic friction are substantially different. Simple mechanical dampers may prove difficult to achieve repeatable damping characteristics, problematic for parametric studies. This can be especially true when temperature and humidity change during testing, and where surfaces may be wet or dry.

Mooring design and construction can also be a demanding task. This is especially the case for floating WECs that aim to realistically represent mooring-captor-PTO interactions. In early-stage tests, simple soft elastic moorings can be used for WECs that do not use moorings as part of their PTO. For later stage tests, 'hard' moorings are used, including single point, spread, catenary, taut, and multi-element mooring systems. Where tests are only focused on power capture, accurate representation of catenary moorings is generally not required, as these have been sown to have little impact on the device response of oscillating bodies [120, 121]. However, methods are available to appropriately model catenrary moorings [13]. In contrast, taut moorings can significantly impact responses and thus power capture, so should be simulated accurately (free oscillation tests are recommended for taut moorings). For survival tests, mooring simulation is an important requirement. In such extremes moorings can strongly influence motions and loads of floating WECs. Further guidance on mooring design and implementation is given in ITTC's 7.5-02-07-03.1 [65] and 7.5-02-07-03.4 [65].

2.3.2 Construct: experimental setup and calibrations

In the Construct phase, the individual components are assembled into the overall experimental apparatus and calibrations are performed on the model, environment, and instruments [60]. Given the assembly of components – experimental setup of the equipment and apparatus – will greatly differ from test to test, this section focuses on calibrations.

2.3.2.1 Model calibrations

Dry and wet calibrations of the model may be carried out before and during a test. Dry calibrations may involve: determining the centre of gravity by some means (see [13] for approaches) and determining model mass moments of inertia by measuring the oscillations of a suspended model in air (using for example the bifilar method). Wet calibrations may involve: ballasting the model to obtain the correct waterline, trim, and heel; determining mass moments of inertia by varying mass distributions (if structural loads are being investigated, the full-scale mass distribution needs to be modelled); validating calculated natural periods through in-water tests; inclining tests to measure metacentric height of the model (with and without mooring); free oscillation/decay tests to determine natural frequencies (with and without mooring); or forced oscillation tests, using waves to excite the model to produce RAOs [65, 13, 48]. For descriptions of said parameters and other mass and hydrodynamic properties refer to [13].

2.3.2.2 Environment calibrations

Before testing it is necessary to characterise the test environment. In the Plan and Design phases, users should have obtained details of the wavemeker, the facility general arrangement, and available equipment and instrumentation. The first task in this Construct phase is to characterise the test environment, the wave climate in the working zone and upwave (and current and wind if relevant). There are three approaches: (1) calibrating incident waves at the location of the model prior to installation, (2) use specifications of previously calibrated wave climate, provided they are accurate and data available in the vicinity of model location, or (3) measuring waves upwave of the model, with waves separated into incident, reflected, and radiated components through post-processing. The wavemaker transfer functions should also be checked to ensure appropriate agreement between input and measured waves. If there is noticeable disparity, calibration tests may be carried out in which the transfer functions are adjusted to achieve better agreement of input/measured waves. During wave characterisation and throughout the tests, a phase wave probe, used to obtain wave phasing in relation to model measurements, is usually installed flanking the model at far enough distance away to reduce interference of the model on their measurements.

A relatively wide test area to WEC width is required to avoid reflection and/or blockage effects, especially because WECs typically affect the wave field in a more complex manner than conventional floating structures. Water depth scaling is also important in many cases due to hydrodynamic effects and mooring requirements [64]. Another important consideration is that all wave basins have some degree of spatial and temporal variation of generated waves. The uncertainty of a varied wave field has implications for floating WECs that move around their deployment site, hence some distance from the assumed incident wave measurements [39]. Arrays testing with multiple floating devices is, as one would expect, further implicated by wave variation, where intra-array effects to be quantified can be in the same order of magnitude as the variation of incident waves [38].

At a more technical level, all wave types intending to be measured should be characterised, such as regular, and long- and short-crested irregular waves. Wave analysis should be carried out in the stationary part of the time series, and include time and frequency domain analyses. Details on regular and irregular wave analyses is provided in several ITTC guides [122, 123, 95]. Analysis of short-crested irregular waves should use the Maximum Likelihood Method (MLM) or Bayesian method. The most popular model for directional spreading is a cosine squared cos^{2s} function. See ITTC [124] and [125] for further details on multidirectional wave analysis. If investigating extreme waves in survival tests, see ITTC 7.5-02-07-03.7 [95] for wave generation methods and [126, 113, 13] for analysis techniques.

2.3.2.3 Instrument Calibrations

Calibrating instruments requires establishing a relationship between a measured signal unit (e.g. current, voltage) and the physical quantity being measured (e.g. wave elevation, force, pressure). This process produces calibration factors used to convert measured signals into their engineering units for analysis. Most instruments require calibration before a test and, often, periodically during a test. For example, wave probes require calibrating each day before tests begin, sometimes multiple times a day. Experience and common sense guides if and when instruments need calibrating.

2.3.3 Debug and execute

Now initial runs are carried out and problems addressed in the Debug phase, followed by the Execute phase in which experimental runs carried out. Results from the Debug phase may indicate the need to modify the test program or apparatus as appropriate. The Execute phase begins once the measurement system, model, and environmental conditions are operating as expected, and the dominant parameters contributing to uncertainty are well understood. Now, experimental runs are carried out and the data are acquired, recorded, and stored [60].

Often, the operation of the measurement system is monitored using checks that were designed into the system to guard against unnoticed and unwanted changes or operating conditions. During debugging, and periodically during execution, it is recommended to validate the raw data by examining the time series of all signals. A simple quality control measure is to compare statistical values of similar, or consecutive, records. Large variations may indicate error. In some cases, using analysed rather than raw data can improve error detection by enhancing the error, for example by plotting power to detect erroneous spikes [13]. The techniques of digital signal processing [127] can also be applied to decontaminate signals and manipulate them so as to provide clear output data. The techniques relevant for typical WEC test data typically involve filtering and smoothing. It is also prudent to evaluate uncertainty in measured quantities whenever new information becomes available.

2.3.4 Analyse and report

In the Analyse phase, data are analysed to determine whether, or the degree to which, the results satisfy the defined test objectives and expected outcomes. In the Report phase, which is often carried out concurrently with analysis so is here presented together, users report the test goals and objectives, methodology, results and discussion, and conclusions (Table 2.4 details common reporting and presentation requirements). Outcomes should be presented in a form that maximises the usefulness of the results and any key lessons learned [60]. This phase also involves addressing stage gate criteria if defined.

Table 2.4 Reporting and presentation requirements of a WEC model test.

Section	**Details**
Introduction	Summary and purpose of tests: design statement; test objectives; stage and scale; plan and schedule; type of model and facility; expected outcomes.
Methodology	*Test facility:* specifications, wave generation characteristics, beach and absorption characteristics, pre-calibration of waves; *Model:* specifications and materials, scale calculations and comment on non-similitudes, method of validation (dry and wet), special features, mooring, PTO specification and characteristics *Instrumentation:* sensor specifications, calibration procedures and results, measurement accuracies, position of sensors on model and in basin, mooring details *Environment:* wave heights/periods/directions of regular waves, durations, summary statistics of irregular wave sea states, spectral shapes selected, short-crested sea states selected, calibration evidence of wave climate, run durations *Data acquisition, processing and analysis:* measurement system specifications, description of hardware/software, signal synchronisation, media recording relevant formulae and equations, data reduction methods, analysis techniques with examples of analysed data *Procedures and test matrix:* assumptions, coordinate systems and sign conventions, set-up procedures, tests conducted including model changes, failure modes
Results & Discussion	Typically includes: tabulated and graphical results for each condition (e.g. model configurations, PTO settings, wave types) and key measurands, accompanied by explanatory text (results presented as RAOs, scatter diagrams/matrix, and/or variables against a set of iso-variables, including uncertainty analysis results (table of uncertainty results and error bars on graphical results); key results extrapolated to full-scale, including scaling methods and discussion of scale effects; and comparisons of model-scale and prototype results if available.
Conclusions	Conclusions on whether, or the degree to which, the results satisfy defined test objectives and expected outcomes; any other significant findings; recommendations for further work; and addressing stage gate criteria.

Regarding data analysis, both time-domain and frequency-domain analysis are applied to analyse the raw data obtained in regular and irregular wave tests. Both analyses should be performed on the stationary region of the timeseries. Characteristics of resonant type WECs can be determined through harmonic analysis (see ITTC 7.5-02-07-03.2 [122]). Time-domain analysis includes plotted time series of key parameters overlayed, such as waves, and WEC motions, loads and power. From this, relevant information regarding the characteristics of a WEC can be determined directly, including amplitude and phase of parameters, Response Amplitude Operators (RAOs), signal quality, and signal statistics. An RAO is the ratio between a relevant magnitude (amplitude/height/integral/spectral density) of a WEC response/measurand/performance indicator (motions, power, loads) and a similar magnitude of the characterised incident wave. RAO curves are a common form of results presentation.

Spectral and statistical analyses are carried out for irregular waves (see ITTC 7.5-02-07-03.114 [123]). RAOs of irregular wave results are calculated from the square root of the ratios between spectral density of a WEC performance indicator and incident waves. The method of spectral smoothing should be included in the reporting. Irregular wave results are also often presented in a bi-variate matrix, with significant wave height and energy/peak period, and a relevant performance indicator as the z-axis quantity. Such presentations should include a discussion of the appropriateness of the power (or load) matrix, given the issues outlined above in § 2.3.1.2. For example, if generic spectral distributions were used (JONSWAP, PM, Bretschneider, etc.) rather than actual wave climate data of a specific site that may have multi-mode systems, then the discussion should comment on the expected difference in performance due to the simplifying assumptions. Also, direction-sensitive WECs may require multiple matrices with varied directional spreading sea states tested.

In both regular and irregular waves, capture width ratio should be calculated and presented in the forms described above. Capture width ratio is a non-dimensional quantity that relates absorbed power to input wave power per device width, thus enabling comparison against all other WECs.

2.4 High-level requirements

This section presents the high-level requirements for WEC model tests that are recommended to be addressed at some point in the development path. The requirements are, in roughly chronological order in which they are addressed: proof-of-concept, numerical model calibration and validation, energy capture performance optimisation, survivability, installation and tow-out methodologies, power production validation, and arrays and clusters. The section focuses on objectives and methodology for each requirement. It is based on the guidelines listed below, primarily the ITTC guide [11]. The subsequent section § 2.5 identifies and discusses the guidance coverage and consensus for each high-level requirement, parameter, and procedure. Thus, this section is not heavily referenced but the guidance comparison matrix in § 2.5 and supporting text highlights which guidelines address the various high-level requirements. Some references are however given where needed for clarity or distinction.

- SuperGen project guide (2008), “SG” [12]
- European Marine Energy Centre guide (2009), “EMEC” [13]
- IEA Ocean Energy Systems guide (2010), “OES” [14]

- EquiMar project research reports (2007-2013), "EQM" [15]
- MaRINET 1 project research reports (2011-2015), "MNT" [16]
- ITTC Recommended Procedures and Guidelines (2017), "ITTC" [46]
- IEC TC 114 Marine energy (2019), "IEC" [10]

2.4.1 Proof-of-concept

Table 2.5 Overview of test requirement: proof-of-concept

Objectives	**Methodology overview**
· Validate the working principle of the WEC concept · Provide empirical data for theoretical evaluation · Determine hydrodynamic coefficients	*TRL*: 1-3 *Scale*: 1:50 – 1:100 *Model*: idealised, lightweight, adaptable *PTO*: idealised/generic simulator, simple damping mechanism; passive, fixed step control. *Mooring*: idealised or not simulated *Waves*: Regular *Other tests*: free and forced oscillations *Key parameters*: RAOs of DoFs contributing to absorbed power, hydrodynamic coefficients, PTO characteristics, mooring loads, WEC body loads

Table 2.5 provides and overview of the objectives and methodology for proof-of-concept tests. A simple, idealised, and adaptable model should be used for these tests, within the scale range of 1:50 to 1:100. A simple PTO simulator may be used, but is not essential. Special attention should be paid to minimise scale and laboratory effects. Sharp corners, for example, introduce excessive hydrodynamic damping and thus viscous effects, which are poorly represented by Froude similitude. For more complex WECs with multiple bodies, tests can be carried out separately. The number of degrees of freedom may also initially be restricted.

In many cases visual feedback is sufficient to validate the working principle. Tests should be recorded with video for later inspection. Other instrumentation and data acquisition may not be necessary in these tests; however, if power absorption as well as response data are collected, it should be in a form that can validate and calibrate numerical models being developed concurrently.

Free oscillation tests may be used to determine added mass and damping values at the natural period. If testing with a PTO, sensors and drive mechanisms can be used to measure hydrodynamic coefficients across the range of wave conditions tested. These coefficients, including viscous damping, added mass, radiation damping, and diffraction forces, can improve the depth and breadth of the theoretical evaluation. However to be conducted accurately these tests require rather more attention than wave excitation response monitoring, consequently increasing the allocated time and budget.

All primary design variables should be evaluated during this phase so results are principally used for comparative purposes rather than to produce absolute values. Once again this provides the testing with a robustness in the results that increases confidence levels. These are not exclusively incompatible requirements, however, and the absolute values should be reasonably accurate ($< 30\%$ uncertainty). Scale effects are more difficult to quantify and may result in deviations in the results, for example due to viscous effects. This will be of particular importance to linear theoretical models that do not include drag losses.

Regular wave tests should be carried out. Response characteristics of the WEC are the principle criteria for these tests. ITTC [11] recommends investigating WEC response in waves with periods in the range $5 - 15$ seconds and heights ranging from $0.5 - 5$ meters (full scale values). Sample higher, finite waves should be randomly included to establish higher order differences in the response characteristics.

Results should be presented as RAOs for comparisons.

The following are essential formulae for determining energy capture performance of a typical WEC, based on [11]. Energy capture performance is generally expressed as capture width ratio, a ratio of absorbed device power to the input wave power (wave energy flux) as a function of device width.

Beginning with incident waves, assuming linear wave theory with regular long-crested two-dimensional waves of elevation η_{inc}, angular frequency ω, and water depth h, the regular wave power $P_{W_{reg}}$ per unit length in general water depth is

$$P_{W_{reg}} = \frac{1}{8}\rho_w g H^2 c_g \tag{2.1}$$

where H is the incident wave height, ρ_w the water density, g the gravitational acceleration, and c_g the group velocity. Group velocity c_g is calculated from wave celerity c and wave number k,

$$c_g = \frac{c}{2}\left[1 + \frac{2kh}{\sinh(2kh)}\right] \tag{2.2}$$

where h is water depth

$$c = \frac{\omega}{k} \tag{2.3}$$

with k determined through an iterative process by solving the dispersion relationship

$$\omega^2 = gk\tanh(kh) \tag{2.4}$$

The total average irregular wave power $P_{W_{irr}}$ in finite water depth for a given spectrum is

$$P_{W_{irr}} = \frac{1}{2}\rho_w g^2 \int_0^\infty C_h(\omega) S(\omega) \frac{d\omega}{\omega} \tag{2.5}$$

where $S(\omega)$ is the power spectral density function and $C_h(\omega)$ is a correction that modifies the wave power in deep water to wave power in finite water depth [128]:

$$C_h = \left(1 + \frac{2kh}{\sinh(2kh)}\right)\frac{k_0}{k} \tag{2.6}$$

where k_0 is the wave number in deep water. For a given spectrum, the significant wave height H_{m0} is

$$H_{m0} = 4\sqrt{m0}, \tag{2.7}$$

and various wave period statistics of energy period T_e, zero up-crossing period T_z, and mean wave period T_{m01} are respectively:

$$T_e = \frac{m_{-1}}{m_0}, T_z = \sqrt{\frac{m_0}{m_2}}, T_{m01} = \frac{m_1}{m_0} \tag{2.8}$$

with the spectral moments defined as

$$m_n = \int_0^\infty S(\omega)\omega^n d\omega \tag{2.9}$$

where $n = -1, 0, 1, 2, \ldots$

If P is the mean power absorbed by the WEC (calculated by multiplying the PTO kinematic and dynamic quantities, e.g. flow rate and pressure, or velocity and force) then the capture width ratio is defined by

$$C_W = \frac{P}{P_W B} \tag{2.10}$$

where B is the characteristic dimension of the WEC (often device width) and P_W can be for regular or irregular waves. C_W is a dimensionless number relates the amount of power absorbed by the WEC to the amount of wave power as a function of its width. While it is considered the hydrodynamic efficiency [99], in fact C_W can be greater than 1, as resonating WECs can concentrate energy, drawing in more energy than what is directly in front of them [129].

2.4.2 Numerical model calibration and validation

Table 2.6 provides and overview of the objectives and methodology for numerical model calibration and validation tests. There are many numerical tools for modelling WEC systems and subsystems. It remains necessary however to calibrate and validate these numerical models with empirical data. Such tests require accurate measurements of various hydrodynamic and PTO parameters, thus increasing the time and cost of the test program. Collected data should be in a form that can calibrate and validate both frequency and time domain numerical models. Ideally, these models are developed as *wave-to-wire* models, which model

Table 2.6 Overview of test requirement: numerical model calibration and validation

Objectives	**Methodology overview**
· Collect empirical data to calibrate/validate numerical models, so they can be used to predict prototype behaviour and performance · Accurately measure hydrodynamic coefficients	*TRL*: 1-4 *Scale*: 1:10 – 1:50 *Model*: idealised, lightweight, adaptable *PTO*: idealised/generic simulator, simple damping mechanism; passive, fixed step control. Numerical model may be calibrated without PTO. *Mooring*: idealised or not simulated *Waves*: Regular, irregular long- and short-crested *Other tests*: free and forced oscillation (to determine hydrodynamic coefficients and natural period) *Key parameters*: RAOs of DoFs contributing to absorbed power, hydrodynamic coefficients, PTO characteristics

the entire energy conversion chain from the hydrodynamics to the electricity feeding into the grid [130]. To calibrate numerical models, users may compare timeseries' of numerical and experimental data, such as waves, motions, pressures, and forces. For validation, users may compare statistical quantities such as means, standard deviations, and distributions.

The scale range is typically 1:10 to 1:50. A PTO simulator may or may not be included in these experiments depending on the scale and the complexity. The numerical model may be calibrated without a PTO. If a PTO simulator is included, it should be carefully characterised so that its effect can be taken into account in the wave-to-wire model. In some cases, it may be difficult or practically impossible to build an exact Froude-scaled model of the WEC system because of, for example, air compressibility in an OWC chamber or due to material stiffness for flexible WECs. In such cases, an approximate experiment model may still be built in order to calibrate and validate the numerical model. For calibration and validation, the characteristics of the experimental model shall be considered in the wave-to-wire model. Once validated, the numerical model may be used to predict the behaviour and performance of a full-scale prototype WEC.

To obtain hydrodynamic coefficients (e.g. added mass, radiation and diffraction forces, viscous damping) free oscillation/decay tests are carried out. Such tests may also characterise mooring stiffness. WEC response should first be measured in small regular waves to determine the accuracy of the numerical model in linear conditions. Thereafter, increasing wave amplitude may provide a measure of the numerical model limitations, and therefore its domain of validity. ITTC [11] recommends the wave conditions in Table 2.7, taken from [131].

For direction dependant WECs, different wave headings should be investigated. Eventu-

Table 2.7 Suggested set of regular waves for numerical model calibration and validation tests. If WEC response is dependent on wave direction, these waves may be run with headings that are appropriate for this device and location. Spectra parameters should be appropriate for the location of the device.

T (s)	H_1 (m)	H_2 (m)	H_3 (m)
6	0.5	1	2
7	0.5	1	2
8	0.5	1	2
9	0.5	1	2
10	0.5	2	4
12	0.5	3	6

ally, long-crested irregular waves should be investigated in order to compare numerical and experimental models under realistic wave conditions. Again, ITTC [11] recommends using wave conditions of Table 2.8, using the Bretschneider spectrum. If wake response is dependent on wave direction, directional spreading should be taken into account. A spreading parameter of s = 25 may be used.

Table 2.8 Suggested set of irregular waves for numerical model calibration and validation tests. A generic spectrum may be used. If WEC response is wave direction dependent, a spreading parameter of s=25 may be used.

T_p (s)	H_s (m)
6	1
7	2
8	3
10	4
12	5

Noted, for calibration and validation knowledge of the incident wave elevation at the location of the model is critical. It should be measured at the deployment position prior to the model being deployed, during wave calibration tests.

2.4.3 Energy capture performance optimisation

Table 2.9 provides and overview of the objectives and methodology for energy capture performance optimisation tests. These tests are extensions of previous tests (i.e. proof-of-concept, and numerical model validation and calibration), now focusing on optimising energy capture performance in realistic waves. Efforts are directed toward analysing and developing the PTO system, and the mooring system if it is fundamental to energy conversion.

The typical model scale range is 1:10-25, and the same model may be used as that used in the proof-of-concept and numerical model validation and calibration tests. Model design should allow for different configurations of geometry, kinematics, and dynamics that can

Table 2.9 Overview of test requirement: energy capture performance optimisation

Objectives	**Methodology overview**
· Investigate design variables to optimise absorbed power in relevant wave conditions · Test and develop PTO control strategies · Validate concept in more extensive wave conditions · Verify mooring design	*TRL*: 1-3 *Scale*: 1:10 – 1:25 *Model*: idealised, lightweight, adaptable *PTO*: full-scale representative simulator; fixed step or active control *Mooring*: idealised or Froude-scaled *Waves*: irregular long- and short-crested *Other tests*: free and forced oscillation (to determine hydrodynamic coefficients and natural period) *Key parameters*: RAOs of DoFs contributing to absorbed power, PTO characteristics, power matrix/scatter diagrams, Mean Annual Energy Performance

quickly and easily be changed. This provides the capability of a physical model parametric study, beneficial to optimisation. A full-scale representative PTO simulator should be included. The PTO simulator should realistically represent the damping characteristics of the captor (the part that interacts directly with waves) and its relative motion to some reaction mass. PTO characteristics shall be measurable, controllable, and repeatable. If these requirements cannot be achieved at the selected scale, the scale shall be increased or another approach selected (e.g. relying on the numerical model for optimisation).

Because models may be physically larger in these tests, a more sophisticated PTO simulator can be implemented. Additionally, on-board sensors and equipment can be accommodated without adversely affecting the model behaviour. While these options are not essential, it could prove advantageous in terms of development progress through the TRLs. The primary requirement for all configurations is that the characteristics of the final PTO are reproduced. This statement assumes the PTO is known, which might not be the case. Experience has shown that unless a very complex system is to be used a high-quality energy dissipater provides a generic representation suitable for most options. The exception is if the PTO will include a control feedback option that attempts to tune a WEC to the incoming waves as a time domain system. For such experiments a more complex PTO model is required.

Regarding control, the minimum requirement is that the PTO characteristics are manually adjusted in stepped values. These adjustments should provide an accurate determination of the relationship between energy capture motions and absorbed power. Automated PTO control is, however, better. The goal of a control system is to change damping settings in real-time in order to tune the WEC to incoming waves, thus optimising absorbed power. Examples of such control systems include electro-magnetic motors (point-absorber) or butterfly valves (OWC). The control strategy, or strategies if investigating the efficacy of different types, shall be representative of the full-scale control system. It is recommended to quantify the similarity between model-scale and expected full-scale PTO control.

Quantifying absorbed power requires measuring both the motions of the primary converter and its resulting force across the PTO. That is, mathematically, $Power = Force \times Velocity$. By equipping the PTO with a force or pressure transducer, and measuring the captor motion with, for example, an LVDT (point absorber) or wave probe (OWC), instantaneous absorbed power can be calculated for each PTO setting. Force and velocity parameters can be plotted to verify that a representative PTO simulator has been selected. Noted, PTO simulators often do not have the same constraints as that of the full-scale design, such as end stops and decoupling. Therefore, the primary goal of the PTO simulator is to provide environmental load data, including extremes, from which the full-scale PTO rating can be derived.

Unless the mooring plays a crucial role in energy capture performance, investigating mooring options is typically reserved for survivability tests. If in place, mooring loads and extensions should be monitored throughout performance tests.

Tests may initially be carried out in regular waves, to verify variables of interest, then in irregular waves for the majority of the test program. Otherwise, tests may be carried out only in the irregular waves. Previous tests (i.e. Requirement 2 or 3 above) may inform the selection of wave conditions for these optimisation tests. Classical spectral shapes or measured data may be used. JONSWAP spectrum may be used with a frequency spreading factor matching that of the target deployment location of the WEC. If the location is not known, the Brettschneider spectrum may be used. Whichever the source of wave conditions, it is important to cover a spread of conditions such that the annual power production figure can be extrapolated.

It is not necessary to test all of the scatter diagram elements of a selected wave resource. The offshore industry recommended practice is to select 15–20 of these H_s/T_p combinations such that the overall behaviour of a structure can be determined. This strategy is adopted for evaluating WEC performance across the spectrum of expected wave conditions. When selecting elements to test within the scatter diagram, it is recommended to select elements along constant lines of significant wave height and peak period [13]. This allows extrapolation graphs to be drawn up such that, if required, all elements of a bivariate table (power matrix) can be computed. These graphs often show a deterministic relationship between changes in sea states, with no discontinuities, thus enhancing confidence in the extrapolation procedure. (See [13] for example of graph). It is noted that a WEC typically produces more power in higher waves, but with diminishing returns due to decreasing efficiency.

WEC design variables should be sequentially changed to obtain a power matrix for each configuration, with this data used to assess options for optimising the device. Performance sensitivity to the wave resource should also be investigated, including wave direction, crest length, and spectral profile. If the WEC energy capture is dependent on wave direction, variation in approach angle of generated waves will reveal the effect on performance due to wave direction. Moreover, directional spreading will reveal the effect on performance due to long- and short-crested seas. The directional spread should match the target deployment location, if known. Otherwise, a spreading parameter of s=25 may be used. For resonator type WECs, it is also important to vary classical spectra profiles if data from the deployment location are not being tested. Model tests in irregular waves should normally be carried out for a duration corresponding to at least 30 minutes at full-scale (250-500 waves) in order to gain statistically valid results (see ITTC 7.5-02-07-01.1 [124] for further guidance on modelling irregular waves).

Again, the requirement of these tests is to consider all identified relevant device variables and investigate their influence on overall WEC performance. Without this information, feedback loops between the waves, WEC hydrodynamics, and power conversion would not be known. As such, results can be concatenated and presented in a way that clearly shows the relations between performance indicators. From this inductive inference process it should be possible to verify the theoretical working principle. Combining these experimental observations with numerical and theoretical models, the optimisation can begin in earnest, with the primary goal being to maximise the techno-economic performance of the WEC. In practice, this optimisation requires balancing Mean Annual Energy Production (MAEP) with operational factors, such as survivability, installation, and maintenance.

2.4.4 Survivability

Table 2.10 Overview of test requirement: survivability

Objectives	**Methodology overview**
· Establish the seaworthiness and survival characteristics of a WEC and its subsystems, especially the mooring · Identify and validate fatigue, ultimate and accidental limit states, and failure modes	*TRL*: 1-5 *Scale*: 1:20 – 1:100 *Model*: idealised, lightweight *PTO*: realistic; able to be fully open and blocked *Mooring*: realistic *Waves*: extreme waves (regular, irregular, focused) *Other tests*: survival mode, if separate from operational mode; wave slamming *Key parameters*: RAOs of all DoFs, loads (mooring, cross-sectional, local)

Table 2.10 provides and overview of the objectives and methodology for survivability tests. Two fundamental design drivers for all WECs are (1) power performance in operational conditions and (2) survival in extreme conditions. Survival tests are therefore central to developing WEC technology.

Survival tests can be carried out from TRL 1-5, typically at a model scale ranging from 1:20 to 1:100. Model size tends to be small due to limitations in generating extreme waves (relative to the model) and basin boundaries. It is recommended, however, to test a medium-scale model after small-scale tests in an appropriately sized wave basin. Testing a small-scale model in a medium basin would still be recommended.

Data from previous tests can be used to design moorings and survival strategies for subsequent survival tests. Similarly, earlier tests can provide qualitative information useful for defining environmental conditions. In addition where appropriate the PTO should be tested both in the fully undamped condition and in the fully locked condition in order to simulate typical failure scenarios which could result in excessive body motions and/or end stop problems. Note that it may be challenging to include an appropriate PTO simulator at the smallest scales.

Survival tests are designed to evaluate WEC behaviour under survival conditions, including structural integrity and the mooring system dynamics. These tests must provide statistically significant distribution of motion and loads exerted on the WEC body and/or captor, the PTO, moorings, and foundations for fixed or gravity structures. The distribution should cover Ultimate Limit States (ULS) and Accidental Limit States (ALS) conditions for the target deployment site. It implies that metocean data of the target deployment site is known beforehand and that survival conditions for both ULS and ALS have been defined.

Selecting these conditions is a difficult and somewhat unresolved issue. Not only are conditions site dependent, but the largest wave does not necessarily cause the extreme response and loads [113], and using focused waves may not be the most appropriate approach for investigating the survivability of WECs. Indeed, a series of sub-maximum height waves near device resonance may cause larger forcing on the WEC structure and mooring relative to the largest wave [105]. Moreover, due to widely diverse WEC designs, selecting ULS and ALS conditions is not obvious for WECs with unique working principles.

WEC responses to ULS and ALS conditions depends on whether it has been designed to withstand the environmental forcing, or designed to have an alternative mode of operation for survival conditions, known as survival strategies or mode. In either case, the goal remains of determining a statistical representation of structural and mooring loads across a broad spectrum of environmental conditions. ULS includes testing the intact WEC, whereas ALS requires testing different failure modes with one or more mooring lines disconnected during experiments to simulate line breaking scenarios. Note that survival conditions for ALS maybe different to those for ULS. ULS and ALS conditions should be provided by the WEC developer. If ULS and ALS are not provided, [113] offers guidance on determining appropriate conditions for such tests.

Another method involves testing a range of conditions and combinations of spectral shapes through a systematic sweep approach [13]. This involves selecting bins from a wave scatter diagram, based on the Bretschneider spectrum. From the worst cases a set of adjusted JONSWAP spectra offering increasing peak factors will reveal the sensitivity of the device to wave steepness. Twin peaked and bimodal seas can contribute to these and the previous survival tests. Short-crested irregular waves should also be included in the test program.

Other environmental parameters, such as tides, current, and wind (e.g. see [101]), should be reviewed, and if regarded as important, investigated in survival tests.

Survival tests are typically carried out for three hours at full-scale. This is approximately 30-45 minutes at model-scale. Theses long duration tests may restrict the number of sea states investigated due to time and cost constraints. Thus, the selection of environmental conditions is especially important to obtain statistically significant results that are representative of expected full-scale conditions.

It is recommended to conduct tests along the wave breaking limit, and test the model in each of the six degrees of freedom natural periods. This is achieved either by angled wave generation or rotating the model and its mooring. Short-crested irregular waves, while they do not tend to induce maxima, tend to excite all the motions simultaneously.

Survival tests are crucial, as they generate design data for full-scale subsystems, including the mooring, PTO, and structure of the WEC body. This data can be used to validate nonlinear numerical models to facilitate the full-scale design process.

2.4.5 Installation and tow-out methodologies

Table 2.11 Overview of test requirement: installation and tow-out methodologies.

Objectives	**Methodology overview**
· Validate the installation and tow-out methodology · Provide distribution of motions and relevant loads (towing lines)	*TRL*: 4-5 *Scale*: 1:10 – 1:25+ *Model*: idealised, lightweight *Waves*: irregular (site-specific) *Key parameters*: RAOs of all DoFs, towing line loads

Table 2.11 provides and overview of the objectives and methodology for installation and tow-out methodologies tests. A key operation in the implementation of a WEC technology is the installation and tow-out to its deployment site. This operation is often high-risk, so

model-scale tests may be carried out to validate these procedures and reduce the risks.

These tests are typically carried out in the design validation stage (TRL 4-5), at a model scale range between 1:10 and 1:25. An appropriate test program shall be defined based upon a description of the installation and tow-out methodology provided by the WEC developer. Tests should include irregular waves corresponding to the site-specific wave resource if known, typically in operational conditions. Tests involving failure modes and/or sea conditions greater than operation conditions may be considered.

2.4.6 Power production validation

Table 2.12 Overview of test requirement: power production validation

Objectives	Methodology overview
· Validate power production at target deployment site	Same as Energy Capture Performance Optimisation tests, except using actual wave conditions measured/modelled at the target deployment site.

Table 2.12 provides and overview of the objectives and methodology for power production validation tests. These tests are similar to the Energy capture performance optimisation requirement, except that actual wave conditions from the target deployment site wave resource are used. The developer provides the wave conditions to be tested, based on in-situ measurements or sophisticated numerical models. For each condition, the directional frequency spectrum shall be provided. Tests in irregular waves should be carried out for at least 30 minutes full-scale to gain statistically valid results. Guidance and procedures for the laboratory simulation and measurement of irregular short-crested sea states is provided in ITTC 7.5-02-07-01.1 [124].

2.4.7 Arrays and clusters

Table 2.13 Overview of test requirement: arrays and clusters

Objectives	Methodology overview
· Investigate behaviour of WEC array · Validate WEC array power performance · Validate/calibrate numerical model of WEC array	*TRL*: TBD *Scale*: ~1:20 – 1:100 (TBD) *Models*: idealised, lightweight, adaptable *PTO*: idealised or realistic *Mooring*: idealised or realistic *Waves*: regular, irregular *Key parameters*: RAOs of DoFs contributing to absorbed power, PTO characteristics, q-factor

Table 2.13 provides and overview of the objectives and methodology for arrays and clusters tests. Future wave energy installations will likely include several to tens or hundreds

of proximal WECs operating in an array or farm. However, there is limited research and experience in testing arrays, both at the model and prototype scale. Guidance on these tests is therefore limited. Consequently, it is not clear at which TRL stage these tests are required and at which model scale. Neither researchers nor developers have much practical experience in this regard. Thus WEC array behaviour may be evaluated by numerical modelling.

A key parameter for these tests is determining the q factor, which relates the total power captured by the array to the power captured by a single isolated WEC multiplied by the number of WECs in the array (q factor greater than one indicates constructive interference) [132, 133]. For an array with many WECs installed, the interaction of WECs may be inferred from tests involving a limited number of devices. An array can consist of individual devices separately moored, or a cluster of devices on the same mooring. Due to cost and scale constraints related to basin boundaries, it may not be possible to evaluate experimentally the behaviour of arrays involving a large number of WECs. Arrays testing may only be performed in basins of a reasonable width relative to the wavelengths being produced.

Whichever system is under investigation, wave field spatial and temporal variations must be taken into account [38, 39]. Given there is no physical way to separate wave components, wave field variations must be accounted for in the analysis, which requires multiple wave measuring points.

While the literature of WEC arrays model testing is not extensive, recent research may be informative [134, 135, 136, 68, 137, 70, 138, 139, 71].

2.5 Guidance comparison and gaps

This section evaluates WEC model test guidelines, identifying and discussing the degree of guidance coverage, consensus, and gaps. For this analysis we created a guidance comparison matrix (Table 2.14). This matrix is based on text search queries of each parameter and procedure that is (or is not) included in the guideline documents (some guidelines include multiple documents, e.g. EquiMar [15], MaRINET [16], and ITTC [11, 17]). The parameter/procedure structure is based on the ITTC WEC guide 7.5-02-07-03.7 [11].

For each parameter and procedure, the coloured cells in Table 2.14 represent the number of occurrences of relevant words or phrases in the guideline document(s). NVivo was used as the text search software to find said word/phrase occurrences. For example, search terms for 'Staged development / TRL' were: "stage* dev* OR structured dev* OR phase dev* OR TRL OR technology readiness level". The black cells correspond to about 300 occurrences, the white cells zero occurrences. This text-search approach is somewhat crude, the main limitation being that the guideline documents have different numbers of words. The approach, however, does provide a more 'objective' means to compare the degree of coverage of

Table 2.14 Guideline comparison matrix. For each parameter and procedure, the coloured cells represent the number of occurrences of relevant words or phrases in the document(s) of included guidelines (see notes below). NVivo was used as the text search software to find said word/phrase occurrences. For example, search terms for 'Staged development / TRL' were: "stage* dev* OR structured dev* OR phase dev* OR TRL OR technology readiness level". The black cells correspond to about 300 occurrences, the white cells zero occurrences.

Parameters and procedures	[12]	[13]	[14]	[15]	[16]	[46]	[10]
Parameters							
Staged development / TRL							
Test facilities							
Model parameters & scale							
Envionmental parameters							
Mooring systems							
Quality & accuracy of results							
Requirements:							
· Experimental proof-of-concept							
· Numerical model calibration / validation							
· Energy capture performance optimisation							
· Survivability							
· Installation and tow-out							
· Power production validation							
· Arrays and clusters							
Procedures							
Model construction & installation							
PTO modelling & control							
Wave generation							
Environment calibration							
Instrumentation & model calibration							
Data acquisition							
Data analysis & reporting							
Uncertainty analysis							
Design of experiment							

[12] = "SG" = SuperGen project guide (2008)
[13] = "EMEC" = European Marine Energy Centre guide (2009)
[14] = "OES" = IEA Ocean Energy Systems guide (2010)
[15] = "EQM" = EquiMar project research reports (2007-2013)
[16] = "MNT" = MaRINET 1 project research reports (2011-2015)
[46] = "ITTC" = ITTC Recommended Procedures and Guidelines (2017)
[10] = "IEC" = IEC TC 114 Marine energy (2019)

each parameter/procedure between and among the guidelines, and identifies gaps and areas requiring further technical investigation and refinement.

The following subsections discuss, first for parameters followed by procedures, the results of this guideline comparison matrix, in terms of the degree of coverage, consensus and differences of guidance, and guidance gaps requiring technical investigation and refinement. The gaps have largely been identified through reviewing recent studies and related literature on WEC model tests and WEC development in general. Noted, the MaRINET 2 project carried out a review of guidelines for the wave energy industry, which identified guidance gaps on a broader, sector level [50]. This report highlighted a need for additional standards on a number of topics, including the PTO subsystem (scaling, simulation at model scale, and performance prediction/assessment) and moorings systems. In particular, there is a lack of guidance on how to transition between TRL levels, dealing with progressing from controlled laboratory setting to the uncontrolled marine environment.

2.5.1 Parameters

Staged development / TRL. Guidance on this aspect of model tests is substantial, with consensus that testing and developing WECs requires this TRL staged-based approach. Points of difference are in the demarcation of TRLs and development stages. ITTC suggests TRL 4-5 are addressed in Stage 2; OES and IEC suggests Stage 2 is TRL 4 only; and EMEC does not make specific reference to TRLs in stages, instead setting out guidance according to stages only. A gap is the omission of Technology Performance Levels (TPLs) in all guides. Some researchers are arguing the TRL approach should be integrated with a TPL scale [140, 141, 142, 143, 54, 144, 47]. The TPL scale focuses on performance as a combination of social, environmental and legal acceptability, power absorption and conversion, system availability, capital expenditure (CapEx) and operational expenditure (OpEx). That is, a focus on improving LCOE at low TRL, cost, and risk. Adoption of a TRL/TPL matrix may introduce different or additional requirements for WEC development, to be incorporated into future guidelines.

Test facilities. The characteristics of test facilities for WEC model testing are well-covered and described, with consensus on the use of smaller wave basins and towing tanks for Stage 1 tests (e.g. proof-of-concept, numerical model validation, optimisation), and larger basins and tanks for Stage 2 tests (e.g. survivability, installation and tow-out power production validation).

Model parameters and scale. Guidance here is substantial. Froude similitude is accepted as the scaling law for almost all model-scale tests, and it is agreed that in general a larger scale more accurately represents prototype behaviour. MNT provide especially detailed descriptions on model parameters and scale. The key drivers for model scale selection are well-known: WEC similitudes, development stages and test goals, and test facility characteristics such as boundaries and wave generation. It is agreed that modelling a PTO system is a key challenge for all WEC model tests. Scale effect issues related to air compressibility, friction, and viscous effects are reasonably well-discussed and some guidance is available on methods to account for scale effects. However, technical investigation is required for other kinds of scale effects, especially due to nonlinear interactions between waves and PTOs (which Chapter 4 deals with). The stage at which a PTO simulator is to be implemented, and its fidelity, differs somewhat between guides.

Environmental parameters. Guidance on environmental parameters is also substantial. There is consensus on which parameters are relevant for which test stages, and how they may be characterised and simulated in the laboratory. A gap is in the requirement to replicate realistic, site-specific wave climates, including wave-current interactions and the uncertainty in neglecting these [101]. Another gap is a neglect of methods to investigate the uncertainty arising from variation of frequency and directional distributions associated with the same H_s/T_p values of irregular sea states (i.e., power matrix uncertainty).

Mooring systems. Some guidance is available on the various types of WEC mooring systems, from catenary to taut to multi-element systems, and this guidance has improved over time. In particular, ITTC [11] has drawn on mooring-related guidance from other ITTC guides for offshore structures (e.g. [65]). A gap is in cases where WECs incorporate moorings that are dissimilar to those used by other offshore applications [82, 50]. Due to different operational objectives of WECs and mature offshore structures, and immature design of WEC mooring systems, there is a substantial gap in methods for physical modelling. This gap may be addressed through systematic investigations into the practical bounds of physical modelling adapted from mathematical models of WEC mooring systems outlined in [82]. This may produce guidance that addresses three categories of WEC mooring systems: (1) passive mooring, where the sole purpose is station-keeping; (2) active mooring, where in addition to station-keeping, the mooring system also has a significant influence on the dynamic response and power extraction of the WEC; and (3) reactive mooring, where the mooring system provides reaction forces for the WEC to extract energy from the waves. A further area lacking guidance is in measuring multi-component hydrodynamic loads on fixed WECs (Chapter 3 describes such a measurement procedure).

Quality and accuracy of results. These parameters are not as well-covered as other aspects of model testing. EQM sought to address this gap, and their main guide [42] provides some description of and methods to account for the parameters that affect quality and accuracy of results. Further work is needed in this area, such as that presented in Chapter 3. Moreover, there is limited guidance on procedures or limiting criteria to avoid, compensate, or correct for other significant sources of uncertainty that affect the quality and accuracy of results, such as scale effects and laboratory effects. Chapters 4 and 5 address these gaps.

For the high-level ***Requirements***, while most guides make reference to the requirements as they are defined in this work, this aspect of the guidance is not as well covered compared to the general considerations. There are also differences in the guidance structure regarding test requirements. EMEC and OES have a structure that specifies requirements within define test stages (Stage 1 and 2 for laboratory tests); ITTC specifies the requirements as being tests in themselves, which this work is based on; and IEC proposes a new structure, one based on a twin-track approach following the development stages and also goal-oriented requirements of power performance, kinematics and dynamics in operational environments, and kinematics and dynamics in survival environments. The following paragraphs discuss the requirements in Table 2.14 separately.

Experimental proof-of-concept. There is consensus on the first major step in WEC development being the experimental proof-of-concept through relatively simple hydrodynamic model tests, with the goal of validating the working principle. It is also agreed that these tests may use a simplified, idealised model with limited degrees of freedom, tested in regular waves under a limited set of wave frequencies and small to moderate wave heights. Some minor discrepancies include EMEC recommending testing five reference irregular wave tests; OES-IEA recommending a sample set of steep waves, as well as measuring hydrodynamic coefficients; and ITTC setting out specific values for wave parameters (0.5-5 meter and 5-15 second regular waves).

Numerical model calibration and validation. Guidance here is relatively lacking. ITTC is the only guide that specifies specific tests for this requirement, while other guides imply that tests in Stage 1 and 2 should be in the form such that they are useful to calibrate and validate numerical models. ITTC suggests a set of regular and irregular waves (Tables 2.7 and 2.8). A comprehensive review of has been undertaken on the wide range of numerical modelling techniques available to WECs, and which are most appropriate for a particular WEC concept and modelling objective [36]. A major concern raised in this work is the need for empirical validation. Using the modelling techniques outlined in this work, a systematic series of experiments could be carried out in order to identify the physical modelling practicalities, issues, and accuracy, and in this way, the best practice could be improved for tests dedicated to calibrating and validating the wide range of numerical models. The guidance may include requirements for both linear and nonlinear models in the time-, frequency- and spectral-domains. Another gap is in the modelling of extreme events, both experimentally and numerically [126]; technical investigation and refinement is needed to develop best practices in these areas.

Energy capture performance optimisation. It is well-established that experimentation is central to energy capture performance optimisation of WECs. There is consensus on the primary objective of these tests: to optimise the energy capture performance in relevant conditions. There is also consensus on when to perform optimisation tests which typically occurs at the end of Stage 1 testing, the scale range to be tested in, the use of a high-quality full-scale representative PTO simulator, type of waves (irregular, realistic waves), and test duration (30 minute full-scale equivalent). ITTC offers some generic wave conditions for optimisation tests (Tables 2.7 and 2.8). It is agreed that special attention is directed toward the analysis and development of the PTO system, and the mooring system if it is fundamental to energy conversion. Moreover, these tests are considered extensions of previous tests (proof of concept and numerical model validation and calibration).

Survivability. Guidance is reasonably well-covered, with some guides offering substantial information about the model and environment parameters relevant for these tests. There is consensus on the primary objective of these tests: to establish the seaworthiness and survival characteristics. In addition, consensus is apparent for which stage to carry out these tests, key measurements, test durations (3 hours full-scale), and specific tests for concepts with a separate survival mode. Some differences include ITTC recommending Ultimate Limit State (ULS) and Accidental Limit State (ALS) wave conditions, where ULS tests are for an intact WEC and ALS tests are for a damaged WEC mooring, for example due to line breaking. EMEC recommends to identify the most demanding sea state, which is the sea state that causes the most extreme motions and loads, through a systematic sweep of wave conditions and spectral shapes. Guidance gaps include recognised challenges in defining wave conditions for survival tests, and further technical investigation is required to improve best practices to clarify which combination of WEC configuration and wave conditions will likely produce maximum motions and loads. i.e. PTO fully damped, or fully open, or partially damped. Noted, the specific number of survival sea states is not defined by any guideline. Selecting survival sea states is a somewhat arbitrary endeavour, so numerical tools can facilitate the selection.

Installation and tow-out. This requirement has the least amount of WEC-specific guidance, with only ITTC recommending tests; other guidance is however available in offshore structures [65]. The lack of guidance on this aspect of WEC testing is likely due to the lack of full-scale operational experience in the wave energy industry, or the lack of it being integrated into model-scale guidance. With limited full-scale WECs operating in the ocean, knowledge feedback loops are similarly limited. These tests, however, may prove to be crucial in the success of a technology. A recent example illustrates this criticality, whereby a full-scale WEC technology sank during tow-out to its deployment site [28].

Power production validation. Only ITTC specifies the requirement of power production validation tests, while some of guides imply that the objective of validating power production is important, and should be carried out in Stage 2. There is consensus on the necessity to validate power performance at the target deployment site. While it is recommended to use actual wave conditions from the target deployment site, treatment of obtaining such data is lacking in the guidelines considered in this work. However, EMEC refers to another of its guides which defines site characterisation methodologies [145]. The IEC also has a technical specification detailing wave energy resource assessment and characterisation (IEC TS 62600-101:2015). The potential to use wave modelling data is not discussed.

Arrays and clusters. Arguably the guidance is most lacking in terms of arrays and clusters, though most guides mention arrays. There is consensus on the test objectives, however, which are to investigate the behaviour of the array of WECs and validate the power performance in terms of q-factor. But it is still not clearly defined when such tests should be performed in WEC development. Issues with non-uniform wave fields [39] and other uncertainties [38] have been investigated but not yet incorporate into guidance. Some outstanding questions to be address are, can modelling a limited number of WECs in an array, or using symmetry against basin boundaries, accurately predict the behaviour of a large number of WECs in a full-scale array? What influences does the facility boundaries have on array model test results?

2.5.2 Procedures

Model construction and installation. These procedures are well-covered by most guides, adapting guidance from related maritime fields. Construction materials for WECs are similar to most ocean structures (e.g. fibreglass, wood, plastics, and light alloys). There is consensus on the importance of hydrostatics of a model when considering its construction, and the importance of installing the model carefully to ensure it has the correct heading, hydrostatics (draft, trim, CoB, etc.). There is a potential gap in guidance for construction related procedures for sophisticated, actively controlled PTOs in later stage tests. MNT addresses some of these issues.

PTO modelling and control. All guides provide some information about PTO modelling and control, and ITTC provides an overview and categorisation of the main types of PTO systems (direct drive, hydraulic systems, pneumatic systems, overtopping). There is consensus on the said challenges of PTO modelling, and that a crude/simple/generic PTO can be used for early stage tests but later stage tests require increasingly realistic PTOs with control capability. Gaps include procedures for PTO subsystem or dry bench tests (MNT documents D2.25 and D4.2 provide information on this); validated extrapolation procedures for various types of PTOs; and procedures to implement various control strategies, for example latching, passive, or reactive [47, 146, 147]. Another gap is guidance on open-loop tests for system identification with active or reactive control.

Wave generation. This procedure is well covered by SG and MNT, and in many other related maritime fields guides and reference books.

Environmental calibration. Procedures for calibrating the test environment are well-contrived and covered by all guides, and there is consensus on the importance of characterising the environmental conditions at the model deployment position without it installed. MNT provides detailed descriptions for more sophisticated wave field measurement techniques. Wave reflection characterisation is not well-described in the considered guides, but these procedures are easily found in prominent papers [148] and books [92].

Instrumentation and model calibration. Similarly, the procedures for instrument calibration are well-known and widely used. Regarding model calibration procedures, such as dry and wet calibrations, these too are well-described and based on procedures developed and proven by the offshore oil and gas industry.

Data acquisition. All guides mention to some extent data acquisition procedures, and the required hardware and software. This aspect of model testing is generally well-known with detailed descriptions. It is agreed that the main measured quantities are all degrees of freedom (DOF) motions, PTO forces and displacements/velocities, pressure/flow or overtopping rates, and mooring forces where relevant.

Data analysis and reporting. Data analysis techniques, in both time and frequency domain, are well-described and consistent between guides. Recommendations for what is required in test reporting generally converge.

Uncertainty analysis. There has been a gradual realisation of the importance of uncertainty analysis in model tests, with later guides placing more emphasis on it and describing procedures. EQM and ITTC provide the most guidance on uncertainty analysis procedures, with ITTC recently publishing a specific guideline on uncertainty analysis for WECs [17]. However, the guidance is lacking in pre-test or general uncertainty analysis, and alternative uncertainty propagation methods such as the Monte Carlo Method (which Chapter 3 addresses). The MCM has been demonstrated to be an accurate uncertainty propagation method for nonlinear systems and where uncertainty magnitudes are of a similar order to measurand magnitudes [60, 118].

Design of experiment. This aspect of WEC model tests is not well-covered in the guidance, with only EQM providing some guidance on DoE procedures. However, general DoE procedures for all experimentation is developed and can be implemented in most applications.

2.6 Conclusions

Hydrodynamic model test experiments are integral to early-stage WEC development. Model tests, however, are a demanding task; they require significant effort, considerable money, and not a small degree of technical experience and knowledge to plan, design, construct, debug, execute, analyse, and report. Despite challenges and drawbacks, the advantages of model tests still justify their costs in time, money, and resources, and their central role in early-stage WEC development. This is especially true when compared to the alternative of fabricating a prototype for deployment in open water, which is far more cost- and time-intensive. Additionally, while numerical tools are being increasingly developed for and used in wave energy, becoming increasingly user-friendly and accurate, they still rely on experimental data to be calibrated and validated. Therefore, the role of model tests in early-stage WEC development will likely remain as important in the next decade as previous decades.

Despite substantial progress in developing technical guidelines and literature on hydrodynamic model test experiments of WECs, there is a continued need to develop WEC-specific model test best practices. While WECs are similar to other maritime structures, suggesting knowledge and guidance developed in mature maritime industries may be used for WEC development and testing, WECs typically have two fundamental differences: they maximise motions (except in storms) and use a PTO system. WEC-specific guidance is thus necessary, as using unspecific guidance increases technical and financial risks. Recognising this, over two decades of efforts developing technical guidelines and literature has culminated in international guidelines on WEC model tests, informed by a cohort of experts in the field. Despite this achievement, the wave energy industry is still immature, with many WEC designs under RD&D due to a lack of proven techno-economic solutions. This suggests the circular relationship between WEC model tests and full-scale performance is not fully understood. It follows that there is a continued need for technical investigations in the laboratory, along the lines of the present research, and the integration of knowledge feedback loops from full-scale demonstrations, to refine the model test guidelines toward a standardised set of robust and validated recommended best practices. Such guidelines are important to streamline the development path from concept to product, to minimise technical and financial risks, to maximise the reliability of model test results, and to ultimately reduce the LCOE of wave energy.

The high-level requirements of hydrodynamic model test experiments of WECs are: experimental proof-of-concept, numerical model calibration and validation, energy capture performance optimisation, survivability, installation and tow-out methodologies, power production validation, and arrays and clusters. Guidance, however, is lacking for some of these requirements. Despite substantial progress in developing these requirements, supported by general considerations (parameters and procedures) and recent advances in modelling practices, this review revealed the guidance is dispersed across many documents, is inconsistent in some parameters, procedures, and high-level requirements, and is lacking in several areas. WEC-specific guidance was found to be lacking in the modelling of moorings, PTOs, and arrays and clusters; identifying and modelling extreme events; installation and tow-out tests; specific tests for calibrating and validation numerical models; methods for extrapolating model-scale results; full-scale validation; and, most important to this research, knowledge of and methods to account for the experimental uncertainties of measurement uncertainty, scale effects, and laboratory effects. Therefore, technical investigations and refinement are needed in these lacking areas.

Broader reviews of guidelines and standards in marine renewable energy found similar gaps in the guidance on hydrodynamic model test experiments of WECs. An additional key gap was that there is lacking guidance on how to transition between TRL stages. It was also emphasised that continued efforts are needed to develop a coherent and consistent set of guidelines/standards, and that proper dissemination of these is important to ensure they are widely accessible, understood, and used by test facilities.

Literature and guidelines are especially lacking for experimental uncertainty in hydrodynamic model test experiments of WECs. While an international guideline on uncertainty analysis for WECs was recently published (by ITTC [17]), it is lacking in pre-test or General Uncertainty Analysis and alternative methods for uncertainty propagation, such as the Monte Carlo Method. This finding motivated and directed the experimental investigation into measurement uncertainty and uncertainty analysis methods for WECs (Chapter 3). Additionally, a review of WEC scale effects (Table 2.3) found that there are many possible sources of uncertainty due to scale, and that while a growing number of studies are addressing various scale-related issues in WEC model tests there remain outstanding issues in how scale influences WECs characterised by nonlinear interactions - nonlinear waves, motions, and PTOs. This finding motivated and directed the experimental investigation into scale effects of OWC WECs, focusing on said outstanding issues (Chapter 4). Finally, while limited guidance from related maritime fields is available on how wave basin laboratories may influence hydrodynamic model test results, WEC-specific investigations into laboratory effects were yet to be carried out. This finding motivated and directed the experimental investigation into laboratory effects of OWC WECs (Chapter 5).

Considering this chapter within the context of the thesis, not only has it generated the knowledge required to ensure that the right experimental investigations are carried out – by revealing the major experimental uncertainties needing investigation – but also that these experimental investigations could be carried out right. It has engendered a sound understanding of the best practices needed to carry out the subsequent experiments designed to investigate these uncertainties in a rigorous manner, to obtain high-quality and relevant results. Thus it has provided an answer to the question, *What are the best practices in hydrodynamic model test experiments of WECs*? This study contributes to the field by providing stakeholders in WEC model test experiments – such as developers, researchers, students, facility managers, and investors – with a comprehensive resource that identifies, describes, and evaluates the best practices, recent advances, and uncertainties in WEC model tests. In doing so, it helps to reduce experimental uncertainty in a general sense. Further, it gives perspectives on future research required to produce relevant, robust, and accurate future best practices specified by international guidelines. reduce experimental uncertainty in the wave energy field.

Chapter 3

Comprehensive Uncertainty Analysis of an OWC Wave Energy Converter Model Test Experiment

Uncertainty analysis (UA) is inseparable to experimentation, but it is neither well understood nor widely used in hydrodynamic model test experiments of Wave Energy Converters (WECs). This chapter presents a comprehensive UA methodology applied to the 1:30 scale model experiment of the case study OWC WEC, which forms the basis of the uncertainty analyses applied to subsequent experiments on scale and laboratory effects. It outlines UA principles, identifies parameters causing measurement uncertainty, and develops several WEC-specific UA methods. It closes with conclusions and recommendations for refining international guidelines on uncertainty analysis for WECs.

3.1 Introduction

Suppose you are to compare two sets of experimental data. How do you determine if the results agree or disagree? Uncertainty analysis is key. The analysis of uncertainties in an experiment quantifies the quality of results, so that those who use them can assess their reliability and determine whether they agree or not [21]. Uncertainty analysis also assures the quality of results: experimentalists can use it to decide which out of possible approaches might best answer a question or attain the objectives, and design and monitor the conditions in which high-quality results will be the likely outcome [60]. Uncertainty analysis is thus inseparable to experimentation. However, it is neither well understood nor widely used in wave energy converter (WEC) experiments, and has been largely overlooked in the boarder wave energy field [18]. This situation represents a serious gap in the knowledge required to develop techno-economic WECs.

This gap is apparent by (1) few WEC experimental studies reporting results *and* uncertainty, (2) undeveloped WEC-specific guidelines, and (3) limited studies to inform said guidance [18, 16, 15]. These limitations are striking, given wave energy technology developers, researchers, and investors make critical decisions based on the results of hydrodynamic model tests; the results are used, for example, to prove a concept, validate and calibrate numerical models, design prototypes, predict cost of energy, or to attract or justify investment [11, 10, 47]. In response to this situation, research projects have sought to produce uncertainty-related guidance for WECs [16, 15]. Recently, the International Towing Tank Conference (ITTC) published the first international guidelines, *Uncertainty Analysis for a Wave Energy Converter* 7.5-02-07-03.12 [17]. While these efforts are a step toward rigorous, standardised best practices, the guidance is undeveloped because it lacks important uses of uncertainty analysis that can significantly improve the processes and outcomes of WEC experiments. Such uses are pre-test or General Uncertainty Analysis (GUA) and other appropriate methods to propagate uncertainty such as the Monte Carlo Method (MCM) [60]. Technical investigation is therefore needed to extend and refine the guidance.

There are, to our knowledge, four studies that focus on uncertainty in WEC experiments. One study showed that the experimental uncertainty in an array of heaving buoy WECs was of such significance that it concealed the array interactions, making power predictions unreliable [38]. This study extended previous work carried out to assess how wave basin homogeneity impacts WEC array studies, which revealed the difficulty in separating array interactions and spatial variations of generated waves [39]. Two recent studies, which this chapter is based on, presented practical applications of uncertainty analysis in OWC wave energy converter experiments [40, 41] (Appendices D and E). More broadly, uncertainty-related studies have been carried out in other areas of the wave energy field, including the uncertainty in wave energy resource assessment [100, 105, 149, 150, 107, 151] , ocean test results [152], and Mean Annual Energy Production estimates [151, 109]. Outside of wave energy, in related maritime fields, uncertainty analysis for hydrodynamic model test experiments has been studied [153] and international guidelines produced [154, 155, 156]. While some aspects of this literature may be useful for WEC experiments, the literature does not address specific challenges and uncertainties associated with WECs, most significantly the modelling of PTOs [18, 11].

This chapter seeks to explain, extend, and refine uncertainty analysis methods for WEC model test experiments, through a comprehensive experimental uncertainty analysis applied to a 1:30 scale model test experiment of the Wave Swell Energy (WSE) OWC WEC. The structure is as follows. § 3.2 provides an overview of experimentation, uncertainty analysis, and their relations. § 3.3 describes the WSE WEC and physical model considerations of the experiment. Two subsequent sections describe the exemplary experiment as it progressed through a series of experimental phases, from initial planning and design, to construction and debugging, to execution, analysis and reporting. At each phase, introduced in chronological order, we first describe the relevant uncertainty analysis principles then immediately describe their implementation into these experimental phases. The two sections are General Uncertainty Analysis (§ 3.3), comprising the plan and preliminary design phases, followed by Detailed Uncertainty Analysis (§ 3.4), comprising the phases of design, construct, debug, execute, analyse, and report. A general discussion on the implications and limitations of the work follows, with the chapter closing with conclusions and recommendations for future guidelines on uncertainty analysis for WECs.

There are two main contributions of this work, one specific to this PhD research, the other being broader. For this PhD, the 1:30 scale experiment that is described in this chapter was one of the scale models used in the experimental investigations into scale effects (Chapter 4) and laboratory effects (Chapter 5). This chapter, then, describes the methodology of the uncertainty analyses performed in these subsequent experiments, such that their results could be objectively compared to determine whether there was agreement across scales in the same laboratory, and between laboratories at the same scale. The broader contribution is that, while the work focuses on extending the understanding and methods of uncertainty analysis for OWC WECs, it may nevertheless be used as a procedure for performing uncertainty analysis in hydrodynamic model test experiments of other WEC designs. Thus, the work lends itself to be incorporated into future international guidelines on uncertainty analysis for WECs.

3.2 Overview of experimentation and uncertainty analysis

Uncertainty analysis is the analysis of uncertainties in an experiment to assure and quantify the quality of results. Fig. 3.1 shows at a high-level the relation between uncertainty analysis, its uses, and experimentation, its phases and activities (cf. Fig. 3 in [17]). Uncertainty analysis may be split up into two categories: (1) General Uncertainty Analysis (GUA), used in the Plan phase of an experiment, and (2) Detailed Uncertainty Analysis (DUA), used in the remaining experimental phases: Design, Debug, Construct, Execute, Analyse, and Report (adapted from [60]). These experimental phases, informed by GUA and DUA, are often iterative. For example, insoluble problems or new significant sources of uncertainty encountered in the Debug phase may require changes to be implemented back in the Design phase.

At a technical level, in GUA we evaluate the relative importance of overall (general) uncertainties in experimental parameters, to evaluate various approaches, instruments, apparatus, and overall measurement procedures that might best answer questions or attain objectives of interest. In DUA, we evaluate uncertainties at a detailed level, to guide deci-

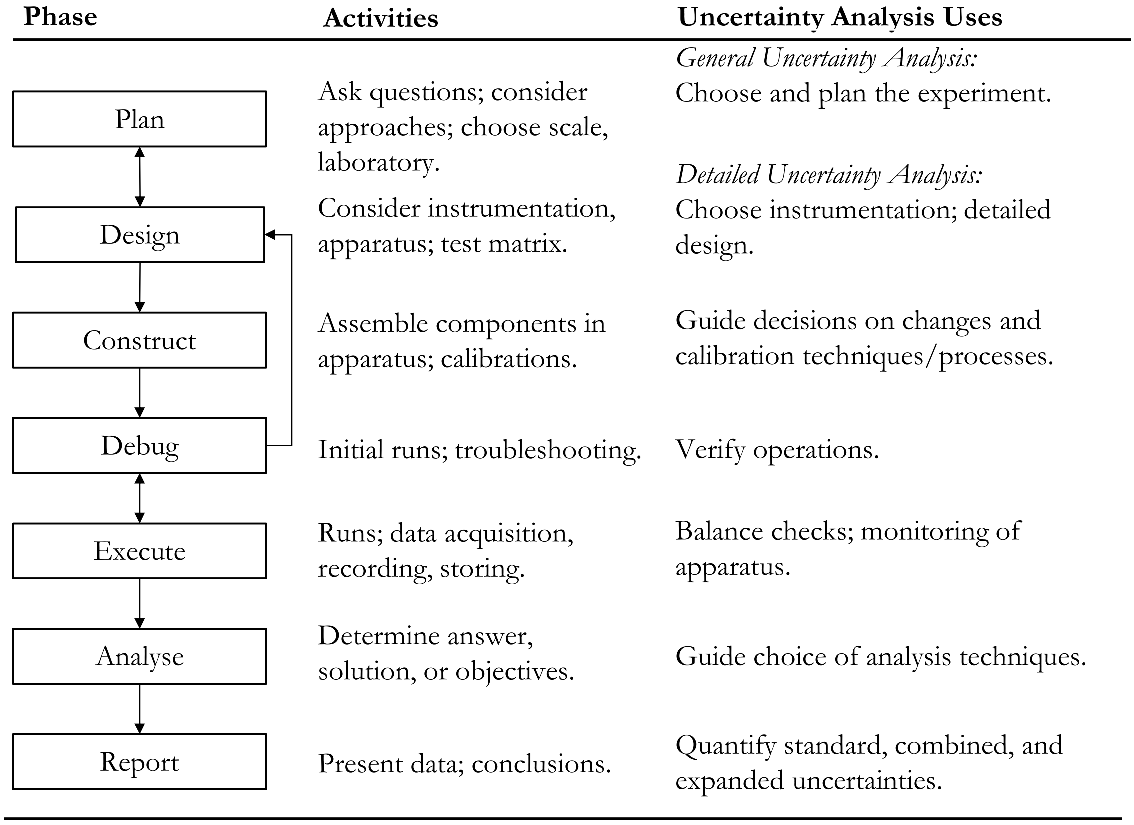

Figure 3.1: Experimental phases with descriptive activities and corresponding uses of uncertainty analysis.

sions on measurements and procedures, to monitor data and its uncertainty, and quantify the quality of results throughout the experiment. To provide a systematic means of performing both GUA and DUA, a three-stage structure of uncertainty analysis is introduced: (1) formulate, (2) propagate, and (3) summarise [21, 118]. Fig. 3.2 shows the concepts in and process of these stages, composed of uncertainty analysis principles for GUA and DUA. Descriptions of key terms in Fig. 3.2 follow.

X_i is an input quantity, where i=1:N number of quantities related to the output quantity Y (the measurand) through a model $Y = f\left(X_1, X_2, \ldots, X_N\right)$. Lowercase x_i, y are the estimates or measurements of quantities. $u_G(X_i)$ is the *general uncertainty* which is a value characterised by an assumed Probability Density Function (PDF) of input quantities X_i. $u_A(x_i)$ is the Type A uncertainty associated with an x_i, evaluated by the statistical analysis of series of observations, that is, the standard deviation of the PDF produced by repeated observations. $u_B(x_i)$ is the Type B uncertainty associated with an x_i, characterised by an assumed PDF, and evaluated by means other than the statistical analysis of series of observations, for example, from instrument calibrations, manufacturer's specifications, or uncertainties taken from handbooks.

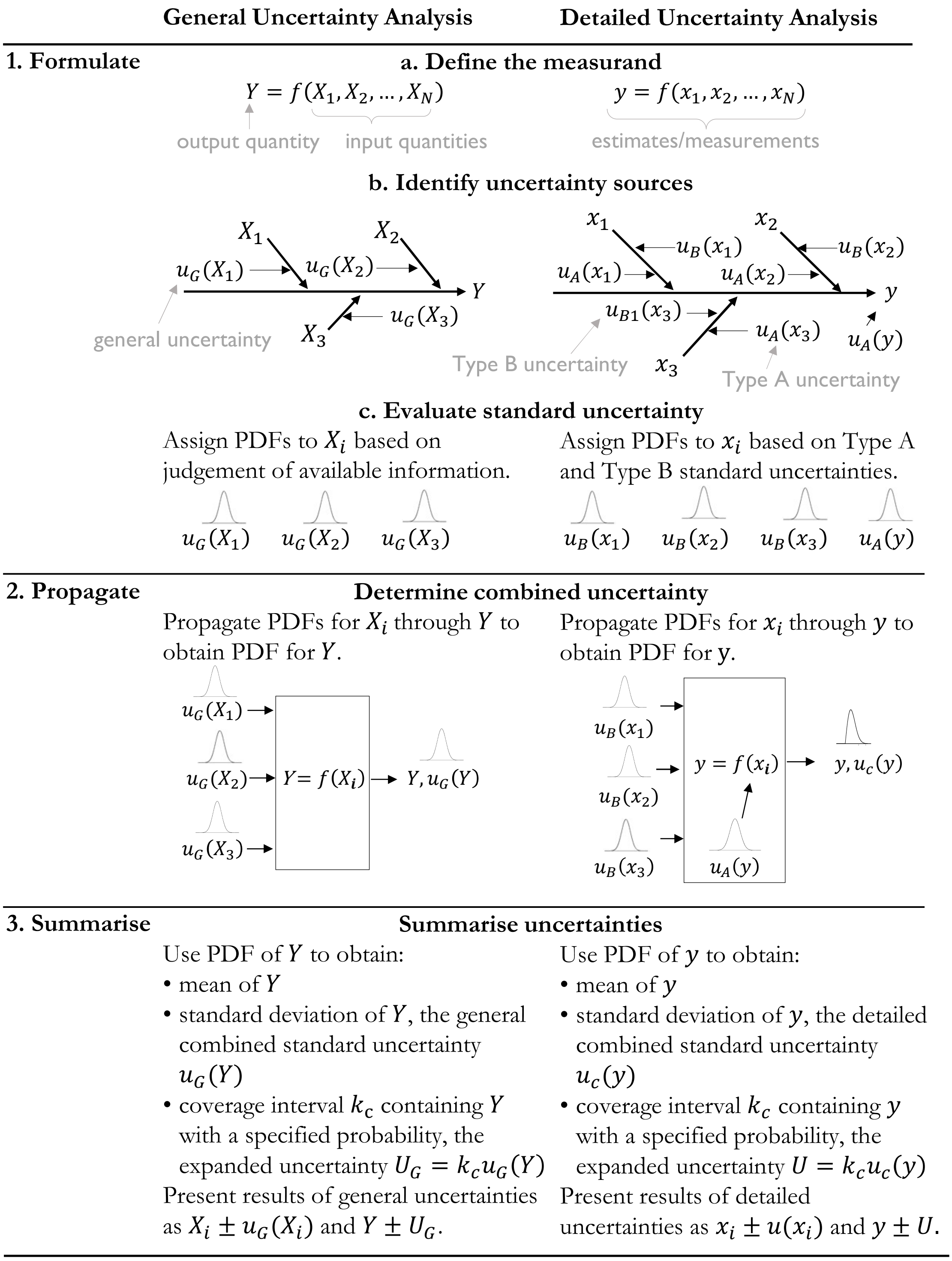

Figure 3.2: Overview of the concepts and processes of uncertainty analysis, structured by three main stages, for General Uncertainty Analysis and Detailed Uncertainty Analysis. The example illustrates $N = 3$ independent input quantities X_i.

The next section describes the OWC WEC technology used in this experiment and key considerations of the physical model. The following two sections §§ 3.4 and 3.6 describe in greater detail the concepts and methodologies shown in Fig. 3.2, and present applications of these to the OWC experiment. The sections are based on the authoritative international ISO *Guide to the Expression of Uncertainty in Measurement* [21, 118], uncertainty analysis for engineers [60] and scientists [157], and the uncertainty-related ITTC Recommended Procedures and Guidelines [154, 17].

3.3 WEC and physical model description

The introduction described the Wave Swell Energy (WSE) Uniwave technology at a high-level, its working principle and key features (Chapter 1 and Fig. 1.1). This section briefly describes the technology at a more technical level, necessary to give context for the following section that describes the mathematical model of the OWC WEC. The prototype PTO comprises a unidirectional nonlinear air turbine, with unidirectional airflow enabled by passive valves that open and exhaust air on the up-stroke, then close on the down-stroke to direct air through the air turbine thereby generating electricity. This PTO system was modelled at scale using an orifice place to represent the quadratic air pressure-flow characteristics of the air turbine (a common practice [28, 158, 159]). Light weight, robust plastic sheets simulated the passive unidirectional flow valves. The prototype was scaled down to 1:30 scale using Froude scaling.

3.4 General Uncertainty Analysis

General Uncertainty Analysis is the analysis of general uncertainties in experimental parameters to inform the planning phase of an experiment. GUA can enforce a complete examination of the experimental procedure; provide an integrated grasp of how to carry out the experiment; identify potential troubles and errors, and why they exist; advise when improved instruments or procedures are needed to achieve a specified uncertainty budget, while minimising the cost; and reveal which parameters contribute most to the uncertainty in results, thereby focusing attention on key measurements and procedures which govern the overall experimental uncertainty [160]. All these uses permit access to otherwise inaccessible information about an experiment before it is carried out, saving time, money and resources.

This section describes the principles and application of GUA according to the three UA stages shown in Fig. 3.2, beginning with Formulate. It also presents a comprehensive example of how GUA was used to help plan the OWC experiment.

Stage 1. Formulate

1.a Define the measurand

To define the measurand(s) of the experiment is to make a clear statement about what is being measured. In most cases a measurand Y is not measured directly but is derived from N other quantities $X_1, X_2, \ldots, X_N$ through a functional relationship denoted a measurement model: $Y = f(X_1, X_2, \ldots, X_N)$. The quantities X_i may themselves be lower-level measurands, measured directly, assumed constants, or unique values that compensate for uncontrolled factors (e.g., environmental factors). For this experiment, to define the measurands a simple sketch of the intended experiment was created (Fig. 3.3). The sketch shows the processes and objects of the experiment, consisting of a model of the WSE prototype (see Fig. 1.1) and its interaction with ocean waves, along with key quantities to be measured, derived, or assumed. The quantities X_i are assembled into the measurand functions (boxed equations), in the form $Y = f(X_1, X_2, \ldots, X_N)$.

The equations presented in § 2.4.1 describe the mathematical model used to characterise the WSE WEC in terms of the wave and model quantities and measurands of the experiment. Additional descriptions are given below for the PTO modelling in this experiment.

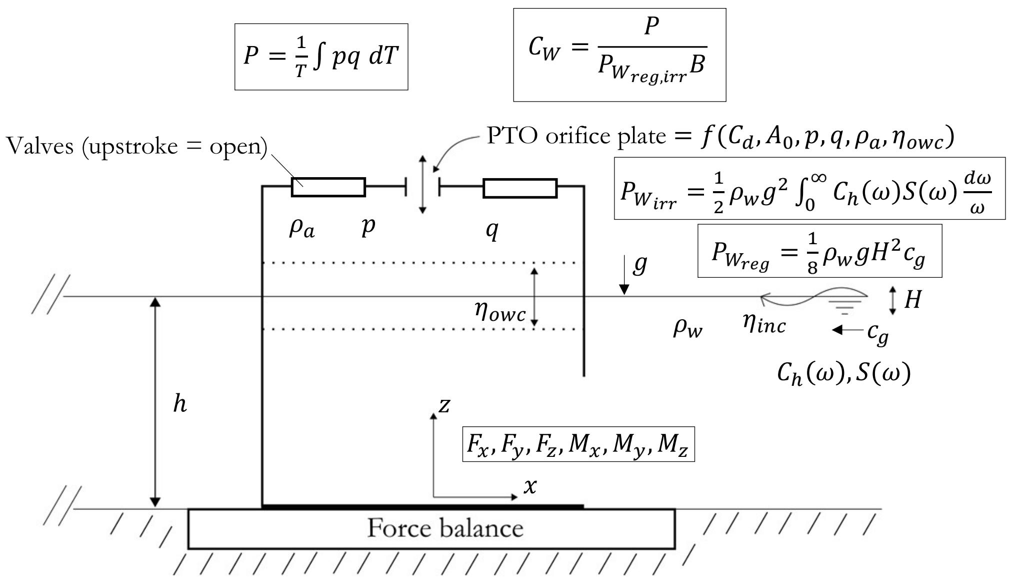

Figure 3.3: Simple sketch of the OWC wave energy converter experiment in regular waves, showing all the defined measurands and input quantities on which they depend.

To characterise the power absorbed by the model OWC WEC, a unidirectional PTO would be modelled using an orifice place to represent the quadratic air pressure-flow characteristics of the air turbine (a common practice [28, 158, 159]). The unidirectional flow valves would be modelled using passive flaps constructed from light weight, robust plastic sheets. Pneumatic power P, henceforth 'OWC power', is derived from the differential air pressure p

measured inside the OWC chamber, and air volume flow rate q displaced by the motion of the inner free-surface. In regular waves,

$$P = \frac{1}{T} \int pq \, dT \tag{3.1}$$

where T is the characteristic wave period. There are two key methods of deriving q in Eq. (3.1); § 3.4.1 describes these methods and presents an example of how GUA was used to choose which method would result in the least uncertainty.

Fig. 3.3 also shows the hydrodynamic loads imposed on the OWC by waves, to be measured using a six-component force balance. The six load measurands are surge force F_x, sway force F_y, heave force F_z, roll moment M_x, pitch moment M_y, and yaw moment M_z. This work focuses only the important components of F_x, F_z, and M_y.

1.b Identify uncertainty sources

There are many possible uncertainty sources in a measurement, including: incomplete definition of the measurand; imperfect realisation of the definition of the measurand; inadequate knowledge of the effects of environmental conditions on the measurement or imperfect measurement of environmental conditions; personal bias in reading analogue instruments; approximations, assumptions, and inexact values of constants and other parameters; or variations in repeated observations of the measurand under apparently identical conditions [21]. A broader perspective on 'experimental uncertainty' reveals still more sources. All or at least the relevant uncertainties should be considered and, when required, evaluated. To assemble a comprehensive list of possible uncertainty sources, relevant for this experiment but also in general for all kinds of WEC experiments, we reviewed the literature on hydrodynamic experimentation to understand which uncertainties may be important (Fig. 3.4). This visual list identifies and categorises uncertainty sources, including references to studies and guidelines (see Appendix C for the list of references relating to the superscripts in the figure).

Relating identified uncertainty sources (Fig. 3.4) to the sketch of quantities and measurands (Fig. 3.3), a general uncertainty $u_G(X_i)$ was then assigned to all the X_i of the experiment. A useful tool to aid this process is the cause-and-effect diagram (Fig. 3.5). These diagrams effectively account for the uncertainties in all the X_i and show their relative influences on the overall uncertainty in Y. The diagrams also avoid double counting of uncertainties.

1.c Evaluate standard uncertainty

The last step in the Formulate stage is to evaluate the general standard uncertainty (Fig. 3.2). This requires assigning PDFs – Gaussian (normal), rectangular (uniform), etc. – to the X_i on the basis of available knowledge, and assigning instead a joint PDF to those

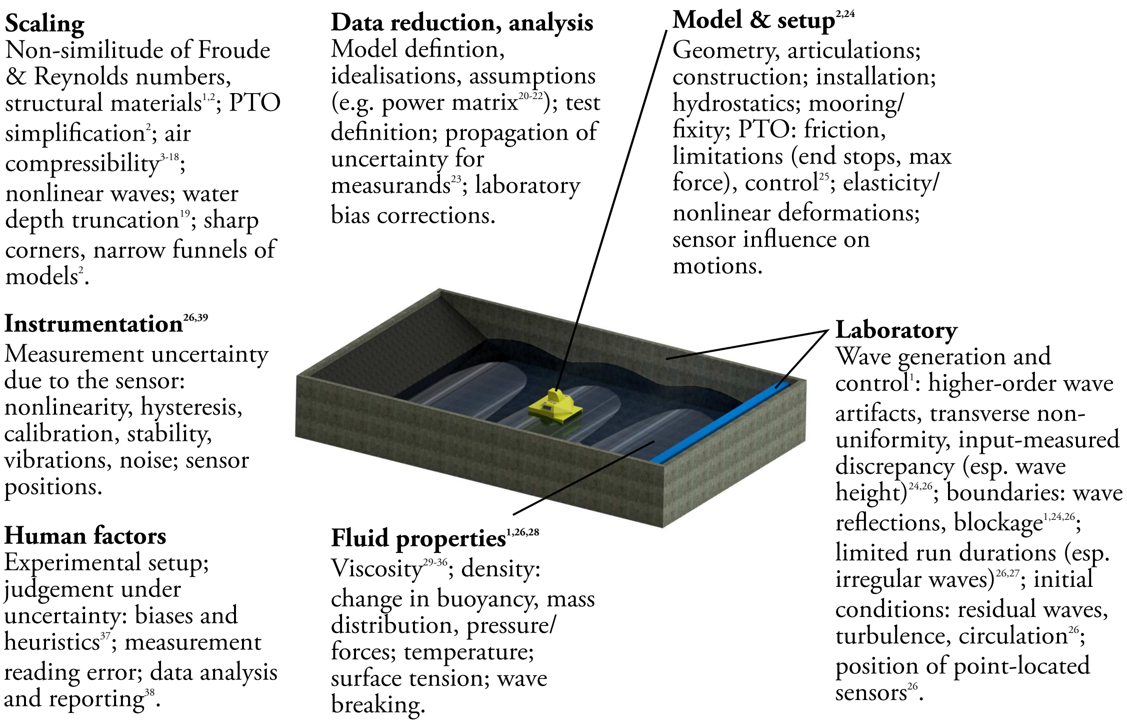

Figure 3.4: Diagram of potential sources of uncertainty in a typical wave energy converter experiment. See Appendix C for the list of references (superscripts).

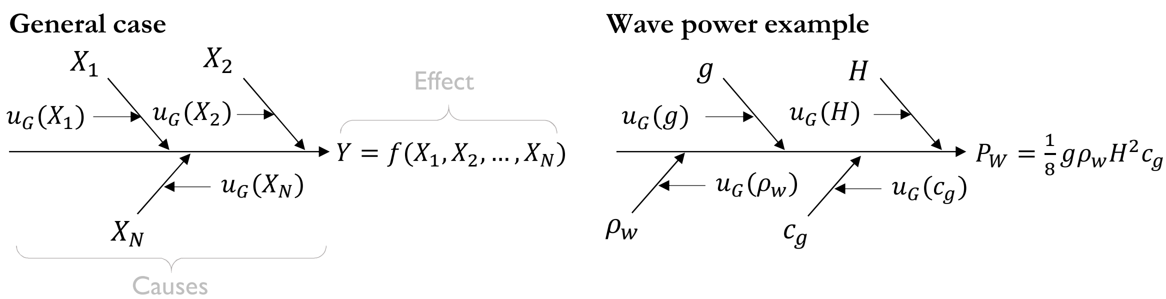

Figure 3.5: A cause-and-effect diagram used to identify uncertainty sources in a measurand Y, where X_i are input or influence quantities upon which Y depends, and $u_G(X_i)$ is a general uncertainty associated with X_i. Example is for N=3 independent X_i.

X_i that are not independent. Available knowledge may include, for example, previous measurement data, experience with similar experiments, or reference materials. Often a simple Gaussian PDF is assumed at the pre-experiment stage.

Stage 2. Propagate: Determine combined uncertainty

Uncertainty propagation is the combinatorial effect of quantities' uncertainties, characterised by PDFs, on the uncertainty of a measurand function based on them. Fig. 3.2 shows the basic principle of uncertainty propagation, in which we propagate the X_i PDFs through a model to produce an estimate and PDF of Y. The propagation of PDFs can be implemented either analytically, through the *law of propagation of uncertainty* based on a first-order Taylor series approximation (i.e., the Taylor Series Method (TSM) or GUM uncertainty framework [21]), or statistically by performing random sampling from PDFs using, for example, the Monte Carlo method (MCM) [118, 60]. The MCM is a practical alternative to the TSM. It has value when linearisation of the model provides an inadequate representation, or the PDF for Y is nonlinear and departs appreciably from a Gaussian distribution or a scaled and shifted t-distribution, e.g. due to asymmetry. Further, the MCM directly propagates uncertainty through measurand functions and so does not contain approximations (therefore errors) that the TSM does; it is generally easier to implement and reduces the analysis effort; and is more reliable when an estimate of Y and the associated uncertainty are approximately of the same magnitude. For these reasons the MCM has become the primary method for propagating uncertainties in many engineering fields [60]. The MCM is, therefore, the focus of this work. It is especially useful in this application, and probably most WEC experiments, because the experiment is characterised by multiple time-dependent nonlinear processes – nonlinear waves inducing nonlinear motions of the OWC's internal free surface which interacts with a nonlinear PTO.

Fig. 3.6 shows the process of the MCM in GUA, presenting an example where a measurand Y depends on two input quantities X_1 and X_2 such that $Y = f(X_1, X_2)$. The method is, however, general for measurands with any number of inputs. A description of the method and its implementation follows.

First, assumed nominal values are input for each quantity $X_{1,nom}$ and $X_{2,nom}$, as well as their assumed general uncertainties $u_G(X_1)$ and $u_G(X_2)$. Each u_G is a unique value encompassing all kinds of uncertainty components, and is assumed to be the standard deviation of the assumed PDF, which is commonly Gaussian but other distributions can be assumed based on better knowledge. Then, at each iteration j, $u_G(X_i)$ is multiplied by a randomly sampled number drawn from the assumed PDF (varying about 1), and added to the nominal values of each quantity to obtain the "measured" values X_1(j) and X_2(j). From these measured values the result of the measurand Y is calculated. This sampling process is repeated M times to obtain a PDF for Y. The output of the MCM is the standard deviation of the PDF of Y, taken as the general uncertainty $u_G(Y)$. An appropriate value for M is determined by calculating the standard deviation of Y at each iteration and stopping the process when a converged value is reached (see Appendix E). A converged value to within 5% is considered to give an acceptable approximation of $u_G(Y)$ ($M \approx$ 5,000 is often sufficient).

At this pre-experiment stage, a sensitivity analysis may be performed through a series of simulations over a range of nominal values and uncertainties within the anticipated parameter

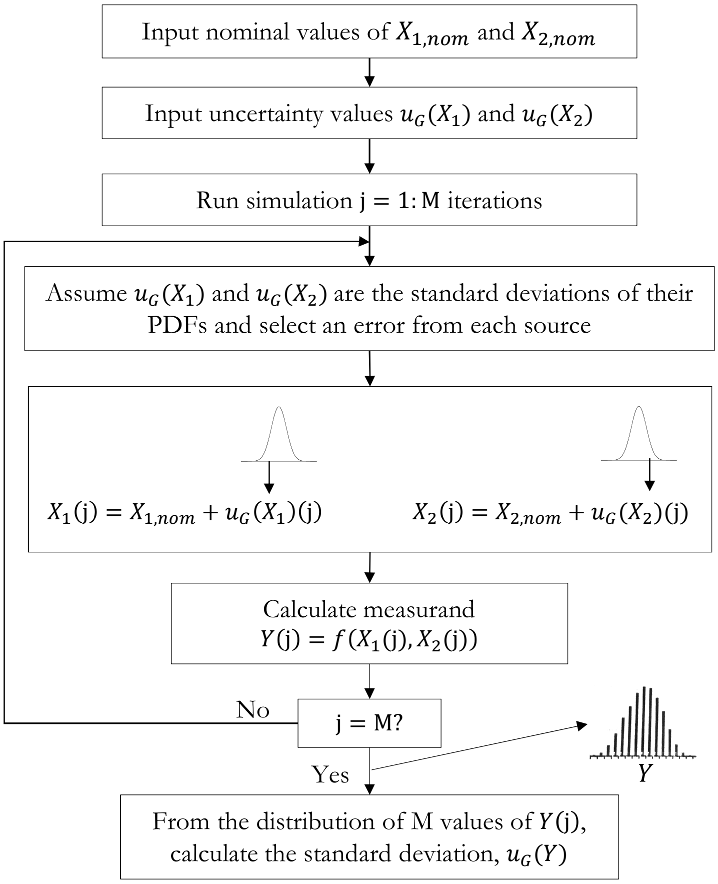

Figure 3.6: Flow diagram of the Monte Carlo method to propagate uncertainty in general uncertainty analysis, showing an example where the measurand result Y is a function of two input quantities X_1 and X_2.

space of the experiment. Here, one input quantity is subject to random sampling at a time, while the other quantities remain constant. Such an analysis reveals the relative importance of input quantities and their uncertainties on the output result. This process yields insights into which parameters contribute most to the overall experimental uncertainty, valuable information that informs the subsequent experiment design phase. Following the Summarise section below, § 3.4.1 presents an example of a kind of sensitivity analysis.

Stage 3. Summarise: Summarise uncertainties

To summarise propagated uncertainties, we use the PDF for Y to obtain: an estimate (the mean) of Y; the standard deviation of Y, taken as the general uncertainty $u_G(Y)$ associated with Y; and a coverage interval k_c containing Y with a specified probability, which gives the expanded general uncertainty $U_G = ku_G(Y)$ (Fig. 3.2).

Determining an MCM coverage interval for Y is straightforward, even if the PDF for Y is asymmetric, occurring when Y is nonlinear or the uncertainties are relatively large. First, the vector of Y values that form the PDF are sorted from smallest to largest. Then, for a chosen coverage probability p_c, the lower bound of the coverage uncertainty interval is $Y_{low} =$ sorted vector $\{[(1 - p_c)/2]\, M\}$, with the upper bound $Y_{high} =$ sorted vector $\{[(1 + p_c)/2]\, M\}$. For example, to obtain 95% coverage interval limits ($p_c = 0.95$), $Y_{low} =$ result number $(0.025M)$ and $Y_{high} =$ result number $(0.975M)$ (i.e., the 2.5% and 97.5% quantiles, with the interval containing 95% of the MCM results).

In addition, this Summary stage includes presenting the general uncertainties in key input quantities and any other important information that informs experiment planning. The form of presentation will differ, but generally it involves presenting in tables or graphs the nominal values and uncertainties in the form $X_i \pm u_G(X_i)$ and $Y \pm U_G$.

3.4.1 Example: Using the MCM to determine the method for deriving OWC power

This example describes how we used the MCM in GUA to help plan an aspect of the experiment. The analysis determined which out of two methods for deriving OWC power P would result in the smallest uncertainty. It further informed experimental design and procedures required to achieve the estimated uncertainty. The example shows how the MCM quantifies the sensitivity of a measurand, its uncertainty, to a range of nominal values and uncertainties of input quantities upon which it depends. It also highlights how GUA can be especially helpful in determining whether or not a new procedure should be pursued in an experiment, or whether a previously developed GUA could be used in a new experiment.

The problem of deriving P in experiments is as follows. From Eq. (3.1) it is seen that P is a function of air pressure p multiplied by volume flow rate q. Measuring q in OWCs, however, is challenging because the air flow changes continuously and rapidly, in both magnitude and direction. Therefore, q is derived using two main methods [161]:

Method (a): q is derived through a numerical derivation of air volume displaced from the OWC internal free surface η_{owc} oscillations measured using multiple wave probes inside the OWC, hence $q_{\eta_{owc}}$:

$$q_{\eta_{owc}} = \iint_{S_c} \frac{d\eta_{owc}}{dt}\, ds = \iint_{S_c} v_s\, ds \tag{3.2}$$

where S_c is the free surface area and v_s the free surface velocity.

Method (b): q is derived from measured p and a calibrated orifice (used to simulate the PTO) characterised by a discharge coefficient C_d, hence q_{C_d}:

$$q_{C_d} = \frac{p}{|p|} C_d A_0 \sqrt{\frac{2|p|}{\rho_a}} \tag{3.3}$$

where A_0 is the orifice cross-sectional area, and ρ_a the density of air, assumed to be 1.2 kg/m^3. This equation for deriving q from flow through an orifice is according to ISO 5167

[162].

An in-situ orifice calibration procedure can be used to determine C_d, which is a two step process. The first step requires rearranging Eq. (3.3) for C_d. Then, using data from all regular wave runs (either measurement data obtained during the experiment or data based on assumed values before the experiment), calculate C_d from values of p, q_{C_d}, A_0, and ρ_a. Obtaining q_{C_d} here first requires the use of Method (a), such that $q_{C_d} = q_{\eta_{owc}}$ in the rearranged Eq. (3.3). After, from the regular data set we calculate the mean of C_d, which is approximately independent of wave height and period. The second step is to simply use this mean C_d value to derive q_{C_d} using Eq. (3.3). This GUA example demonstrates how C_d can be derived using data based on assumed values before the experiment, which was necessary to derive q_{C_d} and enable the comparison of Method (a) and (b). We present the results of this pre-experiment orifice calibration after describing the MCM sensitivity analysis of Method (a) and (b), as follows.

Two sets of MCM simulations were set up as per Fig. 3.6, one set for Method (a) and one for Method (b). The first step is inputting nominal values of the quantities used to derive P. To obtain such nominal values required developing a simple mathematical model, based on the scale of the experiment, selected to be 1:30 based on the wave basin characteristics (location, dimensions, water depth, and wavemaker capability) and other practical aspects including model build and instrumentation implementation (see Chapter 2 for details on model scale selection). The model consisted of an assumed sinusoidal wave profile of 101 data points representing the free surface elevation inside the OWC, $\eta_{owc} = A_{\eta_{owc}} sin(kx - \omega t)$ where $A_{\eta_{owc}}$ is the amplitude. From this profile, q was derived using Eq. (3.2), assuming the cross-sectional area of the OWC to be $S_c = 0.168$ m^2 (based on previous knowledge). In turn, we derived p from q by rearranging Eq. (3.3), and substituting $C_d = 0.6$ (the theoretical discharge coefficient), air density $\rho_a = 1.2$ kgm^{-3}, and orifice area $A_0 = 0.011$ m^2 (based on available knowledge). Finally, P was calculated from $P = pq$. Fig. 3.7 shows the results from this modelled OWC system, where all profiles are normalised against their maximums to conveniently graph them together. p and q are negative because the WSE WEC has a unidirectional flow PTO, described above in § 3.3 and elaborated on below.

Nominal values obtained from above and visualised in the profiles of Fig. 3.7 were then input into two sets of MCM simulations. The MCM was implemented here by subjecting the 101 data points of the profiles to the random sampling process. That is, at each iteration, every data point has an assigned uncertainty value which is multiplied by a randomly sampled number. After M iterations, each data point is an M-by-1 vector that forms a PDF, such that the 101 PDFs for each data point form the uncertainty bounds along the profile. From the uncertainty bounds, the uncertainty was summarised at one point along the profiles –

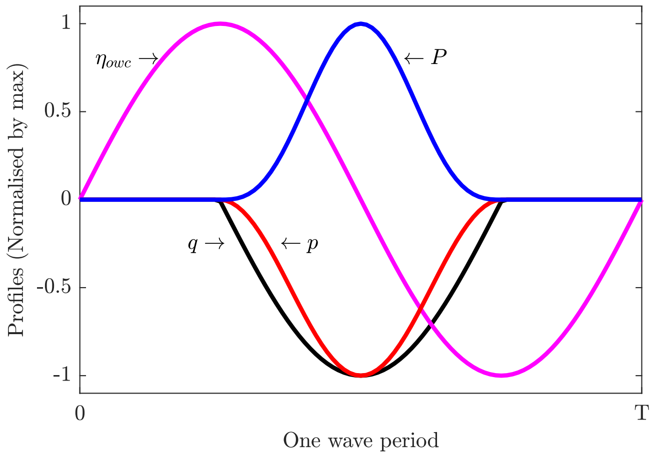

Figure 3.7: Profiles of variables, normalised against their respective maximums for one wave period

the amplitude. This will become clear once we present the relevant results below.

In **Method (a)**, sixteen simulations were run consisting of combinations of input uncertainty values of pressure $u_G(p)$ and OWC internal free surface elevation $u_G(\eta_{owc})$, across a range of amplitudes of OWC internal free surface elevation $A_{\eta_{owc}}$. Fig. 3.8 shows these MCM simulation results. The results show $U_G(P)$ decreased as $A_{\eta_{owc}}$ increased, due to the absolute uncertainties of input quantities $u_G(p)$ and $u_G(\eta_{owc})$ being relatively smaller than the amplitudes of those quantities. Also, $U_G(P)$ was strikingly sensitive to a small change in $u_G(\eta_{owc})$ (from 1 to 2 mm), whereas an equal relative magnitude change in $u_G(p)$ (from 15 to 30 Pa) barely influenced $U_G(P)$. This result indicates how sensitive $q_{\eta_{owc}}$ is to a slight departure of sinusoidal linearity in the η_{owc} profile, induced by free surface sloshing inside the OWC. The worst case, or highest uncertainty in $U_G(P)$ of 45%, occurred when $A_{\eta_{owc}}$ was smallest, and $u_G(p)$ and $u_G(\eta_{owc})$ largest, as expected.

To emphasise how GUA can be used in preliminary experimental design, this new knowledge of the sensitivity of $q_{\eta_{owc}}$ to η_{owc} nonlinearities may be used to design the experimental apparatus to have at least three but preferably six wave probes installed in the OWC, so that the η_{owc} free surface behaviour is more accurately captured.

In **Method (b)** a similar set of MCM simulations were run. To compare the MCM results between Method (a) and (b), we selected to show results from the best case and worst case as highlighted in the Method (a) results (Fig. 3.8). The results for the best and worst case for each method are presented in Fig. 3.9, at a more detailed level than before. In this figure the coloured bands along profiles are the uncertainty distributions for each data point. Inset onto each subplot is a histogram showing the MCM produced PDF of $U_G(P)$ at the amplitude of P. The titles of the subplots specify the assumed nominal and uncertainty values for each case. In the **Method (b) MCM results** there is an additional uncertainty value assumed for volume flow rate $u_G(q_{C_d})$, which is of approximate equal magnitude to the

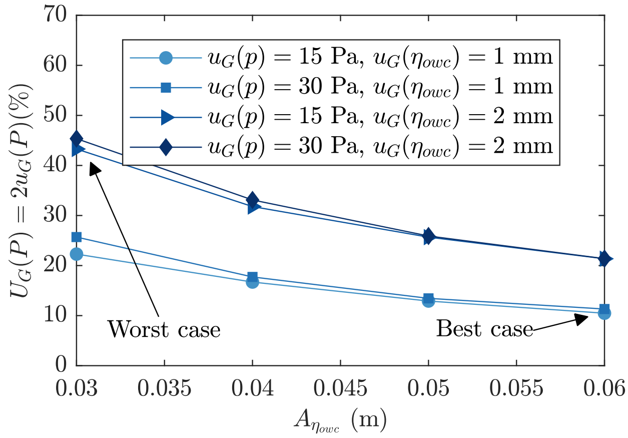

Figure 3.8: MCM simulation results of **Method (a)**, showing the sensitivity of general expanded uncertainty $U_G(P)$ in OWC power P to a combinatorial set of input uncertainty values of pressure $u_G(p)$ and OWC internal free surface elevation $u_G(\eta_{owc})$, across a range of amplitudes of OWC internal free surface elevation $A_{\eta_{owc}}$.

quantities' uncertainties seen in **Method (a) MCM results**.

The MCM results clearly show $U_G(P)$ was about twice as small in Method (b) compared to Method (a), for both the best and worst cases (Fig. 3.9). An explanation of this result is the following. The orifice discharge coefficient C_d used in Method (b) is averaged from all the pressure-flow characteristics in the OWC under all wave conditions, and it is approximately independent of wave height and period. Such averaging reduces the uncertainty in q_{C_d} (therefore P). Conversely, in Method (a), $q_{\eta_{owc}}$ is sensitive to the nonlinear sloshing behaviour of the η_{owc} free surface elevation, which depends on wave height and period. Therefore, based on these MCM results, Method (b) was chosen to derive P in the experiment.

The general uncertainty value of the orifice discharge coefficient $u_G(C_d))$ used in the above MCM sensitivity analysis for Method (b) was obtained from the pre-experiment orifice calibration procedure. Fig. 3.10 shows the results of this calibration, where C_d is plotted against p. The C_d data in this figure were generated through a MCM simulation, using the same quantity profiles and uncertainty values assumed for the main MCM sensitivity analysis described above (see figure title for values). These data are representative of all the regular wave data of the intended experiment. The black data points bounded by red dashed lines (two standard deviations σ) and $p < 200$ Pa were included in the calculation of the mean of C_d, and its standard deviation equal to the general uncertainty $u_G(C_d)$. It is seen that C_d is approximately independent of wave height or as a proxy the height of η_{owc} (in reality it is also independent of wave period, although in this pre-experiment calibration the sinusoidal profiles used to generate the data were considered to have one general wave period T).

The foregoing example demonstrates one of the many uses of GUA with the MCM to help plan an experiment and design some aspects of it. The technical outcomes and information

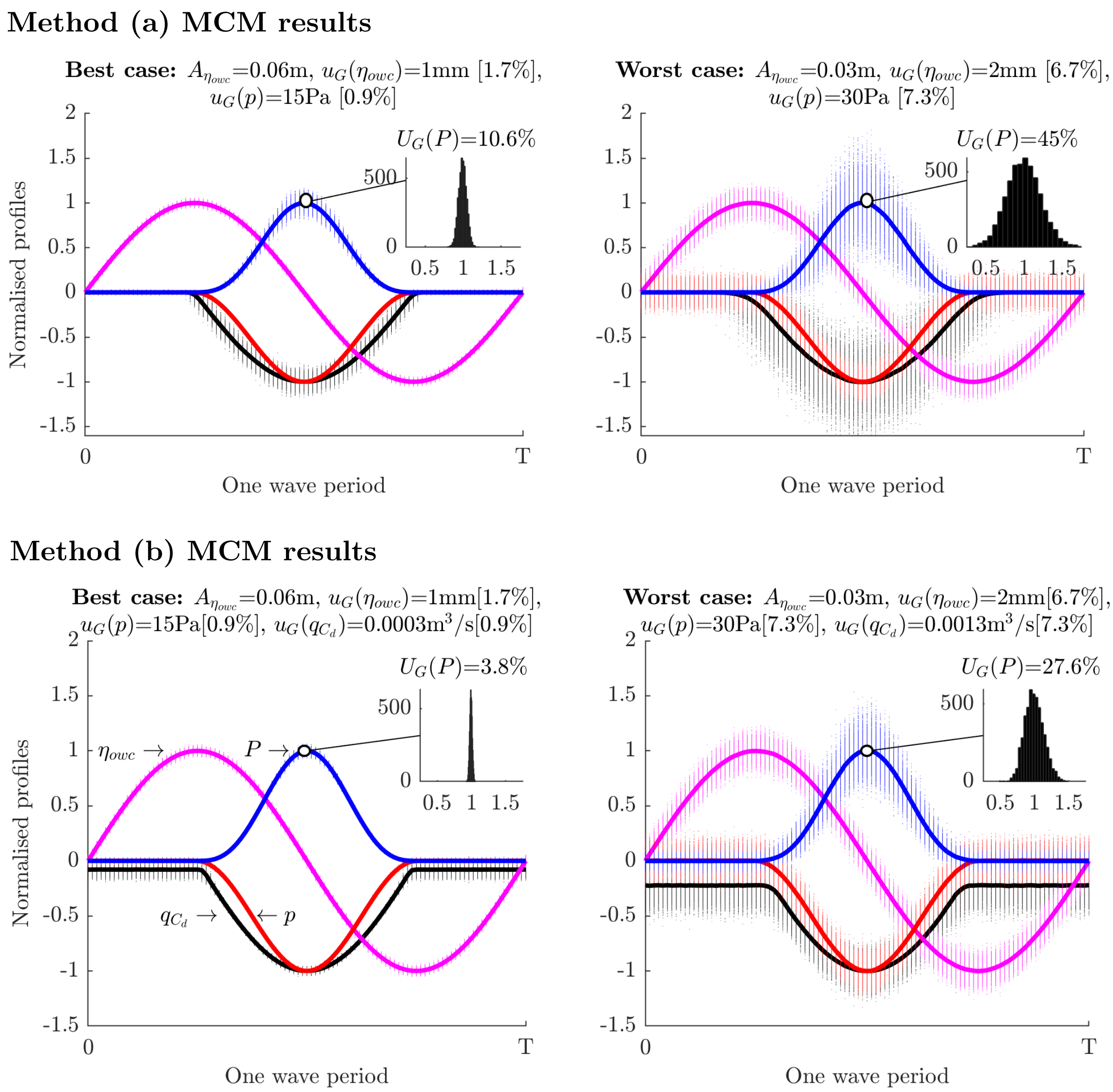

Figure 3.9: MCM simulation results of **Method (a)** and **Method (b)**. The top graph shows for **Method (a)** combinatorial set points of assumed nominal and uncertainty values (uncertainty values are ±); the bottom graphs show the profiles of cases with smallest $u_c(x_i)$ (left) and largest $u_c(x_i)$ (right), and a histogram of normalised P_{max}, where $U(P) = 2u_c(P)$. **Method (b)** results are below for comparison. Title includes $u_c(C_{d_{TSM}}$ and $u_c(C_{d_{MCM}}$ that show virtually equal results for u_c calculated from TSM and MCM respectively. Results show that $U(P)$ for Method (a) is higher than Method (b), therefore, Method (b) is better.

generated in this GUA were (1) an informed decision on the least uncertainty method to derive OWC power, and (2) an enhanced understanding of OWC power sensitivity to a range of nominal and uncertainty values of its input quantities. Moreover, the knowledge gained in (2) revealed critical measurements to be made – such as the OWC internal free surface using an appropriate number of wave probes – and where extra attention may be required to assure the desired uncertainty level is achieved.

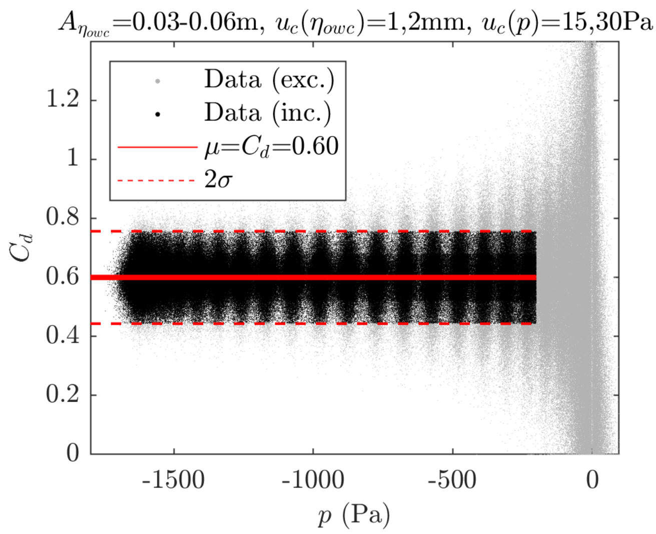

Figure 3.10: Orifice calibration graph showing the C_d-p relationship, and the method to estimate an appropriate value for C_d within defined limits.

More broadly, this section provides an argument for the value of GUA in an experimental program, that it is worthwhile because it generates otherwise inaccessible insights and information which can inform the subsequent design phase and create the conditions for a successful, high-quality experiment. It follows that each new experimental procedure developed in a laboratory should be linked to a GUA and, once applied, to a DUA as part of quality control. If similar experiments using well developed procedures are performed, the previously developed GUA could be used. Because WEC testing often brings new complexity (e.g. valves, PTO control, targeted wave climate) a new GUA may often need to be developed. Even if a seemingly similar experiment is performed, some small changes in parameters (wave properties, different instrumentation etc.) could change the results of the GUA. Checking that the parameters fits within the boundary of the developed GUA is important, otherwise redoing the GUA might be necessary. As part of the quality control and improvement strategy, a review of procedures and related GUA should be performed. (A new instrument might favour a different method).

3.5 Detailed Uncertainty Analysis

Detailed Uncertainty Analysis is the analysis of detailed uncertainties in experimental parameters to inform the remaining experimental phases, building on the information and knowledge generated in the GUA (Fig. 3.1). It involves evaluating uncertainties as separate components to investigate their detailed behaviour as they propagate through the measurands into the results. DUA has many uses, for example, in the Design phase to guide decisions on suitable instrumentation or inform the design of new instruments and procedures; in the

Construct phase, to determine whether changes in procedure are required to drive accuracy under the uncertainty budget; in the Debug phase, to verify operations of the measurement system and calibrations; in the Execute phase, to provide balance checks and monitor the operation of apparatus; in the Analysis phase, to guide the choice of analysis technique; and in the Report phase, to quantify the quality of reported results [160, 60].

Reported results thus consist of obtained values and clear statements of the uncertainty associated with those values, and are not considered complete without such uncertainty statements. It follows these uncertainty statements provide the basis to decide whether, for example, numerical results agree with data or lie outside the experimental uncertainty, or data sets between two model scales or different laboratories agree or disagree. It is now common practice for quality journals, funding bodies, and due diligence audits to request uncertainty statements with reported results [160].

This section presents the principles of DUA according to the three uncertainty analysis stages shown in Fig. 3.2, and alongside the applications to this OWC experiment.

Stage 1. Formulate *1.a Define the measurand*

Here we assume the measurands of the experiment have already been defined in the GUA (§ 3.3 and Fig. 3.3). The only difference is the measurands y and input quantities x_i may now be considered as an expectation (the result of a measurement), so the notation is lower case: $y = f(x_1, x_2, \ldots, x_N)$.

1.b Identify uncertainty sources

Identifying uncertainty sources is practically the same process here as in GUA, except now the uncertainties of the x_i are considered in more detail – separate components evaluated differently, as described in the next step.

3.5.1 Example: Identifying uncertainty sources in wave power

Figure 3.11 shows an example of a cause-and-effect diagram used to identify uncertainty sources for key measurands wave power P_W and OWC power P.

1.c Evaluate standard uncertainty

Every x_i has a standard uncertainty associated with it, consisting of components evaluated using two methods: Type A and Type B. Evaluating Type A standard uncertainty $u_A(x_i)$ requires estimating the mean $\bar{q}$ of n independent observations/repeats q_k which are characterised by a PDF,

$$\bar{q} = \frac{1}{n}\sum_{k=1}^{n} q_k, \tag{3.4}$$

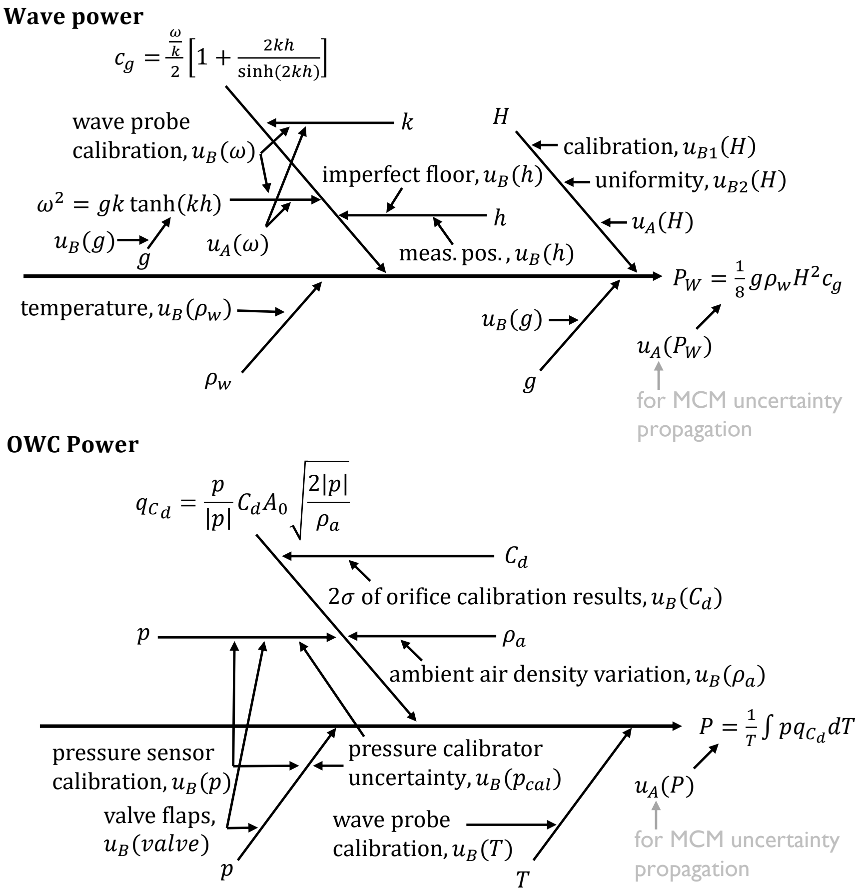

Figure 3.11: A cause-and-effect diagram used to identify uncertainty sources. Example is of wave power P_W and OWC power P, where the $u_A(x_i)$ is the Type A uncertainty and $u_B(x_i)$ the Type B uncertainty.

and the experimental standard deviation of the mean $s(\bar{q})$,

$$u_A(x_i) = s(\bar{q}) = \sqrt{\frac{\frac{1}{n-1}\sum_{j=1}^{n}(q_j - \bar{q})^2}{n}}. \tag{3.5}$$

According to *GUM* [21] the general conditions for experiment repeatability [17] are: (1) the same measurement procedure; (2) the same measuring instrument used under the same test conditions; (2) the same laboratory or field site; and (4) repetition over a short period of time, roughly one day. The repeats should comprise sequential and non-sequential runs [17].

Evaluating Type B standard uncertainty $u_B(x_i)$ requires judgement, experience, and all available information to first identify which of the large number of possible uncertainty sources are significant and, second, to estimate numerical values for the significant sources. Means other than statistical analysis are used, but $u_B(x_i)$ is also characterised by the standard deviation of an assumed PDF. Assigning the $u_B(x_i)$ PDF, or a set of PDFs as often quantities have several Type B sources, is based on the scientific judgement of a pool of comparatively reliable information on the possible variability of x_i. As the experimental program progress so to increases the available $u_B(x_i)$ information. At the Design phase, the information typically consists of (1) previous measurement data; (2) previous experience with or general knowledge of the nature of the phenomena or process and instrumentation; (3) reference material provided by suppliers in terms calibrations and other certificates; and (4) uncertainties assigned to reference data taken from handbooks. In subsequent experimental phases, the available information increases as apparatus is assembled, instrumentation installed, calibrations performed, and experimental runs run.

Insofar as it is possible, $u_B(x_i)$ evaluations should be based on quantitative information. Such an evaluation is as much an art as it is a science; it depends on detailed knowledge of the measurand, the measurement procedure, and common sense and experience. The quality and utility of a $u_B(x_i)$ estimate therefore relies on the understanding, critical analysis, and integrity of those who assign its value [157]. This does not, however, preclude $u_B(x_i)$ estimates from being as realistic as $u_A(x_i)$.

Stage 2. Propagate: Determine combined uncertainty

In this uncertainty analysis stage the standard uncertainties of the x_i, identified using cause-and-effect diagrams (Fig. 3.11), are propagated through the measurand function y to determine the combined standard uncertainty $u_c(y)$. There are various methods to propagate uncertainty, however as said, this work focuses only on the Monte Carlo Method.

Fig. 3.12 shows the process of MCM uncertainty propagation in DUA. It illustrates the general process for propagating uncertainty through any number of measruand levels, where the top-level measurand can be a function of multiple lower-level measurands and quantities. Multi-level measurands are common for WEC experiments, as shown in the wave power measurand example in the cause-and-effect diagram (Fig. 3.11). The MCM process is as follows. First, we input measured nominal values of each quantity $x_{i,nom}$, and $u_{B,k}(x_i)$ (where $k = 1 : N$ number of Type B uncertainty sources). The $u_A(y)$ is also input for the top-level measurand y (in this example, $u_A(y)$ is included only for the top-level measurand, however, $u_A(x_i)$ can be used for each x_i and propagated that way - see [60]). The standard uncertainty components are assumed to be the standard deviations of their PDFs. The PDFs for $u_{B,i}(x_i)$ are here assumed to be Gaussian, but others may be used. If two x_i's share a u_B, or two x_i's are correlated, a joint PDF can be assigned. Then, at each iteration j, $u_{B,k}(x_i)$ is multiplied by a randomly sampled number from the assumed PDF (varying about 1), and added to $x_{i,nom}$ obtain the 'measured' values x_i(j). The top-level measurand y(j) is then calculated with the included $u_A(y)$ term multiplied by a randomly sampled number from the

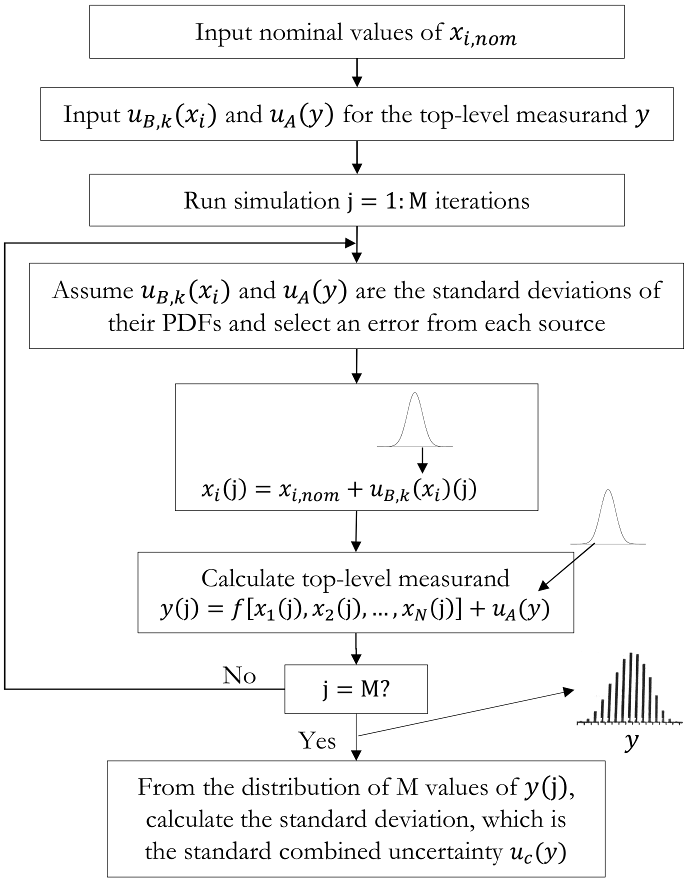

Figure 3.12: Flow diagram of the Monte Carlo Method to propagate uncertainty in detailed uncertainty analysis. The example shows the flow of the MCM when there are multiple levels of measurands with one or more input quantities. It also shows a case where input quantities are correlated, so a joint PDF is assumed for $u_{B,2}$.

PDF, comprised of the repeated observations of y in the experiment. The sampling process is repeated M times to obtain a PDF for y. The output of the MCM is the standard deviation of the PDF of y, taken as the combined standard uncertainty $u_c(y)$, which is part of Stage 3 as below.

Stage 3. Summarise: Summarise uncertainties

To summarise propagated uncertainties in DUA is essentially same procedure as in GUA (§ 3.3), where we use the PDF of y to obtain: the mean of y; the standard deviation of y, taken as the combined standard uncertainty $u_c(y)$; and a coverage interval k_c containing y with a specified probability, which gives the expanded uncertainty $U = ku_c(y)$. This Summary stage includes presenting the detailed uncertainties in key quantities and measurands and any other important uncertainty-related information. The form of presentation generally consists of uncertainty results presented in tables or graphs, in the form $x_i \pm u_{A,B}(x_i)$ and $y \pm U$.

The rest of this section describes the details of the OWC WEC experiment and demonstrates how GUA was and could be used at key phases of the experimental program. The structure of the section is based on the experimental phases of Design, Construct, Debug, Execute, Analyse, and Report (Fig. 3.1).

3.5.2 Design, construct, and debug

These phases are often iterative, so are here presented together (Fig. 3.1). The Design phase builds on the information and knowledge generated in the GUA to specify instrumentation and details of experimental apparatus configurations. The test plan, parameters, and procedures are also identified and decisions made on the data to be obtained, and the scope and sequence of conditions and runs. This process can be guided by Design of Experiment (see for example [17, 42]). Additionally, at this point technical drawings of the model and moorings are created and issued for manufacture.

The parameters of this experiment are summarised in Table 3.1 and Fig. 3.13. The table and figure describes the model and environmental parameters, measurement and data parameters, and the experimental conditions. All values are given in full-scale unless otherwise stated (apply the Froude scaling law to obtain model scale values).

In the Construct phase, the apparatus is assembled, calibrations carried out, and initial runs performed. The Debug phase follows, in which unforeseen problems are addressed. The completion of these phases is indicated by the apparatus operating as expected and factors influencing uncertainty in the results well understood. In addition, incoming data are monitored using built in checks to guard against unnoticed and unwanted changes in the apparatus or operating conditions. DUA can inform all these processes. This section describes how DUA was applied to quantify and assure the quality of instrument calibrations in the Construct phase and throughout the OWC experiment.

3.5.2.1 Example: Evaluating Type B uncertainty from instrument calibrations

This section presents two examples that demonstrate the use of DUA for instrument calibrations, one for wave probe calibration and one for the in-situ force balance calibration. The example concerns step 3 of the Formulate uncertainty stage: Evaluate standard uncertainty (Fig. 3.2). In this experiment the instrumentation was calibrated before the experiment, and when required at experimental condition changes. Wave probes were calibrated at the beginning of each day and after an experimental condition change. The method used to calibrate the wave probes was, briefly, establishing a linear relation between known distances of probe insertion into the water and the corresponding voltage response. The output of

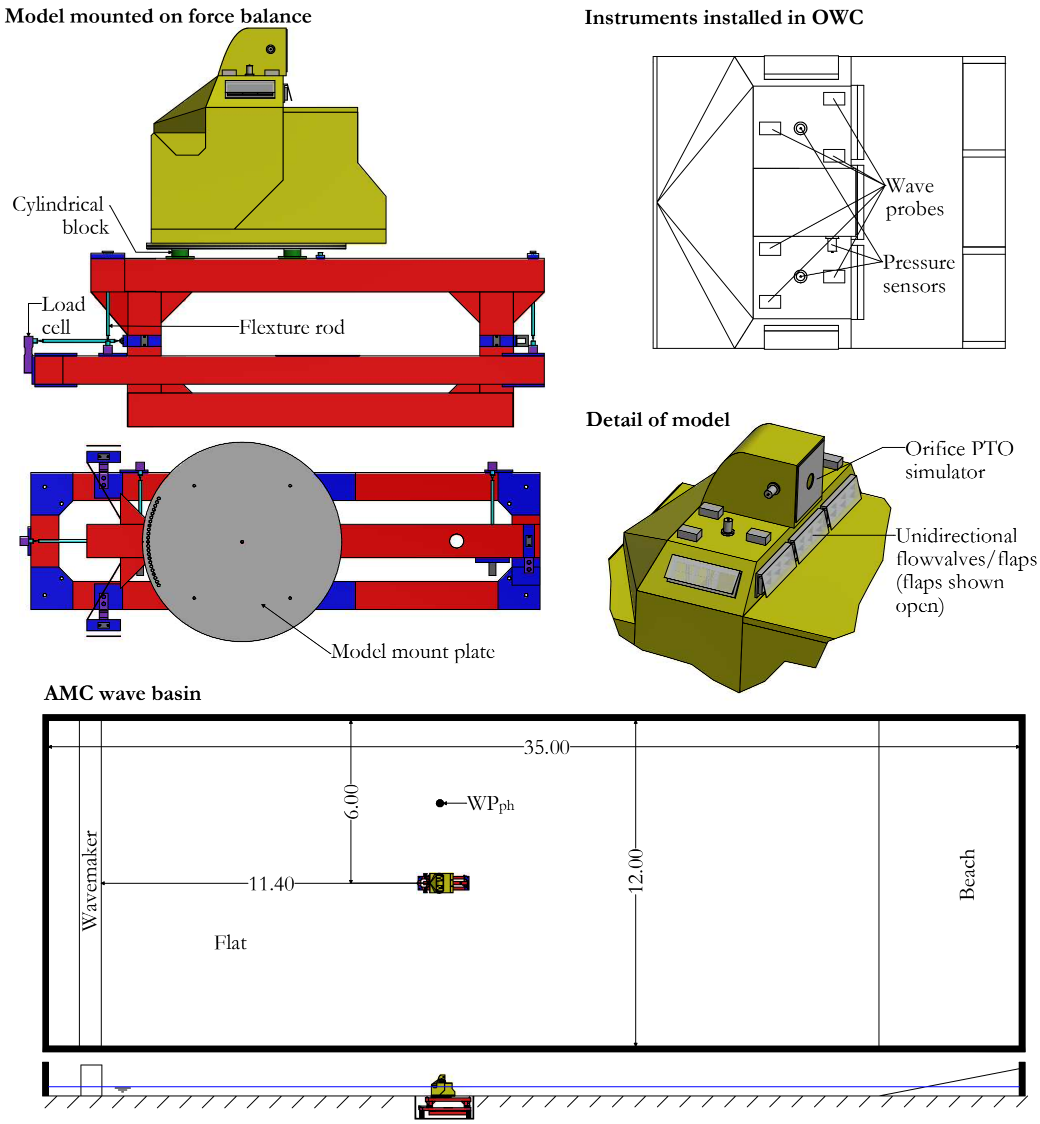

Figure 3.13: Diagram of important aspects of the OWC model and the AMC Model Test Basin. Annotations reveal instrumentation configurations and the general layout of the model installed in the wave basin. WP_{ph} is the phase wave probe.

such a calibration and way in which we evaluate the Type B standard uncertainty associated with the calibration is as follows. Given wave probes output a linear response, a linear fit of the calibration data is applied. The estimate of $u_B(x_i)$, where the x_i could be any wave parameter of interest such as wave height H or period T, is the standard error of the estimate (SEE):

$$u_{s,B} = SEE = \sqrt{\frac{\sum (y_j - \hat{y}_j)^2}{M-2}} \tag{3.6}$$

Table 3.1 Parameters of the experiment.

Parameter	**Details**
Model	Bottom-standing unidrectional flow OWC. 1 Froude-scaled model (λ_{30}). Body constructed from marine plywood, Perspex, and fibreglass. Orifice plate PTO simulator: 1:150 orifice/chamber area ratio. Unidirectional flow valves simulated with passive flaps (thin, robust plastic sheets) designed to negligibly influence OWC pressure on the upstroke when the valve flaps open, and create an airtight seal on the downstroke when the valve flaps close. The mass properties of the flaps was not Froude-scaled because the material/mechanism for the prototype was unknown at the time.
Environment	Shallow water wave basin - 35 m L x 12 m W x 0-1 m D. Sixteen element Piston-type wavemeker; vertical walls; passive beach. Fresh water, at 15-20 °C Water depth for experiments = 10 m.
Measurements; instrumentation; calibrations;	Wave elevation in basin; conductive wave probe; calibrated daily. Wave elevation in OWC; 6 conductive wave probe (see Fig. 3.13 for layout); calibrated daily. Pressure in OWC; 3 x Honeywell Controls TruStability pressure sensor connected to Ocean Controls KTA-284 instrumentation amplifiers; calibrated weekly to ±2000 Pa. Hydrodynamic loads on model; 6-component force balance; calibrated before and after each scale experiment.
Data acquisition	National Instruments PCI-6254M Multifunction Data Acquisition Card, recorded on a HP computer, controlled with Labview software. All data acquired at 200 Hz.
Data recording	Regular waves: 30 seconds (model-scale). Irregular waves: 30 minutes
Wave conditions	Regular waves: $H = 1.8, 2.4, 3.0$ m; $T = 8 - 15.8$ s ($kh = 0.41 - 0.98$). Irregular waves (JONSWAP): 15 sea states: $H_s = 0.75 - 4.75$ m, $T_p = 7 - 19$ s.
Model conditions	Incident waves without model: all waves. Power matrix: operational waves. Loads (system open): operational waves.

where M is the number of calibration points, y_j is the calibrated data point, and $\hat{y_j}$ is the fitted value. Further details on linear and nonlinear calibration curve fitting and uncertainties is provided in ITTC 7.5-01-03-01 [163]. An example of a calibration curve of a wave probe in the experiment, and its standard Type B uncertainty ($u_B(x_i) = SEE$), is given in Fig. 3.14. The residuals (blue squares) are also shown on the secondary axis to emphasise the variation of each data point (black circles) about the regression line. The $u_B(x_i)$ estimate here forms one component of the multiple Type B components of η_{inc} and its related wave parameter quantities of H, T, c_g, etc. (see Fig. 3.11). A similar process can be carried out to estimate $u_B(x_i)$ for other instruments such as pressure transducers. For a pressure transducer, however, there is an additional significant u_B component to estimate, the pressure calibrator used to calibrate the pressure transducer in the first place. Such an estimate is based on manufacturers specifications.

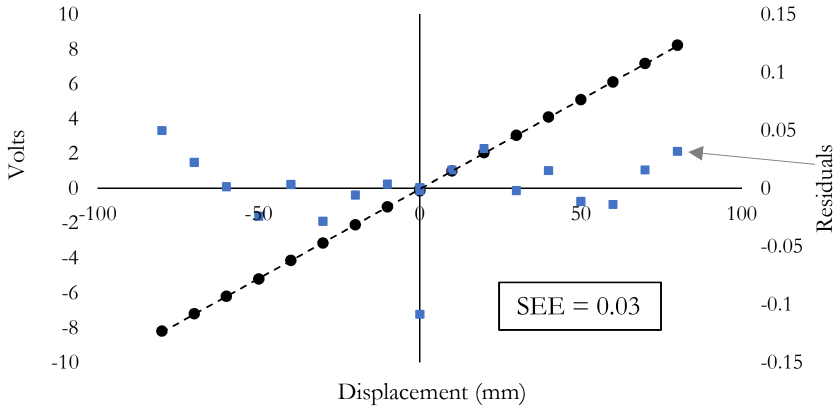

Figure 3.14: Example of a calibration curve of a wave probe, with included residuals and SEE calculation

The more complicated six-component force balance calibration method and uncertainty evaluation is as follows. The following section describes first the measurement procedure and calibration method, with Appendix A presenting detailed information on the instrument itself and the calibration method. After, it describes how DUA was applied to reduce the uncertainty in the calibration that contributes to the overall uncertainty in the load measurements.

The complete hydrodynamic loads imposed on the OWC by waves were measured with a six-component external force balance (see Fig. 3.13). In addition to measuring forces/moments the force balance, which was secured in a pit below the basin floor, provided a console for mounting the model such that its bottom was aligned and planer with the basin floor. The calibration was done in-situ, with the rationale here based on two advantages with respect to reducing measurement uncertainty, thereby giving greater confidence in the load measurements. First, 'in-situ' means that the force balance was installed in its exact place of measurement and conditions of use, with all its model connections and components installed, and water covering the instrument for temperature consistency. This eliminated the possibility of structural or sensor changes that might occur if the calibration was carried done out of water and then installed. The second advantage is that the sensor cables from the six load cells were connected directly to the DAQ used in the experiment, thus reducing systematic effects related to instrumentation, and enabling an end-to-end calibration, as specified in

ITTC Procedures and Recommendations [11]. A full calibration routine was carried out before and after experimental runs, producing two calibration data sets. The post experiment calibration data set provided both a check to see if the calibration matrix had changed significantly during the tests, and also additional data to estimate the measurement uncertainty of the hydrodynamics loads.

During the calibration, to determine if the calibration matrix had been sufficiently resolved and had acceptable uncertainty, DUA was applied. The Type B uncertainty $u_B(x_i)$ of the calibration matrix was evaluated by calculating the standard deviation of the applied and fitted loads, and including other $u_B(x_i)$'s related to the calibration procedure (see following section for details). If the uncertainty was too high during the calibration, with the standard deviation of applied/fitted loads being the dominant factor, an additional combined loading condition was carried out to better resolve the calibration matrix and reduce the standard deviation (therefore uncertainty). Appendix A shows examples results of the applied vs. fitted loads after a calibration. Furthermore, the force balance was calibrated before and after the experiment, to generate a 'repeat' data set from which the Type A uncertainty was evaluated. The foregoing example thus demonstrates how DUA can be used in the Construct phase to reduce uncertainty in loads measurements arising from the calibration.

3.5.3 Execute

In the Execute phase runs are carried out and the data acquired, recorded, and stored. During this phase the focus of DUA shifts toward evaluating Type A standard uncertainty, assuming the Type B standard uncertainties have already been evaluated. Evaluating Type A uncertainty requires performing a series of repeat runs at representative set points at various times throughout the experiment. To avoid the laborious, time-consuming task of performing many repeat tests for all quantities at all set points in all conditions, a sound approach is to select several representative set points and conditions, and work backwards from the top, that is, backwards from the highest-level measurands. This top-down approach generates a data set from which we calculate $u_A(y)$ of the top-level measurand y. If this $u_A(y)$ data set cannot be produced directly, then the x_i upon which y depends can be split up and data sets produced for the groups of x_i, which may themselves be lower-level measurands with input quantities. In this way, producing a $u_A(y)$ data set for y inherently produces a Type A data set for the input quantities $u_A(x_i)$, so that if the uncertainty results of these x_i are useful to report, no extra effort is required to do so. To illustrate this top-down approach of evaluating Type A uncertainty, examples for regular and irregular waves follow.

3.5.3.1 Examples: Evaluating Type A uncertainty

This section presents two examples of Type A uncertainty evaluation, one for regular waves and one for irregular waves. It is concerned with step 3 of Formulate stage, that is, evaluating standard uncertainty (Fig. 3.2). We being with the regular wave example. The top-level, power-related measurand is capture width ratio, $C_W = P/P_W B$ (Eq. (2.10)), with OWC power $P = (1/T)\int pq\, dT$ (Eq. (3.1)), wave power $P = (1/8)\rho_w g H^2 c_g$ (Eq. (2.1)), and OWC width B. It was not possible to directly produce one data set of repeats to calculate $u_A(C_W)$, because P_W required measurements of incident waves at the WEC model location but without it installed. On the other hand, P required the model to be installed. So, there needed to be two separate $u_A(C_W)$ data sets, one for wave power $u_A(P_W)$ and one for OWC power $u_A(P)$. A reasonable $u_A(P_W)$ data set required repeats of regular waves at several set points in various experimental conditions, in this case, several wave periods and wave heights that span their respective ranges. With regards to selecting the number of repeats n, the general rule of thumb is at least 10 [17], which produces a reasonably representative sample of a quantity's population PDF from which the relevant statistics may be calculated (mean, standard deviation, coverage interval). Thus if one n is considered to be one run then 10 runs are required. However, because a typical regular wave run in WEC experiments contains multiple individual waves, these individual waves can themselves be considered to be an n, as per the method developed in [41] (Appendix D). In effect, the required number of repeat runs for each set point can be reduced from 10 runs down to 3-5 runs consisting of a total of at least 10 'repeat' waves, thus saving time and money.

The x_i that significantly contribute to the random variation in P_W are incident wave elevation η_{inc} (from which wave height H is determined) and group velocity c_g (which is inferred from η_{inc}). Normally significant x_i require separate sets of repeats, however, in this case the x_i are derived from the same measurement of η_{inc}. So the $u_A(P_W)$ data set was produced by three to five repeat runs of incident waves at the model location without it installed. Each set of repeats were performed for a low, medium, and high wave frequency, at multiple wave heights. From this data set, $u_A(P_W)$ was calculated. The Type A data set for OWC power $u_A(P)$ was similarly obtained, with the same several set points for repeat tests, except with the model installed. A similar Type A uncertainty evaluation process was carried out for the other main measurands of this experiment, the hydrodynamic loads of surge force Fx, heave force Fz, and pitch moment My.

Fig. 3.15 presents a visualisation of these $u_A(x_i)$ data sets, which contain several set points of data of the significant quantities, for one regular wave height. The overlayed profiles seen in this figure show (1) individual waves representing independent repeats n; (2) the several representative set points of repeats, here with three set points of the lowest, mid,

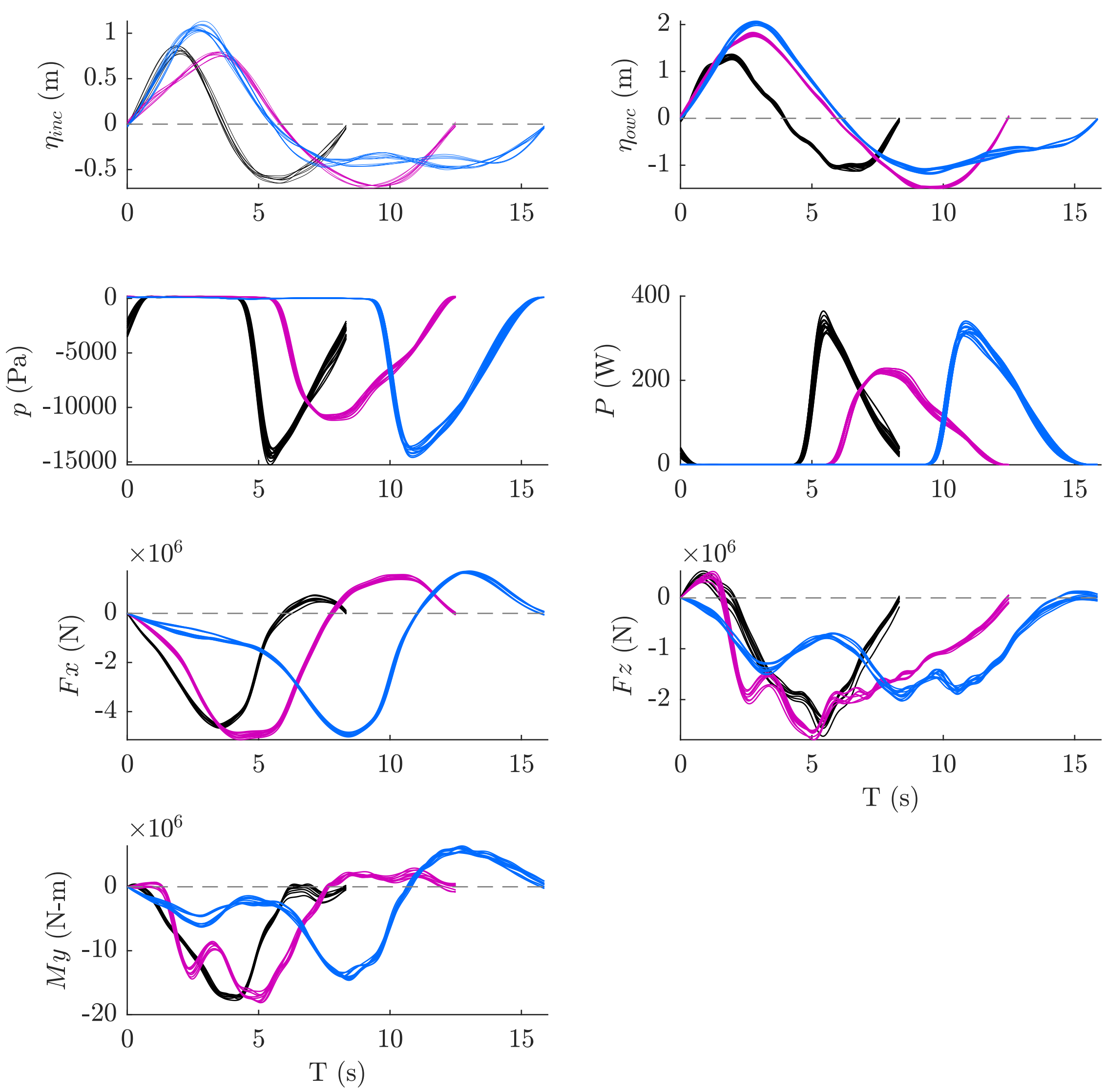

Figure 3.15: Overlayed wave profiles of individual waves taken from time series data of repeated independent observations. Plots show three wave periods (lowest, mid, highest) and one wave height. The magnitudes (e.g.., the amplitude, height, or integral) calculated from each individual wave are input into the Type A uncertainty calculation.

and highest wave period; and (3) how the variation in the key input quantity η_{inc} induces a similar variation in all other dependent quantities of η_{owc}, p, P, Fx, Fz, and My. Depending on the quantity, the magnitude that is used to calculate $u_A(x_i)$ is either an amplitude (as for Fx, Fz, and My), a height (as for η_{inc}), or an integral (as for p and P). Noted, $u_A(x_i)$ should be calculated whenever more information becomes available during the experiment. This simple, useful practice allows us to track uncertainties and decide if more repeats are needed to drive down the expanded uncertainty in the results. All Type A uncertainty results for this experiment are presented in the uncertainty summary given at the end of this main section (Fig. 3.18).

For irregular waves, Type A uncertainty evaluation was similar to regular waves in that a set of repeats were run in incident waves only and with the model installed to generate the necessary data sets to evaluate $u_A(x_i)$. This process involved performing a set of repeats for five sea states that ranged the wave climate considered, typically five repeats for each of the five sea states which was considered to generate a reasonably representative sample and realisation of the sea states under time constraints (irregular wave runs are much longer than regular waves). From the irregular wave $u_A(x_i)$ data sets the power- and load-related statistics were calculated, and an average of these was taken to represent the Type A uncertainty for the entire power matrix and load matrix. These $u_A(x_i)$ for important quantities and measurands were then used as input, along with the $u_B(x_i)$, into the Monte Carlo simulations to propagate uncertainty to determine combined uncertainty. The next section presents these results.

3.5.4 Analyse and report

In these experimental phases the data are analysed and reported in a useful presentation that maximises the understanding and utility of the results. This section first describes data analysis techniques used in this work, followed by descriptions and examples of detailed uncertainty analysis applied in these experimental phases. Focus is on the second and third stages of uncertainty analysis: combined uncertainty, and summarising uncertainties (Fig. 3.2).

Data were analysed according to the ITTC Recommended Procedures and Guidelines [46]. For regular waves analysis, timeseries data were trimmed such that data used for analysis contained only that which was considered stationary (<5 % difference in wave heights), and waves that were not influenced by reflections (the number of individual was for a run ranged from 2-12, with low frequency waves having fewer waves selected for analysis per run due to shorter time for the reflected waves to reach the model). This analysis avoided having to perform a reflection analysis. A phase-averaging technique was applied to the regular wave timeseries to reduce the repeating wave cycles into one representative wave cycle (see [40] for detailed description of the technique). Briefly, phase-averaging reduces any number of repeating waves or polychromatic wave sequences into one averaged wave phase (0 to 2π), by assembling the sampled data points into bins (for example 101 bins per wave cycle) and averaging all the data points within in each bin and corresponding bins in the timeseries. From this phase-averaged profile various wave parameters can be calculated – wave height, period, etc. This serves to reduce uncertainty in the analysis, and simplifies the usage and presentation of data sets. For the irregular waves analysis, a Fast Fourier Transform (FFT) was applied to the cropped timeseries data. Welch's power spectral density estimate method (pwelch function in MATLAB) was used to transform time domain data into the frequency domain. Irregular wave parameters (significant wave height, energy period, etc.) were calculated from the spectral moments of the energy density spectrum as per equations above (§ 3.3).

3.5.4.1 Example: Determining combined uncertainty

The combined uncertainty $u_c(y)$ was determined by propagating uncertainty using the Monte Carlo Method. For regular waves, Monte Carlo simulations were set up as per Fig. 3.12, one simulation for each regular wave frequency and height. The assigned $u_A(x_i)$ and $u_B(x_i)$ was unique for each frequency across several wave heights, differing depending on the number of repeats, the instrument calibration corresponding to the data, and other $u_B(x_i)$ sources. The power and load-related measurands were calculated for $M = 10,000$ iterations, from which $u_c(y)$ was calculated (the standard deviation of the PDF). A 95% coverage interval was selected and applied to the measurand PDFs to obtain the expanded uncertainty and summarise the uncertainties (see § 3.3). A similar process was performed for irregular wave results. The main differences were (1) one MCM simulation per sea state, and (2) for each sea state the $u_A(x_i)$ was a unique, averaged value of the repeats from five sea states (as described in the above example). The results from the data and uncertainty analyses are shown in Fig. 3.16 for regular waves and Fig. 3.17 for irregular waves. Fig. 3.18 also summarises the uncertainties in key measurands in a table-like form.

3.5.4.2 Example: Summarising uncertainties

Regular wave results showed a reasonable level of uncertainty (Fig. 3.16 and **??**). The largest expanded uncertainty overall was in C_W, averaging ±16% with a maximum of ±25%. These uncertainty levels were expected considering C_W is a top-level measurand that is a function of P_W and P, which are themselves functions of many inputs, thereby making C_W sensitive to uncertainty due to its many inputs. These uncertainty results are comparable to similar experiments [40, 41] and to similar work [39, 38, 164]. The uncertainty in loads of F_x, F_z and M_y were relatively smaller, averaging ±6% with a maximum of ±10%. The uncertainty in kh was small, less than ±2%, which is to be expected for wavemakers that generate highly repeatable wave period. In both regular and irregular waves, u_B tended to be larger than u_A.

Uncertainty results in irregular waves are summarised in a power matrix and load matrix (Figs. 3.17 and 3.18; see figure caption for guidance on reading the plots in Figure 3.17). The uncertainty results were similar to those in regular waves, but with C_W uncertainty relatively smaller, averaging ±11%. The loads uncertainties were practically the same.

Key causes of uncertainty in C_W were measurements used to derive the lower level measurands (wave power P_W and OWC power P) and PTO modelling. For P_W, the critical

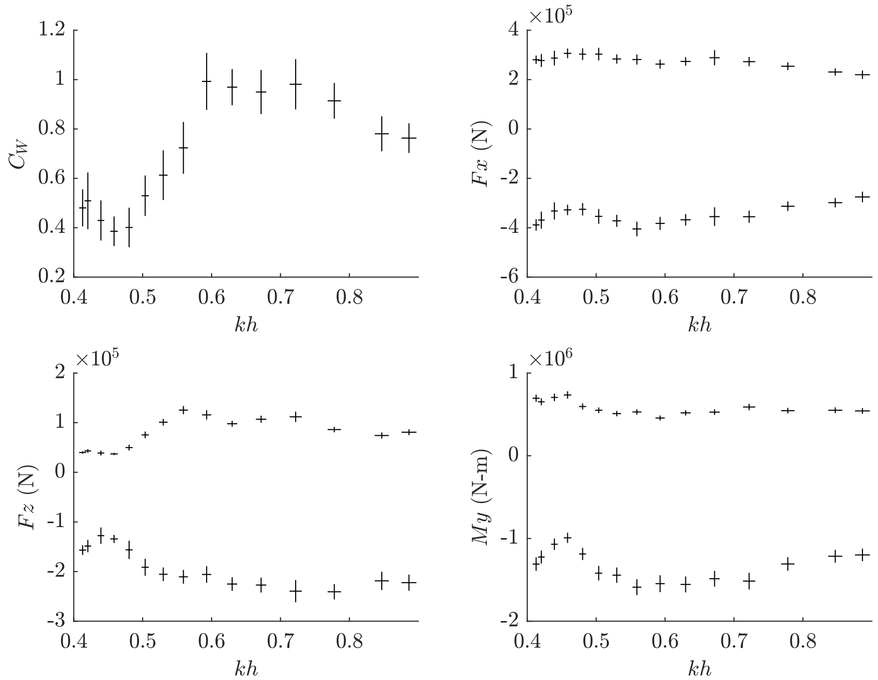

Figure 3.16: Key power and load measurands in regular waves, with error bars representing expanded uncertainty to 95% coverage interval.

measurement, therefore key uncertainty in this measurand, was incident wave elevation. For P, the dominant uncertainties were measurements of p and η_{OWC} used to derive q and, in turn, C_d. Another possible key uncertainty source in P is the modelling of the valve flaps as robust yet lightweight flaps, whose mass properties were not froude-scaled to 1:30 scale. It is plausible that this aspect of the PTO modelling may be a dominant uncertainty in power, if in the prototype the valve flaps have a strong influence on OWC chamber dynamics. With neither knowledge of the mass properties of the prototype valve flaps nor full-scale results to compare with, it was difficult to assign a Type B uncertainty to the modelled valve flaps. This represents a modelling challenge that requires further research. However, because $u_A(P)$ was relatively small, this indicates that the simulated valve system was well-designed for the model-scale tests.

3.6 Discussion

To appropriately address the specific needs of this PhD and the wave energy field, this work is necessarily a compromise between describing the main aspects of the experimental work and uncertainty analysis relevant for the following two chapters, and a broader investigation that has useful implications for the WEC model test community. As a result, there are several limitations that require highlighting and discussion, to ensure the methods and results are properly applied and implications understood.

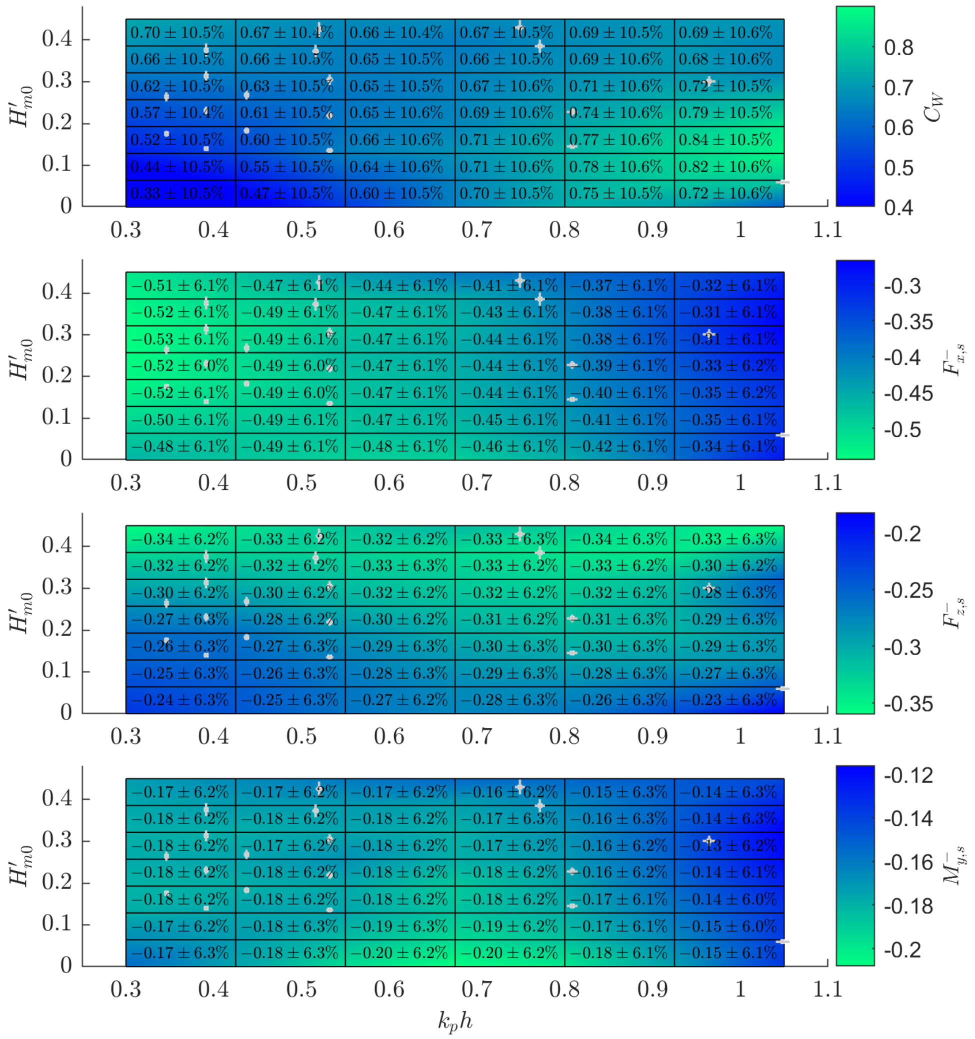

Figure 3.17: Key power and load measurands in irregular waves, for a matrix of H_{m0} vs k_ph sea states. Measurands are dimensionless and normalised by the calculated H_{m0} for each sea state. The text in each coloured cell is in the form of "interpolated value of the measurand (z-axis) $\pm$ expanded uncertainty. The white markers indicate the actual H_{m0}/T_e values, with error bars representing expanded uncertainty to 95% coverage interval. Colour of cells: green represents greatest magnitude, whether positive or negative.

First, the work is a case study, with one WEC type, the OWC, investigated under one kind of experiment typical of TRL 1-4. Therefore, the examples of uncertainty analysis given are specific to OWC WECs and similar experiments. Uncertainty analysis principles are however independent of application. So although the work focuses on evaluating uncertainties of a realistic OWC WEC with a unique PTO (vented unidirectional air flow), it may nevertheless be informative for future experiments with different WECs at different TRLs. Despite ITTC's *Uncertainty Analysis for a Wave Energy Converter* publication, it is apparent that further research is needed in this area to investigate the unique challenges of uncertainty

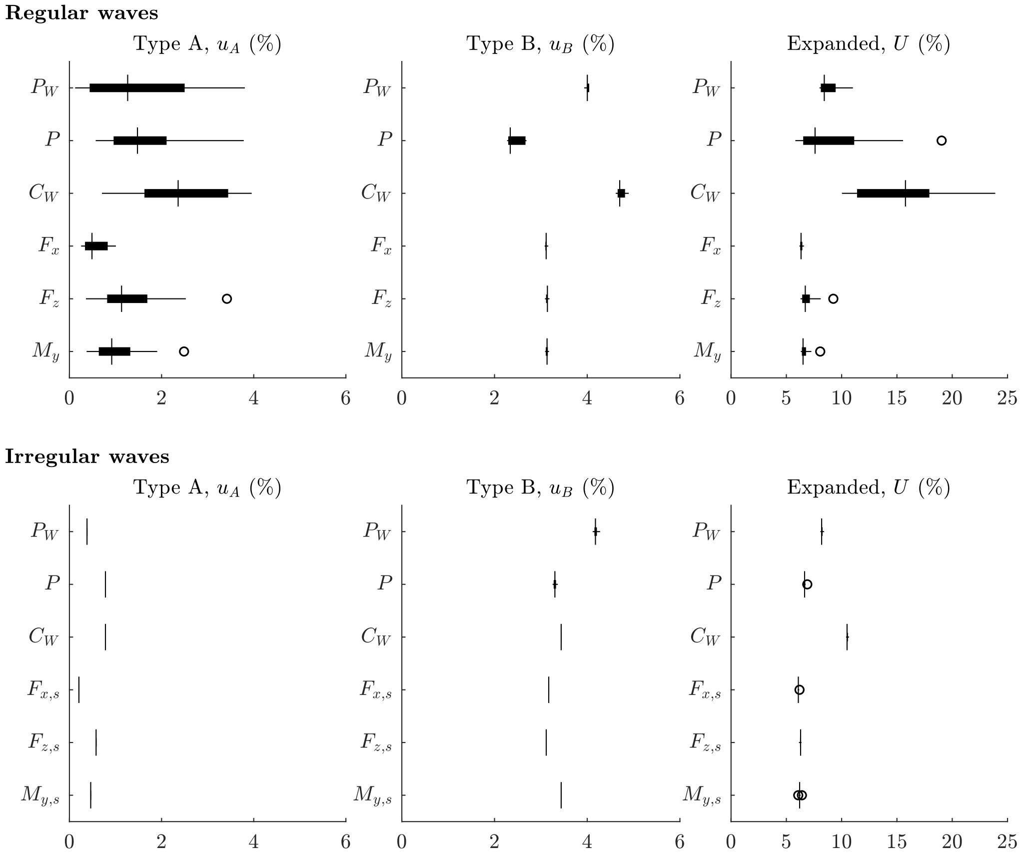

Figure 3.18: Uncertainty of key measurands shown as box and whisker plots (distributions). For **Regular waves**, the u_A distribution includes all wave frequencies and heights; the u_B distribution includes all instrument calibrations carried out throughout the experiment and other u_B sources; the U distribution includes all standard uncertainties, determined by the Monte Carlo Method. For **Irregular waves**, u_A is based on five representative sea states, and u_B and U were obtained similarly as regular waves.

analysis in a range of experiments, WEC types and arrays, for example, point-absorbers (like [38, 39]), terminators, attenuators, and designs with flexible materials. In addition, much work is still to be done on uncertainty analysis for ocean tests of WECs, building on the seminal work in this area [152].

Second, we presented but a small sample of the many uses of uncertainty analysis in experimentation. Other references provide many more applications that can be drawn upon to aid the understanding and use of uncertainty analysis in still further applications in WEC experiments [60, 118].

Third, this work focuses on the MCM for uncertainty propagation. The MCM is the preferred method according to [60], and the *Guide to the expression of uncertainty in measurement* [118] recommends it for applications relevant to WEC experiments which are often characterised by multiple nonlinear, time-dependent quantities — waves, power-related quantities, and their interactions. The MCM is advantageous in such situations due to its relative ease of implementation especially for phase-averaged quantities (e.g. OWC power), its ability to reduce uncertainty analysis effort, and its superior accuracy compared TSM which linearises the measurement model and thus may provide an inadequate representation. However, this work does not substantiate the claimed advantages of the MCM over the TSM, which would require a rigorous comparison of uncertainty results when propagated by the MCM and by the TSM. This is reserved for future work.

Fourth, the uncertainty analysis for irregular waves here presented may be considered basic, not comprehensive. Dedicated investigations are needed on this subject as there are many identified issues with simulating and measuring realistic irregular wave sea states, and WEC responses to these, in wave basin experiments [101, 20]. To a large degree evaluating uncertainty in the power matrix and load matrix, based on a reduced set of wave parameters, is not well understood [105, 104, 102, 107, 103, 109]. Further, extrapolating model scale data and uncertainty to predict prototype performance and risk is a subject in need of further investigation [18].

Fifth, we used linear wave theory to calculate wave power of the nonlinear waves, which may have introduced a non-negligible uncertainty into wave power calculations. This uncertainty could perhaps be reduced by applying a higher order theory [165]. This uncertainty could be investigated in future work.

Finally, while the work provided a comprehensive list of possible uncertainty sources in WEC experiments (Fig. 3.4), it focuses more on *measurement* uncertainty, less on *experimental* uncertainty. Whereas measurement uncertainty generally includes uncertainties arising from environmental and model parameters, instrumentation and its implementation, human factors, data reduction and definition of the measurands, experimental uncertainty includes said sources plus broader uncertainties such as scale effects and laboratory effects. The following two chapters address these (Chapters 4 and 5).

The foregoing discussion reveals the contributions of the work to this PhD and to the wider wave energy field. The work (1) argues for the importance of understanding and using uncertainty analysis and its interdependent relation to experimentation, that is, its ability to assure and quantify the quality of experimental results; (2) provides a comprehensive demonstration of why, how, and when uncertainty analysis can be used in various phases of an experiment such as a hydrodynamic model test; (3) introduces the wave energy field to new aspects of uncertainty analysis, including GUA, means to identify uncertainty sources (cause-and-effect diagrams), and the MCM to propagate uncertainty; and (4) provides the means to objectively compare experimental data sets obtained at different scales and in different laboratories in the other parts of this PhD research (Chapters 4 and 5).

3.7 Conclusions

Uncertainty analysis is neither well understood nor widely used in hydrodynamic model test experiments of WECs. This finding became apparent by (1) scarce WEC experimental studies reporting results *and* uncertainty; (2) undeveloped WEC-specific uncertainty analysis guidelines; and (3) limited studies to inform said guidance. These limitations are striking given critical decisions in WEC development are based on the results of model tests. Therefore, further technical investigations are needed to enhance the understanding and uses of uncertainty analysis in WEC model test experiments, and such investigations should be incorporated into future guidelines.

Uncertainty analysis assures and quantifies the quality of experimental results. Through a comprehensive uncertainty analysis applied to the 1:30 scale WSE OWC model experiment, we demonstrated how uncertainty analysis assures the quality of results through GUA, and quantifies the quality of results through DUA. A three-stage structure – formulate, propagate, summarise – composed of the uncertainty analysis principles provides a systematic means to carry out both GUA and DUA.

GUA is an effective and efficient means to help plan and design an experiment. Through a comprehensive example of determining the least uncertain method to derive OWC power, we demonstrated how GUA can provide an integrated grasp of and generates valuable information about an experiment before it begins. GUA can also give insight into and guide decisions on which approach might best achieve the test goals, which quantities will likely govern the overall uncertainty and therefore require special attention, or which aspects of the laboratory, apparatus, or measurement system might cause troubles. The initial extra time, effort, and resources invested in performing GUA will almost certainly lead to a higher quality experiment and may save time, effort, and resources in the long run. Therefore, GUA should be used in WEC model tests and incorporated into future guidelines.

Cause-and-effect diagrams effectively and efficiently identify uncertainty sources. A review of uncertainty sources in hydrodynamic experiments, focusing on WEC experiments, revealed for the first time a broad and detailed list of possible uncertainty sources. Having defined the measurands of an experiment, cause-and-effect diagrams enforce a complete examination of all dependent quantities of the measurands and their many possible uncertainty sources, through a concise visual representation. They also prompt such questions as: Which uncertainty sources are significant? How to avoid/evaluate/quantify/combine these uncertainties? Therefore, these diagrams should be used in WEC model tests and incorporated into future guidelines.

The MCM is an accurate and straightforward to implement method for uncertainty propagation. It is accurate due to its direct numerical application to propagate uncertainties of any magnitude through nonlinear measurand functions (more accurate than the Law of Propagation of Uncertainty (Taylor Series Method) in cases with considerable nonlinearity or the uncertainty is relatively large). Its implementation is relatively straightforward, and the analysis effort often reduced, due to the direct numerical application and avoiding having to provide partial differentials of difficult measurand functions, which may be time-varying quantities or contain multiple lower-level measurands or both (such as capture width ratio). In many engineering fields the MCM has become the primary uncertainty propagation method. Therefore, the MCM should be used in WEC model tests and incorporated into future guidelines.

DUA involves evaluating Type A and Type B standard uncertainties, propagating these to produce PDFs of the output measurands, and summarising the uncertainty (standard, combined, expanded) in at least the main results. For DUA of the 1:30 scale WSE OWC model experiment, we introduced a new method for evaluating Type A uncertainty that arguably more accurately quantifies this uncertainty component with fewer repeat runs required, thereby saving time and cost of experiments. Type B uncertainty evaluation was found to be a demanding yet important task; it requires judgement, experience and common sense, and interpreting whether, or to what degree, an uncertainty source is to be assigned to a quantity. Despite this, Type B uncertainty can be as quantitatively accurate as Type A uncertainty. The MCM was used to propagate uncertainty. Regarding the uncertainty results of the experiment, the expanded uncertainty in regular waves for capture width ratio was $\pm 16\%$ on average and $\pm 6\%$ on average for the surge and heave forces and pitch moment. Irregular wave results showed similar, yet slightly smaller uncertainty. Type B uncertainty tended to be slightly higher than Type A uncertainty. It is reasonable to infer that most WEC experiments will contain similar levels of uncertainty as in this experiment, because most WECs are characterised by nonlinear interactions (waves, motions, PTO) that increase measurement uncertainty and, likely, scale and laboratory effects.

Assessing power performance is a key requirement in most WEC model tests, but it is likely the most uncertain. This conclusion was based on several findings from the literature review and experimental investigations: (1) PTOs are generally modelled as simplified damping mechanisms rather than an exact scale-down version of the prototype PTO; (2) absorbed power is not measured directly but derived from measured or derived kinematic (motion) and dynamic (force) quantities, with the kinematic quantity often derived from the integral of the captor's displacement over time, which can introduce considerable uncertainty into the derived power; and (3) the model-prototype power disparity, where power is scaled to full-scale prototype values by the length scale raised to 3.5, which suggests that this highly nonlinear similitude condition is sensitive to errors when extrapolating model test results. Therefore, it is crucial to invest time and resources into evaluating uncertainties in power-related experimental results.

The demonstrated utility, arguably necessity, of uncertainty analysis in WEC model tests suggests further investigations are needed to expand the understanding and uses of WEC-specific uncertainty analysis. These investigations should include the various main WEC types, including oscillating bodies, other OWC WEC designs, overtopping devices, and flexible material-based WECs. Prioritising this work is important because uncertainty analysis can significantly improve the overall execution and outcomes of experiments. In particular, it can assure and improve the quality of experiments, and yield uncertainty statements about experimental results that enable those who use or have a stake in them — engineers, researchers, investors, auditors, publishers, etc. — to assess their reliability, to objectively compare them with similar results (e.g. compare results between multiple scales as in Chapter 4 or multiple laboratories as in Chapter 5), to assign appropriate risk levels when integrating them into broader contexts, and to make critical decisions based on the results and the known unknowns. On the contrary, if uncertainty in experiments is not evaluated or poorly understood, this could lead to reduced confidence in engineering design, incorrect comparisons within the literature, disillusionment with LCOE projections or other key techno-economic performance metrics, or increased business risk and investment barriers.

Importantly, uncertainty analysis is neither a routine task nor one in which a set of instructions are merely followed; it requires sound knowledge of experimental processes, measurands, and external influence factors, and demands scientific integrity, critical thinking, and interpretation of how the principles are to be implemented in different situations. This may appear to be a daunting task, but it is worthwhile, especially for WEC experiments that are relatively new, with new challenges and complexities. While laboratories are putting significant effort into developing procedures or improving existing ones to support these new kinds of experiments, the use of UA could enhance these efforts and lead to improved quality control. Noted, even with a well-developed UA, some sources of uncertainties cannot easily be removed or improved. Therefore, further research is needed to emphasise the key role UA can play in WEC model tests and to improve WEC-specific procedures for evaluating measurement uncertainty.

3.7.1 Recommendations for refining the international guidelines on uncertainty analysis for WECs

The following recommendations are offered based on this chapter. While the test laboratories should be responsible for the uncertainty, clients (developers, researchers, etc.) should also seek to understand the UA-related guidelines, as this will help with interpreting the uncertainty in experimental results and its implications for subsequent uses of the results.

1. Include a description and example of General Uncertainty Analysis.
2. Include the Monte Carlo Method as an alternative method to propagate uncertainty, with an example.
3. Include a description and example of cause-and-effect diagrams for identifying uncertainty sources.
4. Include an more comprehensive example of uncertainty analysis for a wave energy converter, including General Uncertainty Analysis and Detailed Uncertainty Analysis.
5. Define desired uncertainty levels for each Technology Readiness Level stage.
6. Define reporting minimums, such as: Type A, Type B, combined standard uncertainty, and expanded uncertainty, in at least the key measurands.

Chapter 4

Experimental Investigation into Scale Effects of an OWC Wave Energy Converter

Models help us understand, assess, predict; but they are limited, uncertain. To maximise the utility of WEC model tests it is critical to understand how limitations and uncertainties, such as scale effects, can influence model-prototype similarity. This work investigates uncertainty in model tests of the case study OWC WEC due to scale effects. It reports a series of 3D experiments at three model scales, through which we identify, quantify, and evaluate parameters causing scale effects in power and loads results.

4.1 Introduction

Two major sources of experimental uncertainty in hydrodynamic model tests can be scale effects and laboratory effects, with measurement uncertainty also important. The previous chapter addressed measurement uncertainty. The following chapter addresses laboratory effects. This chapter addresses scale effects. We consider 'scale effects' as a general term that encompasses all that which causes model-prototype dissimilarity, including 'model effects' arising from incorrect reproduction of prototype features such as geometry, wave generation, or fluid properties [23].

Scale effects are inseparable from hydrodynamic model tests due to physical and practical constraints, resulting in deviations between up-scaled predictions and prototype observations. Physical constraints arise from the inability to correctly model all force ratios [22, 23]. Typically one governing force ratio is scaled, such as inertia/gravity (Froude scaling) or viscosity/gravity (Reynolds scaling), and other forces assumed to negligibly affect the processes under investigation. However, sometimes the non-scaled forces in the model may not be negligible, causing scale effects. Practical constraints arise from the impracticability of modelling a feature of the prototype because it is too complex or not worth the investment to model it. A common example of this practical constraint in WEC model tests is that the Power Take-Off (PTO) is generally modelled as a simplified damping mechanism (see Chapter 2 and [11, 10]) rather than a scaled-down prototype of the PTO. Another practical constraint may be linear approximations in the generation of nonlinear shallow-intermediate waves.

To achieve model-prototype similarity experimenters must know or seek to find out which possible parameters might cause significant scale effects. Having identified such parameters, scale effects can be avoided, compensated, or corrected [23, 166]. To *avoid* scale effects, limiting criteria or rules of thumb may be followed, such as minimum model scale, allowing for scale effects to be reliably neglected. To *compensate* may involve distorting an aspect of a model, such as enlargening an OWC air chamber volume to correctly reproduce air compressibility [167, 88, 89, 168, 87, 169], or truncating water depth [57]. To *correct* may involve using empirical equations derived from sufficient information on the quantitative influence of scale effects [23]. What if the parameters causing significant scale effects are unknown or poorly understood?

To a large extent, this question characterises the situation in the wave energy field. Related maritime fields, such as offshore oil and gas structures [57] and hydraulic engineering [23], have accrued a substantial body of knowledge to account for scale effects, which may be applied to WEC model test. Doing so, however, carries risk [50], because WECs have unique characteristics which present unique modelling challenges [11]. For example, whereas offshore structures minimise motions, WECs tend to maximise them and use a PTO to convert such motions into useful energy. Thus, WECs are uniquely susceptible to scale effects.

While the WEC-specific body of knowledge to deal with scale effects is generally undeveloped [18], and very limited literature on scale effects between the laboratory and full-scale prototypes (one example is [170]), there are a growing number of studies addressing scale effects of WECs. Regarding OWC WECs, the focus of this study, most studies have focused on the air compressibility scale effect, including the approaches mathematical/numerical modelling [171, 172, 173, 174, 175, 159, 176, 177, 169, 178, 87] and physical/experimental modelling [167, 88, 35, 159, 179, 177, 168]. These studies mainly show that air compressibility can be detrimental to wave energy absorption and performance diminishes with the chamber volume, which could lead to 5–15% overprediction of OWC power performance.

A recent 2D experiment of a fixed OWC WEC claimed its behaviour was Reynolds number dependent, leading to a hydrodynamic scale effect that was the main cause of a $\sim$30% relative difference in capture width ratio between a small and larger model, the larger model having better performance [164]. This study also highlighted the practical difficulties of scaling the orifice PTO system. Another recent 2D experiment of a fixed OWC WEC investigated scale influences on both power-related and loads quantities [168]. The approach involved a small model with two chamber heights (chamber volume scale ratios of λ^3 and $\lambda^{2.7}$ where λ is the length scale) compared to a large model to examine air compressibility effects and hydrodynamic loads on the outer front wall of the caisson type OWC. The loads results were sporadic, with the smaller models encountering 10-200% relatively larger loads in smaller wave conditions, and ~20% relatively smaller loads in the largest wave conditions.

The present work builds on these previous works, but differs in the following ways. Here we report an experimental investigation into scale effects of an OWC WEC, which consisted of a set of 3D experiments with three scaled models of the case study OWC WEC (the Wave Swell Energy WEC described in Chapter 1). Given the sound knowledge of the air compressibility scale effect, and methods to compensate for it, this work focuses instead on identifying, quantifying, and evaluating other potential parameters causing significant scale effects in power-related and load quantities of OWC WECs. Thus, air compressibility is neglected in the modelling. The work reveals several newly identified parameters causing significant scale effects, and quantifies and evaluates their relative importance so that they may in the future be avoided, compensated, or corrected.

4.2 Dimensional analysis and similitude

This section briefly describes the dimensional analysis and similitude considerations for designing the scaled physical models (Appendix D provides the full description).

The relation between the model and prototype parameters is denoted by the *scale ratio* or simply the *scale*, defined as the ratio of a parameter X in the prototype (subscript p) to the value of the same parameter in the model (subscript m). That is

$$\lambda_X = \frac{L_p}{L_m} = \frac{\text{Value of L in the Protoype}}{\text{Value of L in the Model}} \tag{4.1}$$

where λ_L is the prototype-to-model scale ratio of the length parameter L. This definition of the scale ratio leads us to define the length scale ratio as $\lambda_L = L_p/L_m$.

From the dimensional analysis and hydrodynamic modelling considerations above, we decided to use three model scales – λ_{40}, λ_{30}, λ_{20} – to identify and quantify scale effects of the OWC WEC and, in doing so, investigate their contribution to experimental uncertainty. To compare the experimental results across scales, we organised the data into dimensionless quantities comprising the performance indicators of the OWC WEC (Table 4.1). All experimental data were first scaled up to full-scale according to Froude's scaling law, then nondimensionalised by the quantities given in Table 4.1.

Table 4.1 Dimensionless quantities used to compare experimental data across scales.

Dimensionless quantity	**Definition***
Wavelength-water depth ratio	$kh = \frac{2\pi h}{\lambda}$
Wave height-water depth ratio	$H' = \frac{H}{h}$
Wave steepness	$s = \frac{H}{\lambda}$
Wave power	$P'_W = \frac{P_W}{\rho g^{3/2} h^{5/2}}$
Pressure	$p' = \frac{p}{\rho g H}$
Amplification factor	$H_{\eta_{AF}} = \frac{H_{\eta_{owc}}}{H_{\eta_{inc}}}$
Capture width ratio	$C_W = \frac{P}{P_W B}$
Force coefficient	$F' = \frac{F}{\rho g A_d H}$
Moment coefficient	$M' = \frac{M}{\rho g A_d h H}$
Froude Number	Fe= $\frac{U_v}{\sqrt{gL}}$
Reynolds Number (aerodynamic)	$\mathrm{Re}_o = \frac{U_o D_o}{\nu_a}$
Reynolds Number (hydrodynamic)	$\mathrm{Re}_h = \frac{A\omega D_c}{\nu_w}$

*Notation: h = water depth, λ = wavelength, $k = 2\pi/\lambda$ = wave number, H = tough-to-crest wave height, ρ = 999 density of fresh water at ~17°C, g = 9.807 gravitational constant, $p = 1/T \int p\,dT$ OWC chamber pressure, T = wave period (phase-averaged), P = OWC absorbed power, B = OWC chamber width, A_d = horizontal area of the device, L = characteristic length, U_v = characteristic velocity, U_o = air flow velocity through the OWC orifice, D_o = orifice diameter, ν_a = kinematic viscosity of air, A = amplitude of η_{owc}, $\omega = 2\pi/T$ angular wave frequency, $D_c = \sqrt{4A_c/\pi}$ diameter of OWC chamber, ν_w = kinematic viscosity of water.

4.3 Experimental overview

Chapter 1 described the case study OWC technology and Chapter 3 described the mathematical model of the OWC and its interaction with waves. This description included linear wave theory equations and quantities that characterise the OWC power performance, which combined to form the key performance measurands. Table 4.2 presents all the relevant parameters of the experiment, and the following subsections provide details where needed.

4.3.1 Laboratory and model particulars

Experiments were conducted in the Australian Maritime College Model Test Basin, consisting of a series of 3D experiments with three different sized scale models (λ_{40} λ_{30}, and λ_{20}) of the WSE OWC WEC. Fig. 3.13 shows diagrams of the experimental setup, illustrating a correctly dimensioned drawing of the λ_{30} model deployed in the wave basin, a close up of the model mounted on the six-component force balance used to measure the complete hydrodynamic loads, configuration of the instruments installed in the OWC used to measure air pressure and internal wave elevation, and details of the simulated PTO system.

The prototype OWC WEC technology (see Fig. 1.1 in Chapter 1) was scaled using

Froude scaling. The prototype PTO comprises a unidirectional nonlinear air turbine, with unidirectional flow enabled by passive flaps that open and exhaust air on the up-stroke, then close on the down-stroke to direct air through the air turbine duct only. This PTO system was modelled at scale using an orifice place to represent the quadratic air pressure-flow characteristics of the air turbine (a common practice [28, 158, 159]). Light weight, robust plastic sheets simulated the passive unidirectional flow flaps/valves.

Figure 4.1: Photograph of the three models used in the experiments, from left λ_{40}, λ_{30}, and λ_{20}

4.3.2 Measurements, instrumentation, and calibrations

Chapter 3 described the measurement methods of incident wave elevations and wave elevations inside the OWC chamber, as well as the air pressure measurement inside the OWC chamber. Fig. 3.13 illustrates the configurations of the wave probes and pressure sensors instruments in and around the model. For readability we present below the key equations and methods used to quantify the OWC WEC power performance.

The incident wave power equation is seen above in Table 4.1. For OWC WEC parameters, the pneumatic power P, the measurand for quantifying the absorbed power of the OWC, is calculated from gauge pressure p measured inside the OWC chamber, and derived air volume flow rate q displaced by the OWC free-surface motion. For regular waves,

$$P = \frac{1}{T}\int pq\, dT \tag{4.2}$$

where T is the characteristic wave period. In irregular waves, Eq. (4.2) is the smae except T is the time vector of the whole irregular wave time series.

Air flow rate q is derived from pressure p and a calibrated orifice C_d [162]:

$$q = C_d A_0 \sqrt{\frac{2|p|}{\rho_a}} \tag{4.3}$$

Table 4.2 Parameters of the experiment.

Parameter	**Details**
Model	Bottom-standing unidrectional flow OWC. 3 Froude-scaled models ($\lambda_{40,30,20}$). Body constructed from marine plywood, Perspex, and fibreglass. Orifice plate PTO simulator: 1:150 orifice/chamber area ratio. Unidirectional flow valves simulated with passive flaps made from thin but robust plastic sheets.
Environment	Shallow water wave basin: 35 m L x 12 m W x 0-1 m D. Sixteen element Piston-type wavemaker (no active absorption); vertical walls; passive beach. Fresh water, at 15-20 °C Water depth for experiments = 10 m.
Measurements; instrumentation; calibrations;	Wave elevation in basin; conductive wave probe; calibrated daily. Wave elevation in OWC; 6 conductive wave probe (see Fig. 3.13 for layout); calibrated daily. Pressure in OWC; 3 x Honeywell Controls TruStability pressure sensor connected to Ocean Controls KTA-284 instrumentation amplifiers; calibrated weekly to ±2000 Pa. Hydrodynamic loads on model; 6-component force balance; calibrated before and after each scale experiment.
Data acquisition	National Instruments PCI-6254M Multifunction Data Acquisition Card, recorded on a HP computer, controlled with Labview software. All data acquired at 200 Hz.
Data recording	Regular waves: 30 s (model-scale). Irregular operational waves: 30 mins. Irregular survival waves: 3 hrs.
Wave conditions	Regular operational waves: $H = 1.8, 2.4, 3.0$ m; $T = 8 - 15.8$ s ($kh = 0.41 - 0.98$). Regular survival waves: $H = 4, 5$ m; $T = 16 - 18$ s ($kh = 0.36 - 0.4$). Irregular operation waves (JONSWAP): 15 sea states: $H_s = 0.75 - 4.75$ m, $T_p = 7 - 19$ s. Irregular survival waves (JONSWAP): 2 sea states: $H_s = 6$ m, $T_p = 9$ & 13 s.
Model conditions	Incident waves without model: all waves. Power matrix: operational waves. Loads (system open): survival waves; some operational waves.

where A_0 is the orifice cross-sectional area, and ρ_a is the density of air, assumed to be 1.2 kg/m^3.

The orifice plates for the three models were all calibrated using an in-situ method, described in Chapter 3 and elsewhere [161]. We report and discuss the results from the in-situ calibrations across scales in Appendix B. These results are often referred to in the results and discussion section on OWC hydrodynamics and power (§ 4.4.2), as they indicate a scale effect arising from the nonlinear PTO system.

The complete hydrodynamic loads on the WEC body were measured with a six-component external force balance (see Fig. 3.13). Chapter 3 described the instrument and in-situ calibration method, with Appendix A describing these in detail including example calibration results. A full calibration routine was carried out before and after experimental runs for each scale, producing two calibration data sets per scale. The post experiment calibrations provided a means of estimating measurement uncertainty of the hydrodynamics loads. The method of uncertainty analysis for loads was presented in Chapter 3.

Regarding calibrating the test environment, the key parameters to calibrate were the regular and irregular incident waves. Careful calibration of the incident waves was performed to obtain close agreement between the relevant wave statistics across scales. The statistic in regular waves was wave height H, and the statistics in irregular waves were significant wave height H_{m0} and peak period T_p. Given the λ_{30} experiment was performed first, the incident waves statistics in λ_{40} and λ_{20} were calibrated to match the λ_{30} wave statistics, aiming for within 5%.

4.3.3 Data analysis and uncertainty

Chapter 3 described the data analysis techniques and uncertainty analysis methods undertaken for this experiment. Where some results show expanded uncertainty bars, these represent 95% confidence interval (CI). The complete uncertainty analysis results for the three model scales are given in Appendix B.

4.3.3.1 Presenting results in time and frequency domains

We present time domain results in the form of phase-averaged profiles of measured quantities, including incident wave elevation η_{inc}, internal OWC wave elevation η_{owc} and pressure p, and hydrodynamic loads F_x, F_z, M_y. The method of phase-averaging was described in Chapter 3, but essentially encodes all regular wave cycles for a given frequency by overlaying them, starting at the zero up-crossing point, and taking the average. This method produces a single representative wave cycle/phase, a kind of statistical summary, and so is useful for the analysis and display of data.

We analyse the frequency domain results through the use of a modified description of the well-known Response Amplitude Operators (RAOs). RAOs are effectively transfer functions describing the effect a wave, or sea state of waves, has on the motion of a floating body in six degrees of freedom. They consist of two parts: (1) the response amplitude, or the degree of wave-induced motion of a floating body, and (2) the operator, or a factor that is applied to define the motion in terms of wave amplitude, thus nondimensionalising the motions.

RAOs, then, describe the response per unit amplitude of excitation, as a function of wave frequency. This conventional description is useful for WEC body motions (or motions of working surface that is used for wave energy conversion, e.g., fixed OWCs), however does not readily apply to power related quantities of a WEC, as these are often nonlinear (e.g., unidirectional air flow in the OWC of this work means the pressure differential is almost always negative, has no positive amplitude), or depends not on amplitude but the area under the curve (integral) as a function of wave frequency. To maintain the usefulness of RAOs as descriptors of wave-WEC interactions, however, we can modify the description in the following way. The RAO is the ratio of the magnitude – amplitude, height, or integral – of a WEC response measurand to the height of the wave, as a function of wave frequency. This description is based on that given in the international technical specification for WEC model tests [10] and similar texts [47]. As a result the RAO is not always dimensionless. However, it remains a convenient way to present results as transfer functions relating WEC responses to wave excitation forces, and also to correct for slight variations in wave height across scales for a given frequency, enabling proper comparisons of results across scales.

4.4 Results and discussion: Regular waves

§§ 4.5 and 5.4 provide the results of the experiments for regular and irregular waves respectively. The sections each present the incident wave measurement results, where the waves were those measured at the location of the OWC model prior to it being deployed. Following this is the analysis of results from the OWC hydrodynamics and power, and hydrodynamic loads. Where data are missing this is due to either no experimental run or omission of the data due to it being deemed incorrect. In each subsection, we first report and discuss the OWC WEC behaviour in terms of the key measurands, then examine the differences of these measurands across scales. For clarity, the following terminology and quantitative scale is used to describe the (relative percentage) differences in results across scales: *negligible* (<5% relative percentage difference (RD)); *minor* (5-10% RD); *moderate* (10-30% RD); and *major* or *significant* (30+% RD).

4.4.1 Incident waves

Incident regular waves were mostly nonlinear across wave height H and period or wavenumber kh, and this nonlinearity deviated across scales resulting in sometimes significant differences in wave profile (Fig. 4.2). The smallest H and largest kh combination were the most linear (top left), with nonlinearity increasing as H increased and kh decreased (bottom right). As kh decreased down the 15 wave periods for a given H, an asymmetry developed between the wave peak and trough, where the wave peak amplitude A_P became peakier and the amplitude

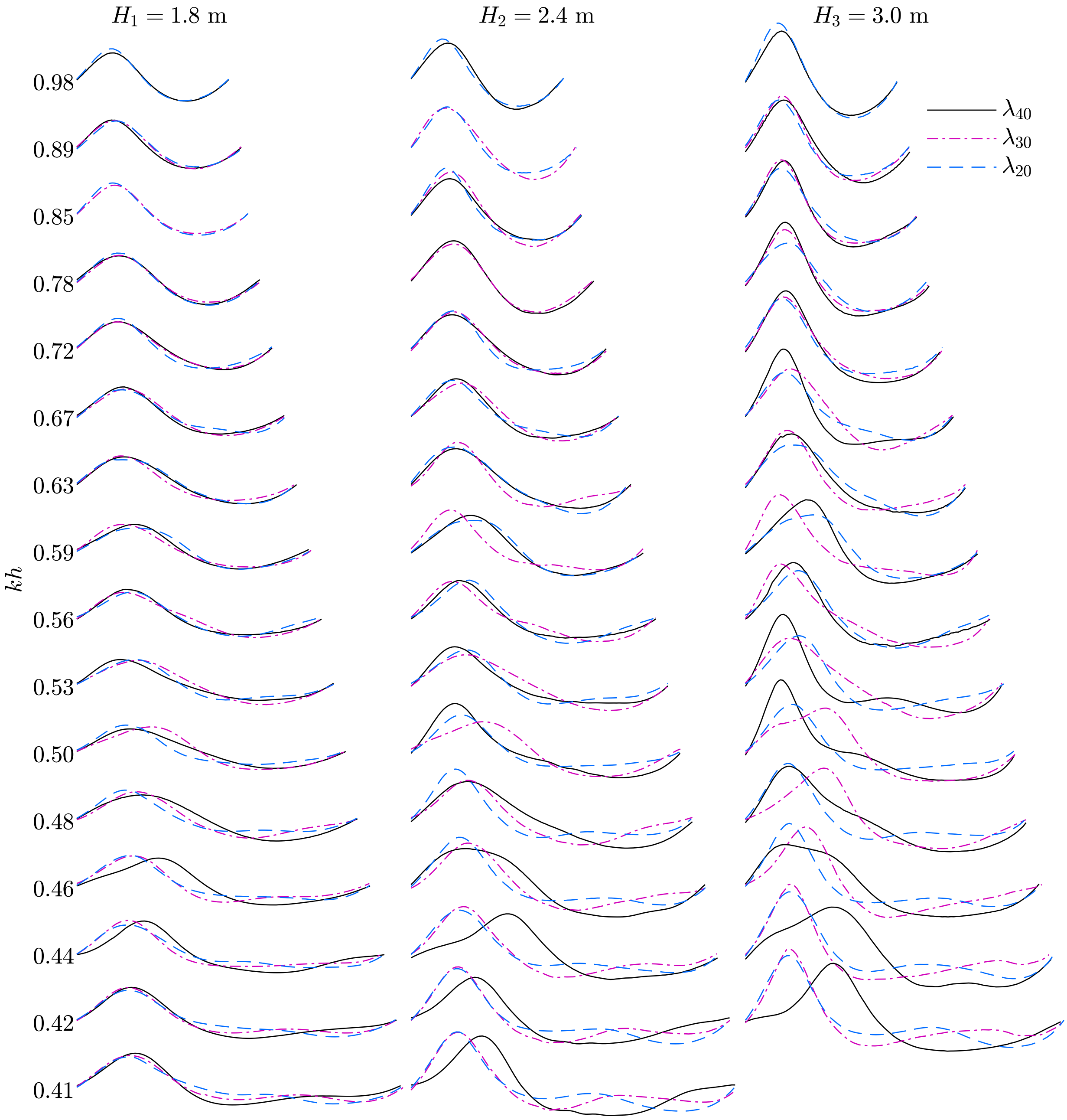

Figure 4.2: Comparison of incident wave measurements η_{inc} of three wave heights H and 15 wave periods (shown as kh). Phase-averaged wave profiles shown as a table format with H along three columns and kh down 15 rows. Axes are omitted to aid the visual comparisons; quantitative H and kh values are shown in Fig 4.3.

trough depths A_T flatter. As H increased for a given kh, η_{inc} tended to have a similar shape, but with enlarged peaks and troughs, with the peak amplitude A_P greater than trough depth A_T, again expected with nonlinear waves. These trends reflect the characteristics of nonlinear regular waves [94, 180]. This was expected given the waves were intermediate and shallow waves. The three wave parameters that determine which wave theory is applicable for a given problem are H, T, and λ. These parameters can be used to define three non-dimensional parameters that determine ranges of validity of different wave theories: wave steepness parameter $S = 2\pi H/gT^2$, the shallow water parameter $\mu = 2\pi h/gT^2$ and the Ursell number $U_s = H\lambda^2/h^3$. The experimental waves in this study ranged between shallow ($h/\lambda < 0.05$) and intermediate depth ($0.05 < h/\lambda < 0.5$) (see Appendix B).

Profile shape of η_{inc} differed across scales up to major degree (Fig. 4.2). The difference between scales was negligible to minor for small short waves (high kh), tending to moderate to major differences with increasing wave height and length. Inspecting H_1, as wavelength increased the wave crest occurred at slightly different points at each scale, due to the interference of higher order waves. The λ_{20} crest occurred around $kh = 0.59$, λ_{30} crest occurred around $kh = 0.5$, and λ_{40} crest occurred around $kh = 0.59$ and again around $kh = 0.46$. This trend persisted for the larger wave heights, albeit the magnitude and variation becoming more pronounced.

A possible explanation for observed η_{inc} deviation across scales is that, because the model position was fixed in the basin, the relative distance for the waves to propagate before reaching the models differed. This meant the shallow-intermediate waves transformed in a different manner. Another factor is the interaction of higher order waves with the first order wave was different for each scale. For instance, the trough of higher order wave might coincide with the crest of the first order wave, in effect flattening and delaying the wave peak in a destructive interference (e.g. λ_{40} scale η_{inc} for H_3 and $kh = 0.44$).

In terms of the quantitative values of H across the kh range, H tended to increase toward at the lowest kh, dip around $kh = 0.5$, and then level out as $kh \to 1$ (Fig. 4.3). This trend was consistent across heights. This apparent dip was due to an interference between the first order wave and higher order waves around the crest, causing the crest to flatten, as seen visually in the profile of λ_{30} scale around $kh = 0.5$ (the λ_{30} scale experiment was conducted first, with subsequent scales' H attempted to be matched to the λ_{30} scale H, explaining the similar trends across scales). The variation of H across the kh range increased as wave height increased.

Regarding the agreement of H across scales, agreement was best for H_1 and least for H_3. This larger difference for larger waves was due to a greater sensitivity of the relationship between the input H for the wavemaker and measured H, where the intermediate to shallow water waves transformed considerably between the wavemaker and the model location, making the matching of H difficult under time constraints. Wave power P'_W increased exponentially with increasing wave steepness s (Fig. 4.3**B**). This result was expected because P'_W varies with H^2. While the individual values between the scales differed, they all collapsed onto a trend line, indicating that s did not appreciably affect P'_W across scales.

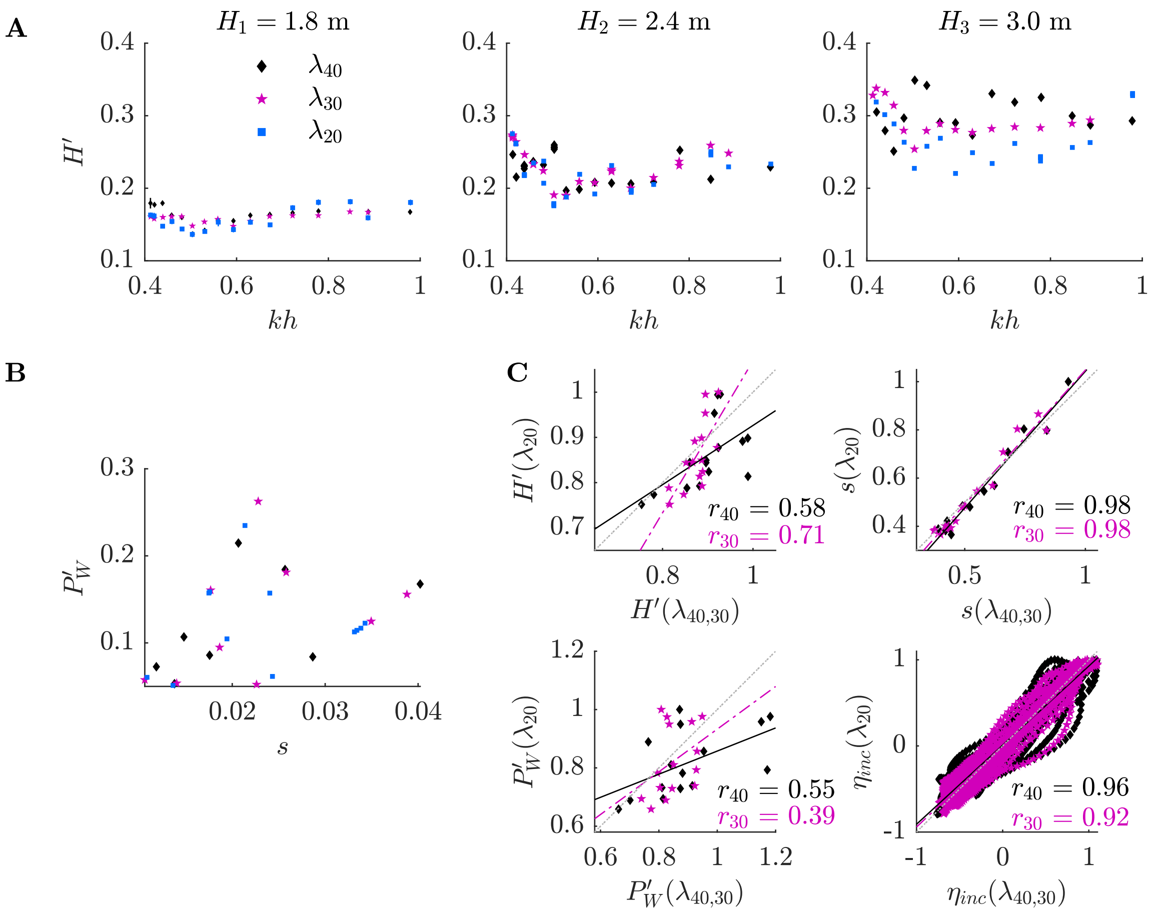

Figure 4.3: Incident wave measurands in the absence of the model. (**A**) Dimensionless wave height $H' = H/h$ across the kh range tested, with H_1 showing expanded uncertainty bars (95%)). (**B**) Relationship between wave steepness $s = H/\lambda$ and dimensionless wave power $P'_W = \rho g^{3/2} h^{5/2}$ (data shown here include P'_w values for three instances of s, including three wave heights included). (**C**) Pearson's product moment correlation coefficient r plots of said wave quantities, as well as η_{inc} profiles, for λ_{40} and λ_{30} (x-axis) relative to λ_{20} (y-axis). Data are from H_1 only. The numeric values of r for both scales (r_{40} and r_{30}) are also given. All data in these correlation plots are normalised against the maximum λ_{20} value for each respective variable.

The correlation plots visualise and quantify the differences across scales, where the smaller two scales (λ_{40}, λ_{30}) are plotted against λ_{20} for several measurands (Fig. 4.3**C**). A high correlation across scales was found for kh, wave steepness s, and η_{inc}, with the Pearson's correlation coefficient r quantifying this correlation. The correlation for H' and P'_w across scales was reasonable, with r values of above 0.55 for both scales, except r_{30} for P'_w, resulting in 0.39. This lower correlation of H and P'_w was due to the variation of H across the kh range and across scales. The near perfect correlation of kh indicates that H' was the dominant parameter contributing to the deviation of P'_W. While the correlation of η_{inc} is above 0.96 for both scales, there was considerable variation about the regression line, caused by the wave profile deviation across scales.

Two implications arise from these incident wave results. First, WECs operating in intermediate to shallow water will encounter similar nonlinear waves as those in this experiment. This raises questions about assuming linear wave theory to estimate average wave power and how this affects C_W, and whether nonlinear wavemaker inputs are required. Moreover, it is conceivably a difficult task to correct for deviating nonlinear η_{inc} across scales, or otherwise account for this scale effect, if it is not practical or economical to conduct a series of experiments at different scales, which is invariably the case for WEC developers. Without testing at different scales the sensitivity of η_{inc} to scale and its subsequent influences on WEC behaviour would be unknown. Therefore, further research is needed to understand how this scale effect might be accounted for.

Second, all WECs have a working surface (a *captor* that interacts directly with waves) that captures and converts wave energy [47, 8, 36]. A captor's hydrodynamic response to incident waves can be significant due to resonance, amplified by two or three times (e.g., see [129]). Consequently, even slight deviations in incident regular waves – in height, period, or nonlinear profile – could be amplified to produce significantly different WEC motions, power, and loads, depending on the scale tested. The degree to which incident waves and their differences across scales influence OWC WEC behaviour is reported and discussed in the following sections (§§ 4.4.2 and 4.4.3).

4.4.2 OWC hydrodynamics and power

To examine OWC hydrodynamics and power results, including how scale influences these, we produced a dense data display showing key measurands across time and frequency domains, and across scales (Fig. 4.4). Time domain results consist of a set of synchronised **Phase-averaged profiles of five *kh* values** of incident waves (η_{inc}) and OWC quantities (air pressure p and internal wave elevation η_{owc}). They are overlayed to show the relationship between waves and OWC hydro-aerodynamic responses, which are linked to the frequency domain responses through response amplitude operators (**RAO**) curves of power-related measurands. The differences across scales are visualised by **Correlation plots** and quantified by Pearson's correlation coefficients r. This set of three displays thus enforces global and local comparisons of OWC WEC behaviour in terms of how all the quantities interact and the influence of scale on these.

Describing the OWC WEC working principle and behaviour first, we refer to **The phase-averaged profiles of five *kh* values** (Fig. 4.4). As an incident wave η_{inc} passes the model, the rise to its peak induces a similar but amplified and slightly phase-delayed rise in η_{owc}. During this wave-rising-to-peak stroke, p is approximately zero indicating air exhausting from the chamber enabled by the unidirectional flow valves. No OWC power P is absorbed during

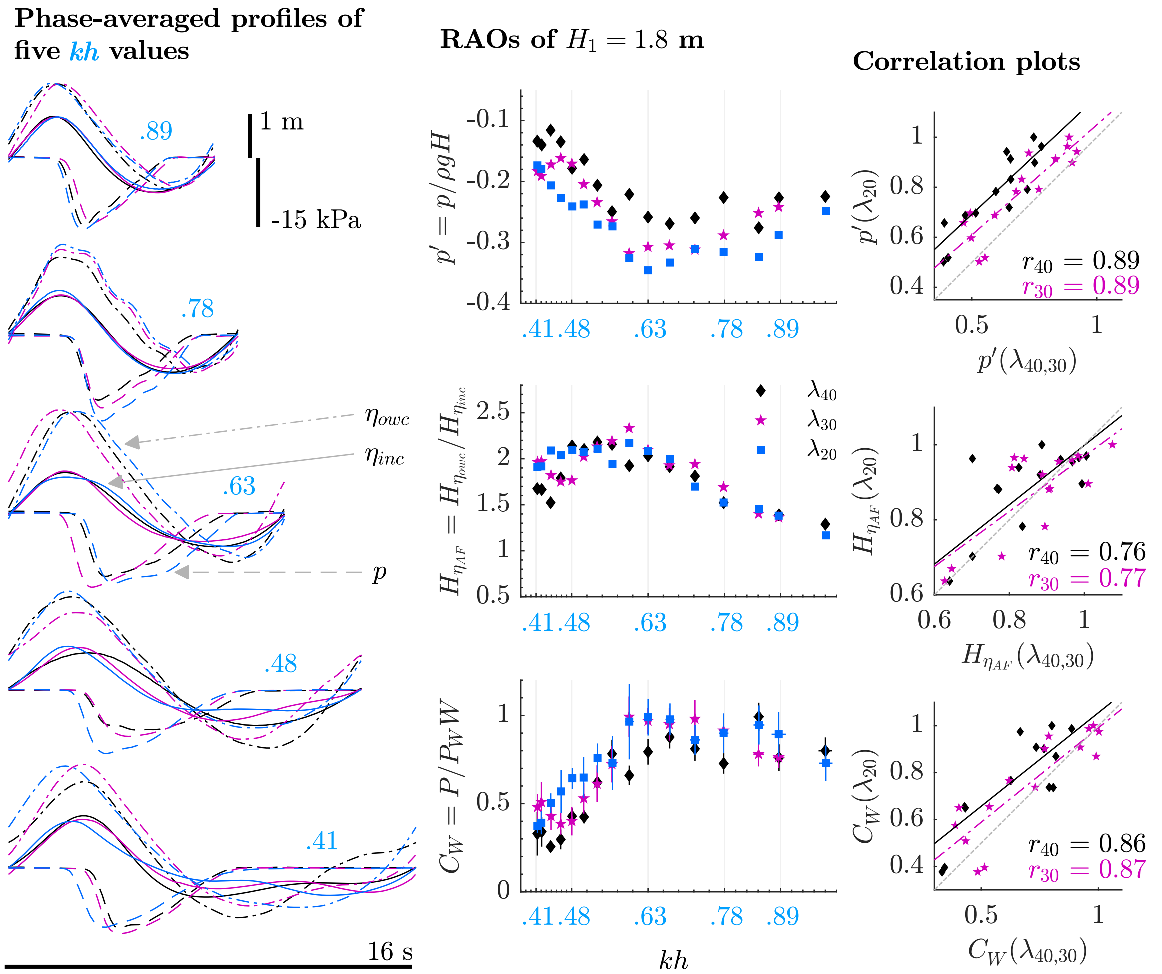

Figure 4.4: Comparisons of OWC hydrodynamics and power across dimensions of time, frequency, and scales, showing incident waves η_{inc}, OWC hydro-aerodynamics of internal wave elevation η_{owc} and air pressure p, and capture width ratio C_W (expanded uncertainty bars to 95% CI). All results are for H_1=1.8 m. The **Phase-averaged profiles of five *kh* values** displays plot η_{inc} and η_{owc} on one y-axis, and p one another y-axis of different scale (1 m wave amplitude, -15 kPa pressure, and 16 s wave period). The ***kh*** values correspond to the x-axis ticks in the **RAOs for $H_1 = 1.8$ m**. **Correlation plots** show and quantify differences across scales, including perfect correlation ( ). Correlation data are normalised against the maximum value obtain for λ_{20} for each respective measurand.

this up-stroke, but energy is being stored as potential energy in the water column heave [33]. Once the incident wave peak passes, η_{owc} falls, causing a negative pressure differential in the OWC that induces air flow, which, in turn, closes the undirectional flow valves to direct air flow through the orifice into the chamber. Kinetic and stored potential energy is now being absorbed. Peak negative p corresponds to the maximum rate of change of η_{owc} w.r.t time, thus maximum volume flow rate q and P. Having peaked, p and q tend back to zero as η_{inc} and η_{owc} bottom out to the trough. Once η_{owc} is minimum, at the trough, p, q, and P are approximately zero. The cycle begins again with the next wave.

This time domain OWC behaviour is linked to the frequency response through the curves of **RAOs of $H_1 = 1.8$ m**, showing power-related measurands of dimensionless pressure p', amplification factor $H_{\eta_{AF}}$, and capture width ratio C_W (Fig. 4.4). The highest responses for all measurands occurred in mid-length waves (kh values), 10-12 seconds full-scale wave period, which is the resonance zone. Either side of the peak responses of p' and C_W, there was a sharp decrease for longer waves ($kh < 0.6$), but a relatively constant high response for shorter waves ($kh = 0.6 - 1$). The p' and C_W RAO curves were similar but flipped as p' is negative. $H_{\eta_{AF}}$ showed a broad peak for longer waves, decreasing steadily to 1 for the shortest, highest kh waves. While $H_{\eta_{AF}}$ was relatively high for low kh waves, p' and C_W were relatively low. This is explained by smaller $d\eta_{owc}/dt$ occurring in less steep, longer waves, or in other words a lower rate of change of energy (power) that can be absorbed by the OWC WEC.

Across scales, larger model scales tended to show minor to moderate increases in OWC hydrodynamic responses and power, and the frequency domain response shapes differed across the kh range (Fig. 4.4). The **phase-averaged profiles** show the OWC hydrodynamic responses tending to be higher for larger scales despite H being approximately equal, and the profiles evidently deviating across scales. These time domain results are reflected in the **RAOs**, where the dimensionless OWC responses of p', $H_{\eta_{AF}}$, and C_W tended to be relatively higher for larger scales, and the RAO shapes differed. Focusing on capture width ratio, $C_{W,\lambda_{30}}$ was +21% RD compared to $C_{W,\lambda_{40}}$ when averaged over the kh range, and $C_{W,\lambda_{20}}$ averaged +16% RD compared to $C_{W,\lambda_{30}}$. Across the scale range, $C_{W,\lambda_{20}}$ was +25% RD on average relative to $C_{W,\lambda_{40}}$. A maximum of +56% RD between λ_{20} and λ_{40} was found at $kh = 0.44$. These magnitude differences are outside the measurement uncertainty indicated by the uncertainty bars, which supports our hypothesis that OWC WEC results from tests at different scales can differ by an amount larger than the measurement uncertainty. This finding agrees with observations from similar studies of OWC WECs [58, 164].

$H_{\eta_{AF}}$ showed a negligible difference in short waves ($kh > 0.63$), and a minor difference in longer waves. The p' RAO showed similar magnitude differences to C_W, albeit slightly higher because C_W varies with H^2 whereas p' varies with H. The finding of $H_{\eta_{AF}}$ differing less across scales relative to p' supports observations from similar studies [159, 178, 164].

Examining the **Correlation plots** provides another layer of the analysis of differences in results across scales (Fig. 4.4). The key feature in these plots is the trendlines, where an up-shifted trendline on the y-axis indicates λ_{20} was consistently higher relative to the smaller scales along the x-axis. As seen, p' trendlines showed the largest up-shift (bias) to λ_{20}, followed by C_W and $H_{\eta_{AF}}$ trendlines. In all cases λ_{40} trendline was higher than λ_{30} which were both higher than perfect correlation (······). The Pearson's correlation coefficient was highest for p' at $r = 0.89$ for both scales, and lowest for $H_{\eta_{AF}}$ with $r_{40} = 0.76$.

An interpretation of these results leads us to consider which parameters most likely caused the significant scale effects, manifest in the differences in OWC hydrodynamics and power results across scales. One likely parameter is PTO damping. The in-situ orifice calibrations, which produced the orifice discharge coefficient C_d (see results in Appendix B), show that C_d decreased by about 8.5% RD per scale, or 16.5% RD between λ_{20} and λ_{40}. In other words, larger model scales experienced greater PTO damping (larger damping coefficient δ). This discrepancy in PTO damping seems to have been a consequence of maintaining the geometrical similitude condition of constant orifice to OWC chamber area ratio, which was optimal at 1:150 (this geometric similitude condition was also maintained in [168]). Such a geometric similitude condition may have led to dynamic dissimilarity of PTO characteristics – air pressure and flow rate – across scales. This non-similitude was likely exacerbated because of the quadratic damping of the orifice that induces nonlinear air pressure and flow characteristics, and because the PTO strongly influences OWC WEC motions and power [181].

Incident waves were also a likely parameter causing scale effects. Incident wave measurement results showed that the shape of the nonlinear wave profiles depended on the scale (Fig. 4.2). These profile deviations may have been due to a combination of the fixed model deployment position relative to the wavemaker that allowed for relatively different wave transformations in space and time, and the differing paddle transfer functions for generating waves at different water depths. Regarding how these nonlinear profile deviations influenced OWC behaviour across scales, as previously discussed and clearly shown in Fig. 4.4 the OWC hydrodynamic responses are not only sensitive to wave height and period but also the nonlinear profile variation along the wavelength. Therefore, incident waves were likely a significant contribution to the differences in OWC hydrodynamics and power results.

These newly identified scale-dependent parameters and their associated impacts expose a concern: without testing this OWC WEC at different scales the evidently significant influence of scale on power-related results would be unknown. If only one model scale were tested, which is invariably the case for most WEC developers conducting experiments, the experimental results could be unreliable and misleading because their sensitivity to model scale is concealed. In such cases, the consequences range from erroneous predictions of full-scale power performance based on model-scale extrapolation, to uncertain design data that compromises the design of prototype subsystems, to unreliable quality assurance documentation used in due diligence of the technology. In terms of experimental uncertainty, scale effects of OWC WECs is evidently a significant part of experimental uncertainty, so they should be evaluated.

The results of OWC hydrodynamics and power across waves heights show that wave height had a negligible effect on the overall trend of better power performance for larger model scales (Fig. 4.5). Regarding the OWC responses to wave height, increasing wave height tended to increase the OWC hydrodynamic responses but slightly reduce C_W because of the relative nonlinear increase in P'_W, which varies with H^2. Such a reduction in C_W in more energetic waves is a common observation for WECs in general [182] and OWC WECs [183, 184], likely due to real fluid effects [166]. Across scales, wave height tended to amplify the relative differences at some kh values and attenuate them in others, resulting in more pronounced RAO shape differences and greater data scatter. This was most noticeable for the $H_{\eta_{AF}}$ RAO in longer waves, where λ_{40} peaked at $kh = 0.44$ and was as maximum for all scales, leading to a relative gain of $C_W(\lambda_{40})$ compare to other scales. This amplified λ_{40} response may be explained by inspecting the η_{inc} profiles (Fig. 4.2), where for H_3 and long waves the λ_{40} profiles show a major deviation from the other scales, with markedly delayed peaks, due to higher order wave interactions differing across scales. Indeed, this delayed *einc* peak correlated with the peak of the $H_{\eta_{AF}}$ RAO for all scales, and similarly the peak of the C_W RAO. Interestingly, $\eta_{inc}(\lambda_{40})$ had another delayed peak trend around $kh = 0.59$, which corresponded to a secondary local maxima for the RAO of $H_{\eta_{AF}}$. This trend indicates the OWC's sensitivity to such nonlinear incident wave behaviour.

How these OWC hydrodynamics and power results relate to the relevant literature is as follows. A well-known concern in hydrodynamic physical models is an inconsistency between Froude and Reynolds scaling laws. Their force ratios cannot be satisfied simultaneously as Froude similarity is governed by inertia, Reynolds viscosity [158, 57]. If a small model's Reynolds number Re is lower than *critical*, viscous effects may be non-negligible as the model sees laminar flow whereas the flow would be turbulent in the prototype. For WEC model tests, a critical Re has been estimated to be $\sim$1e5 [158]. It is therefore important to estimate Re for the range of model and environment conditions to determine if it can be reliably ignored as a scale effect parameter. For OWCs, to check for Re dependence in power related quantities requires estimating Re for the hydrodynamics Re_h and aerodynamics Re_a [164]. We made such estimates for the smallest model scale (therefore smallest Re range), as follows:

$Re_h = A\omega D_c/\nu_w$ where A is the incident wave amplitude, ω the wave frequency, D_c the characteristic dimension of the model, assumed here to be the equivalent OWC chamber diameter if the rectangular model were circular, i.e., $D = \sqrt{4A_c/\pi}$ where A_c is the cross-sectional area of the OWC chamber, and ν_w is the kinematic viscosity of water at basin temperature. This estimate yielded a Re_h range of 1.4e5-4.5e5 for all the regular wave heights/periods tested. This estimate places Re_h higher than the recommended critical number, indicating turbulent flow, therefore suggesting Re_h was not a significant parameter contributing to scale effects in power and loads results.

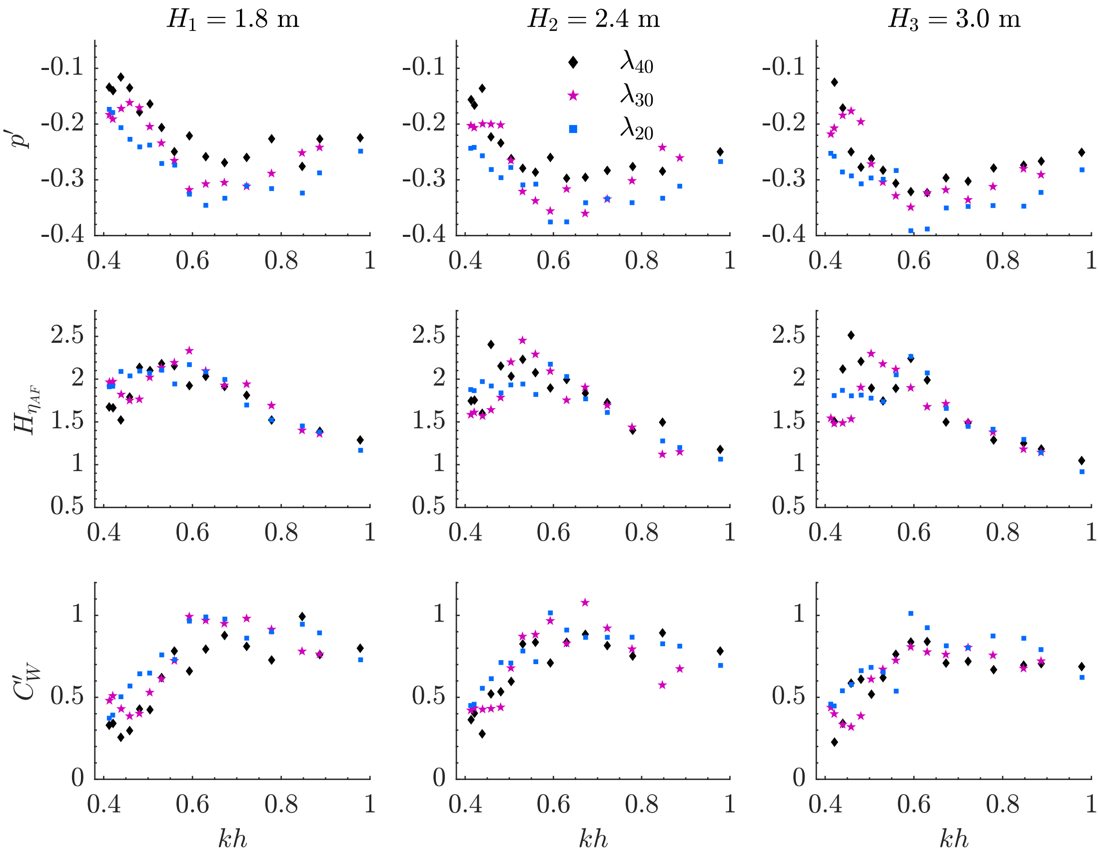

Figure 4.5: Effect of wave height on RAOs of performance indicators across three heights $H_{1,2,3}$ and scales $\lambda_{40,30,20}$. See Fig. 4.4 for explanation of shown measurands. Larger wave heights induced larger OWC responses but reduced C_W due to wave power varying by H^2, and across scales varied the relative differences.

For the aerodynamic condition, also called the orifice Reynolds number [164], Re_a was estimated from $Re_a = D_c v_s / \nu_a$ where D_c is the same as for Re_h (this definition differs from [164] who claim the characteristic dimension should be 2 times the orifice diameter, however, based on [185] it is arguably better to assume D_c is related to the OWC chamber diameter (i.e., the 'pipe'), not the orifice diameter), v_s is the volumetric velocity of air displaced by the OWC internal free-surface (3.2), and ν_a is the kinematic viscosity of air. This estimate yielded a Re_a range of 1.2e5-7.3e5 for all the regular wave heights/periods tested. Again, Re_a was beyond the critical Reynolds number. In contrast to the conclusions from [164], our experimental results were likely Reynolds number independent, suggesting observed scale effects were due to other parameters (evaluated in Table 4.5).

Another possible scale-dependent parameter influencing OWC power performance is air compressibility [167, 88, 89, 159, 168, 87, 169, 178, 177, 174, 35]. These studies generally show that air compressibility may be lead to 5–15% under- or over-prediction of C_W, but is mainly detrimental to wave energy absorption. Some of these experimental based studies have compensated for the air compressibility scale effect by enlargening the model air chamber or with and additional air reservoir to maintain the condition $V_m/V_p = \delta^{-1}\lambda^2$ where V is the air chamber volume, and δ is basin water to seawater ratio. Doing so apparently reproduced the air compressibility effect in the chamber. However, even a basic experimental uncertainty analysis is not evident in these studies. The additional experimental apparatus and complexity undoubtedly introduced uncertainties into the experiment, which were no evaluated through an uncertainty analysis. This was the basis for why the present work neglected to model the air compressibility effect, and to focus on other scale effects.

Nevertheless, to determine whether air compressibility might be influencing the pressure-flow relationship and thus OWC power in this scale series, we calculated the compression number Ω, which determines the relative importance of air compressibility to the OWC characteristics, denote as [177]:

$$\Omega = \frac{K\omega h}{\gamma_p p_0} \tag{4.4}$$

where K is the relationship between pressure p' and air flow velocity $\bar{v}$ inside the chamber ($K = p/\bar{v}|\bar{v}|$), ω is the angular frequency, h is the height of the chamber (from the water mean water level), $\gamma_p = 1.4$ is the polytropic expansion index for air, and p_0 is the atmospheric pressure. For the worst case, which is at the largest wave height and highest wave frequency (and kh) for the λ_{20} scale, we obtained $\Omega = 0.07$. Because this 0.07 value is less than 0.1, air compressibility is sufficiently small so as to be neglected. Moreover, there was no phase shift detected between measured p and derived q displaced by the OWC free-surface motion in the timeseries. Given such a phase shift indicates the air is compressing and so air compressibility is an important part of the energy conversion process [87], the absence of phase shift in our results further suggests that air compressibility was negligible.

4.4.3 Hydrodynamic loads

Here we report and discuss the results of horizontal surge force F'_x, vertical heave force F'_z, and overturning pitch moment M_y, as these degrees of freedom are the most important. Noted, the F''_z and M_y data for λ_{40} are omitted due to unreliable data (discussed below). Uncertainty results for loads are presented in Chapter 3 and Appendix B.

The load components exhibited a complex set of responses due to an interplay of the nonlinear incident waves, OWC hydrodynamic responses, and the PTO damping (Fig. 4.6). Considering first $H_1 = 1.8$m, loads were approximately twice as high in the negative direction than the positive (higher in the direction of wave propagation). This was expected given the higher-peak-to-trough asymmetry of the nonlinear incident waves (Fig. 4.2). The maximum force for F'_x was -0.53 (-427 t), which was higher relative to F'_z at -0.38 (-306 t). The maximum moment for M'_y was -0.28 (-2253 t-m). The shape of the load RAO curves showed

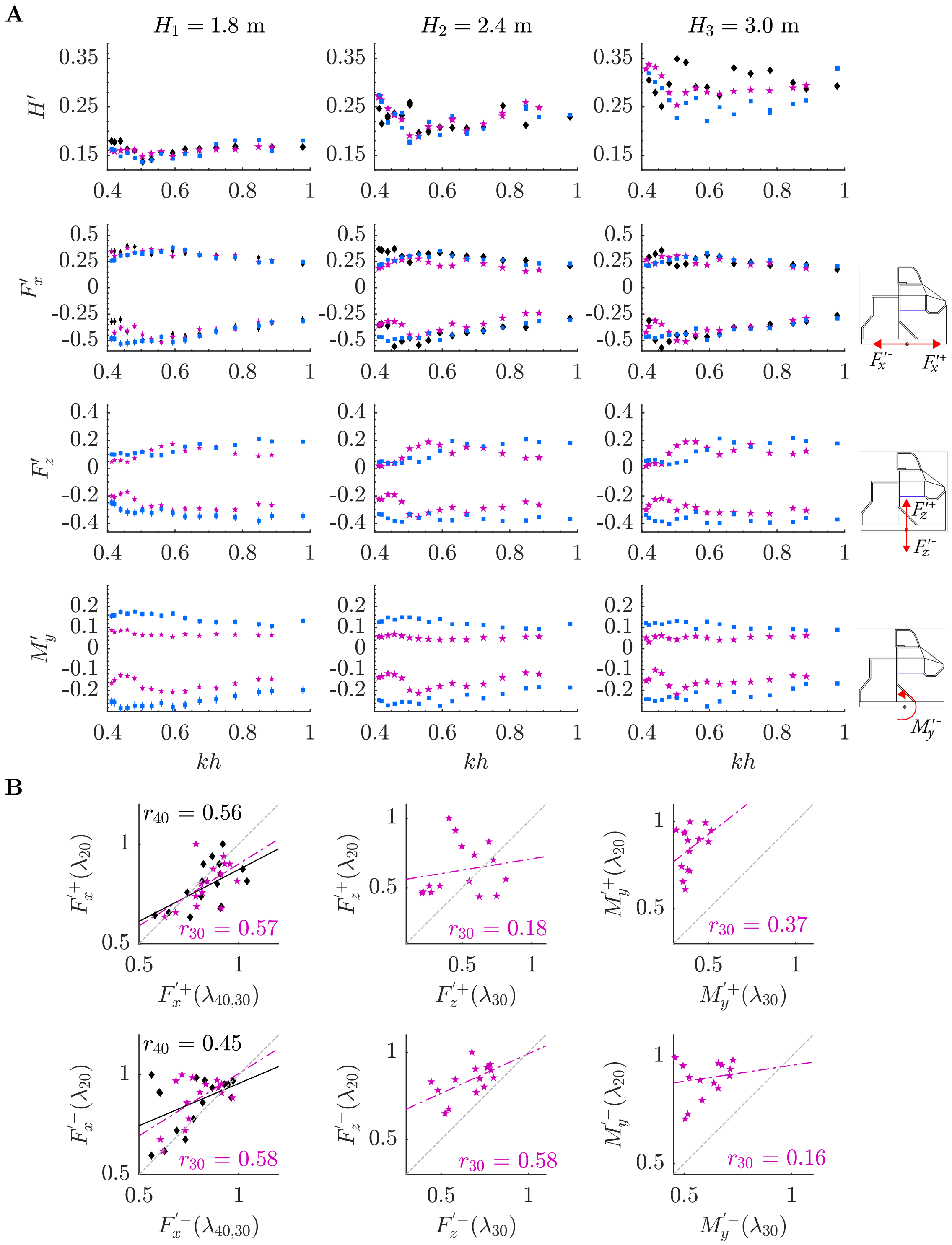

Figure 4.6: Hydrodynamic loads and correlations. (**A**) shows dimensionless wave height $H' = H/h$, horizontal surge force coefficient $F'_x = F_x/\rho g A_d H$, vertical heave force coefficient $F'_z = F_z/\rho g A_d H$, and pitch moment force coefficient $M'_y = M_y/\rho g A_d h H$. H_1 results show expanded uncertainty bars (95% CI). The inserted diagrams of the three models show the force/moment directions according to the coordinate system. (**B**) Pearson's product moment correlation r for above forces/moments.

similar responses to power-related RAO curves (shown in Fig. 4.4), especially in longer waves ($kh < 0.6$), but less so in shorter waves. F_x' and M_y' showed similar responses to amplification factor $H_{\eta_{AF}}$, tending to peak around $kh = 0.6$, decreasing in longer waves at lower kh's, and decreasing linearly in shorter waves as $kh \to 1$. This suggests the water volume in the OWC and its dynamics were key drivers of F_x' and M_y'. F_x' was affected by the downward-acting water column heave due to the angled bottom of the bent-duct OWC design, and sloshing (tilting/pitching back and forth, or mode oscillations) inside the chamber. This slosh also contributed to the sum of forces/moments in M_y', as did the model buoyancy force F_B', which became more dominant in long waves. The F_z' RAO curve was similar to pressure p' and capture width ratio C_W. This suggests the PTO damping was a key driver of F_z'. However, F_z' is also a function of the varying hydrostatic force of η_{inc} and η_{owc}, and up-acting F_B'. This interplay of forcings and the OWC hydro-aerodynamic responses led to F_z' being similar for low kh but then tending to increase for $kh > 0.6$, when C_W was highest.

Across scales, larger model scales tended to encounter relatively higher loads, with the magnitude of the differences depended on the load component (Fig. 4.6). While F_x' showed negligible differences in short waves, in long waves F_x' showed moderate to major differences, 13% RD on average and up to a maximum of 53% RD between the λ_{40} and λ_{20}. The relatively larger PTO damping for larger scales may have also been a key contributor to these differences, because larger PTO damping would impart higher loads to the larger models. The F_x' and $H_{\eta_{AF}}$ scatter plots also showed similar trends, albeit F_x' had a lower correlation coefficient r (Fig. 4.6 **B**). The expanded uncertainty was 8% on average, consistent across scales, and similar for F_x', F_z', and M_y' (the uncertainty bars extend only very slightly beyond the data points).

For $F_z'^{-}$, λ_{20} was consistently higher than λ_{30} by 22% RD on average, and 51% RD maximum at $kh = 0.46$. These moderate to major differences were similar to those found in the pressure RAO (Fig. 4.4). Again, the PTO was a likely key parameter causing these differences. Another possible parameter contributing to the difference was slight differences in model buoyancy force between models due to standard material thicknesses, but this is estimated to be smaller than the experimental uncertainty. For $F_z'^{+}$, the relative differences varied across the kh range, thus scattered correlation data and low r. The trough of the η_{owc} internal free surface governed the behaviour of $F_x'^{+}$, so the differences here observed are linked to the differences in the nonlinear η_{inc} waves.

For both positive and negative M_y', λ_{20} was consistently higher than λ_{30} by 41% RD on average, and 75% RD maximum at $kh = 0.44$ for M_y'-. This represents a major difference. The likely explanation of this difference is the coupled increases in both F_x' and F_z' load components for the larger scale. The PTO damping also likely contributed to this difference.

However, the pitch moment also seemed to be sensitive to slight deviations in the load distributions in and around the model acting at a moment arm, with sloshing also influencing this behaviour.

These moderate to major differences found in load results across scales suggests that if only one model scale were tested, the extrapolated results could lead to erroneous predictions of full-scale loads, on the order of many hundreds of tonnes and tonne-meters. This finding reveals that if the sensitivity of model-scale loads results to scale is unknown or poorly understood, this could be seriously detrimental to the structural and foundational design of prototype OWC WEC.

Wave height had a negligible effect on the overall trend of higher loads for larger scales (Fig. 4.6). However, wave height tended to amplify the relative differences at some kh values and attenuate them in others, due mainly to larger variation in H, resulting in more pronounced RAO shape differences and greater data scatter. Loads tended to increase linearly with wave height, evident by similar load coefficient magnitudes due to these being normalised by the wave height. The trends reported and discussed above for H_1 reflected the behaviour of higher waves.

Regarding the interplay of diffraction and inertial forces, and their relative importance across the kh range, a useful distinction called the diffraction parameter D/λ indicates whether flow separation is important. Here, D is the characteristic horizontal dimension, taken as $D = \sqrt{4A_d/\pi}$, were $A_d = LW$ is the horizontal area of the device (see Fig. 4.1 for L and W). When $D/\lambda > 0.2$, diffraction is considered predominate [186]. Given this definition, the Keulegan-Carpenter number K_n will usually be approximately less than one; therefore, it is assumed that appreciable flow separation should not occur for $kh > 0.48$ and the effects of viscosity will be confined to the boundary layers on the body surface. This, then, suggests flow separation may be occurring when $kh < 0.48$, which would not scale exactly due to the inconsistency of Reynolds and Froude numbers, and which therefore could in part account for the variation of the forces and moments across scales in the longest waves. Noted, according to [186], the influence of diffraction tends to reduce wave loads.

Another scale dependent parameter that may cause scale effects is vortex shedding. However, wave force experiments with square and rectangular sections have indicated that the influence of vortex shedding on the total force is generally not noticeable for large diffraction regime bodies [186].

4.5 Results and discussion: Irregular waves

4.5.1 Incident waves

As with regular wave results, this analysis of irregular wave results begins with the incident waves, examining the trends and scale differences of energy density spectra S for the range of sea states tested, along with its key statistics of significant wave height H'_{m0} and peak wavenumber $k_p h$ (Fig. 4.7). General trends showed S tended to increase with larger sea states (top right), except when wave breaking began to occur for the largest sea states. Also with more energetic seas a secondary peak emerged in the spectra at higher frequencies.

Across scales, the largest model scale resulted in the most energetic seas overall, therefore larger H'_{m0} and T_p values (Fig. 4.7). However, λ_{30} resulted in the smallest S, smaller than λ_{40} on average. $H'_{m0,\lambda_{20}}$ was 13% larger than $H'_{m0,\lambda_{30}}$ on average, and 7% larger than $H'_{m0,\lambda_{40}}$; T_p showed minor differences, with λ_{20} 5% different to other scales. These differences across scales are despite efforts to calibrate H'_{m0} of the λ_{40} and λ_{20} experiments to the H'_{m0} of the λ_{30} experiment. Spectrum shapes agreed well between scales, except for larger sea states where λ_{20} showed a second energy peak at a higher frequency.

There are several possible explanations for the differences observed in incident waves across scales. One is that the model deployment position relative to the wavemaker was different for each scale. This suggests the wave transformations occurring between the wavemaker and wave measurement location were appreciable, due to waves being intermediate to shallow water. Another source of difference may be the wavemaker transfer functions differing to a degree for each scale (therefore water depth) to generate a sea state for the same H_s, T_p and gamma inputs, and the wave reflections that build up during the long timeseries runs required to sufficiently represent a stationary sea state (30 minutes full-scale).

4.5.2 OWC hydrodynamics and power

Irregular waves trends of OWC hydrodynamics and power were generally similar to those observed in regular waves in terms of responses across the wave frequency range and due to increases in wave height (Fig. 4.8). As seas became more energetic, P_W and p' increased, showing a peak between $k_p h = 0.6 - .08$ (T_p=11-15 s). $H_{\eta_{AF}}$ showed a broadband peak around the middle frequencies and heights, and C_W tended to peak at higher $k_p h$ and lower H'_{m0}, with a value of around 0.9.

Across scales, as model scale increased the power performance tended to increase, with minor to moderate differences found across scales on average (Figs. 4.8 and 4.9). $C_{W,\lambda_{20}}$ was +15% RD on average compared to $C_{W,\lambda_{30}}$. However, λ_{30} generally showed a poorer power performance compared to λ_{40}. While this finding was not expected and deviates from

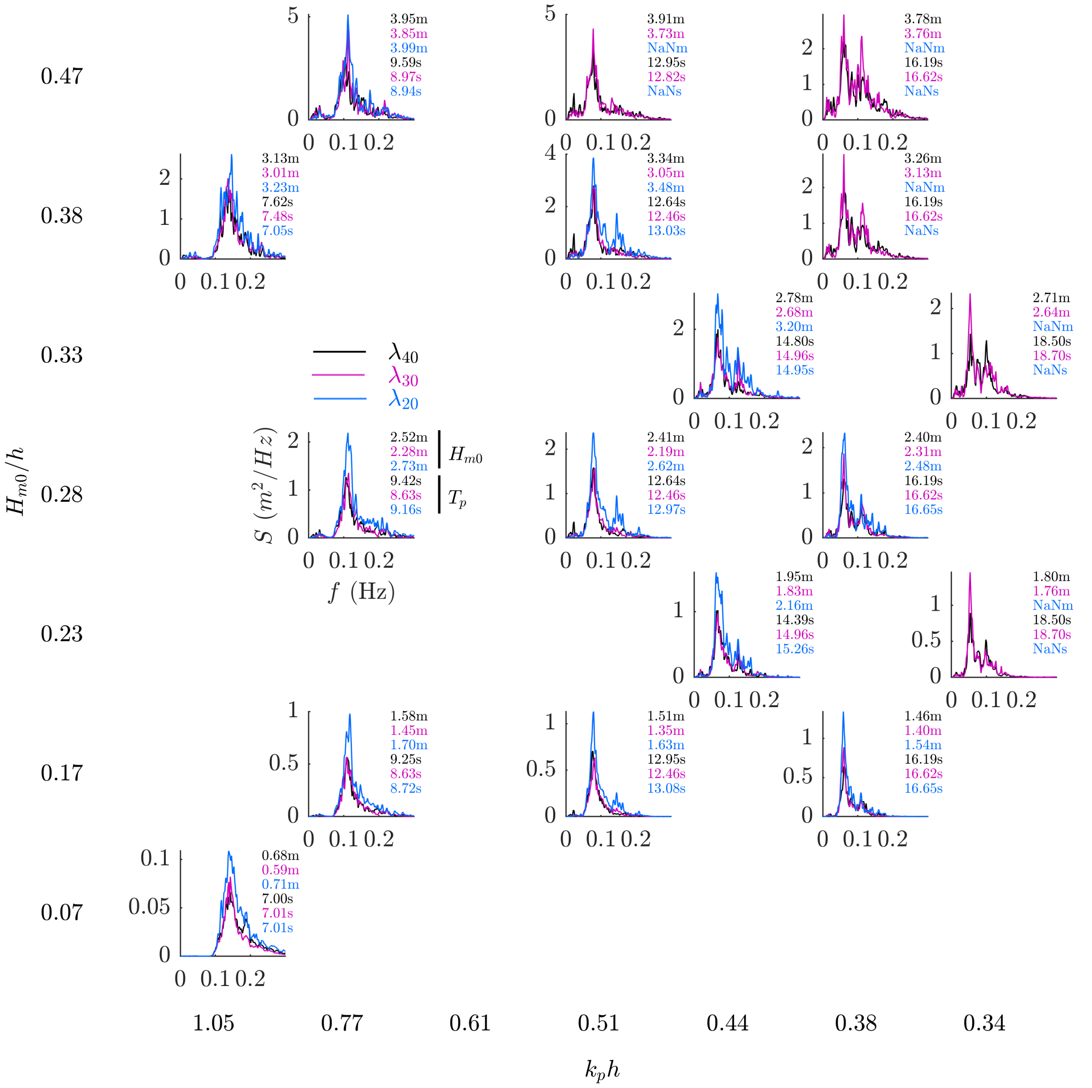

Figure 4.7: Incident irregular wave spectrum energy density S for three scales across the range of sea states tested (see middle subplot for axes labels and legend). The significant wave height H_{m0} and peak period (shown as peak wavenumber $k_p h$) matrix also shows the statistics obtained for H_{m0} and peak period T_p to the right of each subplot for reference. Results show larger model scales tended to have larger wave power spectra S.

the regular wave trends, there are several possible explanations. First, $P_{W,\lambda_{30}}$ was smallest overall, 11% smaller than $P_{W,\lambda_{40}}$ on average, which would have contributed to the relatively smaller C_W (see correlation plots for comparison Fig. 4.9). Another factor may have been the minor differences of $k_p h$ (or T_p) for each sea state (seen visually in Fig. 4.8 by the relative horizontal position of the overlayed white symbols showing the measured values). It is seen that λ_{30} had a consistently higher $k_p h$, which equates to a relatively less energetic sea state. Third, despite carefully calibrating the H_s/T_p statistics of sea states across scales, S

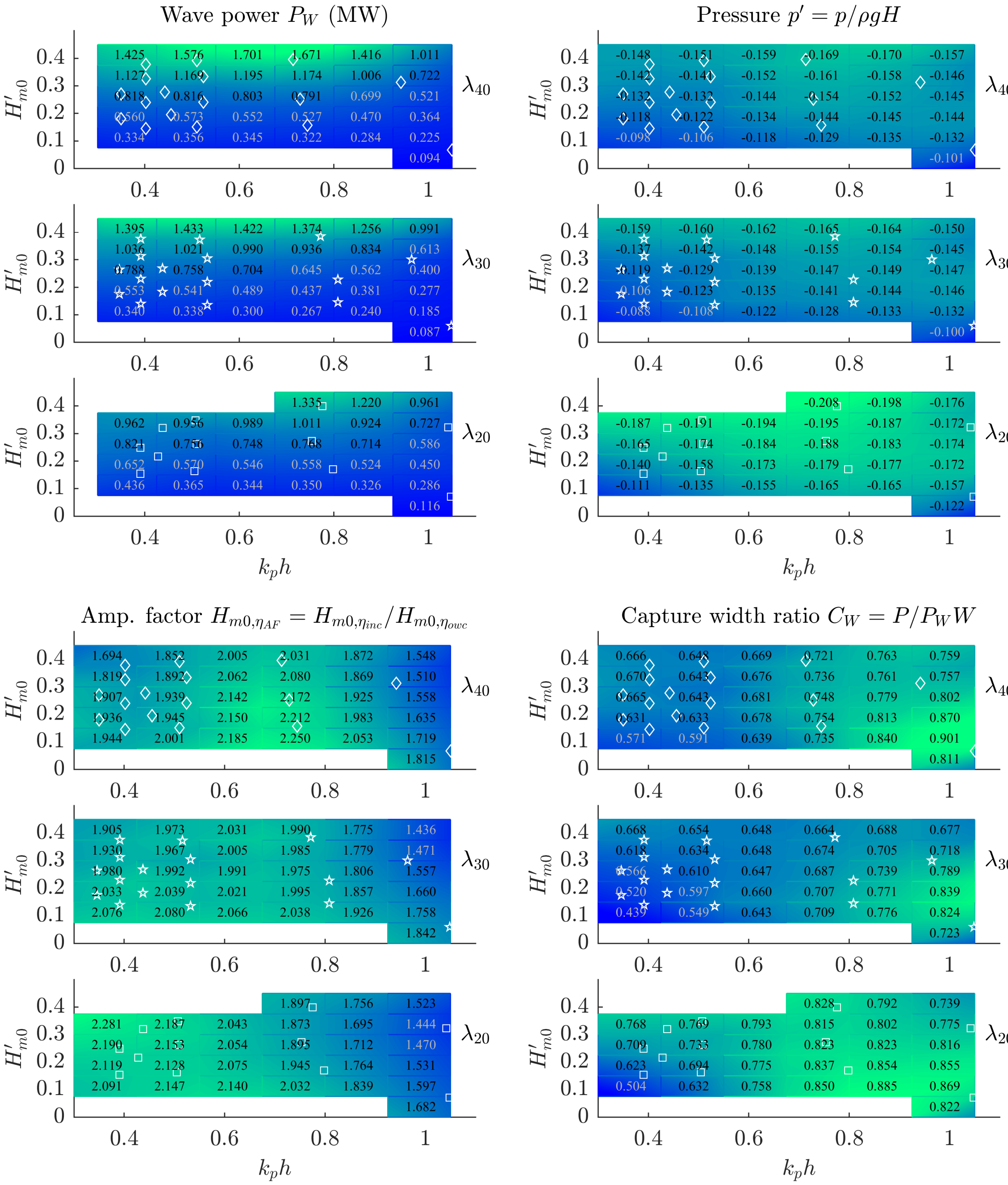

Figure 4.8: Relationship between incident wave power, and OWC hydrodynamics and power across three scales. Scales λ_i are the rows of subplots. Measurands are dimensionless and normalised by the calculated H_{m0} for each sea state. Coloured cells with text are interpolated values; white markers indicate the actual H_{m0}/T_e values; the colourbar is such that green is always the greatest magnitude, whether positive or negative. Results show generally better performance for the largest model scale, but λ_{30} was moderately smaller than λ_{40}.

deviated to a minor degree, and more in more energetic sea states. However, the sea sates were composed of nonlinear regular wave components, because of the intermediate to shallow

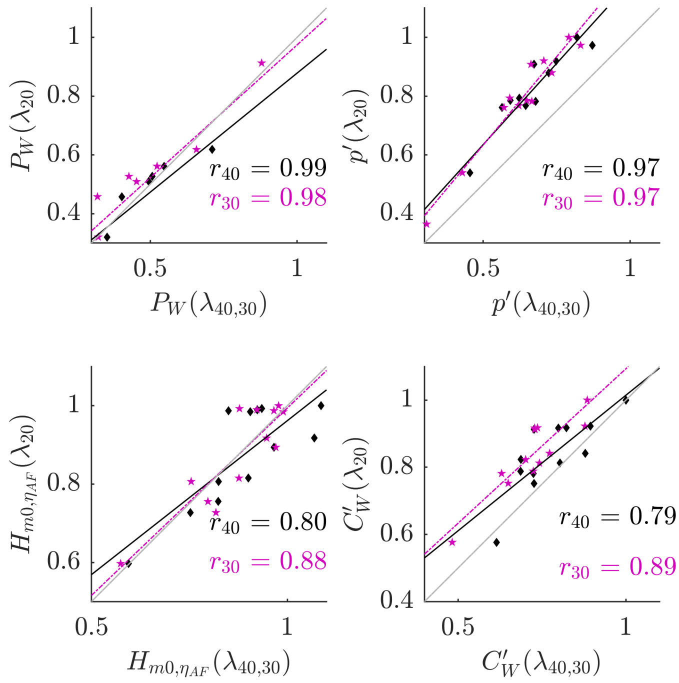

Figure 4.9: Pearson's product moment correlation r for said quantities (only measured data included, not interpolated).

water depth. Given irregular wave statistics calculations assume linear waves and are in the frequency domain, the nonlinear waves inducing nonlinear OWC responses are not captured in these statistics. In effect, even if the relevant statistics match perfectly across scales, the sea states may still differ at the individual (nonlinear) wave level. These slight differences at the wave level may accrue over the duration of the sea state run, leading to appreciable differences in the overall statistics of OWC hydrodynamics and power. It is possible that the irregular wave sea states λ_{30} were composed of nonlinear regular wave components that induced consistently smaller OWC responses.

The implication of considerably different OWC hydrodynamic and power matrices across scales is similar to that discussed for regular waves: erroneous predictions of prototype power performance based on extrapolated model-scale results. An additional factor here is that irregular wave results are used to estimate Mean Annual Energy Production (MAEP) and used as input into LCOE projections. Therefore, experimental uncertainty in these matrices due to scale effects should be evaluated and accounted for when using model test results.

4.5.3 Hydrodynamic loads

This section presents results of hydrodynamic loads in the direction that had the greater magnitudes, which was always the negative forces/moment (see Fig. 4.6 for coordinate system). For each of the important load components, two measures are given. One is the significant load calculated by averaging the third highest waves in the timeseries (analogous to significant wave height) denoted with the subscript s. The other measure is the maximum load, denoted with the subscript 4, calculated by averaging the four highest waves in the timeseries, which roughly corresponds to the 1/250 maximum load because there were $\sim$1000 waves in the timeseries (as seen in [168]).

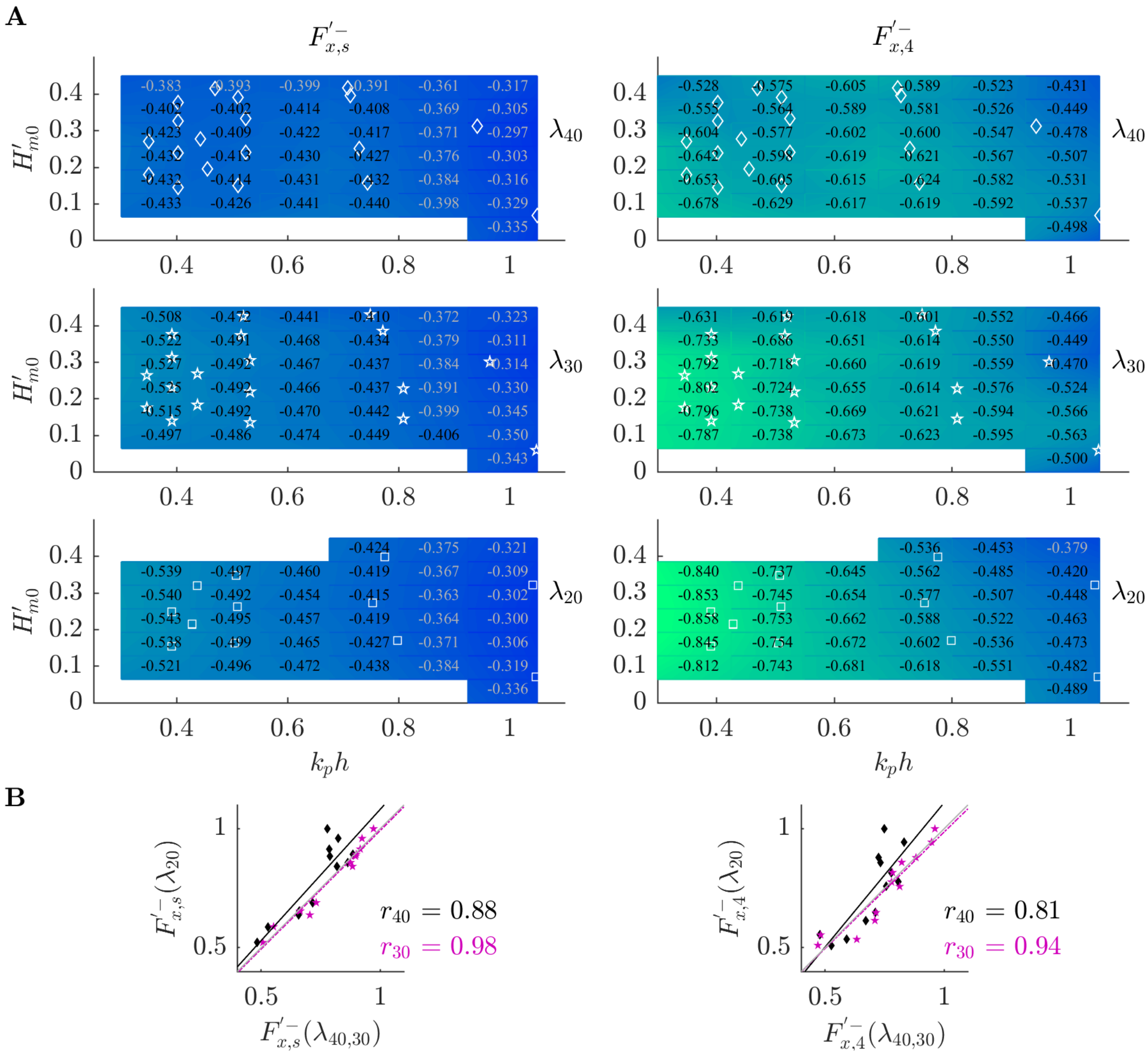

Figure 4.10: Hydrodynamic load matrices of surge force. (**A**) Significant surge force $F'^{-}_{x,s}$ (left column) and maximum negative surge force $F'^{-}_{x,4}$ (right column) for three scales, where $F'^{-} = F^{-}/\rho g A_d H_{m0}$. (**B**) Pearson's product moment coefficient r graphs, with λ_{40} and λ_{30} against λ_{20}. Results show surge force tended to increase with increasing significant wave height and energy period, and minor-moderate higher forces for the larger scale.

The general trends of loads in irregular waves were similar to those observed in regular waves, with surge force and pitch moment peaking at lower $k_p h$ and reducing as $k_p h \to 1$, and heave force showing a local peak at low-mid $k_p h$ and generally increasing as $k_p h \to 1$

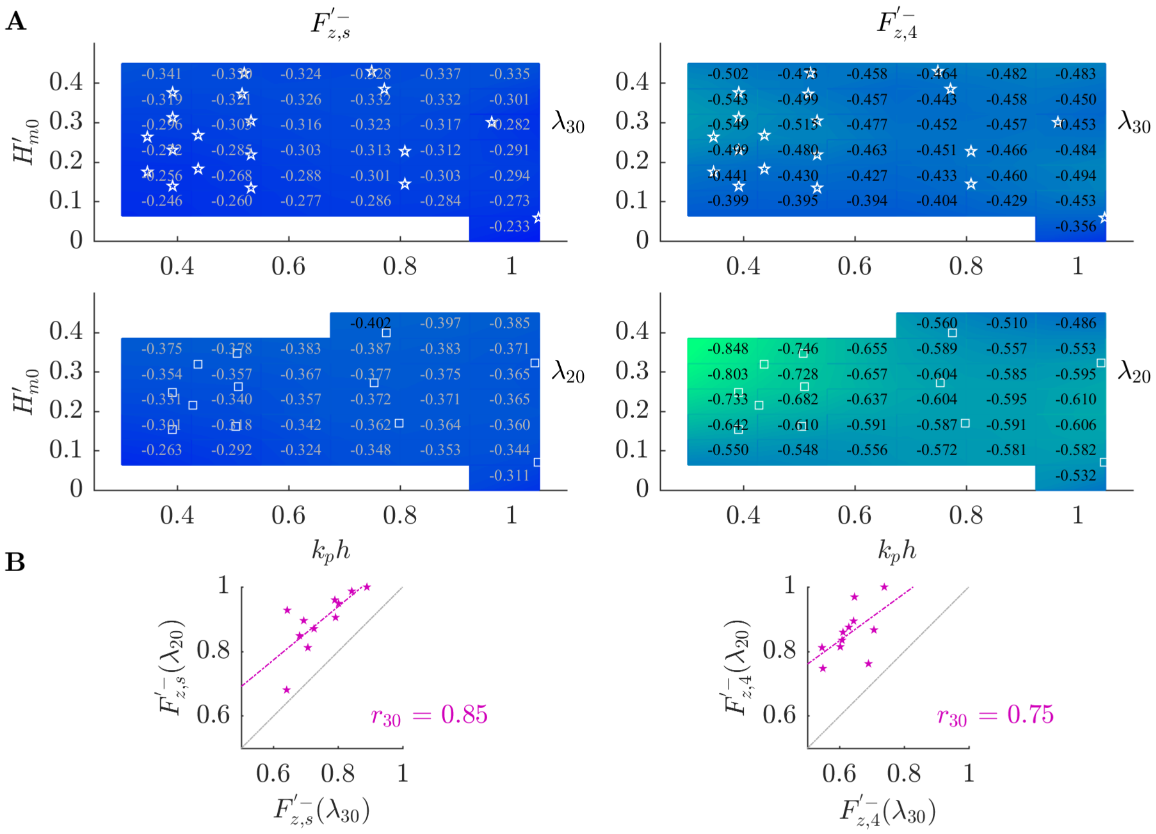

Figure 4.11: Hydrodynamic load matrices of heave force. (**A**) Significant negative heave force coefficient $F'^{-}_{z,s}$ (left column) and maximum negative heave force coefficient $F'^{-}_{z,4}$ (right column) for three scales, where $F'^{-} = F^{-}/\rho g A_d H_{m0}$. (**B**) Pearson's product moment coefficient r graphs, with λ_{30} against λ_{20}. Results show two peaks, one aligned with peak p, the other with peak $H_{\eta_{AF}}$, and moderately higher forces for the larger scale.

(Figs. 4.10 to 4.12). Another general trend was the maximum loads being 30-40% larger than the significant loads. $F'_{x,s,4}$ tended to increase with increasing H_{m0} and more so with longer wavelengths (decreasing $k_p h$), suggesting surge forces varies mostly with wavelength. Slight reduction in force at high H_{m0} was due to wave breaking. $F'_{z,s,4}$ had two peaks, one aligned with the peak of p, the other with the peak of $H_{\eta_{AF}}$ (Fig. 4.8). Like regular waves, down-acting pressure and water column heave govern the heave forces, with model buoyancy force playing a role in longer waves. $M'_{y,s,4}$ showed a similar trend to $F'_{x,s,4}$.

Across scales, the largest scale tended to encounter the highest loads (Figs. 4.10 to 4.12). Magnitude differences across scales were similar to the regular wave results: $F'^{-}_{x,s,\lambda_{20}}$ was 8% higher than $F'^{-}_{x,s,\lambda_{40}}$ and 3% higher than $F'^{-}_{x,s,\lambda_{30}}$, with these differences slightly higher for $F'^{-}_{x,4}$; $F'^{-}_{z,s,\lambda_{20}}$ was 19% higher than $F'^{-}_{z,s,\lambda_{30}}$, and 32% higher in terms of $F'^{-}_{z,4}$; and $M'^{-}_{y,s,\lambda_{20}}$ was 27% higher than $M'^{-}_{y,s,\lambda_{30}}$, similar for $M'^{-}_{y,4}$. These results indicate the maximum loads result in greater differences. The results also suggest the parameters contributing most to the differences in loads were similar to those contributing most to the differences in power-related

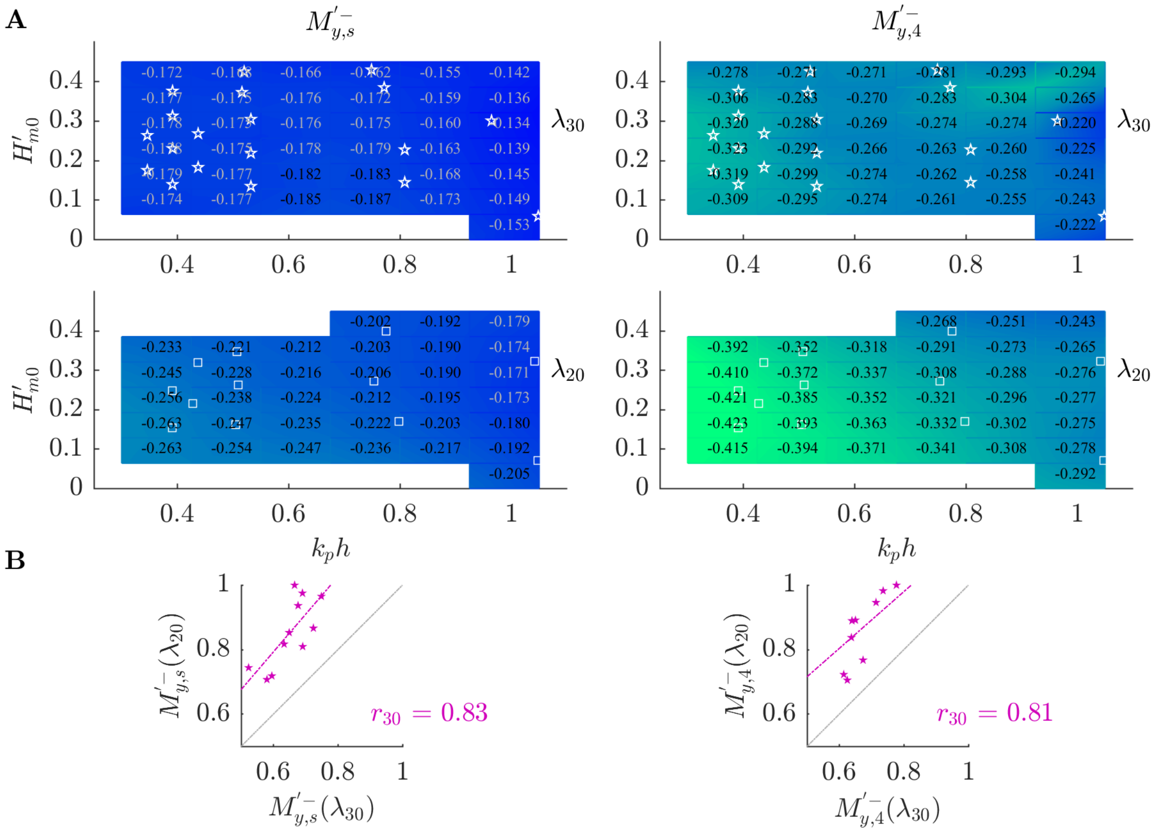

Figure 4.12: Hydrodynamic load matrices of pitch moment. (**A**) Significant negative pitch moment coefficient $M'^{-}_{y,s}$ (left column) and maximum negative pitch moment coefficient $M'^{-}_{y,4}$ (right column) for three scales, where $M'^{-} = M^{-}/\rho g A_d H_{m0}$ (significant is the average of the top third highest loads, analogous to significant wave height). The white markers indicate the actual H'_{m0}/T_e values. (**B**) Pearson's product moment coefficient r graphs, with λ_{30} against λ_{20}. Results show pitch moment tended to increase with decreasing $k_p h$, and moderate higher moments for the larger scale.

measurands. That is, nonlinear incident waves, interacting with a nonlinear PTO which had a higher damping as scale increased.

In terms of correlations, λ_{30} correlated better with λ_{20} than λ_{40} did with λ_{20}. The correlation was best for F'_x, followed by F'_z then M'_y. Additionally, the correlation between scales was always better for the significant loads than the maximum, expected given significant loads are averaged over a greater range of wave heights. Overall, these hydrodynamic load irregular wave results, compared to regular waves, had better agreement across scales, evidenced by less data scatter and stronger correlations. Where differences can be observed across scales, trends are easier to discern. This may enable better correction for the differences when scaling up model-scale results to the prototype.

Another factor to point out is the force regime governing the OWC WECs operation in the test wave climate, and how this may be affected by scale. The OWC WEC size and wave conditions tested are such that the force regime was inertia-dominated, because of the large volume structure. This means the global loads due to wave diffraction are significantly larger than the drag induced global loads [94], suggesting viscous effects, which are not Froude-scaled, contributed negligibly to the differences observed across scales.

4.6 Evaluating scale effects

Table 4.3 Scoring system indicating the likelihood (**Lh**) that a parameter causes non-negligible scale effects, and the size of the effect (**E**) that parameter may have on the overall results. The demarcation for the effects – Negligible (N), Minor (M), Significant (S) – is based on an approximate percentage contribution to the overall difference in results, as follows: N< 3%; 3% <M< 10%; S> 10%.

		Effect (E)		
		Negligible (N)	Minor (M)	Significant (S)
Likelihood (Lh)	Unlikely (U)	1	2	3
	Possible (P)	2	4	6
	Likely (L)	3	6	9

To identify and evaluate the degree to which experimental parameters contributed to the set of important scale effects, we carried out a qualitative evaluation. This evaluation consisted of a scoring system (Table 4.3) that indicates the likelihood of a parameter causing non-negligible scale effects, and the size of the effect that parameter may have on the overall results (Table 4.5). The scoring system is not dissimilar to a risk scoring matrix. The assignment of the likelihood and effect are based on the findings from this study and from the work carried out throughout this PhD research (Chapters 2, 3 and 5). The set of experimental parameters was adapted from [153] and informed by Chapter 3.

This evaluation of scale effects highlights several parameters causing most of the deviation in results, leading to scale effects. The parameters are those associated with the environment, the model, and the instrumentation and apparatus (Table 4.5), discussed in order as follows.

Incident waves (regular and irregular) were among the parameters contributing most to scale effects. Generating intermediate to shallow water waves and slightly differing wavemaker transfer functions for different water depths combined to generate incident waves that differed appreciably across scales, due to often strong nonlinearity and therefore higher order wave interactions with the first order wave. Wave reflections were considered to have a minor effect on results, with the reflections expected to be negligible in short wavelengths but minor in the longest wavelengths. A reflection analysis was not performed, however, so this is an assumption. Future work could investigate the actual degree to which wave reflections affect results across scales, which is not anticipated to be significant.

The model deployment position from the wavemaker also likely caused differences in results. Due to experimental constraints, the model deployment position was fixed in the basin

Table 4.4 List of identified experimental parameters evaluated by the scoring matrix described in Table 4.3. The result (**R**) is the multiplication of **Lh** and **E**. Notation: U = Unlikely, P = Possible, L = Likely; N = Negligible, M = Minor, S = Significant.

Parameter	**Lh**	**E**	**R**	**Comments**
Water properties				
Temperature	P	N	2	Temperature variation was < 2 C
Density	U	N	1	See above.
Viscosity	P	M	4	Differences in nonlinear waves may cause varied turbulence in and around the OWC, which may have had a minor effect on responses.
Surface tension	U	N	1	Model scales are large enough for this to be negligible.
Environment				
Incident waves	L	S	9	Shallow nonlinear waves; differing wavemaker transfer functions for different water depths. (Figs. 4.2 and 4.7)
Wave reflections	P	M	4	Un-scaled basin boundaries leading to relative differences of energy build-up in irregular wave runs; possible sources: beach, wall/edge, model.
Bathymetry	U	N	1	Bathymetry was flat.
Run duration: regular	U	N	1	Same durations across scales.
Run duration: irregular	U	M	2	Same (scaled) durations.
Data analysis	U	M	2	Same analysis.
Blockage	U	N	1	Wide basin.
Initial conditions	U	M	2	Remaining waves, circulation, or turbulence from remaining waves.
Model				
Geometry	P	M	4	Model construction limitations due to standard material dimensions.
Installation	U	M	2	e.g., alignment to wave front.
Deployment position	L	S	9	Model deployment position fixed in basin, so relatively different distance from wavemaker, leading to differing shallow nonlinear wave transformations.
Mooring	U	M	2	i.e., securing model to force balance for bottom-fixed OWC.
PTO	L	S	9	Maintaining optimal orifice-chamber area ratio (1:150) led to dynamic dissimilarity, where PTO damping increased by a minor-moderate degree as scale increased.
Weight/buoyancy	P	M	4	Consequence of model construction limitations said above, affecting loads results.

Table 4.5 continued

Parameter	Lh	E	R	Comments
Instrumentation, apparatus				
Wave probe	U	M	2	i.e., accuracy (repeatability, linearity, hysteresis). Unlikely, and low uncertainty (see Chapter 3)
Pressure sensor	U	S	3	i.e., accuracy (repeatability, linearity, hysteresis). Unlikely, but appreciable uncertainty (see Chapter 3).
Force balance	P	S	6	i.e., accuracy (repeatability, linearity, hysteresis). λ_{40} loads results unreliable in heave and pitch moment.
Installation	U	S	3	Wave probes and pressure sensors required insertion through top of model to measure quantities inside, potentially compromising air tightness of chamber if not properly installed.
Human factors				
Experimental setup	U	S	3	Lead researcher was helped by several people less informed of the experimental details, potentially affecting, e.g., instrument calibrations.
Record keeping	U	M	2	Lead researcher responsible for all record keeping.
Data analysis	U	M	2	Lead researcher performed all analysis with same codes.

so it could be mounted to the force balance. Consequently, the intermediate to shallow water waves propagating toward the model transformed differently in space and time, resulting in the models encountering different nonlinear wave profiles. In addition, the PTO simulation play a key role due to maintaining the optimal orifice-chamber area ratio of 1:150. This geometric similitude condition led to a dynamic dissimilarity, evident by higher PTO damping for larger scales. While the PTO had lightweight flaps that simulated passive valves to create unidirectional flow, great care was taken to ensure these flaps created air-tight seals and that they were correctly setup before and during all tests. Therefore, experimental setup of this PTO feature was considered contribute negligibly to the differences in results.

The key instrumentation and apparatus parameter was the force balance. As mentioned, there were challenges in using the same force balance to measure loads for three model scales, due to the Froude-scaled relations of forces (λ^3) and moments (λ^4). This constraint presented challenges for the in-situ calibrations of the force balance to cover the full measurement range, from the relatively small loads for λ_{40} (~30 kg max) to the relatively large loads for λ_{20} (~240 kg max). These challenges led to unreliable loads data for λ_{40} in the heave force and pitch moment components. As such this was identified as a likely significant scale effect, and in general highlights the challenge of measuring hydrodynamic loads in already complex WEC experiments.

Regarding human factors, despite all scale series experiments conducted in the same way, support was provided by a number of others less informed of the details of the experiment, support with instrumentation setup and calibrations, model setup, and other construction and debugging activities. Given this test program was large in scope, with several conditions requiring changes of models, configurations, and wave types, errors and mistakes in these processes, while unlikely, could affect the results.

Finally, we discuss implications and limitations of this investigation. First, without full-scale prototype data of this case study OWC WEC operating in the ocean, it is impossible to examine scale effects between the laboratory and the ocean. Thus, there is unknown uncertainty of whether or not the largest model itself is already affected by non-negligible scale effects [23]. Given the significant differences between the middle and largest scale, which confirms one part of the hypothesis of this PhD research, and experimental simplifications such as using an orifice to simulate an air turbine, which is likely a rough approximation of the damping of a prototype air turbine operating in the ocean [87], this suggests it is likely the largest scale is also affected by non-negligible scale effects.

This investigation also reveals a possible limiting criteria – to avoid significant scale effects – for similar hydrodynamic model tests of WECs that are characterised by nonlinear environments (waves and currents) and nonlinear subsystems (catpor motions and PTO). If accurate power performance estimates are required then model scale should be 1:30 or larger. If yet more accurate estimates are required, it is recommended to carry out a series of model test experiments at different scales to assess the sensitivity of results to scale. Another implication is the establishment of a baseline (in)accuracy of hydrodynamic model tests of similar WECs. Our results show significant deviations of power and loads results due to scale effects, on the order of 20-30+%, which is outside the measurement uncertainty. These findings not only yield insights into the overall experimental uncertainty that is to be expected if only one model scale is tested, but can be useful to inform developers and researchers when they plan, execute, and report a model test program and use the experimental results.

4.7 Conclusions

Despite the hydrodynamic model test experiments of the WSE OWC WEC at three model scales being conducted to a high standard according to international guidelines, key power and loads results differed by an amount larger than the measurement uncertainty. This finding supports the hypothesis proposed in the Introduction (Chapter 1). Measurement uncertainty results were similar across scales, suggesting measurement uncertainty had a negligible contribution to the differences in results. The parameters that contributed most to these differences in results – evaluated through a scoring matrix that scored the likelihood of a parameter that causes non-negligible scale effects and the size of the effect that parameter may have on the overall results – were associated with incident waves and model parameters, with instrumentation and apparatus also playing a non-negligible role.

Increasing model scale tended to show better power performance and larger hydrodynamic loads. Across scales, results of incident waves, OWC hydrodynamics, power, and loads showed moderate to major differences (30+%) on average, with some differences exceeding 50%. The differences were slightly less for irregular waves. Key parameters causing these scale effects were evaluated to be the nonlinear incident wave profiles and PTO damping. In particular, waves deviated across scales due to relatively different distances between the models and wavemaker, giving rise to different wave transformations, and different wavemaker transfer functions for each water depth. Despite careful wave calibration, these circumstances led to deviating regular wave profiles and irregular wave energy density spectra, both of which induced deviating OWC hydrodynamic responses which, in turn, influenced power and loads. Regarding the PTO, damping increased by 8.5% on average per scale, which was a key contributor to the relatively larger power and loads for larger scales. The main cause of this scale effect was likely due to satisfying the geometric similitude condition of optimal orifice-chamber area ratio, which suggests the nonlinear air pressure-flow characteristics induced by the orifice quadratic damping did not scale well. Noted, experiment difficulties in loads measurements led to some load components in the smallest model being omitted from the analysis. This suggests that the force balance likely had a minor influence on loads results across scales. Overall, these findings lend further support to the current best practice that model scale should generally increase as WECs progress through the TRLs, with the aim to achieve more accurate model-prototype similarity.

A commonality that emerged from these findings is the influences of nonlinearities. Nonlinear processes and interactions between waves, OWC hydrodynamics, and PTO damping seem to be key factors contributing to scale effects. With multiple interacting nonlinearities, even slight deviations across scales in environmental forcing or model parameters amplify the differences in OWC hydrodynamics, power, and loads. Therefore, the findings of this study may be relevant for other WEC designs characterised by nonlinear waves, nonlinear motions, and nonlinear PTOs. In such cases, without testing multiple scales, it should be expected that experimental uncertainty due to scale alone may be $\pm 15\%$. The finding here should also be considered in the context of the literature on the potential scale effect of air compressibility in OWC WECs, and the potential Reynolds number scale effect.

This investigation clearly shows that scale can significantly influence the results of OWC WEC model tests, thereby increasing experimental uncertainty. Scale effects, therefore, should not be ignored when conducting these experiments and when using the results. Resources should be prioritised at the planning and design phase of the experiment to evaluate the potential influence of scale on the results. General Uncertainty Analysis, demonstrated in Chapter 3, might be useful for such an evaluation. When using experimental results, it is recommended to consider how the results will scale. Such consideration is critically important because extrapolations of model-scale results play a key role in WEC development. If scale effects are not accounted for in these uses, this could lead to increased development risks or disillusionment with the overall technology performance and reliability.

An apparent outstanding challenge in WEC model tests is that the means to account for scale effects is still not well understood. There is a lack of best practices that provide guidance on how to avoid, compensate, or correct for scale effects. Therefore, further research is needed to enhance the understanding of WEC-specific scale effects and develop means to account for them. One limiting criterion emerging from this study, which might help avoid scale effects of bottom-fixed OWC WECs, is that model scale should be as large as the laboratory can handle. In our case, 1:30 scale was most suitable for the basin and experiment, allowing for operational and some survival waves. If in future experiments survival tests are the focus, smaller models may be needed to achieve representative extreme wave conditions. If smaller models are used, this should be carefully considered in the results, and a larger scale will be required to be tested at higher TRLs. More limiting criteria are undoubtedly needed. Moreover, compensation techniques that distort the physical model to achieve better dynamic similarity should be thoroughly investigated, as should empirically-derived factors that can be applied to correct power and loads results for the quantitative influence of scale effects. A key part of improving the knowledge of and means to account for scale effects might be to reverse engineer the problem, by carrying out open water tests on a prototype and then going back to the laboratory to model an exact version of the prototype, and comparing results. To date, such investigations are very limited. Like the present investigation, these future investigations should aim to improve the international guidelines on WEC model tests.

While this work focused on a case study OWC WEC, it nevertheless provides a sound reference for stakeholders of WEC model tests to gain insights into the possible sensitivity of model-test results to scale. It thus extends the understanding of scale effects of OWC WECs specifically and WECs generally. The main recommendation arising from this investigation is that, until more knowledge is available on scale effects of WECs, it might be prudent for developers to carry out a series of model tests at multiple scales to generate confidence in the experimental results and, therefore, confidence in the technology as it progresses beyond the laboratory into the open water at higher Technology Readiness Levels.

Chapter 5

Experimental Investigation Into Laboratory Effects of an OWC Wave Energy Converter

Consistent results obtained when an experiment is repeated — reproducibility — is key to advancing science and de-risking engineering. However, whether consistent results are obtained when a WEC model test experiment is repeated has not been investigated. This chapter is a first step. It reports a 1:30 scale experiment of the case study OWC WEC reproduced in two wave basin laboratories, carried out to identify, quantify, and evaluate parameters causing laboratory effects.

5.1 Introduction

Hydrodynamic model test experiments are central to developing Wave Energy Converters (WECs), as they are used to test and progress WECs through several stages of the Technology Readiness Levels (TRLs). Model tests are carried out in TRL 1 to prove a concept, in TRL 2-3 to validate and optimise power and survival performance, and in TRL 4+ to advance the technology for prototype demonstration in the ocean [11, 10, 187]. However, no two wave basins are the same; they are neither uniformly configured nor have the same capabilities. If a different laboratory was chosen at any of the TRLs there is little if any literature in wave energy, neither studies nor guidance nor projects, on the differences that might be expected between results obtained from different, though nominally similar laboratories (the MARINET 1 project attempted this task but was abandoned [43]). This is an alarming situation because laboratory effects can be a major source of experimental uncertainty [22]. It follows there is a pressing need to address the lack of knowledge of how wave basin laboratories – their parameters and uncertainty sources – influence WEC model test results, and the largely unknown role laboratory effects play in overall WEC development [10].

To better understand the limitations and uncertainties of WEC model test experiments, a Specialist Committee of the International Towing Tank Conference (ITTC), who develop guidelines for marine renewable energy, assigned to their terms of reference the investigation of laboratory effects [19, 20]. The aim of the terms of reference related to laboratory effects was to undertake a round robin test campaign, similar to the ship Resistance Committee [25]. To realise this aim requires a series of reproduced experiments to determine which parameters likely cause laboratory effects, leading to non-negligible differences in the results; that is, to test the sensitivity of results to the choice of laboratory. The work in this chapter is a first step.

What are laboratory effects? They can arise due to such modelling limitations as the inability to simulate realistic forcing conditions, basin boundaries influencing waves and reflections, and variation of experimental procedures [22]. Moreover, each laboratory is uniquely configured, employs one method among many to generate and absorb waves and other environmental conditions, uses particular instrumentation, has different model building capabilities, different ambient conditions, and so on. All these experimental parameters can influence the results to some degree, so it is important to investigate which parameters have a non-negligible degree of influence relevant for WEC model tests.

Related maritime engineering fields have studied laboratory effects. A succession of ITTC Resistance Committee's undertook an ambitious initiative, a worldwide campaign across 41 towing tanks [25]. The objectives were to benchmark tests, identify laboratory effects ("facility biases"), evaluate uncertainties, and gain insight into each laboratory's operation. The campaign consisted of testing similar ship models in standard tests of resistance, sinkage, and trim. The interlaboratory comparisons yielded both informative and surprising results, with significant differences between laboratories found in both the values of said measurands ($\sim$30%), and their associated uncertainty (5-50+%). Key conclusions from this campaign where the following: extrapolating model data to full-scale gives different results, depending on the laboratory, and to reliably compare results they need correction; the campaign was valuable despite great difficulties in worldwide model transportation and obtaining acceptable data for inclusion; it served as a stark reminder of the challenges in conducting high-quality experiments; and laboratories were challenged to consider whether they are actually delivering experimental uncertainty to levels stated in documentation.

In ship manoeuvring, several studies have observed significant variation in interlaboratory comparative results of manoeuvring performance predictions [188, 26]. The likely cause of the variation between laboratories, sometimes significant, was systematic in nature; that is, the experimental procedures were ill-contrived or insufficiently defined [26]. Various studies have also been carried out on laboratory effects relevant for coastal engineering problems

[22]. Lastly, the MaRINET 1 project did succeed in a round robin test campaign of a tidal turbine, comparing results between towing and circulating tanks [27].

Given even mature maritime fields still show significant differences in interlaboratory results and uncertainties, this underscores the need to undertake similar lines of research into laboratory effects within the relatively immature wave energy field. This is especially because WECs are often complex machines operating in complex environments, with unique geometries, large relative motions, a PTO system, dynamic mooring systems, and so on (as Chapter 2 details). Thus, WECs are surmised to be uniquely vulnerable to laboratory effects. This work fulfils the need to gain insight into the problem of laboratory effects in WEC experiments.

This chapter seeks to identify, quantify, and evaluate the main parameters causing significant laboratory effects in a typical early-stage WEC experiment (TRL 1-4). The experiment consisted of a range of standard performance assessment tests of the case study OWC WEC at two scales (1:30, 1:20), carried out in two shallow water wave basin laboratories: the Australian Maritime College (AMC) Model Test Basin and the Queen's University Belfast (QUB) Coastal Wave Basin (Fig. 5.1). The results and discussion evaluates identified parameters that cause laboratory effects and presents key findings. This study contributes to enhancing the understanding of experimental uncertainty in wave energy any hydrodynamic-related fields.

5.2 Experimental overview

To distinguish between the experiments, E_{AMC} denotes the experiment at AMC, E_{QUB} at QUB. Many of the methods of the interlaboratory experiments reported in this chapter have already been described in previous chapters. Specifically, Chapter 1 outlined the case study OWC WEC used in these interlaboratory experiments. Chapter 3 described methods relevant for E_{AMC}, including the experimental parameters of the OWC WEC model particulars, environmental and model conditions, measurements, instrumentation, and calibrations, and procedures for data processing and analysis. Chapter 3 also presented a comprehensive uncertainty analysis (UA) performed on E_{AMC}, which is the same procedure performed for the investigations in this chapter. Chapter 4 described the three OWC WEC models used to investigate scale effects. The 1:30 and 1:20 scale models were included in the interlaboratory experiments. Table 5.1 presents the parameters of the interlaboratory experiments. Because the 1:20 scale results were similar to the 1:30 scale, we present the 1:20 results in Appendix C. This brief section describes the methods specific to the interlaboratory experiments, as follows.

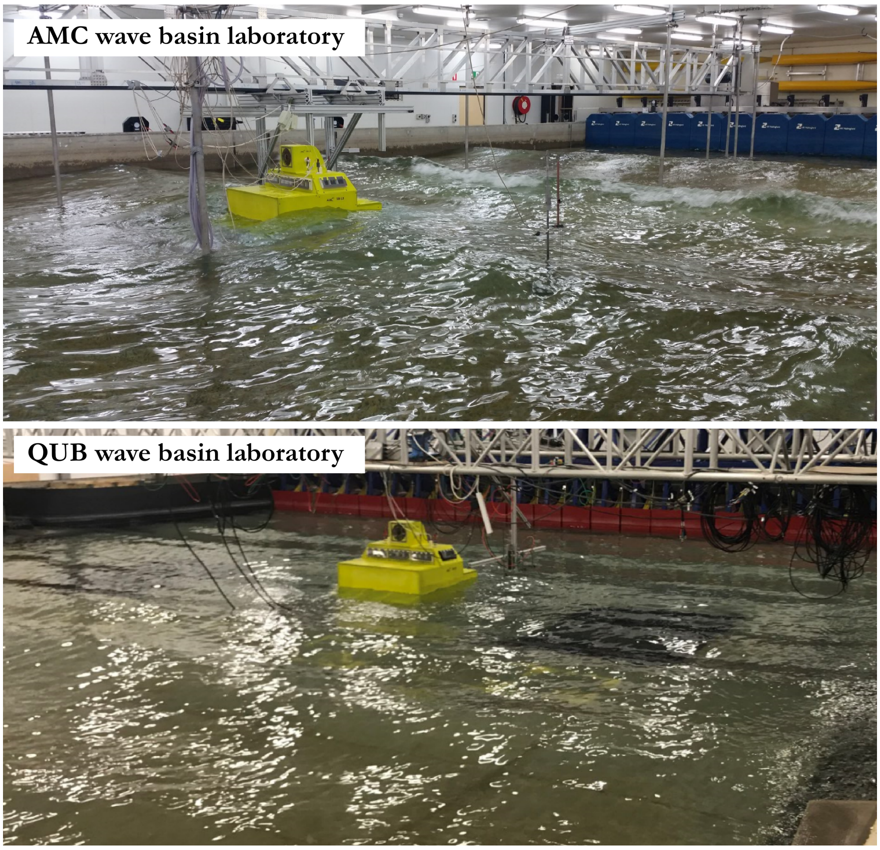

Figure 5.1: Photographs of the wave basin laboratories used in this study, showing the 1:20 scale model in the Australian Maritime College Model Test Basin at top, and the Queen's University Belfast Coastal Wave Basin underneath.

5.2.1 Laboratories

The two shallow water wave basin laboratories in which the experiments were carried out for this study were the AMC Model Test Basin in Tasmania, and the QUB Portaferry Coastal Wave Basin in Northern Ireland (Fig. 5.2). The AMC wave basin laboratory is 35 m long by 12 m wide; has flat bathymetry; a variable water depth of 0-1 m (constant during tests); has a floor level to within ± 3 mm from horizontal; is a fresh water basin having a temperature of ∼16 degrees Celsius; and has a 16-element wavemaker (horizontal motion) at one end and a wave absorbing beach at the other, with vertical side walls. The QUB wave basin laboratory is 18 m long by 12 m wide; has a slope bathymetry; a variable depth of 0-1 m (constant during tests); has a floor level to within ± 5 mm; is a fresh water basin having a temperature of ∼14 degrees Celsius; and has a 24-element piston-type wavemaker (top-hinged rotational motion) at one end and a wave absorbing beach at the other, with 'soft' edges (sloped gravel beaches).

The wavemaker operating principle was different between E_{AMC} and E_{QUB}. The AMC wavemaker generated waves through horizontal motion, whereas the QUB wavemaker gen-

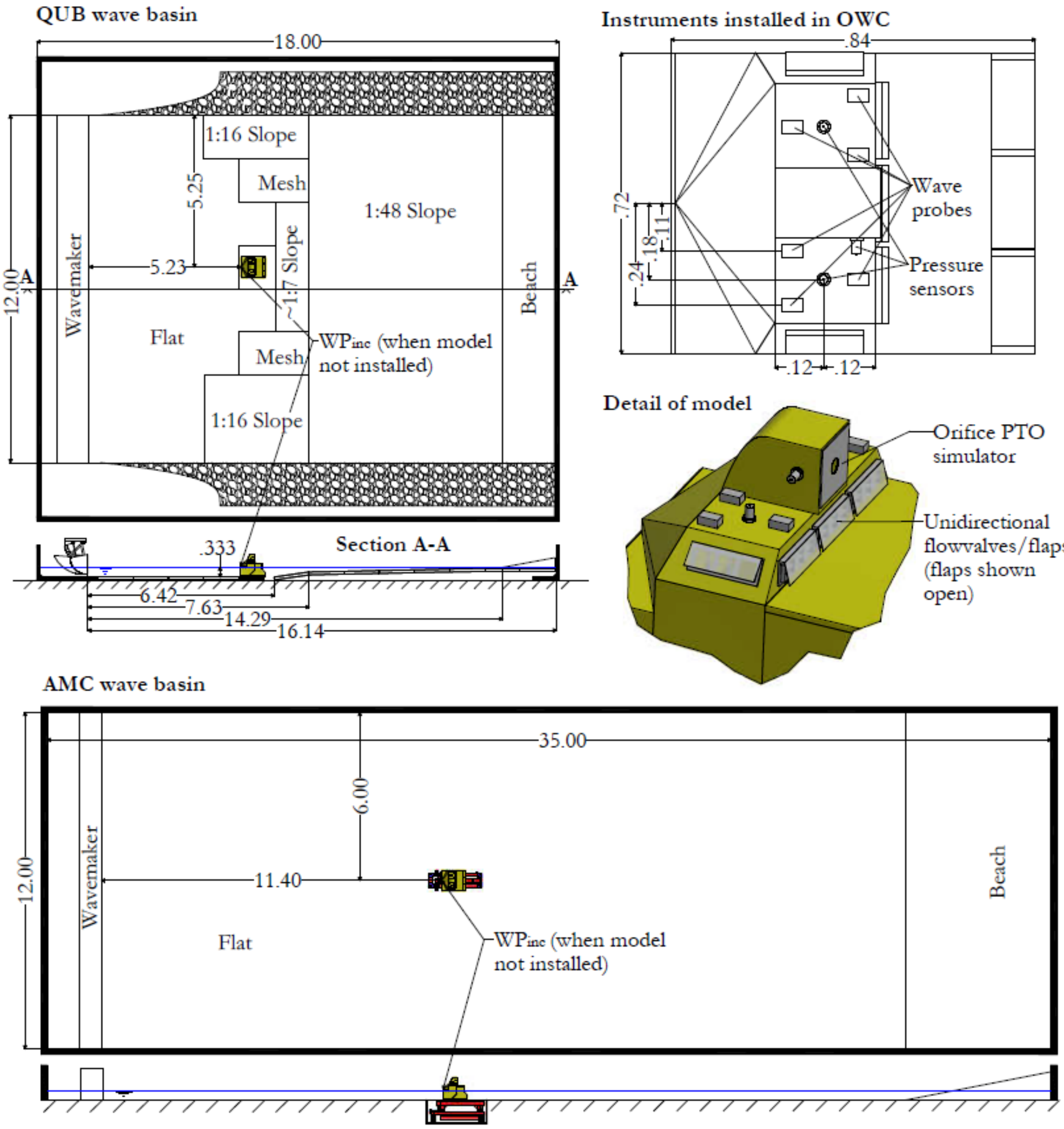

Figure 5.2: Drawings and assemblies showing key laboratory and model particulars and arrangements. The **QUB wave basin** and **AMC wave basin**, and the 1:30 scale model and its respective deployment position in the basins, are drawn to scale with annotated dimensions. WPinc shows the position of the incident wave probe for the incident wave measurements performed before the model was installed.

erated waves through top-hinged rotational motion (Fig. 5.3). The different wave making principles suggest their transfer functions to generate a given sea state, whether regular and irregular, differed to some degree. In addition, the QUB wavemaker also had dynamic wave force absorption that reduces the build-up of wave reflections, thereby giving good control and repeatability.

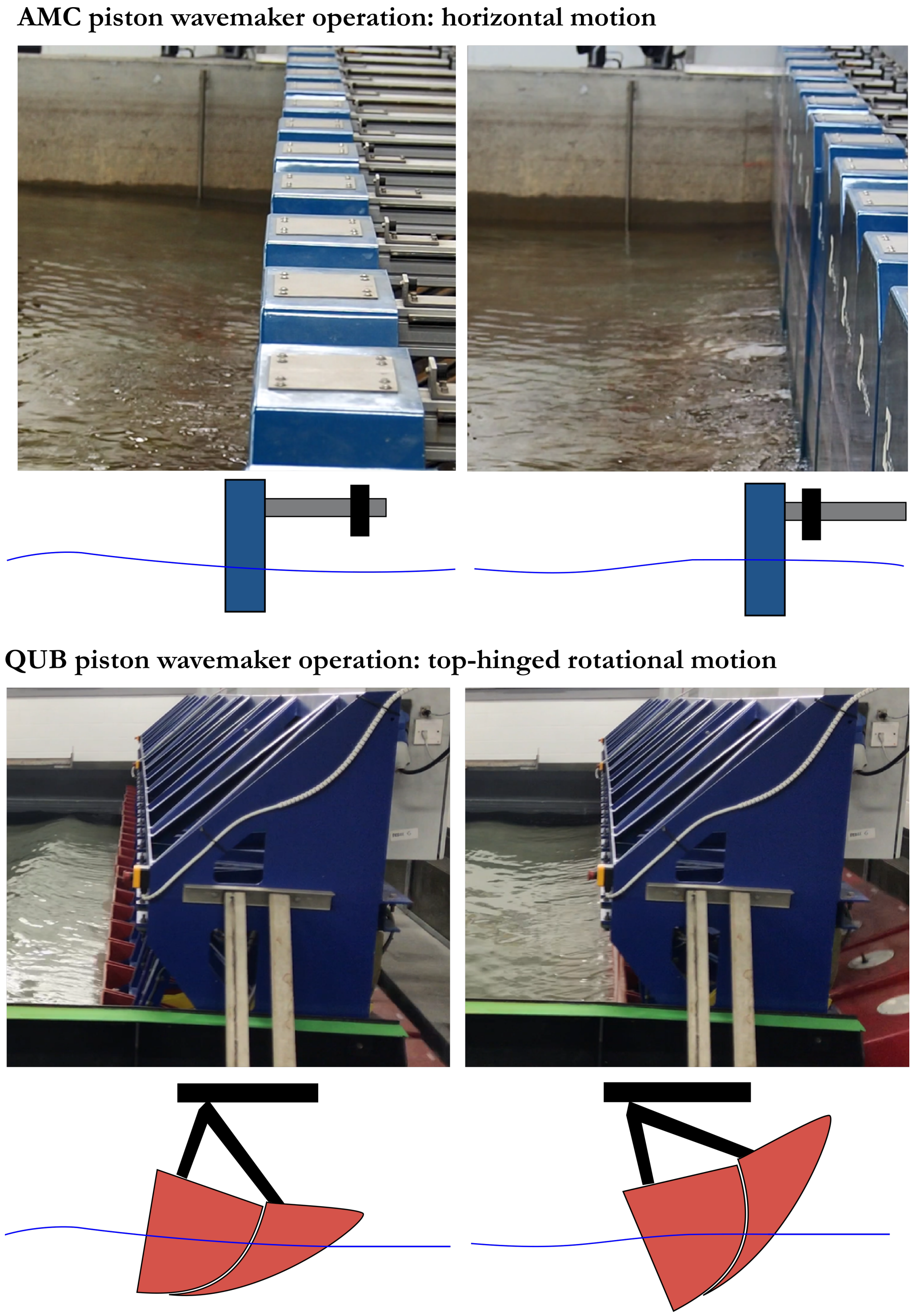

Figure 5.3: Photographs and diagrams showing the different wavemaker operations for E_{AMC} and E_{QUB}. The AMC piston wavemaker generates waves through horizontal motion, whereas the QUB piston wavemaker generates waves through top-hinged rotational motion, and creates no back wave.

5.2.2 Experiment parameters and procedures

Table 5.1 presents the parameters of the experiment, including model and environmental parameters, measurement and data parameters, and the experimental conditions. Fig. 5.2 shows the experimental setup of the model position in each laboratory, along with details of model features and instrumentation configurations.

It is seen in Table 5.1 that hydrodynamic loads imposed on the OWC WEC model were measured in both laboratories. Unfortunately the loads measurements in E_{QUB} were subject to a range of difficulties that lead to the loads results being omitted from the analysis. We elaborate on this further in the general discussion (§ 5.4).

5.2.2.1 Data reduction, analysis, and uncertainty

The quantities, Data Reduction Equations (DREs)/measurands, and data analysis methods for these experiments were described in Chapters 3 and 4. The key quantities and DREs include wave power P_W derived from incident wave measurements η_{inc}; OWC power P derived from pressure p measurements inside the OWC and an in-situ calibrated orifice C_d using wave elevation measurements inside the OWC η_{inc} to derive air flow q; and capture width ratio $C_W = P/P_W B$ where B is the OWC width. All results have been phase-averaged unless stated otherwise. The phase-averaging method was described in Chapter 3 and previous work [40]. The same MATLAB codes were used process and analyse the data from both experiments.

OWC hydrodynamic and power quantities have been non-dimensionalised by the wave height (see table of non-dimensional quantities in Chapter 4, so that slight variation in wave height in a given wave height set is accounted for. This removes the effect of wave height to enable correct comparisons of results between laboratories. The notation for a dimensionless quantity is the quantity symbol followed by a prime (e.g., for air pressure, p'). When discussing results, the term 'dimensionless' is omitted.

The uncertainty analyses performed in the experiments were identical; that is, we used the same analysis methods to evaluate Type A uncertainty u_A and Type B uncertainty u_B, to propagate uncertainty to determine the combined uncertainty u_c using the Monte Carlo Method (MCM), and to calculate the expanded uncertainty U (refer to Chapter 3 for details of the methods). Moreover, the same uncertainty analysis code was used to process the data. The uncertainty analysis results are presented as box-and-whisker plots, showing u_A, u_B, and U, with these distributions described at length in Chapter 3. The table-like layout of the summary uncertainties enables comparison of uncertainty components of directly measured and derived measurands across experiments.

Table 5.1 Parameters of the interlaboratory experiments. Values are full-scale (FS) unless state otherwise.

<table>
<tr><th>Parameter</th><th>E_{AMC}</th><th>E_{QUB}</th></tr>
<tr><td>Model</td><td colspan="2">Bottom-standing unidrectional flow OWC
2 Froude-scaled models (1:30, 1:20)
Orifice PTO simulator</td></tr>
<tr><td rowspan="2">Environment</td><td colspan="2">Operational water depth: 10 m
Shallow water wave basin</td></tr>
<tr><td>35Lx12Wx1H m; Flat bathymetry, vertical walls; 16-element wavemaker (horizontal motion), passive beach (see Fig. 5.2)</td><td>18Lx12Wx1H m; sloped bathymetry, 'soft' edges; 24-element wavemaker (top-hinged rotational motion), passive beach (see Fig. 5.2)</td></tr>
<tr><td rowspan="5">Measurements; instruments; calibrations;</td><td colspan="2">Wave elevation in basin and OWC; conductive wave probes; calibrated daily</td></tr>
<tr><td colspan="2">Pressure in OWC;</td></tr>
<tr><td>3 x Honeywell Controls TruStability pressure sensor with Ocean Controls KTA-284 instrumentation amplifiers; calibrated per model to ± 2000 Pa.</td><td>3 x Sensor Technics HCXM050D6V; calibrated per model to ± 2000 Pa.</td></tr>
<tr><td colspan="2">Hydrodynamic loads on model;</td></tr>
<tr><td>six-component force balance constructed from six multi-element cantilever load cells (MTI 4856-500 load cells) with flexure rods; calibrated before and after each scale experiment.</td><td>six-component force balance constructed from three coupled single-element multi-component transducers (AMTI SP2.5D); calibrated before and after each scale experiment.</td></tr>
<tr><td>Data acquisition</td><td>National Instruments PCI-6254M Multifunction DAQ, acquired at 200 Hz.</td><td>National Instruments cDAQ-9188 CompactDAQ, acquired at 120 Hz.</td></tr>
<tr><td>Data recording</td><td colspan="2">Regular waves: 30 secs (model-scale)
Irregular operational waves: 30 mins
Irregular survival waves: 3 hrs</td></tr>
<tr><td rowspan="2">Wave conditions</td><td>Regular waves:
H_1=1.8 m, H_3 3.0 m; kh=0.41-0.98(T=7-15.8 s)</td><td>
H_1=1.8 m, H_3 3.0 m; kh=0.6-0.98 (T=7-13.7 s)</td></tr>
<tr><td>Irregular waves:
15 sea states: H_s=0.75-4.75 m, $k_p h$=0.4-1.0 (T_p=7-19 s)</td><td>
12 sea states: H_s=0.75-4.75 m, $k_p h$=0.6-1.0 (T_p=7-13.7 s)</td></tr>
<tr><td>Model conditions</td><td colspan="2">Incident waves without model: all waves
Power matrix: all operational waves</td></tr>
</table>

5.3 Results and discussion

We first report and discuss uncertainty analysis results from the two laboratories. Following are analyses of regular and irregular wave results, including results of incident waves and OWC hydrodynamics and power. These analyses focus on the differences in results between laboratories, rather than the OWC WEC hydrodynamics and performance themselves, which were described at length in Chapter 4. Following this is an evaluation of laboratory effects through a scoring matrix. We employ the same terminology and quantitative scale to discuss differences as previously: *negligible* (<5% relative percentage difference (RD)); *minor* (5-10% RD); *moderate* (10-30% RD); and *major* or *significant* (30+% RD).

5.3.1 Uncertainty analysis

To first understand the degree to which measurement uncertainty differed between experiments, we compared the uncertainty analysis results from regular waves (Fig. 5.4). The results show strikingly similar uncertainty results for the measurands, both directly measured and derived. The key measurands of incident wave power P_W, OWC power P, and capture width ratio C_W were similar in both Type A uncertainty u_A and Type B uncertainty u_B, thereby producing similar magnitudes of expanded uncertainty U. The u_A for $C_{W_{AMC}}$ was slightly higher, resulting in U_{AMC} of $\pm 16\%$ on average, whereas U_{QUB} was $\pm 12\%$ on average. These results indicate that both experiments were well-controlled, with highly repeatable waves and little variation in the OWC hydrodynamics and power responses, and that the main u_B uncertainties were of a similar kind and magnitude. Therefore, we surmise that while measurement uncertainty was considerable in both experiments, the levels of uncertainty were similar, so measurement uncertainty had a negligible contribution to laboratory effects.

5.3.2 Regular waves

5.3.2.1 Incident waves

This analysis examined the differences in incident waves, without the model deployed, generated between laboratories for nominally similar inputs of wave height H and period T into the wavemaker (Fig. 5.5). Regarding general trends first, the smallest shortest waves were mostly linear ($H = 1.6, kh = 0.89$), and the highest longest waves mostly nonlinear, as expected (Fig. 5.5**A**). A classic nonlinear wave asymmetry was observed in both laboratory waves, with higher peakier wave crests and flatter wave troughs, as expected given the waves ranges from intermediate to shallow water [94].

Comparing waves between experiments, the incident wave elevation profiles η_{inc} tended to agree for more linear waves, but as wave height and period increased the profiles became

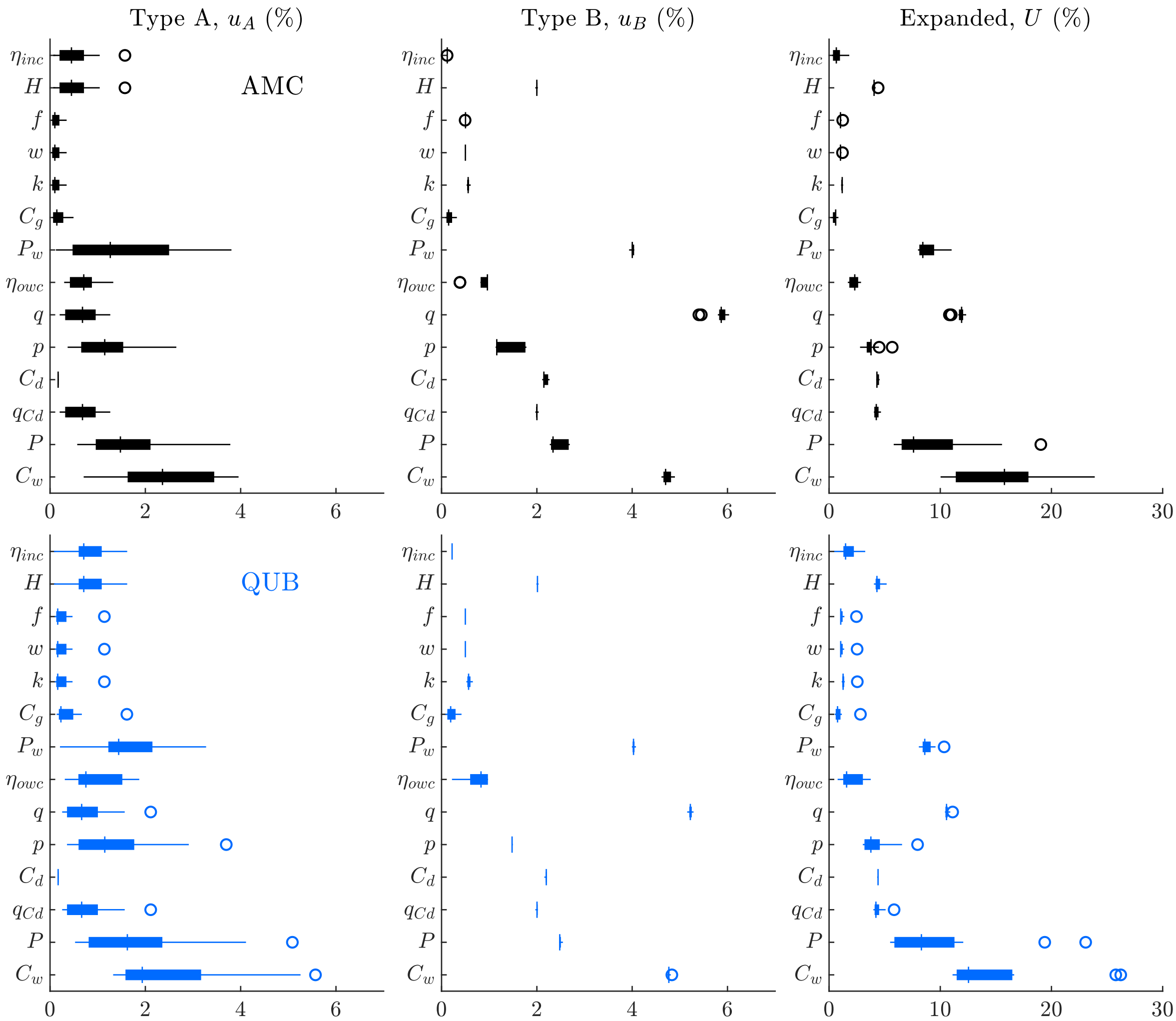

Figure 5.4: Uncertainty of experimental quantities and measurands for E_{AMC} and E_{QUB}, shown as box-and-whisker plots (regular waves only). For u_A, the box-and-whisker distribution includes all wave frequencies and heights; for u_B, the distribution includes all the calibrations carried out throughout the experiment, as well as including other sources of u_B. The distributions of expanded uncertainty U includes everything, and was determined by the Monte Carlo Method (refer Chapter 3 for details).

more nonlinear and diverged moderately, sometimes significantly (Fig. 5.5A). The wave height tended to agree to within 5% for both wave heights (Fig. 5.5B). For wave height H_1', a correlation coefficient of $r = 0.87$ was found for the wave height (Fig. 5.5C). For the wave elevation profile η_{inc} the correlation was $r = 0.98$, but showed moderate divergence about the perfect correlation trendline (Fig. 5.5D). These results show that, despite the wave heights and periods being well-matched (due to calibrating wave heights to achieve $< 5\%$ difference between experiments), there were non-negligible differences in terms of the η_{inc} shape. The effects of these η_{inc} deviations between experiments on OWC responses are examined in the following sections.

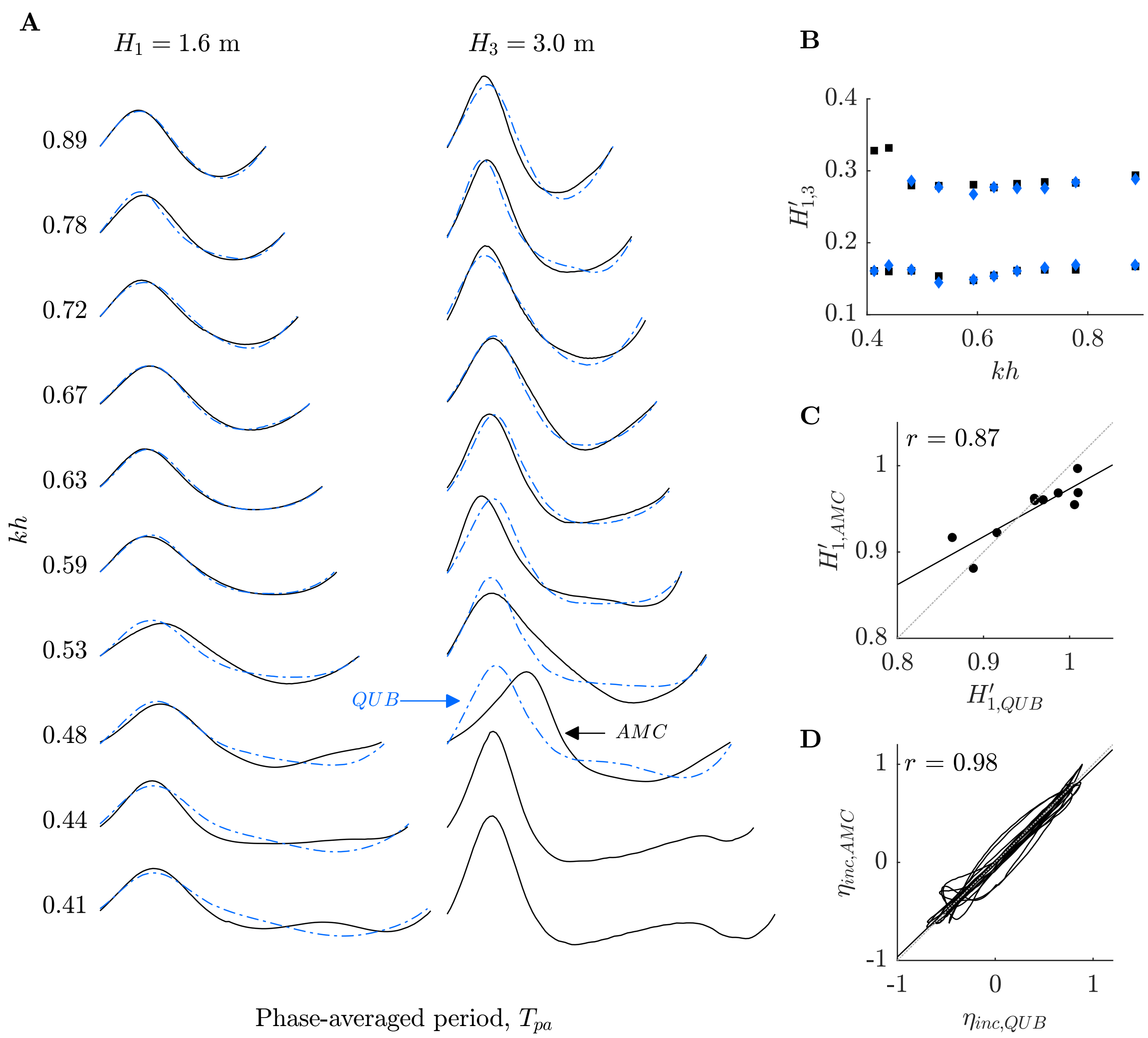

Figure 5.5: Incident regular waves differed between laboratories for nominally similar input wave heights/frequencies to the wavemaker. (**A**) Phase-averaged wave profiles $\eta_{inc,E_{AMC},E_{QUB}}$ shown as a table format with $H_{1,3}$ across two columns and kh down ten rows. (**B**) Dimensionless Wave height $H'_{1,3}$ and dimensionless wavenumber kh derived from $\eta_{inc,E_{AMC},E_{QUB}}$. (**C, D**) Correlation plots of H'_1 and $\eta_{inc,E_{AMC},E_{QUB}}$, showing quantified differences.

There are several likely factors contributing to the differences of η_{inc} between experiments. First, the wavemaker working principles are different, as shown in Fig. 5.3 and discussed, as well as differing paddle transfer functions. Second, due to constraints of the model deployment position, the distance between the model and wavemaker in E_{QUB} was about half that in E_{AMC} (Fig. 5.2). This suggests the waves transformed over a shorter distance in E_{QUB}, resulting in differing (nonlinear) profiles and therefore kinematic and dynamic quantities. Third, although both experiments had a flat bathymetry upwave and abreast the model, E_{QUB} basin sloped at a distance behind the model (Fig. 5.2), but this was considered to have a negligible influence on the wave fields at the model location.

Implications arising from these incident wave results are the following. All WECs except those operating in deepwater will encounter waves with some degree of nonlinearity. These nonlinearities will likely differ across laboratories due to different wavemaker design and operation, model deployment position, and basin boundaries. Thus, these laboratory-dependent parameters and their potential influence on incident waves must be carefully considered in WEC model tests, especially because WECs are typically sensitive to incident waves due to resonance and use a PTO. Without reproducing the same experiment in different wave basins, which is not normally within the time and cost budgets of WEC developers, this information will be unknown, thereby increasing the overall experimental uncertainty and technology risk. Accounting for these laboratory effects that influence incident wave profile shape represents a difficult task, requiring further technical investigation. Future research might focus on developing means to avoid, compensate, or correct for these laboratory effects. In the meantime, it would be prudent for stakeholders of WEC model test to be aware of and understand that WEC model tests could be significantly influenced by these newly identified laboratory effects related to incident waves, and perhaps others that are relevant for other WECs and laboratories.

5.3.2.2 OWC PTO damping

Having observed considerable differences in incident waves between experiments, the next analysis examined the degree to which these incident waves differences influenced OWC PTO damping, and whether other possible laboratory effects that may have influenced PTO damping. Fig. 5.6 presents a comparison of the in-situ orifice calibration results, obtained from the calibration method described in Chapter 3. It shows the respective orifice discharge coefficients C_d that indicate PTO damping characteristics. Despite C_d being an average of all regular wave heights and frequencies tested, we found a minor bias. The $C_{d,E_{AMC}}$ value of 0.739 was slightly higher than $C_{d,E_{QUB}}$ value of 0.713 (3.6% RD). While this is a small difference, its effect is amplified because the PTO strongly influences WEC motions, power, and loads (as shown in Chapter 4).

Two factors may have contributed to this observed difference. One is that the regular wave profiles presented in Fig. 5.5 show E_{QUB} profiles being consistently steeper at the front. An interpretation of the effect of this characteristic is that it may have induced relatively larger OWC hydrodynamic responses, which accumulated over all regular waves to produce slightly different PTO damping characteristics. Another factor in the C_d difference may be attributed to the OWC WEC utilising air as the intermediary energy conversion medium. The air-based PTO of the WSE WEC model may be susceptible to uncontrolled ambient environmental conditions, such as air temperature, density, pressure, and humidity, which likely differed during the experiments in the laboratories. These ambient conditions may have influenced the air pressure and flow properties. Additionally, although the orifice was exactly

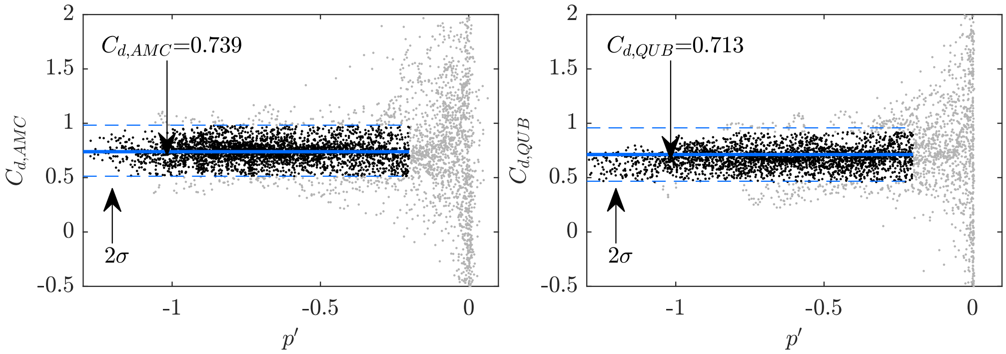

Figure 5.6: Orifice discharge coefficient C_d in E_{AMC} was slightly higher (3.6% RD). C_d was determined from in-situ orifice calibrations (method described in Chapter 3). Mean C_d was calculated for dimensionless chamber pressure $p < -0.2$.

the same, as were the lightweight flaps that simulated passive valves to create unidirectional air flow, slightly different ambient conditions may have changed the mechanical properties of these features leading to non-negligible differences in PTO damping characteristics. The nonlinearity of PTO damping would have likely influenced both of these factors related to the incident waves and test environment ambient conditions.

5.3.2.3 OWC hydrodynamics and power

The general hydrodynamic behaviour of the OWC WEC in the time- and frequency-domain, as depicted in Fig. 5.7, was described previously (Chapter 4). Thus, this section focuses on the differences in OWC hydrodynamics and power between experiments. The effect of wave height did not appreciably change the results described below in terms of differences in measurands between laboratories, only slightly accentuating the differences, so this section includes only one wave height, with the remaining wave height results given in Appendix C.

If the incident wave elevation η_{inc} agreed between experiments, the OWC responses tended to agree (Fig. 5.7). At $kh = 0.63$, η_{inc} agreed between experiments, which produced similar OWC responses (air pressure p and wave elevation η_{owc}) in the **phase-averaged profiles**, in turn producing similar **RAOs** (dimensionless pressure p', amplification factor $H_{\eta_{AF}}$, and capture width ratio C'_W). If, however, η_{inc} deviated in profile shape between experiments the OWC responses similarly deviated. For example, at $kh = 0.78$, the poor agreement of η_{inc} lead to significantly different OWC responses in **profiles** and **RAOs**, with a maximum of 33% relative difference (RD) found for C_W. $H_{\eta_{AF}}$ differed relatively less than p' and C_W. This finding supports observations from similar studies [159, 178, 164]. This difference may be because $H_{\eta_{AF}}$ is calculated with the magnitudes of η_{inc} and η_{owc} (i.e. the height), not the profile shape, so nonlinearities are not captured in this measurand. The expanded uncertainty bars on the C_W **RAO** shows that the differences in results are outside of the measurement uncertainty, which confirms our hypothesis, that experimental results

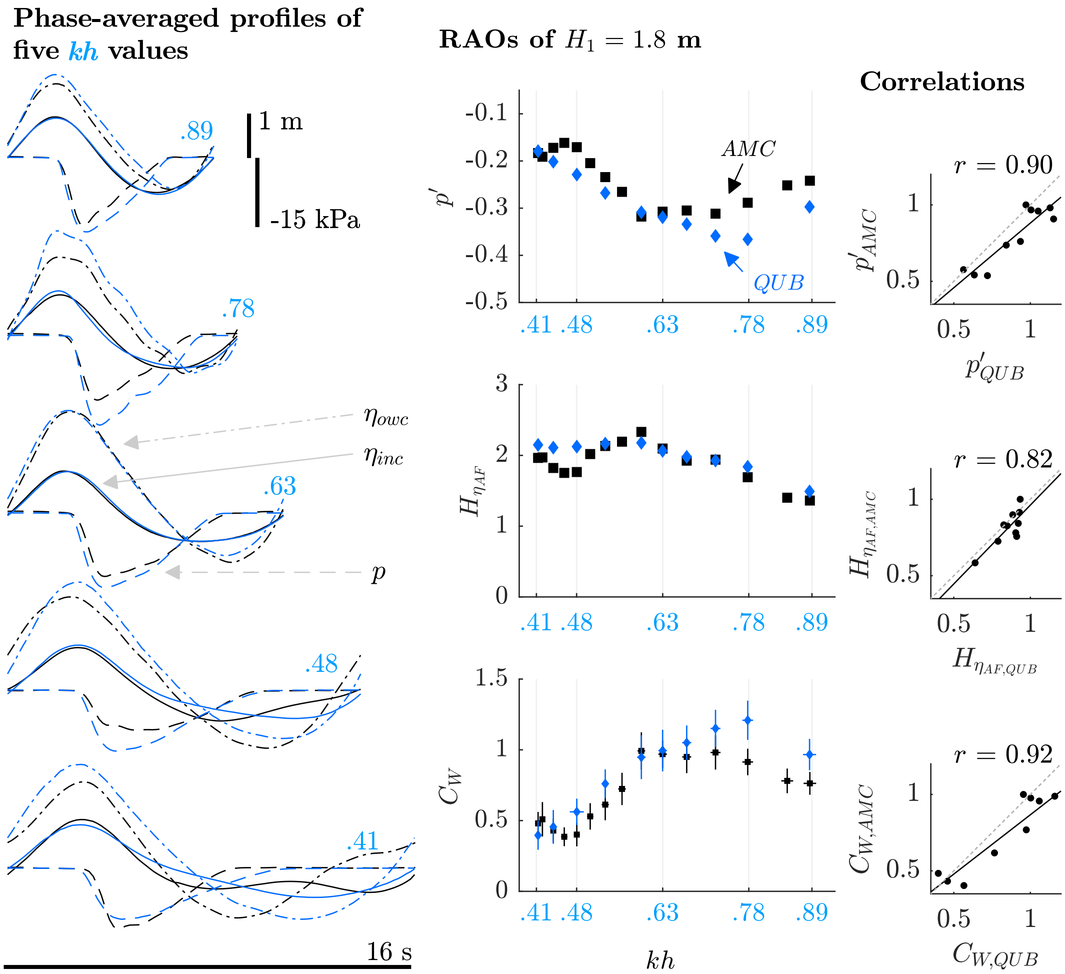

Figure 5.7: Comparisons of OWC hydrodynamics and power between laboratories, showing incident waves η_{inc}, OWC hydro-aerodynamics of internal wave elevation η_{owc} and air pressure p, and capture width ratio C_W (expanded uncertainty bars to 95% CI). All results are for H_1=1.8 m. The **Phase-averaged profiles of five *kh* values** displays plot η_{inc} and η_{owc} on one y-axis, and p one another y-axis of different scale (1 m wave amplitude, -15 kPa pressure, and 16 s wave period). The ***kh*** values correspond to the x-axis ticks in the **RAOs for H_1 =1.8 m**. **Correlation** plots show and quantify differences between results, including perfect correlation (······). Correlation data are normalised against the maximum value obtain for E_{AMC} for each respective measurand.

between laboratories can differ by an amount larger than the measurement uncertainty.

At a higher level, there was a moderate bias in results between experiments, where E_{QUB} had consistently higher values, by 16% RD on average for C_W (Fig. 5.7). This difference is seen visually in the **correlation** plots as the trendline biased down toward E_{QUB}. This observed bias may be attributed to the combined influences of η_{inc} profile deviations and slightly different PTO damping characteristics. Despite $\eta_{inc,QUB}$ having approximately equal wave height as $\eta_{inc,QUB}$, the $\eta_{inc,QUB}$ profiles may have been such that they consistently induced higher OWC responses due to a higher rate of change of energy, allowing more energy to be absorbed on the downstroke of the cycle. In other words, a relatively larger area under the curve of OWC power.

These findings reveal the degree to which the laboratory can influence power-related results in regular waves, with C_W differing by an amount larger than the measurement uncertainty, which supports the hypothesis stated in Chapter 1. The main laboratory-dependant parameters likely causing differences were the incident waves and differing test environment ambient conditions, so these constitute key laboratory effects. Regarding the incident waves, which are a function of the wavemaker, the model position relative to the wavemaker, wave transformations, and water depth, we infer that because most WECs are sensitive to incident waves due to resonance and the PTO, incident waves may be a key parameter that could lead to significant differences in power-related results if an experiment is reproduced in multiple wave basins. This implication is especially relevant for WECs operating in intermediate-shallow water. For WECs with air-based PTOs or other PTOs susceptible to uncontrolled ambient conditions, the test environment ambient conditions may also influences the results in a non-negligible way. These findings suggests the experimental uncertainty evaluated in any given WEC model test, carried out in only one laboratory, will likely be underestimated. This situation impacts the various ways in which model test data are used, such as directly in design of the WEC structure or subsystems like the PTO and mooring, to validate and calibrate numerical models, or to predict prototype power performance and survivability.

5.3.3 Irregular waves

5.3.3.1 Incident waves

Incident irregular wave spectra differed by a minor to moderate degree between experiments across the range of tested sea states (Fig. 5.8). Despite a careful and extensive calibration process of the incident waves, whereby the E_{QUB} sea states in terms of the energy spectra density S were calibrated to those measured at E_{AMC}, S_{AMC} was consistently larger by 8% RD on average and a maximum of 17% RD. The spectra shapes showed moderate agreement between laboratories, though deviating with higher sea states. E_{AMC} exhibited a second energy peak at higher frequencies.

There are several possible explanations of observed differences in incident waves. First, like for regular waves, model deployment position was likely a dominant parameter contributing to the differences in S, due to differing wave transformations. Second, the differences in energy spectra shape were likely because of the different wavemaker transfer functions to generate a sea state for the same H_s, T_p and γ inputs. Additionally, the basin boundaries were different between laboratories, which might have influenced the degree to which wave reflections accumulated during the long timeseries runs required to sufficiently represent a stationary sea state (30 minutes full-scale). Regarding T_p, it is known that determining T_p

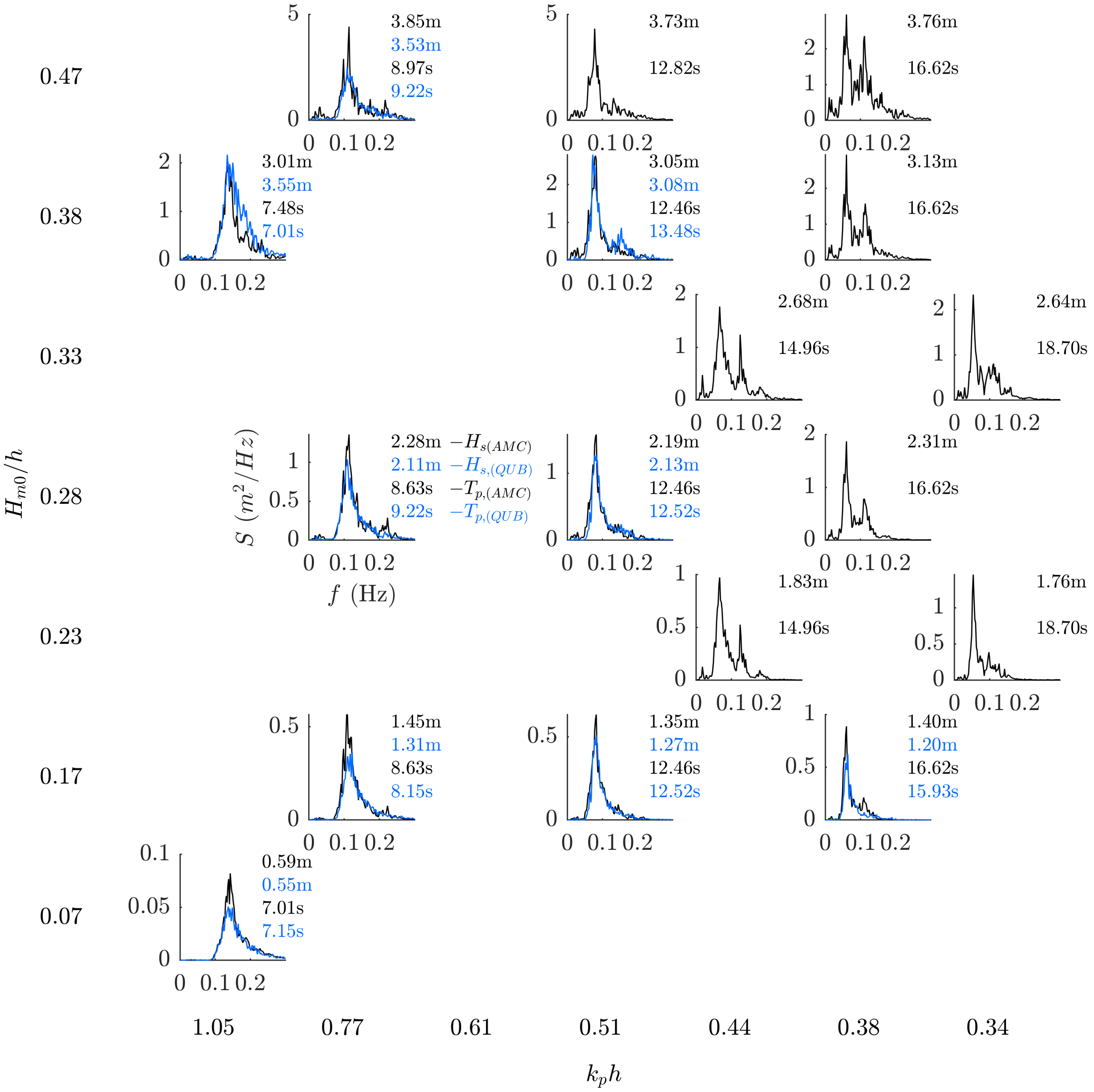

Figure 5.8: Incident irregular wave spectra energy density S for E_{AMC} and E_{QUB} across the range of tested sea states (see middle subplot for axes labels and legend). The significant wave height H_{m0} and peak period (shown as peak wavenumber $k_p h$) matrix also shows the statistics obtained for H_{m0} and peak period T_p to the right of each subplot for reference.

from spectral analysis presents difficulties [13]. Another factor is the wavemaker transfer function that differed between laboratories due to the wavemaker design and basin configurations. Such differences lead to varied irregular wave timeseries simulation for a given sea state, due to the sum of (slightly different) regular wave components of which the sea state is composed.

Some sea states at E_{QUB} are missing from the upper right of the matrix because these sea states could not be generated by the E_{QUB} wavemeker, as they were outside its operational envelope (Fig. 5.8). The E_{AMC} laboratory could therefore test a wider range of wave conditions for a given model scale. While this was not anticipated when designing the sea state scatter matrix, it highlights the challenge of accommodating for a fixed model scale and water depth across multiple laboratories.

5.3.3.2 OWC hydrodynamics and power

A convenient way to compare the OWC hydrodynamics and power results in irregular waves between laboratories was to calculate the relative percentage difference (RD) of values in the measurand matrices, which forms the z-axis (coloured) of the matrix graphs (Fig. 5.9). The RD equation is such that positive/red indicates relatively larger E_{AMC} values, and vice-versa such that negative/blue indicates relatively larger E_{QUB} values. The cell elements for each measurand matrix were interpolated, bi-directionally, from the measured results shown as black symbols. Extrapolated cell elements were omitted to enable appropriate comparisons.

Compared to E_{AMC}, the OWC hydrodynamic responses and power tended to be larger in E_{QUB} (blue), despite a smaller (red) on average incident wave power P_W (Fig. 5.9). The correlation plots also show these trends, where the correlation trendline for P_W was biased toward E_{AMC}, which indicates systematically higher values, and biased toward E_{QUB} for C_W. $P_{W,E_{AMC}}$ was consistently larger by 15% on average, except for high H_{m0} and $k_p h$ sea state where E_{QUB} was larger (top-right of the matrix), with a RD of -14.6%. Differences were relatively minor in p' and $H'_{m0,\eta_{AF}}$, except for p' in small sea states. C_W showed a major difference, with $C_{W,E_{QUB}}$ being +30% RD larger on average, and slightly higher for smaller $k_p h$ (longer waves). The correlations were high for all measurands, larger than 0.92. These differences in key measurands between experiments are comparable to the differences observed in laboratory effects experimental investigations carried out in the field of ship resistance [25].

Possible explanations for why power performance was relatively higher in E_{QUB} despite P_W being relatively smaller are the following. First, $P_{W_{QUB}}$ was relatively smaller due to consistently smaller sea state statistics. These statistics are calculated based on the assumption that the irregular wave spectra is composed of the sum of *linear* regular waves, where wave height is the most important parameter. However, the incident regular wave measurements showed the regular wave profiles were mostly *nonlinear*, and that these nonlinearities were a key contributor to significant differences in OWC hydrodynamics and power despite approximately equal wave height. Thus, the nonlinear incident wave profiles in E_{QUB} were possibly conducive to relatively higher OWC hydrodynamic responses and power. Such nonlinearities, which are not captured by the frequency domain calculation of P_W, would have accrued over the long durations of the sea states leading to overall better power performance. In other words, slightly better power performance at the individual wave level may have accrued

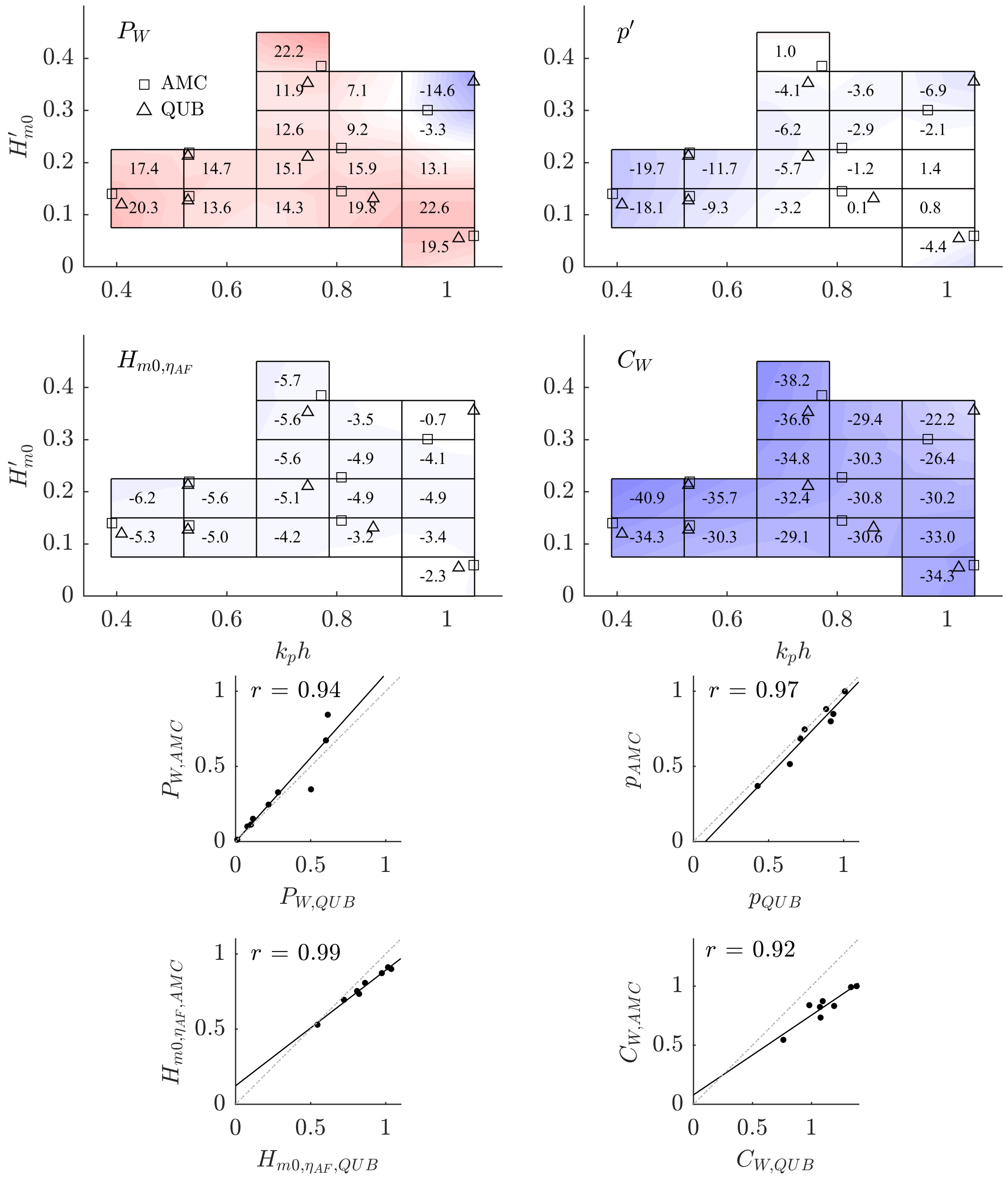

Figure 5.9: Matrices for key measurands showing the relative percentage difference (RD) between E_{AMC} and E_{QUB}, where a positive/red RD value corresponds to E_{AMC} being larger than E_{QUB}, and vice-versa for negative/blue.

to produce significantly better power performance at the sea state level. The implication here is that even slight differences in wavemakers (i.e. design and paddle transfer functions) and wave transformations upwave of the model due to different model position relative to the wavemaker accumulate over the duration of an irregular wave run (about 30 minutes model-scale), resulting in major differences.

Second, deriving P_W from spectral moments is sensitive to small changes in the summary statistics of H_{m0} and $k_p h$. These statistics, shown as black symbols in Fig. 5.9, differed between laboratories by up to 10%. A third factor worth noting is the inherent sensitivity of P due to slight differences in the quadratic pressure-flow characteristics in the OWC, where P is a function of p multiplied by q that are both mostly nonlinear. Finally, slight differences in PTO damping (Fig. 5.6) due to deviating ambient conditions of the test environment air may have influenced OWC hydrodynamics and power to a non-negligible degree. These parameters – incident wave nonlinearities, differing wavemakers and model deployment position, inherently sensitive derivations of key measurands, and PTO damping deviation – provide a likely explanation for the significant difference in C_W found between experiments. Therefore, we surmise that these are key parameters that cause laboratory effects in OWC WEC experiments in irregular waves. Again, the implications and means to deal with these irregular wave-based laboratory effects are similar to those described above for regular waves.

5.3.4 Evaluating laboratory effects

To identify the degree to which experimental parameters contribute to laboratory effects, a qualitative evaluation was carried out. This evaluation consists of a scoring system (Table 4.3) that indicates the likelihood of a parameter contributing to the set of laboratory effects, and the effect that parameter may have on the overall results (Table 5.2). The scoring system is not dissimilar to a risk scoring matrix. The assignment of the likelihood and effect are based on the findings in this study and from the work carried out throughout this PhD research.

Through this qualitative assessment several key findings emerged. The key parameters considered to contribute most to laboratory effects, that is, have a significant effect on the results, were the environment, the model, and the instrumentation and apparatus. Human factors was assessed to be of minor importance, and water properties generally negligible.

Regarding the environment parameters, wave generation both for regular and irregular waves was assessed to be among the parameters contributing most to laboratory effects. A combination of factors led to this assessment, including different wavemaker operating principles, capabilities (i.e., E_{QUB} had force absorption capability), and wavemaker transfer functions, as well as shallow water waves that are inherently nonlinear. In addition, test environment ambient conditions likely contributed to the differences in results, due to influences on the air-based PTO.

The model deployment position from the wavemaker was assessed to be among the most important parameters. In E_{QUB} the model was about twice as close, due to constraints of the working area of the basin. The implication here is that shallow water waves propagating toward the model transform in space and time, dissipating wave energy, so the model likely encountered waves with different transformation characteristics. In addition, the PTO setup and simulation may have contributed to laboratory effects despite the exact same model being

Table 5.2 List of identified experimental parameters evaluated by the scoring matrix described in Table 4.3. The result (**R**) is the multiplication of **Lh** and **E**. Notation: U = Unlikely, P = Possible, L = Likely; N = Negligible, M = Minor, S = Significant.

Parameter	**Lh**	**E**	**R**	**Comments**
Water properties				
Temperature	P	N	2	Temperature was within 5 C.
Density	U	N	1	
Viscosity	P	M	4	Differences in nonlinear waves cause varied turbulence in and around the OWC, which could affect responses.
Surface tension	U	N	1	
Environment				
Wave generation: regular	L	S	9	Different wavemaker operating principles, capabilities (i.e., force absorption), and paddle transfer functions; shallow nonlinear waves. See Figs. 5.5 and 5.7.
Wave generation: irregular	L	S	9	As above, plus see Fig. 5.8.
Wave reflections	P	M	4	Possible sources: beach, wall/edge, model, bathymetry.
Bathymetry	U	S	3	Bathymetry not flat behind and flanking model in E_{QUB}.
Run duration: regular	U	N	1	Same duration.
Run duration: irregular	U	S	3	Same duration. If not, however, the sea state realisation would be significantly affected.
Data analysis				Same analysis.
Blockage	U	M	2	Wide basins.
Initial conditions	U	M	2	Minimal remaining waves, circulation, or turbulence from remaining waves.
Ambient conditions	L	M	6	Air temperature, density, pressure, and humidity differed between experiments, influencing the air-based PTO.
Model				
Geometry	U	M	2	Same model.
Installation	U	M	2	i.e., alignment.
Deployment position	L	S	9	Model was twice as close to wavemaker in E_{QUB}, the implication space and time variations in wave transformations.
Mooring	U	M	2	i.e., securing model to force balance given bottom mounteded OWC.
PTO	L	M	6	Changes in test environment ambient air conditions likely caused changes in PTO damping; experimental setup of PTO required great care to ensure air tightness of OWC chamber.
Weight/buoyancy	U	M	2	Same model.

Table 5.3 continued

Parameter	L	E	R	Comments
Instrumentation, apparatus, and data acquisition				
Wave probe	U	S	3	i.e., accuracy (repeatability, linearity, hysteresis). Unlikely due to low uncertainty. (Fig. 5.4)
Pressure sensor	U	S	3	As above.
Force balance	L	S	9	See § 5.4.
Installation	U	S	3	Wave probes and pressure sensors required insertion through top of model to measure quantities inside, potentially compromising air tightness of chamber if not properly installed.
DAQ	U	S	3	OWC air pressure and wave elevation signals acquired in separate DAQs, resulting in slight time lag. Data processing techniques applied to align signals to be synchronous.
Human factors				
Experimental setup	U	S	3	Lead researcher was helped by several people less informed of the experimental details, potentially affecting, e.g., instrument calibrations.
Record keeping	U	S	3	Lead researcher responsible for all record keeping.
Data analysis	U	S	3	Lead researcher performed all analysis with same codes, however, large data sets are prone to errors and mistakes.

used for both experiments. This was mainly due to the orifice plates and air valve/flaps requiring careful installation to ensure the OWC chamber was air tight, and because of the lightweight plastic sheet flaps used to simulate the unidirectional flow valves. Ambient conditions may have also influenced the mechanical properties of these features.

The key instrumentation and apparatus parameter was the force balance. As mentioned in § 5.2.2, and elaborated in § 5.4, there were great difficulties in measuring loads in E_{QUB}. As such this was identified as a likely significant laboratory effect despite the results not reported here, and in general highlights the challenge of measuring hydrodynamic loads in already complex WEC experiments. In addition, the DAQ may have influenced the power results because the OWC air pressure signal and wave elevation signal used to derive flow rate were acquired in separate DAQs. Data processing techniques were applied to align the signals, to ensure the correct phase shift between p and q, which are multiplied to derive OWC power.

Regarding human factors, despite both experiments being conducted in the same way, support was provided by a number of others less informed of the details of the experiment, support with instrumentation setup and calibrations, model setup, and other construction and debugging activities. Given this test program was large in scope, with several conditions requiring changes of models, configurations, and wave types, errors and mistakes in these processes, while unlikely, could significantly affect the results. Similarly, record keeping and data analysis could significantly affect the results, though unlikely because the methods were consistent for each experiment.

5.4 General discussion

This section provides a general discussion on key findings of the study, its limitations and implications, and the challenges of reproducing a WEC model test experiment in two nominally similar wave basins.

Given the many considerations and effort required to reproduce the experiment in another laboratory and controlling for key parameters – such as using the same model, the same instrumentation, the same instrument and wave calibration procedures, and the same data processing and analysis techniques – the degree to which the results differed between experiments was somewhat surprising. This finding tentatively points to an inconvenient truth: that laboratory effects will likely be a significant source of experimental uncertainty in most WEC model tests and, therefore, must be considered when carrying out WEC model test and using obtained results.

There are several limitations of this study that make this statement tentative. First, this laboratory series experimental investigation includes only two laboratories. It would be further revealing, and statistically sound, to reproduce the same WEC experiment in many more laboratories to better understand the impact of laboratory effects on WEC model test results, which parameters are most important, and the overall impact on WEC development (like in the field of ship resistance [25]). The MaRINET2 programme is currently undertaking such an investigation, with round robin testing of a simple OWC WEC and a hinged barge WEC tested in four different laboratories. A key challenge here, however, is accommodating the same model in all the various wave basins. This work revealed that not all the regular and irregular wave conditions could be generated in E_{QUB}, due to their being outside the wavemaking capabilities. In addition, instrumentation and its implementation may present problems in reproducing the experiment that cannot be overcome under tight time and budget constraints.

A second limitation is that this study considers only one WEC, an OWC WEC with a vented unidirectional flow PTO, which is characterised by nonlinear hydro-aerodynamic responses induced by a moderate to highly nonlinear wave climate. This suggests a need to carry out other experimental investigations with different types of WECs, reproduced in multiple wave basin laboratories.

Third, in E_{QUB} the pressure measurement inside the OWC was acquired in a separate DAQ to the measurement of the OWC internal wave elevation that was used to derive flow rate. To rectify this situation required post-test data processing that synchronised the signals. A consequence of such a measurement procedure is that we could not determine if there was a phase delay between the pressure and air flow signals which would indicate air compressibility occurring in the OWC. However, Chapter 4 argued that this OWC did not exhibit air compressibility, so this issue was not serious for this experiment. Future work might investigate this issue though a Monte Carlo sensitivity analysis, where the sensitivity of OWC power to phase shifts between pressure and air flow rate is assessed.

Finally, acceptable force measurements in E_{QUB} could not be obtained, which resulted in these results being omitted from this laboratory series investigation. As such future work is needed to fulfil this gap, that is, to perform load measurements on WECs using different force balances in multiple laboratories to understand the important load-related parameters causing significant laboratory effects. The load measurement issue for this study is elaborated on, as follows.

In short, the bespoke force balance constructed from three coupled six-component load cells in a triangular configuration was not appropriate for the application (see Appendix C for details on the force balance). The key issue was the calibration matrix changed between the calibration and when mounting the models for testing. Despite determining the calibration matrix through an in-situ calibration, with the force balance in its place of measurement for testing, the model was not mounted on the force balance during the calibration and, when mounting the model to the measuring plate it deformed to some degree, thereby changing the load cell voltage responses under applied loads. While this a disappointing outcome, it highlights the challenges of load measurements in WEC model tests, tests that are already complex due to the requirement to model a PTO system and sometimes realistic moorings. While this is not a laboratory effect per se, it does point to a larger issue of the prospect of how reproducibility will be addressed in a field that is not the beneficiary of oil and gas economics or military applications.

A final few remarks on other challenges in reproducing model tests in multiple wave basin laboratories. Using the same model, or models that are exactly same, is essential to investigating laboratory effects, thus model transportation is likely required. However, transportation introduces non-trivial logistical challenges and costs, such as potential damage to or loss of the model during transit, and import taxes/custom holdings that may very likely cause delays in the test program (see for example [25]). Additionally, for an extensive laboratory effects investigation, ideally each separate experiment would be carried out by different people, as would the data analysis, to better control for and understand human biases [189, 190] and overall human factors in such experimental investigations. From the experience of [25], however, this is a difficult task that requires great procedural and managerial effort. This must be considered when designing a future round robin test campaign. Moreover, [25] concluded that the process of a round robin campaign is valuable, but highlights the significant challenges associated with conducting high-quality experiments across multiple laboratories. It also challenged laboratories to assess whether they are delivering experimental uncertainty to the levels they are stating in their documentation. This admonition should be taken seriously by stakeholders in WEC model test experiments. Finally, matching incident waves across laboratories is a critical part of investigating laboratory effects in WEC model tests because WECs are typically resonant and have PTOs, both of which make then sensitive to linear and nonlinear incident waves. Therefore, careful wave calibration of regular and irregular waves to attain close agreement between laboratories, though time consuming, should be a high priority.

5.5 Conclusions

The 1:30 scale model test experiment of the WSE OWC WEC reproduced in two laboratories showed results that differed by an amount larger than the measurement uncertainty, which supports the hypothesis stated in the Introduction (Chapter 1). Measurement uncertainty results were found to be very similar, suggesting measurement uncertainty had a negligible contribution to the differences in results. Key power results obtained in the two experiments differed from a minor (<10%) to moderate (10<30%) degree on average, up to a major ($>$ 30%) degree at maximum. The identified, quantified, and evaluated parameters that contributed most to these differences in results were those relating to the test environment (wavemeking, nonlinear wave transformations, and ambient conditions of the air), the model (deployment position and PTO), and instrumentation and apparatus (loads measurements). These parameters are therefore considered key parameters that cause laboratory effects. Human factors were of minor importance, and water properties generally negligible.

In regular waves, despite incident wave height agreeing to within ∼5% and wave period agreeing to within ∼1% between laboratories, wave profile shape differed by a minor degree in smaller shorter waves (linear) up to a major degree in higher longer waves (nonlinear). The parameters likely causing most of these differences were the wavemaker design and operation and the model deployment position relative to the wavemaker, giving rise to different nonlinear wave transformations upwave of the model. Deviating regular wave profiles, as well as slightly different PTO damping characteristics, were likely key contributors to moderate to major differences of power-related results, where C_W was 16% larger on average in E_{QUB}, up to 33% difference at maximum. These findings indicate the degree to which incident waves can influence power-related results. Unless incident regular wave profiles highly correlate between laboratories and the test environment ambient conditions are the same, interlaboratory power-related results will likely be inconsistent, other things being equal. A key implication is that, for OWC WECs or other WECs with resonant responses that are sensitive to nonlinear incident waves or have PTOs that are susceptible to changes in ambient air or water properties, the uncertainty in regular wave results due to the laboratory itself should be expected to be $\sim \pm 15\%$.

In irregular waves, despite significant wave height and energy period tending to agree within ~5% between laboratories, power-related results showed moderate to major differences (10<30+%). The OWC hydrodynamics and power tended to be moderately larger in E_{QUB}, with $C_{W_{QUB}}$ larger by a major degree on average. Similar to regular waves, laboratory-dependent parameters likely causing most of the differences in results were the nonlinear incident waves, due to different wavemaker designs and operations and model deployment position, and PTO damping characteristics influenced by ambient air conditions. The sensitivity of deriving the key measurands of wave power and OWC power based on nonlinear quantities also likely contributed to the differences in results. These findings suggest that extrapolations of model-scale results in irregular waves to predict full-scale power performance may be misleading and have significant uncertainty due to the laboratory itself.

It is important to emphasise that despite the reproduced OWC WEC model test experiments being conducted to a high standard according to international guidelines, as well as the exact same model being used, the same or similar instruments, the same data processing and analysis techniques, and careful calibration of incident waves, we found major differences in power performance between laboratories. These finding clearly shows that laboratory effects can significantly influence OWC WEC model test results and, therefore, cannot be neglected when carrying out model tests and extrapolating results. This conclusion likely applies to other WEC designs with similar characteristics, operating in intermediate to shallow water. Therefore, when conducting model test experiments resources should also be prioritised toward evaluating the potential influences of laboratory-dependent parameters on the overall experimental results and uncertainty.

While this study identifies the real and significant problem of laboratory effects in WEC model tests, it does not propose solutions for dealing with laboratory effects in future experiments, with the aim to reduce the overall experimental uncertainty. Accounting for laboratory effects in WEC model tests is not understood. Further research is therefore needed, which may comprise a set of broader interlaboratory round robin test campaigns with various WECs in multiple laboratories. These campaigns should seek to better understand how the laboratory can influence model test results, by how much, and the overall impact on WEC development. The technical aims would be to identify, quantify, and evaluate which laboratory-dependent parameters for a range of WECs and tests cause most of the differences in results, their relative impact on the results, and to develop means to account for laboratory effects by avoidance, compensation, or correction. In addition, the wave energy field needs to develop an uncertainty analysis method for incorporating uncertainties due to laboratory effects (and scale effects) with measurement uncertainty to establish a measure of overall experimental uncertainty. The broader aim of these campaigns would be to synthesise the research into a coherent and robust set of standardised best practices that improve the quality, rigour, and accuracy of hydrodynamic model test experiments of WECs, ultimately helping to reduce wave energy's LCOE.

If the wave energy industry is to continue, if it is to compete with the ever-decreasing cost of wind and solar energy or combine with them to create hybrid renewable energy systems, it must ensure the tools for WEC development, of which physical modelling is key, are robust and the uncertainties well understood – uncertainties such as those arising from laboratory effects. This is critical for developing techno-economic WECs and de-risking their path to commercialisation.

Chapter 6

Summary, Conclusions and Future Work

This chapter first summarises the thesis, then provides a synthesis of the findings and conclusions from each research question. It then discusses broader considerations, recommendations arising from the research, limitations of the research, and future work.

6.1 Summary

This thesis sought to improve the understanding of and develop methods to account for uncertainty in hydrodynamic model test experiments of WECs, with a focus on OWC WECs. The research was motivated by the need to investigate knowledge gaps in model tests, in particular experimental uncertainty, as recognised by Committees such as the ITTC responsible for developing guidelines for WECs. To address this gap, we proposed two questions to direct the research: (1) *What are the best practices in hydrodynamic model tests experiments of wave energy converters?* and (2) *What are the causes and effects of experimental uncertainty in hydrodynamic model test experiments of OWC wave energy converters?* To provide an answer to (1), we reviewed technical guidelines and recent literature on hydrodynamic model test experiments of WECs. To provide an answer to (2), we used the findings from (1) and preliminary experiments to inform a systematic series of model test experiments designed to investigate major experimental uncertainties, focusing on a realistic case study OWC WEC (Wave Swell Energy's Uniwave technology).

The methodology of the research was structured by an incremental build-up approach. A literature review and preliminary experiments first identified the key experimental uncertainties needing investigation: measurement uncertainty, scale effects, and laboratory effects. This initial research phase then generated the knowledge required to design and conduct rigorous experimental investigations into these uncertainties. The set of experiments included a range of model scales, representative of Technology Readiness Levels 1-4, and assessed power performance and hydrodynamic loads in regular and irregular waves.

The research consisted of four main parts, reported in four chapters. Chapter 2 reported a focused, comprehensive review of technical guidelines and recent literature on WEC model test experiments. It identified and described general considerations, experimental uncertainties, recent advances, and high-level requirements corresponding to the TRLs. It also evaluated guidance coverage and consensus to identify gaps and inconsistencies to be investigated in future work. Chapter 3, building on previous experimental work (Appendices D and E), reported an experimental investigation into measurement uncertainty and uncertainty analysis relevant for WECs, consisting of a 1:30 scale model test of the WSE OWC conducted in the Australian Maritime College (AMC) Model Test Basin (MTB). It outlined uncertainty analysis principles, identified parameters causing measurement uncertainty, and developed several WEC-specific uncertainty analysis methods. Importantly, it also generated the knowledge required to determine whether results across scales or between laboratories agreed or disagreed, to test the hypothesis, *If a hydrodynamic model test experiment of an OWC WEC is carried out at different scales or in different laboratories the experimental results will differ by an amount larger than the measurement uncertainty.* Chapter 4 reported an experimental investigation into scale effects of OWC WECs, consisting of a series of model tests at three scales (1:40, 1:30, 1:20) of the WSE OWC conducted in the AMC MTB. It identified, quantified, and evaluated parameters causing scale effects of OWC WECs. Chapter 5 reported an experimental investigation into laboratory effects of OWC WECs, consisting of a reproduced WSE OWC model test at two scales (1:30, 1:20) in a similar shallow water wave basin, the Queen's University Belfast (QUB) Coastal Wave Basin (CWB). It identified, quantified, and evaluated parameters causing laboratory effects in WEC experiments, particularly relevant for OWC WECs.

6.2 Synthesis of the findings, conclusions and recommendations

This section presents a synthesis of the research findings, explicitly discussing how we addressed the two research questions and conclusions drawn from the findings. The section is structured by the research questions. The findings and conclusions discussed provide strong evidence of achieving the overarching research aim: to extend the knowledge of and develop methods to account for uncertainty in hydrodynamic model test experiments of WECs, focusing on OWC WECs.

6.2.1 What are the best practices in hydrodynamic model tests experiments of WECs?

Two primary conclusions can be drawn as a summary of the work presented in Chapter 2, which focused on this first research question. First, substantial progress has been made in developing best practices in hydrodynamic model test experiments of WECs, culminating in recently published international guidelines that specify the best practices. These guidelines are a synthesis of several research projects, numerous WEC-specific experimental studies, and experience and knowledge gained directly with WEC experiments and open water deployments and indirectly from similar activities in related, mature maritime engineering fields. A common theme in the guidance and literature was an emphasis on the importance of model tests in early-stage WEC development (TRLs 1-5). Despite significant effort, money, and technical expertise needed to conduct WEC model tests, the benefits of model tests still justify their costs in time, money, and resources. The results from such tests are key drivers of WEC design and are critical for validating the numerical modelling of WEC power performance and loads. Given WEC power performance and loads directly determine the cost of energy for a WEC, it is critical these variables are predicted with the greatest confidence possible within practical limitations, to mitigate risk in development. Therefore, in the next few decades model tests will likely remain the primary tool to test and develop WECs, supplemented with numerical models that are validated and calibrated by experimental data.

Regarding best practices, guidelines have adopted and adapted the TRL methodology, linking the objectives of TRLs 1-5 to a series of model tests that typically increase in scale, scope, and complexity. During these tests, several high-level requirements should be addressed: experimental proof-of-concept, numerical model calibration and validation, energy capture performance optimisation, survivability, installation and tow-out methodologies, power production validation, and arrays and clusters.

Second, despite achieving international status, the guidance on WEC model tests needs further laboratory-based investigations and deeper integration of knowledge and experience from open water tests. The current state of the guidance is (1) it is not yet at the level of an accepted international standard; (2) it is dispersed across many documents; (3) it is inconsistent in some parameters and procedures; and (4) it has gaps or is inadequate in several areas. Regarding (1) and (2), until there is clear evidence of converged commercial WEC technologies, it is unlikely that an international standard will be developed, so the dispersion of guidance could remain for some time. On (3), while there were no starkly contrasting guidance, there were some notable inconsistencies, including the structure of the guideline documents, the demarcation of TRLs as well as which high-level requirements should be addressed at which TRLs, specification of the high-level requirements, and the degree of accuracy/sophistication of modelling the PTO and mooring systems at the TRL stages. On (4), WEC-specific guidance was found to be lacking in the modelling of moorings, PTOs, and arrays and clusters; identifying and modelling survival conditions; installation and tow-out tests; specific tests for calibrating and validating numerical models; methods for extrapolating model-scale results; full-scale validation; and understanding of and methods to account for measurement uncertainty, scale effects, and laboratory effects. Similar reviews including guidelines on WEC model tests found similar lacks. From these findings we conclude that technical investigations and refinement are needed in these lacking areas.

Although the lack of organisation, inconsistencies, limitations, and gaps of the guidance are potential barriers for those seeking to understand, conduct, or evaluate WEC model tests, this review helps to overcome these barriers by providing a comprehensive overview of WEC model tests – the best practices, advances, and uncertainties. It also offers perspectives on future directions that could refine the guidance. More broadly, this review supports similar reviews emphasis on the importance of and continued need to develop coherent, robust, and validated guidelines/standards on WEC development, and to disseminate them widely to ensure they are accepted and used by developers, technical facilities, and researchers. If these stakeholders peruse this comprehensive, central resource on WEC model tests presented in Chapter 2, they may gain an in-depth understanding of model tests in the context of WEC development. Thus, Chapter 2 equips stakeholders with the necessary knowledge for carrying out high-quality experiments that produce relevant and reliable results, thereby helping to reduce uncertainty in WEC model tests.

6.2.2 What are the causes and effects of uncertainty in hydrodynamic model test experiments of OWC WECs?

Role of uncertainty analysis

The first step in understanding the causes and effects of uncertainty in hydrodynamic model test experiments of OWC WECs was to understand measurement uncertainty and uncertainty analysis. This understanding would be necessary to objectively compare experimental results between scales and laboratories and, in effect, understand the causes and effects of uncertainty related to scale effects (Chapter 4) and laboratory effects (Chapter 5). Reviewing the literature for this work revealed two interrelated issues: that few experimental-based studies on WECs reported results with their associated uncertainty, and that despite recently published international guidelines on uncertainty analysis for WECs [17], the guidance is limited in WEC-specific methods and has several gaps. We found limitations in evaluating Type A and Type B uncertainties and means to identify uncertainty sources, and gaps in the use of General Uncertainty Analysis (GUA) and the Monte Carlo Method to propagate uncertainty. To address these limitations we sought to extend the knowledge of WEC-specific uncertainty analysis, to ensure stakeholders are aware of and understand its critical importance and uses in experimental modelling.

The primary conclusion drawn from Chapter 3 is that uncertainty analysis is required in hydrodynamic model test experiments of WECs, because measurement uncertainty can significantly influence experimental results, and because uncertainty analysis assures and quantifies the quality of experimental results. Key research activities and findings that substantiate this conclusion are as follows.

Through multiple experiments we developed and applied several new WEC-specific uncertainty analysis methods: (1) GUA used to facilitate planning and design of the OWC WEC model test, (2) the MCM used to propagate uncertainty more accurately while reducing the analysis effort, (3) a new method for evaluating Type A uncertainty in regular waves that reduces the number of required repeats thereby saving time and money in experiments, and (4) a method for uncertainty analysis in irregular waves. Furthermore, we described and gave detailed examples of how Type B uncertainty was evaluated in the experiment.

These contributions significantly extend the knowledge of uncertainty analysis in the WEC model test community. The new knowledge equips users of WEC model tests with a substantially better toolkit with which they may bring to bear throughout all experimental phases. If uncertainty in experiments is acknowledged and embraced, manifested by prioritising the use of GUA and DUA, the overall execution and outcomes of experiments could improve significantly. For instance, if a developer or researcher performs GUA (as well as peruses Chapter 2) to facilitate planning and design of an upcoming experiment, including the use of the MCM, they could quickly gain an integrated grasp and virtual experience of the experiment – key parameters and uncertainties and their relative influences on WEC motions, power, and loads. These valuable insights could then be used in the design of high-level components (test goals and schedule) and technical components (model build, test matrix, instruments, apparatus, calibrations, etc.). This gained knowledge and experience could yield better discussions with and advice from test facility staff as well as better communication of key aspects of the WEC and identification of critical measurements. Couple this GUA with a rigorous application of DUA throughout the experiment, including the use of the MCM, the new method to evaluate Type A uncertainty, and serious efforts to evaluate Type B uncertainties, and this will almost certainly increase the likelihood of the experiment completing on time, to budget, with high-quality and relevant results that stakeholders can be confident in.

GUA and DUA in WEC model tests is critical because these tests are typically both complex and expensive. Complexity arises from inherent characteristics of WECs: large motions and a PTO. Large motions often result in nonlinearities that can be difficult to measure accurately and are sensitive to scale effects. PTOs are difficult to model accurately and are sensitive to incident waves due to resonance, which may result in large uncertainty in motions, power, and loads. Regarding expense, under constrained time and cost budgets developers often must design an aggressive test program schedule, resulting in a reduced test matrix, less knowledge gained about the system, fewer data points to calibrate or validate numerical models with, and so on. If the experiment runs into troubles (to be expected), the schedule may be significantly shortened in the debugging process. Therefore, to ensure experiments are conducted carefully and to avoid cost escalations or reduced confidence in the data due to an incomplete test program, it is prudent to seek to understand as much possible about the experiment. This understanding process should prioritise the use of GUA and DUA. If this process is widely implemented in the wave energy field, not only could it maximise the return of investment of model tests but also improve the WEC development path in TRLs 1-5, thereby reducing technology risk and the time and cost for commercialisation.

Finally, it is apparent that the emphasis in WEC model tests has been on assessing WEC power performance and survivability. Far too little attention has been paid to the role of uncertainty and uncertainty analysis in these experiments. Therefore, this research argues for shift in emphasis from assessing power performance and survivability toward ensuring these assessments are accurate and quantifying the accuracy through uncertainty analysis.

Causes and effects of experimental uncertainty

Over the course of the research we have identified and characterised a comprehensive list of causes and effects of uncertainty in hydrodynamic model test experiments WECs, particularly relevant for OWC WECs. Out of the identified uncertainties (Chapter 3), our research focused on those associated with measurement uncertainty, scale effects, and laboratory effects. We explicitly discuss these uncertainties in terms of causes and effects, as follows.

There are many possible causes of measurement uncertainty in OWC WEC experiments. Uncertainties common to most measurement applications include ill-defined measurands, imperfect measurements, constant values, and approximations, and random variation. Substantial knowledge and guidance are available for evaluating these uncertainties, so we do not elaborate on them here. Specific to OWC WECs, we found a range of causes of uncertainty that propagated into the top-level measurands of capture width ratio C_W and hydrodynamic loads. The effect of these standard uncertainties across all experiments was $\pm$10-20% expanded uncertainty (95% CI) on average for C_W and $\pm$6-8% on average for loads.

Key causes of uncertainty in C_W were measurements used to derive the lower level measurands of incident wave power P_W and OWC power P, and the modelling of the PTO. For P_W, the critical measurement, therefore key uncertainty in this measurand, was incident wave elevation. For P, the critical measurements were air pressure p and wave elevation inside the OWC η_{OWC} used to derive air flow rate q and in turn determine the orifice discharge coefficient C_d. It is worth noting here that critical measurements demand special attention. Special attention might manifest as: choosing high-accuracy instruments, calibrating instruments with more care and more often, installing redundant instruments, ensuring instruments physical geometry and installed position negligibly influence the quantity being measured, and prioritising uncertainty evaluation of the measurements. Therefore, to obtain more accuracy in critical measurements and reduce the likelihood of significant uncertainty, we recommend deploying multiple co-located wave probes spanning the width of the WEC model to obtain a better average of the (non-uniform) wave height, and installing at least three pressure sensors and three wave probes inside the OWC for redundancy and to better resolve the fluctuating air pressure and flow rate.

Importantly, measuring PTO kinematics and dynamics (i.e. air flow and pressure, or velocity and force) will be critical for most WEC experiments because of the PTO's major influence on WEC motions, power, and loads. In addition, the kinematic quantity is rarely measured directly but is derived from the integral of the captor's displacement over time, which can introduce significant uncertainty. Moreover, modelling PTOs is widely regarded to be a governing cause of measurement uncertainty. Uncertainty arises because PTOs are often modelled as simplified dampers (including dynamic features such as the valve/flaps of the WSE WEC model) and because PTOs are sensitive to incident waves due to resonance, thereby exhibiting nonlinear characteristics. Therefore, special attention should be paid to the measurements, modelling, and experimental setup of PTOs and to evaluating the associated Type A and Type B uncertainties.

Hydrodynamic loads tended to have smaller expanded uncertainty than power, with the uncertainty mostly due to the force balance calibration. While loads were measured with good accuracy for larger model scales in the AMC experiments, the measurements for the smallest scale in some load components were unreliable, which meant they had to be omitted from our analysis. Furthermore, significant experimental difficulties in the QUB experiments led to all loads measurements being too unreliable to be included at all. This highlights that the force balance instrument will likely be a dominant cause of uncertainty in loads. We discuss the challenges of loads measurements in a later section.

Regarding Type A uncertainty u_A and Type B uncertainty u_B, we found that u_B tended to be relatively higher. u_A was likely smaller because the wave basins used in our experiments were well-controlled; they generate highly repeatable waves especially in period but also in height, and dampened waves relatively quickly after runs. In addition, great care was taken to ensure each model was correctly setup and working before actual run data were obtained. u_B is a function of many different uncertainty sources discussed in the above paragraphs, i.e., instrument calibrations and position/influence, the PTO, wave nonuniformity, environmental conditions, etc. The conclusion here is that resources should be prioritised to evaluate both

u_A and u_B, but if the experimental program is constrained in time, we recommend that evaluating u_B is a higher priority.

Several implications emerge from these measurement uncertainty findings. First, the large uncertainty in C_W means that, when extrapolating these results, the uncertainty in predictions of prototype power performance (e.g. MAEP) is significant, thereby increasing development risks. It also impacts the design of larger WECs and subsystems that are based on the experimental data of power-related quantities (e.g. air pressure and flow). Importantly, because C_W is a function of many lower level measurands and quantities, it is inherently sensitive to uncertainty. Therefore, most WEC experiments will likely result in similar levels of uncertainty in C_W. Second, although the hydrodynamic loads uncertainty was not as significant, when scaled up this still equates to an uncertainty of hundreds of tonnes. To mitigate risk due to this uncertainty, the structural and foundation design of the prototype might take the upper bound as the design load, thereby increasing costs. Third, given the uncertainty of power-related and loads quantities in irregular waves were either similar to or slightly smaller than that in regular waves, predictions of prototype power performance and loads should be based on irregular wave results.

Regarding uncertainty caused by scale effects, the key identified, quantified, and evaluated scale-dependant parameters of the OWC WEC were incident waves, the PTO, and the experimental constraint of fixed model deployment position in the wave basin. In all these parameters nonlinearities played a key role: nonlinear waves induced nonlinear hydro-aerodynamic responses, damped by the nonlinear orifice PTO simulator. These interacting nonlinearities meant that even slight deviations across scales in wave forcing and dynamic dissimilarity of PTO damping resulted in significant differences in motions, loads, and power. Specifically, C_W and loads differed across scales by an amount larger than the measurement uncertainty, which supports our hypothesis stated § 1.2. We also found that increasing model scale tended to show better power performance and higher loads.

These findings clearly show that scale can significantly influence OWC WEC model test results and, therefore, cannot be neglected when carrying out model tests and extrapolating results. We infer that this conclusion is relevant for other WECs that are resonant devices, that operate in intermediate to shallow waters, and that have nonlinear PTOs, or some combination of these. Based on this, we expect that such WECs would show similar differences in results across scales as reported in this research. As mentioned, the PTO is a critical part of the WEC but it is also amongst the components most susceptible to scale effects, for the reasons stated previously and because of the large exponent in extrapolating power results from model- to full-scale (length scale raised to 3.5). Therefore, when conducting model test experiments resources should be prioritised toward evaluating the potential influences of scale-dependent parameters on the overall experimental results and uncertainty.

The experimental investigation into scale effects also lends further support to the current best practice guidance that, to improve prototype representation and reduce uncertainty, model scale should generally increase with TRL progression (except in survivability tests which might require a small model to achieve representative extreme waves). It also suggests that if there are stringent requirements on model-prototype similarity, set by the developer, investors, or funding bodies, the most prudent way to satisfy these requirements might be to carry out a series of model tests at different scales. Such an investigation would yield, as the present investigation did, a broader and deeper understanding of WEC motions, power, and loads over a wider range of conditions and their sensitivities to scale. Doing so could increase confidence in the technology and enable informed mitigative actions to eliminate or control risks. Relevant guidelines should consider adopting this approach as a means to account for scale effects of WECs.

Regarding uncertainty caused by laboratory effects, the key identified, quantified, and evaluated parameters causing laboratory effects of the OWC WEC were those relating the test environment (wavemaker and nonlinear wave transformations), the model (deployment position and the PTO), and instrumentation (loads measurements). Given these parameters are mostly independent of the OWC WEC design, we infer that these parameters will likely be the cause of laboratory effects in experiments with other WECs operating in intermediate-shallow water. The exception here is the PTO of the OWC WEC. The PTO is air-based, so it is susceptible to uncontrolled ambient environmental conditions, such as air temperature, ambient pressure, and humidity. Additionally, the WSE PTO simulator used lightweight flaps to simulate passive valves which create unidirectional flow. While these features are unique to OWC WECs, other WEC designs utilise air flow as the energy conversion medium and may include un-scaled dynamic components in their PTOs that are affected by ambient environmental conditions and experimental setup. Thus, the PTO of a WEC model will likely still be amongst the key parameters causing laboratory effects in experiments with other WECs.

It is important to emphasise that despite the reproduced OWC WEC model test experiments being conducted to a high standard according to international guidelines, as well as the exact same model being used, the same or similar instruments, the same data processing and analysis techniques, and incident waves carefully calibrated, we found that C_W and related results differed between laboratories by an amount larger than the measurement uncertainty, which also supports our hypothesis stated § 1.2. These findings clearly show that, like scale, the laboratory can significantly influence OWC WEC model test results and, therefore, cannot be neglected when carrying out model tests and extrapolating results. As with before, this conclusion likely applies to other WEC designs with similar characteristics. Therefore, when conducting model test experiments resources should also be prioritised toward evaluating the potential influences of laboratory-dependent parameters on the overall experimental results and uncertainty.

A key implication from this work is that if laboratory effects are neglected or poorly understood, extrapolations of model tests results could be misleading and contain large uncertainty due to the laboratory itself. In effect, this makes for uncertain predictions of prototype WEC power performance and loads, which are key drivers of WEC design, and which cost of energy estimates are based. Such uncertainty leads to more risk in development and might conceal risks that manifest at higher TRLs, at greater cost.

Finally, while this work reveals for the first time that laboratory effects are real and significant in WEC experiments, it does not explicitly provide guidance on how to account for laboratory effects. This represents a key challenge in wave energy. The challenge should stimulate others in the field to pursue research in this area. The research should focus on identifying other important laboratory-dependent parameters and on developing means to avoid, compensate, or correct for laboratory effects. To achieve this might require carrying out a set of round robin campaigns with various WEC designs tested in dozens of wave basin laboratories. Until then, it will be difficult to know with a sufficient degree of certainty the quantitative influences of laboratories on WEC model test results. Ultimately, these campaigns are necessary to develop robust, accurate, and validated best practice guidelines that recommend how laboratory effects can be dealt with.

6.2.3 Broader considerations

Experimental uncertainty impacts on WEC development and overall technology uncertainty

Here we discuss a broader perspective on uncertainty associated with all aspects of a WEC technology. This research has focused on the uncertainty in WEC model tests, which broadly translates to the uncertainty in a WEC's hydrodynamic conversion of energy quantified by C_W, and the uncertainty in hydrodynamic loads. In terms of TRLs, these uncertainties contribute to the technology uncertainty in TRL 1-4. Regarding hydrodynamic conversion, this is but one link the wave-to-wire energy conversion chain. This chain consists of, at minimum, hydrodynamic conversion (wave to captor/absorber, quantified by capture width ratio), PTO (captor to generator), generator and electronics, substation and transformation, and grid connection [47]. TRL5+ requires the sequential demonstration and validation of the performance and reliability of these subsystems and the WEC system overall at large-scale, then full-scale. In light of this context, it is apparent that WECs are complex systems, consisting of many interfacing subsystems, all of which contain uncertainties of varying degrees of significance in the overall WEC technology uncertainty in terms of power performance, survivability, operations, LCOE, and other key metrics. Until a WEC has been deployed at full-scale for at least a year, there will be considerable uncertainty in these metrics, and this uncertainty will be higher the further away a technology is from this point. Therefore, key to WEC development, from the beginning, should be to invest time, money, and resources into evaluating uncertainties in all subsystems, to understand their influences and mitigate related risks. Such investments will likely yield a strong return on the investment in terms of power performance and reliability of the technology.

Second, the subsequent uses of experimental results and the consequences of large, poorly understood, or unknown uncertainty in the results could considerably impact WEC development and technology uncertainty. For instance, WEC system design loads are at least an order of magnitude higher than high-power operational loads. Consequently, the performance and cost of a WEC system are sensitive to design loads – their definition and associated uncertainty. If design loads based on experimental results that contain large or unknown uncertainty, or the uncertainty is poorly understood, this could lead to grossly under- or over-designed structural elements or foundations. Structures designed to ill-defined design loads could lead to prototype damage in a storm due to unexpectedly large wave loads, or too massive structures that rapidly escalate fabrication costs. The consequences of ill-characterised uncertainty in power-related results might be disillusionment with prototype power performance (leading to reputational damage or discontinued investments), or damage to the PTO due to uncertain dynamic-kinematic quantities.

Third, the relationship between uncertainty and risk needs considering. In many ways uncertainty and risk are correlated: large uncertainty equals large risks. More qualitatively, understood uncertainty equals understood risks. It follows that efforts to understand uncertainty, beginning with experimental uncertainty but expanding to include other subsystems, engenders a deeper understanding of associated risks. Better understood risks leads to better mitigative actions, better mitigative actions lead to reduced risk, and reduced risk leads to increased confidence in the commercial viability of the technology. This furthers the argument that understanding and evaluating uncertainty is critical to WEC development and its commercial viability.

Fourth, it is instructive to emphasise that developing productive and economical WECs is a demanding, costly venture; it requires a multitude of disciplines within and across engineering, science, technology, law, and economics, as well as at least a decade to reach commercial readiness, and probably tens of millions of dollars. At a technical level, WECs must endure harsh marine environments: extreme waves and wind, tides and currents, corrosion, and biofouling. WECs must also be resilient under challenging deployment/retrieval operations, reliably activate/deactivate a survival mode, and deal with vibrations and large reactions generated by components or the PTO. More broadly, societal, environmental, and financial requirements of technologies are increasing, tolerances for errors are dwindling, and it is apparent that despite considerable investment in wave energy the industry still lacks satisfactory solutions. The aggregate of these factors suggests interest will increase in uncertainty at all levels of a WEC technology, as will requirements to integrate uncertainty in decision-making and quality assurance measures. This research provides a comprehensive overview of uncertainty at the experimental level (TRL1-4) and invites others to pursue further research aiming to understand the influences of uncertainty in all aspects of WEC technologies.

Finally, the wave energy field has seen a proliferation of new concepts, new versions of old concepts, and new construction materials to capture wave energy, primarily aiming to maximise power performance. This expansion of concepts and emphasis on power performance seems to have come at a cost of reliability, in terms of both the reliability of industry knowledge and of WEC systems. That is, there seems to be lacking emphasis on critically evaluating existing knowledge in terms of rigour, completeness, consistency, and other key attributes of knowledge, and on ensuring the reliability of WEC systems. Such critical evaluation may take many forms, but the analysis of uncertainties – in experiments, numerical models, wave energy resource, etc. – is an essential part. These activities will also undoubtedly improve the overall reliability of WECs. This research demonstrates that if experimental uncertainty is neglected, not taken seriously, or poorly understood or characterised, this could lead to significant negative impacts on the execution and outcomes of the technology. Development path delays, technical failures, cost escalations, withdrawn investment, or insolvency are at risk. If, however, uncertainty is embraced and seen as an integral part of testing and developing WECs, it can be effectively managed, mitigated, and reduced. These measures objectively increase confidence in the technology, reduce technical and financial risks, and help reduce the LCOE. Therefore, the wave energy field stands to benefit from this research and from further research focused on uncertainty at all levels of WEC technologies, throughout TRLs 1-9. Future research should be directed toward developing relevant international guidelines and standards, like the present research.

Challenges and lessons learned in carrying out the experimental investigations

Experience is probably the most important factor in the success of an experiment – the quality of the results obtained and rigour of the uncertainty analysis performed. Therefore, this section briefly discusses key challenges and lessons learned in carrying out the model test experiments of this research, in the hope it gives useful insights and virtual experience to others carrying out or involved in WEC model tests.

A key challenge is the important, and as Chapters 2 and 3 clearly showed, necessary tasks of planning and designing model test experiments. The main lesson learned here as that serious efforts should be undertaken to first grasp the overall aspects of WEC model tests (by perusing Chapter 2), then employ GUA to plan and design the technical components specific to the WEC (as in Chapter 3). It is difficult to overstate the positive impact these tasks have on understanding the breadth and depth of possible uncertainties that might need to be evaluated, and on ultimately achieving a high-quality experiment, completed on time, to budget.

Loads measurements also presented various challenges. In the AMC experiments (reported in Chapters 3 and 4), we used a sophisticated six-component force balance, calibrated in-situ. While this took more time it likely reduced the measurement uncertainty. Despite this care taken, the load range for the range of model scales was too large such that most of the smallest model scale (1:40) measurements were deemed unreliable. Serious loads measurement challenges were also encountered in the QUB experiments (Chapter 5). We designed a bespoke force balance consisting of mechanically coupled six-component load cells and went to great lengths to install and calibrate the balance in-situ. Despite our efforts, the loads measurements were deemed too unreliable. While disappointing, it highlights the challenges (likely leading to uncertainties) of loads measurements of bottom-fixed WECs. This finding has wider implications for the accurate assessment of wave-induced loads imposed on WECs under survival conditions, especially because such data may be used directly in the structural design of prototypes.

Another challenge was matching regular and irregular waves across model scales and between laboratories. This process required considerable time to calibrate the waves, to modify paddle transfer functions, and to ensure wave probes were in the same positions in all experiments. The challenge was compounded by the waves being intermediate to shallow water waves (nonlinear). Therefore, similar future investigations into scale effects and laboratory effects should allocate a significant portion of the program to wave calibration.

Reproducing the OWC WEC model test in another laboratory, on a different continent, presented an array of logistical and technical challenges. Model transportation and importation had to be carefully managed. Technical challenges experienced included the effort and time required to modify the QUB bathymetry to be flat, setting up and performing a new method of load measurement in that laboratory (unsuccessfully), and that not all wave conditions could be generated which reduced the data sets for comparison.

Finally, survival-focused tests are challenging because they necessarily push the wavemaker's operational envelope, are difficult to control, and increase the risk of damaging the model, apparatus, or wavemaker. Smaller models may overcome some of these challenges but, in doing so, introduces additional issues regarding scale effects.

6.2.4 Recommendations

The following recommendations arising from the research are directed toward developing relevant guidelines for WEC model tests and to inform future research on experimental uncertainty.
Organisations developing guidelines on WEC model tests should:

- Address the limitations and gaps identified in Chapter 2, especially those relating to experimental uncertainty.
- Consider expanding the emphasis on assessing power performance and survivability to include an emphasis on ensuring these assessments are accurate by prioritising uncertainty analysis.

Future guidelines on uncertainty analysis for WECs should:

- Include a description and example of General Uncertainty Analysis.
- Include the Monte Carlo Method as an alternative method to propagate uncertainty, with an example.
- Include a description and example of cause-and-effect diagrams for identifying uncertainty sources.
- Include a more comprehensive example of uncertainty analysis for a WEC, including General Uncertainty Analysis and Detailed Uncertainty Analysis.
- Define desired uncertainty levels for each Technology Readiness Level stage.
- Define reporting minimums, such as: Type A, Type B, combined standard uncertainty, and expanded uncertainty, in at least the key measurands.

Preliminary recommendations to account for scale effects of OWC WECs:

- Use the experimental investigation presented in Chapter 4 as a template for carrying out further investigations into scale effects of OWC WEC and other WECs.
- To avoid significant scale effects related to power, a limiting criterion might be that model scales should be 1:30 or larger. Further research is needed to identify other limiting criteria.

- To compensate for the scale effect of PTO damping, it might be necessary to violate the geometric similitude condition of the orifice to OWC chamber diameter in order to achieve dynamic similitude. A series of tests may be required with different sized orifices to achieve this. Further research is needed to identify other compensation measures.

- To correct for scale effects, further research is needed to establish correction factors to apply to power and loads results.

Preliminary recommendations to account for laboratory effects of OWC WECs:

- Use the experimental investigation presented in Chapter 5 as a template for carrying out further investigations into laboratory effects of OWC WEC and other WECs.

- Further research is needed to develop measures to account for laboratory effects, through avoidance, compensation, or correction (discussed in § 6.4).

6.3 Limitations of the research

The research methodology regarding the experimental investigations was based on a case study approach, using an OWC WEC technology being developed commercially by Wave Swell Energy. For any case study approach there is inherent assumption that the specific outcomes are applicable within a broader, more general context. This assumption means that the knowledge generated around uncertainty in hydrodynamic model test experiments of the WSE OWC WEC is applicable to other types of OWC WECs, and applicable to other types of WECs in a more general sense. Such generalisations, however, contain caveats which must be carefully interpreted. Future work may corroborate the outcomes of the present case study by investigating other OWC WEC designs and other WECs.

The scope of the experimental investigation into scale effects limited the number of model scales to three. This decision was a trade-off between the possible range of scales the laboratories could accommodate and budget and time restrictions. Related, the experimental investigation into laboratory effects was limited to two laboratories, for similar reasons.

There are other possible model and environmental conditions that would influence the OWC WEC power and hydrodynamic loads, and therefore contain uncertainty components that would contribute to the overall experimental uncertainty. Such model conditions include varying the angle to the incident wave direction or different PTO damping settings for the model conditions, whereas environmental conditions include short-crested irregular waves, different water depths (for tidal variation), or current interactions. However, these conditions were not considered essential to the aim of the research, so they were neglected, thereby considerably simplifying the experiments.

Regarding OWC WEC hydrodynamic modelling, a growing number of studies have shown that neglecting to account for the spring-like effect of air compressibility may lead to a considerable error in power performance predictions of the full-scale prototype (discussed in detail in Chapter 4). In experimental modelling, it has been argued that air compressibility can be simulated in an OWC by scaling the aerodynamic domain of the chamber such that its volume is relatively larger (i.e., ϵ^2 rather ϵ^3 where ϵ is the model-prototype length scale ratio L_m/L_p). This may be done physically by a larger chamber, or virtually by maintaining the chamber's geometrical similitude and including an additional air volume reservoir. However, both these methods significantly complicates the experiments and, importantly, arguably introduces non-negligible uncertainty which would propagate into the final power results. Therefore, to simplify the experiments and avoid introducing potentially significant uncertainty, we neglected to account for air compressibility. This, however, represents a potential avenue for future work.

Wave generation capabilities is also an issue in wave basin laboratories, specifically for extreme waves. The wave climate study at WSEs deployment location at King Island, Tasmania, indicates extreme waves of $\sim$9.5 m high, which are outside of the wave generation capabilities, so the survival waves designed in the experiments are those which are at the maximum of the wave generation capabilities depending on the scale. Thus, some high and long regular waves and large sea states could not be realised for the larger model scales. Moreover, the wave generation systems differed between laboratories, so this placed further limits on the full range of possible wave conditions when investigating laboratory effects.

6.4 Future work

To gain further insights into the causes and effects of uncertainty in hydrodynamic model test experiments of WECs we recommend that further experimental investigations as well as numerical simulations be conducted. There is a pressing need for experimental investigations with various WEC types that identify, evaluate, and quantify key parameters causing measurement uncertainty, scale effects, and laboratory effects, and that develop methods to account for these uncertainties. These investigations should be designed for and their outcomes directed toward developing international guidelines on WEC model tests. In addition, it would be prudent to explore the use of numerical simulations as an auxiliary means to assess the relative influences of measurement-, scale-, and laboratory-related uncertainties on the behaviour and performance of WECs, especially over a broader parameter space. Nonlinear numerical models may be particularly useful to better understand uncertainties that arise in survival tests and extreme waves. The experimental investigations should be designed such that the data are suitable to calibrate and validate the numerical simulations.

Several specific future directions that may extended the research are as follows.

Regarding measurement uncertainty and uncertainty analysis, extensions of the work presented in Chapter 3 would provide further insights into WEC-specific uncertainty analyses. First, Chapter 3 presented only the MCM for propagating uncertainty but did not substantiate the claimed advantages of the MCM over the Taylor Series Method (Law of Propagation of Uncertainty). Therefore, further work could present a rigorous comparison of uncertainty results when propagated by the MCM and by the TSM. Second, future work could expand the presented uncertainty analysis approach from primarily evaluating measurement uncertainty to evaluating experimental uncertainty. Such a method would provide the means to evaluate uncertainties arising from not only measurements but also scale effects and laboratory effects. This method would assemble these uncertainties into one final expanded uncertainty result, for both GUA and DUA, thereby giving a more realistic estimate of the overall uncertainty in the results of a WEC model test experiment. A third extension might be a thorough investigation into human factors in experiments. While experiments are regarded as the gold standard of acquiring and testing knowledge, their results can be seriously misleading if the humans conducting the experiments are careless, inexperienced, or negligent. With many human-experiment interfaces in all experimental phases, human-related uncertainty can arise from ill-designed experiments, ill-defined measurands, incorrect or lousy experimental setup, misrecording of experimental information (runs, wave and model conditions, locations of instruments or the model, etc.), incorrect inputs into the wavemaker, or unconscious biases in data analysis or cherry-picking results for reporting. These uncertainty sources could contribute to the overall experimental uncertainty by a non-negligible, potentially significant, degree. Therefore, research is needed to understand the degree to the which humans likely influence WEC model test results and to develop protocols to eliminate or control human factors insofar as its possible.

Regarding scale effects, extensions of the work presented in Chapter 4 would yield a more integrated, broader understanding of the influences of scale effects of OWC WECs and other WECs. One line of investigation might be to carry out similar series of model test experiments at different scales but with more generic, simpler WEC designs. This work would establish a useful database of knowledge on scale effects, which could be synthesised into relevant guidance and drawn on by developers, test facility managers, and other stakeholders to help deal with scale-related physical modelling challenges faced by unique, techno-economic WEC technologies. Key outcomes of this work would be a set of procedures to account for scale effects by avoidance, compensation, and correction. Such procedures would also enable more accurate extrapolations of model test results to full-scale.

Another set of investigations might focus wholly on scale effects arising from survival tests. Performing survival tests present an array of scale-related challenges, such as the necessarily smaller model size to generate representatively extreme waves and the strong nonlinear interactions between waves, motions, power, and loads. Therefore, this work would yield valuable insights into the potential uncertainty sources in survival tests and the uncertainty in results that can be expected.

Third, experiments might be conducted focusing on the OWC WEC scale effect compensation method of scaling the OWC chamber by the length scale squared and installing either a larger above-water chamber or air reservoir. Importantly, a thorough uncertainty analysis would be required to determine whether the benefit of modelling air compressibility outweighs the introduced experimental complexity, which likely increases both uncertainty in the results and time and cost of the experiments. Fourth, there are very few comparisons of experimental results of model WECs with the results from open water tests of prototype WECs. Such comparisons would provide valuable knowledge about scale effects between the laboratory and open water.

Finally, regarding the six-component force balance used to measure the hydrodynamics loads of the bottom-standing OWC WEC, the AMC Model Test Basin stands to benefit from efforts directed toward improving the calibration of this instrument, especially so that it can measure loads accurately for smaller model scales such as the 1:40 scale model. Modifications to the balance may also be required to measure smaller loads accurately.

Regarding laboratory effects, extensions of the work presented in Chapter 5 would similarly yield a more integrated, broader understanding of the influences of laboratory effects on OWC WECs and other WECs. We recommend a set of round-robin campaigns of model test experiments with several different WEC designs, conducted in at least five but preferably more than ten laboratories. Wave basins as well as towing tanks may be useful to include in these campaigns. The experiments should use the same model, or an exact replica, and include standard tests such as RAOs, power matrix tests, and loads measurements, in both operational and survival conditions. These efforts would provide valuable insights into the non-negligible problem of laboratory effects, by identifying which laboratory-dependent parameters for a range of WECs and tests cause most of the differences in results, and their relative influence on the overall experimental uncertainty. Doing so would help the wave energy industry develop guidelines to account for laboratory effects by avoidance, compensation, or correction. It is recommended that learnings and experiences from the ITTC Resistance Committee's worldwide testing campaign to identify laboratory effects/biases are taken on board. This campaign highlighted many challenges in obtaining enough data of acceptable quality and consistent format to make reasonable comparisons and conclusions.

Bibliography

[1] Valérie Masson-Delmotte, Panmao Zhai, Hans-Otto Pörtner, Debra Roberts, Jim Skea, Priyadarshi R Shukla, Anna Pirani, W Moufouma-Okia, C Péan, R Pidcock, et al. *Global warming of 1.5 C - An IPCC Special Report on the impacts of global warming of 1.5°Cabove pre-industrial levels and related global greenhouse gas emission pathways,in the context of strengthening the global response to the threat of climate change,sustainable development, and efforts to eradicate poverty*. Tech. rep. IPCC, 2018.

[2] GBD 2017 Risk Factor Collaborators et al. "Global, regional, and national comparative risk assessment of 84 behavioural, environmental and occupational, and metabolic risks or clusters of risks for 195 countries and territories, 1990–2017: a systematic analysis for the Global Burden of Disease Study 2017". In: *Lancet (London, England)* 392.10159 (2018), p. 1923.

[3] Christian Aid. *Counting The Cost: A Year of Climate Breakdown*. Christian Aid, 2018. URL: `christianaid.org.uk`.

[4] Mark Z Jacobson, Mark A Delucchi, Zack AF Bauer, Savannah C Goodman, William E Chapman, Mary A Cameron, Cedric Bozonnat, Liat Chobadi, Hailey A Clonts, Peter Enevoldsen, et al. "100% clean and renewable wind, water, and sunlight all-sector energy roadmaps for 139 countries of the world". In: *Joule* 1.1 (2017), pp. 108–121.

[5] IEA. *World Energy Outlook 2019*. 2019. URL: `https://www.iea.org/reports/world-energy-outlook-2019`.

[6] Paul T Jacobson, George Hagerman, and George Scott. *Mapping and assessment of the United States ocean wave energy resource*. Tech. rep. Electric Power Research Institute, 2011.

[7] IEA. *Total primary energy supply (TPES) by source, World 1990-2017*. 2017. URL: `https://www.iea.org/data-and-statistics`.

[8] Aurélien Babarit. *Ocean Wave Energy Conversion: Resource, Technologies and Performance*. Elsevier, 2017. ISBN: 0081023901.

[9] ARENA. *Technology Readiness Levels for Renewable Energy Sectors*. Tech. rep. Australian Renewable Energy Agnecy (ARENA), Australian Government, 2014.

[10] IEC. *Marine energy - Wave, tidal and other water current converters - Part 103: Guidelines for the early stage development of wave energy converters - Best practices and recommended procedures for the testing of pre-prototype devices*. 1.0. IEC TS 62600-103:2018. International Electrotechnical Commission. 2019.

[11] ITTC. "ITTC Recommended Guidelines: Wave Energy Converter Model Test Experiments (7.5-02-07-03.7)". In: *Proceedings of the 28th International Towing Tank Conference (Recommended Procedures and Guidelines register)* (2017).

[12] Gregory Payne. *Guidance for the experimental tank testing of wave energy converters.* Tech. rep. The University of Edinburgh: Newington, Edinburgh, UK, 2008.

[13] Brian Holmes. *Tank Testing of Wave Energy Conversion Systems.* European Marine Energy Centre (EMEC). 2009.

[14] Brian Holmes and Kim Nielsen. *Annex II Task 2.1: Guidelines for the development & testing of wave energy systems.* International Energy Agency Ocean Energy Systems. 2010.

[15] EquiMar. *EquiMar Deliverables.* 2013. URL: `https://www.equimar.org/equimar-project-deliverables.html`.

[16] MaRINET. *MaRINET Research reports.* 2016. URL: `http://www.marinet2.eu/archive-reports-2/research-reports/`.

[17] ITTC. "ITTC Recommended Guidelines: Uncertainty Analysis for a Wave Energy Converter (7.5-02-07-03.12)". In: *Proceedings of the 28th International Towing Tank Conference (Recommended Procedures and Guidelines register)* (2017).

[18] A. H. Day, A. Babarit, A. Fontaine, Y. P. He, M. Kraskowski, M. Murai, I. Penesis, F. Salvatore, and H. K. Shin. "Hydrodynamic modelling of marine renewable energy devices: A state of the art review". In: *Ocean Engineering* 108 (2015), pp. 46–69. DOI: `10.1016/j.oceaneng.2015.05.036`.

[19] S. Day, I Penesis, A. Babarit, A. Fontaine, Yanping. He, M. Krakowski, F. Salvatore, and H. Kyoung Shin. *Specialist Committee on Hydrodynamic Testing of Marine Renewable Energy Devices - Final Report and Recommendations to the 27th ITTC.* Tech. rep. International towing Tank Conference, 2014.

[20] I. Penesis, W. Batten, A. Fontaine, H. Kyoung Shin, Y. L. Shanghai Jiaotong, M. Kraskowski, Petter Andreas Berthelsen, M. Murai, and A. Babarit. *Specialist Committee on Hydrodynamics Modelling of Marine Renewable Energy Devices - Final Report and Recommendations to the 28th ITTC.* Tech. rep. International towing Tank Conference, 2017.

[21] BIPM, IEC, IFCC, ILAC, ISO, IUPAC, IUPAP, and OIML. "JCGM 100:2008: Evaluation of measurement data–Guide to the expression of uncertainty in measurement". In: *Joint Committee for Guides in Metrology, JCGM* 50 (2008), p. 134.

[22] Steven A Hughes. *Physical models and laboratory techniques in coastal engineering.* Vol. 7. World Scientific, 1993.

[23] Valentin Heller. "Scale effects in physical hydraulic engineering models". In: *Journal of Hydraulic Research* 49.3 (2011), pp. 293–306.

[24] J Cândido, Matthew Finn, Keith Dampney, John Lawrence, and L Margheritini. *D2.9 Standards for Wave Data Analysis, Archival and Presentation.* Tech. rep. MaRINET, 2015.

[25] J Gorski, S. Turnock, B. Alessandrini, Ho-Hwan. Chun, U. Hollenbach, T. Mikkola, Y. Tahara, J. Valle, and L. Ying. *Resistance Committee - Final Report and Recommendations to the 26th ITTC*. Tech. rep. International Towing Tank Conference, 2011.

[26] Michael D. Woodward. "Evaluation of inter-facility uncertainty for ship manoeuvring performance prediction". In: *Ocean Engineering* 88 (2014), pp. 598–606. DOI: 10.1016/j.oceaneng.2014.04.001. URL: https://dx.doi.org/10.1016/j.oceaneng.2014.04.001.

[27] B. Gaurier, G. Germain, J. V. Facq, C. M. Johnstone, A. D. Grant, A. H. Day, E. Nixon, F. Di Felice, and M. Costanzo. "Tidal energy "Round Robin" tests comparisons between towing tank and circulating tank results". In: *International Journal of Marine Energy* 12 (2015), pp. 87–109. DOI: 10.1016/j.ijome.2015.05.005.

[28] António F. O. Falcão and João C. C. Henriques. "Oscillating-water-column wave energy converters and air turbines: A review". In: *Renewable Energy* 85 (2016), pp. 1391–1424. DOI: 10.1016/j.renene.2015.07.086.

[29] Gabriel Ibarra-Berastegi, Jon Sáenz, Alain Ulazia, Paula Serras, Ganix Esnaola, and Carlos Garcia-Soto. "Electricity production, capacity factor, and plant efficiency index at the Mutriku wave farm (2014–2016)". In: *Ocean Engineering* 147 (2018), pp. 20–29.

[30] TJT Whittaker, W Beattie, M Folley, C Boake, A Wright, M Osterried, and T Heath. "The limpet wave power project–the first years of operation". In: *Renewable Energy* (2004).

[31] Damon Howe and Jean-Roch Nader. "OWC WEC integrated within a breakwater versus isolated: Experimental and numerical theoretical study". In: *International Journal of Marine Energy* (2017).

[32] MA Mustapa, OB Yaakob, Yasser M Ahmed, Chang-Kyu Rheem, KK Koh, and Faizul Amri Adnan. "Wave energy device and breakwater integration: A review". In: *Renewable and Sustainable Energy Reviews* 77 (2017), pp. 43–58.

[33] AN Fleming, GJ MacFarlane, Scott Hunter, and Tom Denniss. "Power performance prediction for a vented oscillating water column wave energy converter with a unidirectional air turbine power take-off". In: *The 12th European Wave and Tidal Energy Conference (EWTEC)* (2017), pp. 1–7.

[34] Ahmed Elhanafi, Alan Fleming, Gregor Macfarlane, and Zhi Leong. "Numerical hydrodynamic analysis of an offshore stationary–floating oscillating water column–wave energy converter using CFD". In: *International Journal of Naval Architecture and Ocean Engineering* 9.1 (2017), pp. 77–99. DOI: http://dx.doi.org/10.1016/j.ijnaoe.2016.08.002. URL: http://www.sciencedirect.com/science/article/pii/S2092678216304290.

[35] Wanan Sheng, Raymond Alcorn, and Anthony Lewis. "Assessment of primary energy conversions of oscillating water columns. II. Power take-off and validations". In: *Journal of Renewable and Sustainable Energy* 6.5 (2014), p. 053114.

[36] Matt Folley. *Numerical modelling of wave energy converters: state-of-the-art techniques for single devices and arrays.* Academic Press, 2016.

[37] *Wave Swell Energy*. Online. 2020. URL: https://www.waveswell.com/.

[38] Paul Lamont-Kane, Matt Folley, and Trevor Whittaker. “Investigating uncertainties in physical testing of wave energy converter arrays”. In: *Proceedings of the European Wave and Tidal Energy Conference (EWTEC)* (2013).

[39] Louise O’Boyle. “Assessment of Wave Basin Homogeneity for Wave Energy Converter Array Studies”. In: *Proceedings of the European Wave and Tidal Energy Conference (EWTEC)* (2011).

[40] Jarrah Orphin, Jean-Roch Nader, Irene Penesis, and Damon Howe. “Experimental Uncertainty Analysis of an OWC Wave Energy Converter”. In: *Proceedings of the European Wave and Tidal Energy Conference (EWTEC)* (2017).

[41] Jarrah Orphin, Irene Penesis, and Jean-Roch Nader. “Uncertainty analysis for a wave energy converter: the Monte Carlo method”. In: *Proceedings of the Asian Wave and Tidal Energy Conference (AWTEC)* (2018).

[42] T McCombes, C Johnstone, B Holmes, LE Myers, AS Bahaj, and JP Kofoed. *D3.4 Best practice for tank testing of small marine energy devices*. Tech. rep. EquiMar, 2010.

[43] Morten Thott Andersen and Jonas Bjerg Thomsen. *The Inter Facility Testing of a Standard Oscillating Water Column (OWC) Type Wave Energy Converter (WEC)*. Tech. rep. MaRINET, 2014.

[44] IRENA. *International Renewable Energy Agency - Ocean Energy Data*. Online. 2018. URL: `https://www.irena.org/en/ocean`.

[45] Wanan Sheng. “Wave energy conversion and hydrodynamics modelling technologies: A review”. In: *Renewable and Sustainable Energy Reviews* 109 (2019), pp. 482–498. DOI: `https://doi.org/10.1016/j.rser.2019.04.030`. URL: `http://www.sciencedirect.com/science/article/pii/S1364032119302424`.

[46] ITTC. *International Towing Tank Conference Recommended Procedures and Guidelines*. 2020. URL: `http://www.ittc.info/`.

[47] Arthur Pecher and Jens Peter Kofoed. *Handbook of ocean wave energy*. Springer Nature, 2017.

[48] Deborah Greaves and Gregorio Iglesias. *Wave and tidal energy*. John Wiley & Sons, 2018.

[49] John C Mankins. “Technology readiness assessments: A retrospective”. In: *Acta Astronautica* 65.9 (2009), pp. 1216–1223.

[50] D. R. Noble et al. *D2.1 Test recommendations and gap analysis report*. Tech. rep. Marine Renewable Infrastructure Network (MaRINET), 2018.

[51] António F. de O. Falcão. “Wave energy utilization: A review of the technologies”. In: *Renewable and Sustainable Energy Reviews* 14.3 (2010), pp. 899–918. DOI: `10.1016/j.rser.2009.11.003`.

[52] Iraide López, Jon Andreu, Salvador Ceballos, Iñigo Martínez de Alegría, and Iñigo Kortabarria. “Review of wave energy technologies and the necessary power-equipment”. In: *Renewable and Sustainable Energy Reviews* 27 (2013), pp. 413–434.

[53] LE Myers et al. *D5. 2: Device classification template*. Tech. rep. EquiMar, 2011.

[54] Jochem Weber, Daniel Laird, Ronan Costello, Jesse Roberts, Diana Bull, Aurélien Babarit, Kim Nielsen, Claudio Bittencourt Ferreira, and Ben Kennedy. "Cost, Time, and Risk Assessment of Different Wave Energy Converter Technology Development Trajectories". In: *European Wave and Tidal Energy Conference* (2017).

[55] Markel Penalba, Giussepe Giorgi, and John V. Ringwood. "Mathematical modelling of wave energy converters: A review of nonlinear approaches". In: *Renewable and Sustainable Energy Reviews* 78 (2017), pp. 1188–1207. DOI: `http://dx.doi.org/10.1016/j.rser.2016.11.137`. URL: `http://www.sciencedirect.com/science/article/pii/S1364032116308784`.

[56] Adrien Combourieu, Michael Lawson, Aurélien Babarit, Kelley Ruehl, André Roy, Ronan Costello, Pauline Laporte Weywada, and Helen Bailey. "WEC3: Wave energy converter code comparison project". In: *Proceedings of the 11th European Wave and Tidal Energy Conference, Nantes, France* (2015), pp. 6–11.

[57] Subrata Chakrabarti. *Handbook of Offshore Engineering (2-volume set)*. Elsevier, 2005.

[58] JM Forestier, B Holmes, S Barrett, and AW Lewis. "Value and validation of small scale physical model tests of floating wave energy converters". In: *Proceedings of the European Wave and Tidal Energy Conference (EWTEC)* (2007).

[59] EquiMar. *Tank Testing Protocol*. High level EquiMar Protocols. 2013.

[60] Hugh W Coleman and W Glenn Steele. *Experimentation, validation, and uncertainty analysis for engineers*. 4th. John Wiley & Sons, 2018. ISBN: 9781119417514. DOI: `10.1002/9781119417989`.

[61] Wanan Sheng. "Wave energy conversion and hydrodynamics modelling technologies: A review". In: *Renewable and Sustainable Energy Reviews* 109 (2019), pp. 482–498.

[62] Amélie Têtu, Peter Frigaard, Jens Peter Kofoed, Miguel Lopes, Aby Iyer, Sylvain Bourdier, Dorleta Marina, Stuart Stripling, and Lars Johanning. *Report on Instrumentation Best Practice*. Tech. rep. D2.05. Marine Renewables Infrastructure Network, 2013.

[63] Jeremy Ohana and Sylvain Bourdier. *D4.01 Tank test related instumentation and best practice*. Tech. rep. Marine Renewables Infrastructure Network (MaRINET), 2014.

[64] Donald R. Noble, Samuel Draycott, Thomas A. D. Davey, and Tom Bruce. "Design diagrams for wavelength discrepancy in tank testing with inconsistently scaled intermediate water depth". In: *International Journal of Marine Energy* 18 (2017), pp. 109–113. DOI: `10.1016/j.ijome.2017.04.001`. URL: `https://dx.doi.org/10.1016/j.ijome.2017.04.001`.

[65] ITTC. "ITTC Recommended Guidelines: Floating Offshore Platform Experiments (7.5-02-07-03.1)". In: *Proceedings of the 28th International Towing Tank Conference (Recommended Procedures and Guidelines register)* (2017).

[66] Jonas Thomsen, Francesco Ferri, and Jens Kofoed. "Screening of Available Tools for Dynamic Mooring Analysis of Wave Energy Converters". In: *Energies* 10.7 (2017), p. 853. URL: `http://www.mdpi.com/1996-1073/10/7/853`.

[67] Matt Folley and Trevor Whittaker. “Preliminary cross-validation of wave energy converter array interactions”. In: *ASME 2013 32nd International Conference on Ocean, Offshore and Arctic Engineering* (2013), V008T09A055–V008T09A055.

[68] V. Stratigaki, P. Troch, T. Stallard, D. Forehand, M. Folley, J. P. Kofoed, M. Benoit, A. Babarit, M. Vantorre, and J. Kirkegaard. “Sea-state modification and heaving float interaction factors from physical modelling of arrays of wave energy converters”. In: *Journal of Renewable and Sustainable Energy* 7.6 (2015), p. 061705. DOI: `10.1063/1.4938030`.

[69] Svein Ersdal and Anders M Moe. “Model Test of the Aker Wave Energy Converter Concept”. In: *ASME 2013 32nd International Conference on Ocean, Offshore and Arctic Engineering* (2013), V008T09A030–V008T09A030.

[70] Irene Penesis, Richard Manasseh, Jean-Roch Nader, Swapnadip De Chowdhury, Alan Fleming, Gregor Macfarlane, and Md Kamrul Hasan. “Performance of ocean wave-energy arrays in Australia”. In: *3rd Asian Wave and Tidal Energy Conference (AWTEC 2016)*. Vol. 1. 2016, pp. 246–253.

[71] Jean-Roch Nader, Alan Fleming, Gregor Macfarlane, Irene Penesis, and Richard Manasseh. “Novel experimental modelling of the hydrodynamic interactions of arrays of wave energy converters”. In: *International journal of marine energy* 20 (2017), pp. 109–124.

[72] Edgar Mendoza, Rodolfo Silva, Barbara Zanuttigh, Elisa Angelelli, Thomas Lykke Andersen, Luca Martinelli, Jørgen Quvang Harck Nørgaard, and Piero Ruol. “Beach response to wave energy converter farms acting as coastal defence”. In: *Coastal Engineering* 87 (2014), pp. 97–111.

[73] Kjell Larsen and Erling Huse. “Practical procedures for estimation of viscous scale effects in model testing of floating structures”. In: *The Third International Offshore and Polar Engineering Conference* (1993).

[74] Johannes Palm, Claes Eskilsson, Lars Bergdahl, and Rickard Bensow. “Assessment of Scale Effects, Viscous Forces and Induced Drag on a Point-Absorbing Wave Energy Converter by CFD Simulations”. In: *Journal of Marine Science and Engineering* 6.4 (2018), p. 124. URL: `http://www.mdpi.com/2077-1312/6/4/124`.

[75] Siya Jin, Ron J. Patton, and Bingyong Guo. “Viscosity effect on a point absorber wave energy converter hydrodynamics validated by simulation and experiment”. In: *Renewable Energy* 129 (2018), pp. 500–512. DOI: `10.1016/j.renene.2018.06.006`. URL: `https://dx.doi.org/10.1016/j.renene.2018.06.006`.

[76] Giuseppe Giorgi and John V. Ringwood. “Nonlinear Froude-Krylov and viscous drag representations for wave energy converters in the computation/fidelity continuum”. In: *Ocean Engineering* 141 (2017), pp. 164–175. DOI: `https://doi.org/10.1016/j.oceaneng.2017.06.030`. URL: `http://www.sciencedirect.com/science/article/pii/S0029801817303256`.

[77] Pál Schmitt and Björn Elsäßer. “The application of Froude scaling to model tests of Oscillating Wave Surge Converters”. In: *Ocean Engineering* 141 (2017), pp. 108–115. DOI: `http://dx.doi.org/10.1016/j.oceaneng.2017.06.003`. URL: `http://www.sciencedirect.com/science/article/pii/S0029801817302986`.

[78] Yanji Wei, Ashkan Rafiee, Alan Henry, and Frederic Dias. "Wave interaction with an oscillating wave surge converter, Part I: Viscous effects". In: *Ocean Engineering* 104 (2015), pp. 185–203. DOI: 10.1016/j.oceaneng.2015.05.002. URL: https://dx.doi.org/10.1016/j.oceaneng.2015.05.002.

[79] Majid A Bhinder, Aurélien Babarit, Lionel Gentaz, and Pierre Ferrant. "Effect of viscous forces on the performance of a surging wave energy converter". In: *The Twenty-second International Offshore and Polar Engineering Conference* (2012).

[80] Ashish Pathak, Cole Freniere, and Mehdi Raessi. "Advanced computational simulations of water waves interacting with wave energy converters". In: *European Journal of Computational Mechanics* 26.1-2 (2017), pp. 172–204.

[81] A. J. Caska and T. D. Finnigan. "Hydrodynamic characteristics of a cylindrical bottom-pivoted wave energy absorber". In: *Ocean Engineering* 35.1 (2008), pp. 6–16. DOI: 10.1016/j.oceaneng.2007.06.006. URL: https://dx.doi.org/10.1016/j.oceaneng.2007.06.006.

[82] Josh Davidson and John V Ringwood. "Mathematical modelling of mooring systems for wave Energy converters—A review". In: *Energies* 10.5 (2017), p. 666.

[83] B Le Méhauté. "Similitude". In: *Ocean engineering science* 9.Part B (1990), pp. 955–980.

[84] Shaswat Saincher and Jyotirmay Banerjee. "Influence of wave breaking on the hydrodynamics of wave energy converters: A review". In: *Renewable and Sustainable Energy Reviews* 58 (2016), pp. 704–717.

[85] Scott Beatty, Francesco Ferri, Bryce Bocking, Jens Peter Kofoed, and Bradley Buckham. "Power Take-Off Simulation for Scale Model Testing of Wave Energy Converters". In: *Energies* 10.7 (2017), p. 973.

[86] António JNA Sarmento and AF de O Falcão. "Wave generation by an oscillating surface-pressure and its application in wave-energy extraction". In: *Journal of Fluid Mechanics* 150 (1985), pp. 467–485.

[87] António F. O. Falcão and João C. C. Henriques. "The spring-like air compressibility effect in oscillating-water-column wave energy converters: Review and analyses". In: *Renewable and Sustainable Energy Reviews* 112 (2019), pp. 483–498. DOI: https://doi.org/10.1016/j.rser.2019.04.040. URL: http://www.sciencedirect.com/science/article/pii/S1364032119302527.

[88] J Weber. "Representation of non-linear aero-thermodynamic effects during small scale physical modelling of OWC WECs". In: *Proceedings of the 7th European Wave and Tidal Energy Conference* 895 (2007).

[89] António F. O. Falcão and João C. C. Henriques. "Model-prototype similarity of oscillating-water-column wave energy converters". In: *International Journal of Marine Energy* 6 (2014), pp. 18–34. DOI: 10.1016/j.ijome.2014.05.002.

[90] H. Zhang and G. A. Aggidis. "Nature rules hidden in the biomimetic wave energy converters". In: *Renewable and Sustainable Energy Reviews* 97 (2018), pp. 28–37. DOI: https://doi.org/10.1016/j.rser.2018.08.018. URL: http://www.sciencedirect.com/science/article/pii/S1364032118306051.

[91] Giacomo Moretti, Miguel Santos Herran, David Forehand, Marco Alves, Henry Jeffrey, Rocco Vertechy, and Marco Fontana. "Advances in the development of dielectric elastomer generators for wave energy conversion". In: *Renewable and Sustainable Energy Reviews* 117 (2020), p. 109430.

[92] Malcolm John Tucker and Edward G Pitt. *Waves in ocean engineering*. Volume 5. 2001.

[93] Matt Folley. "The wave energy resource". In: *Handbook of Ocean Wave Energy* 7 (2017).

[94] DNV. *Environmental conditions and environmental loads, DNV-RP-C205*. Det Norske Veritas. 2010.

[95] ITTC. "ITTC Recommended Guidelines: Laboratory Modelling of Waves: Regular, Irregular and Extreme Events (7.5-02-07-03.7)". In: *Proceedings of the 28th International Towing Tank Conference (Recommended Procedures and Guidelines register)* (2017).

[96] J. Lawrance, B. Holmes, I. Bryden, D. Magagna, Y. Torre-Encisco, Jean-Marc Rousset, H. Smith, Paul. M., L. Margheritini, and J. Candido. "Wave Instrumentation Database". In: *D2.01* (2012).

[97] David Magagna et al. *D2.14 Wave data presentation and storage review*. Tech. rep. Marine Renewables Infrastructure Network (MaRINET), 2012.

[98] Garry Sutton and B Holmes. *Best Practice Manual for Wave Simulation*. Tech. rep. MaRINET, 2015.

[99] A. Babarit. "A database of capture width ratio of wave energy converters". In: *Renewable Energy* 80 (2015), pp. 610–628. DOI: `http://dx.doi.org/10.1016/j.renene.2015.02.049`. URL: `http://www.sciencedirect.com/science/article/pii/S0960148115001652`.

[100] Marie-Aurélie Kerbiriou, Marc Prevosto, Christophe Maisondieu, Alain Clément, and Aurélien Babarit. "Influence of sea-states description on wave energy production assessment". In: *Proceedings of the Seventh European Wave and Tidal Energy Conference, Porto, Portugal, CD-ROM* (2007).

[101] S. Draycott, B. Sellar, T. Davey, D. R. Noble, V. Venugopal, and D. M. Ingram. "Capture and simulation of the ocean environment for offshore renewable energy". In: *Renewable and Sustainable Energy Reviews* 104 (2019), pp. 15–29. DOI: `10.1016/j.rser.2019.01.011`. URL: `https://dx.doi.org/10.1016/j.rser.2019.01.011`.

[102] D Clabby, A Henry, M Folley, and T Whittaker. "The effect of the spectral distribution of wave energy on the performance of a bottom hinged flap type wave energy converter". In: *ASME 2012 31st International Conference on Ocean, Offshore and Arctic Engineering* (2012), pp. 331–339.

[103] AD De Andrés, R Guanche, J Weber, and R Costello. "Finding gaps on power production assessment on WECs: Wave definition analysis". In: *Renewable Energy* 83 (2015), pp. 171–187.

[104] Jean-Baptiste Saulnier, Marc Prevosto, and Christophe Maisondieu. "Refinements of sea state statistics for marine renewables: A case study from simultaneous buoy measurements in Portugal". In: *Renewable Energy* 36.11 (2011), pp. 2853–2865.

[105] Jean-Baptiste Saulnier, Alain Clément, F de O António, Teresa Pontes, Marc Prevosto, and Pierpaolo Ricci. "Wave groupiness and spectral bandwidth as relevant parameters for the performance assessment of wave energy converters". In: *Ocean Engineering* 38.1 (2011), pp. 130–147.

[106] R Carballo and G Iglesias. "A methodology to determine the power performance of wave energy converters at a particular coastal location". In: *Energy Conversion and Management* 61 (2012), pp. 8–18.

[107] Remy Pascal, G Payne, CM Theobald, and I Bryden. "Parametric models for the performance of wave energy converters". In: *Applied Ocean Research* 38 (2012), pp. 112–124.

[108] Clayton Hiles, ADDA Guitierrez, Scott Beatty, and Brad Buckham. "A case study on the matrix approach to WEC performance characterization". In: *Proceedings of the 11th European Wave and Tidal Energy Conference, Nantes, France* (2015), pp. 6–11.

[109] Clayton E Hiles, Scott J Beatty, and Adrian de Andres. "Wave energy converter annual energy production uncertainty using simulations". In: *Journal of Marine Science and Engineering* 4.3 (2016), p. 53.

[110] Alexis Mérigaud and John V Ringwood. "Power production assessment for wave energy converters: Overcoming the perils of the power matrix". In: *Proceedings of the Institution of Mechanical Engineers, Part M: Journal of Engineering for the Maritime Environment* 232.1 (2018), pp. 50–70.

[111] Tom Mitchell Ferguson, Alan Fleming, Irene Penesis, and Gregor Macfarlane. "Improving OWC performance prediction using polychromatic waves". In: *Energy* 93 (2015), pp. 1943–1952.

[112] Ryan Geoffrey Coe, Vincent Sinclair Neary, MJ Lawson, Y Yu, and Jochem Weber. "Extreme conditions modeling workshop report". In: *NREL* (2014).

[113] Yi-Hsiang Yu, Jennifer Van Rij, Ryan Coe, and Mike Lawson. "Preliminary wave energy converters extreme load analysis". In: *34th International Conference on Ocean, Offshore and Arctic Engineering, OMAE, St. John's, Newfoundland, Canada* (2015).

[114] Sylvain Bourdier, Kieth Dampney, H. Fernandez, Guiomar Lopez, and Jean-Baptiste Rochon. *D4.05 Report on non-intrusive wave field measurement.* Tech. rep. Marine Renewables Infrastructure Network (MaRINET), 2014.

[115] Tom Mitchell Ferguson, Gregor MacFarlane, Alan Fleming, and Irene Penesis. "PIV investigation of 3-dimensional flow within an oscillating water column". In: *International Journal of Marine Energy* 11 (2015), pp. 120–131.

[116] Tom Mitchell Ferguson, Irene Penesis, Gregor Macfarlane, and Alan Fleming. "A PIV investigation of OWC operation in regular, polychromatic and irregular waves". In: *Renewable Energy* 103 (2017), pp. 143–155.

[117] Alan Fleming, Irene Penesis, Laurie Goldsworthy, Gregor Macfarlane, Neil Bose, and Tom Denniss. "Phase-averaged analysis of an oscillating water column wave energy

converter". PhD thesis. National Centre for Maritime Engineering and Hydrodynamics, Australian Maritime College, University of Tasmania, 2012.

[118] BIPM, IEC, IFCC, ILAC, ISO, IUPAC, IUPAP, and OIML. "JCGM 101:2008: Evaluation of Measurement Data–Supplement 1 to the "Guide to the Expression of Uncertainty in Measurement"–Propagation of distributions using a Monte Carlo method". In: *Joint Committee for Guides in Metrology, JCGM* 101 (2008).

[119] Damon Howe, Jean-Roch Nader, and Gregor Macfarlane. "Experimental investigation of multiple Oscillating Water Column Wave Energy Converters integrated in a floating breakwater: Energy extraction performance". In: *Applied Ocean Research* 97 (2020), p. 102086.

[120] Made Jaya Muliawan, Zhen Gao, Torgeir Moan, and Aurelien Babarit. "Analysis of a two-body floating wave energy converter with particular focus on the effects of power take-off and mooring systems on energy capture". In: *Journal of Offshore Mechanics and Arctic Engineering* 135.3 (2013).

[121] Pedro C Vicente, AF Falcão, and PJ Justino. "Slack-chain mooring configuration analysis of a floating wave energy converter". In: *26th International workshop on water waves and floating bodies, Athens, Greece.* 2011.

[122] ITTC. "ITTC Recommended Guidelines: Analysis Procedure for Model Tests in Regular Waves (7.5-02-07-03.2)". In: *Proceedings of the 28th International Towing Tank Conference (Recommended Procedures and Guidelines register)* (2017).

[123] ITTC. "ITTC Recommended Guidelines: Analaysis Procedure of Model Tests in Irregular Waves (7.5-02-07-03.114)". In: *Proceedings of the 28th International Towing Tank Conference (Recommended Procedures and Guidelines register)* (2017).

[124] ITTC. "ITTC Recommended Guidelines: Laboratory Modelling of Multidirectional Irregular Wave Spectra (7.5-02-07-01.1)". In: *Proceedings of the 28th International Towing Tank Conference (Recommended Procedures and Guidelines register)* (2017).

[125] Peter Frigaard, J Helm-Petersen, G Klopman, CT Standsberg, M Benoit, MJ Briggs, M Miles, J Santas, HA Schäffer, and PJ Hawkes. "IAHR List of Sea Parameters: an update for multidirectional waves". In: *The 27th IAHR Congress* (1997).

[126] Ryan G Coe and Vincent S Neary. "Review of methods for modeling wave energy converter survival in extreme sea states". In: *Prcoeedings of the Marine Energy Technology Symposium* (2014).

[127] Steven W Smith. *The scientist and engineer's guide to digital signal processing.* California Technical Pub. San Diego, 1997.

[128] Wanan Sheng and Hui Li. "A Method for Energy and Resource Assessment of Waves in Finite Water Depths". In: *Energies* 10.4 (2017), p. 460. DOI: `10.3390/en10040460`. URL: `https://dx.doi.org/10.3390/en10040460`.

[129] Jean-Roch Nader. "Interaction of Ocean Waves with Oscillating Water Column Wave Energy Converters". PhD thesis. School of Mathematics and Applied Statistics, University of Wollongong, 2013.

[130] Markel Penalba and John V Ringwood. "A review of wave-to-wire models for wave energy converters". In: *Energies* 9.7 (2016), p. 506.

[131] Peter Frigaard, Jens Peter Kofoed, and Kim Nielsen. “Assessment of Wave Energy Devices: best practice as used in Denmark”. In: *World Renewable Energy Congress and Exhibition* (2008).

[132] DV Evans. “Some theoretical aspects of three-dimensional wave-energy absorbers”. In: *Proc. 1st Symp. Wave Energy Utilization*. 1979, pp. 78–112.

[133] Johannes Falnes. “Radiation impedance matrix and optimum power absorption for interacting oscillators in surface waves”. In: *Applied ocean research* 2.2 (1980), pp. 75–80.

[134] Peter Troch et al. “Physical Modelling of an Array of 25 Heaving Wave Energy Converters to Quantify Variation of Response and Wave Conditions”. In: HAL, 2013.

[135] Peter Troch. “An overview of the WECwakes project physical modeling of an array of 25 wave energy converters”. In: *Proceedings of the 3rd IAHR Europe Congress* (2014).

[136] Vasiliki Stratigaki et al. “Physical modelling of wave energy converter arrays in a large-scale wave basin: the WECwakes project”. In: *Proceedings of the HYDRALAB IV Joint User Meeting* 1 (2014).

[137] Pau Mercadé Ruiz, Francesco Ferri, and Jens Peter Kofoed. “Experimental Validation of a Wave Energy Converter Array Hydrodynamics Tool”. In: *Sustainability* 9.1 (2017), p. 115.

[138] M Bennet, I Penesis, A Fleming, G Macfarlane, and J-R Nader. “Experimental Study into the Diffracted Wave Field Downstream of an Array of Wave Energy Converters in Irregular Waves”. In: *European Wave and Tidal Energy Conference* (2017).

[139] A Fleming and R Manasseh. “Preliminary Experimental Observation of Surface Currents Produced by Simulating WEC Radiation and Diffraction Wave Fields”. In: *European Wave and Tidal Energy Conference* (2017).

[140] Jochem Weber. “WEC Technology Readiness and Performance Matrix–finding the best research technology development trajectory”. In: *International Conference on Ocean Energy* (2012).

[141] Jochem Weber, Ronan Costello, and John Ringwood. “WEC technology performance levels (TPLs)-metric for successful development of economic WEC technology”. In: *Proceedings the European Wave and Tidal Energy Conference (EWTEC)* (2013).

[142] Diana Bull, Ronan Costello, Aurélien Babarit, Kim Nielsen, Ben Kennedy, Claudio Bittencourt-Ferreira, Jesse Roberts, and Jochem Weber. “Scoring the Technolgy Performance Level (TPL) assessment”. In: *Proceedings of the 12the European Wave and Tidal Energy Conference (EWTEC)* (2017).

[143] Jesse D Roberts, Diana L Bull, Robert Joseph Malins, Ronan Patrick Costello, Aurelien Babarit, Kim Nielsen, Claudio Bittencourt Ferreira, Ben Kennedy, Kathryn Dykes, and Jochem Weber. *Technology Performance Level Assessment Methodology*. Tech. rep. Sandia National Lab. (SNL-NM), Albuquerque, NM (United States), 2017.

[144] Jochem W Weber and Daniel Laird. *Structured Innovation of High-Performance Wave Energy Converter Technology*. Tech. rep. National Renewable Energy Lab.(NREL), Golden, CO (United States), 2018.

[145] Edward Pitt. *Assessment of Performance of Wave Energy Conversion Systems.* European Marine Energy Centre (EMEC). 2009.

[146] Yue Hong, Rafael Waters, Cecilia Boström, Mikael Eriksson, Jens Engström, and Mats Leijon. "Review on electrical control strategies for wave energy converting systems". In: *Renewable and Sustainable Energy Reviews* 31 (2014), pp. 329–342. DOI: `https://doi.org/10.1016/j.rser.2013.11.053`. URL: `http://www.sciencedirect.com/science/article/pii/S1364032113008022`.

[147] Liguo Wang, Jan Isberg, and Elisabetta Tedeschi. "Review of control strategies for wave energy conversion systems and their validation: the wave-to-wire approach". In: *Renewable and Sustainable Energy Reviews* 81 (2018), pp. 366–379. DOI: `https://doi.org/10.1016/j.rser.2017.06.074`. URL: `http://www.sciencedirect.com/science/article/pii/S136403211731016X`.

[148] Yoshimi Goda and Yasumasa Suzuki. "Estimation of incident and reflected waves in random wave experiments". In: Coastal Engineering, 1977, pp. 828–845.

[149] Edward BL Mackay, AbuBakr S Bahaj, and Peter G Challenor. "Uncertainty in wave energy resource assessment. Part 1: historic data". In: *Renewable Energy* 35.8 (2010), pp. 1792–1808.

[150] Edward BL Mackay, AbuBakr S Bahaj, and Peter G Challenor. "Uncertainty in wave energy resource assessment. Part 2: Variability and predictability". In: *Renewable energy* 35.8 (2010), pp. 1809–1819.

[151] Offshore Renewable Energy Catapult. *Wave and Tidal Energy Yield Uncertainty Reference Document.* Tech. rep. Catapult, Offshore Renewable Energy, 2015.

[152] J. P. Kofoed et al. "A methodology for equitable performance assessment and presentation of wave energy converters based on sea trials". In: *Renewable energy* 52 (2013), pp. 99–110.

[153] Wei Qiu, Joel Sales Junior, Dongyeon Lee, Halvor Lie, Viacheslav Magarovskii, Takashi Mikami, Jean-Marc Rousset, Sergio Sphaier, Longbin Tao, and Xuefeng Wang. "Uncertainties related to predictions of loads and responses for ocean and offshore structures". In: *Ocean Engineering* 86 (2014), pp. 58–67.

[154] ITTC. "ITTC Recommended Guidelines: Guide to the Expression of Uncertainty in Experimental Hydrodynamics (7.5-02-01-01)". In: *Proceedings of the 28th International Towing Tank Conference (Recommended Procedures and Guidelines register)* (2014).

[155] ITTC. "ITTC Recommended Guidelines: General Guideline for Uncertainty Analysis in Resistance Tests (7.5-02-02-02)". In: *Proceedings of the 28th International Towing Tank Conference (Recommended Procedures and Guidelines register)* (2008).

[156] B. Wu, M. Woodward, S. Nishio, A. Olivieri, L. Perez Rojas, M. van Rijsbergen, and A. Derradji-Aouat. *The Specialist Committee on Uncertainty Analysis - Final Report and Recommendations to the 26th ITTC.* Tech. rep. International Towing Tank Conference, 2011.

[157] Eurachem / CITAC. *Quantifying Uncertainty in Analytical Measurement.* QUAM:2012.P1. Co-Operation of International Tracability in Analytical Chemistry. 2012.

[158] Wanan Sheng, Raymond Alcorn, and Tony Lewis. "Physical modelling of wave energy converters". In: *Ocean Engineering* 84 (2014), pp. 29–36. DOI: 10.1016/j.oceaneng.2014.03.019.

[159] Ahmed Elhanafi, Gregor Macfarlane, Alan Fleming, and Zhi Leong. "Scaling and air compressibility effects on a three-dimensional offshore stationary OWC wave energy converter". In: *Applied energy* 189 (2017), pp. 1–20.

[160] SJ Kline. "The purposes of uncertainty analysis". In: *Journal of Fluids Engineering* 107.2 (1985), pp. 153–160.

[161] Alan Fleming and Gregor Macfarlane. "In-situ orifice calibration for reversing oscillating flow and improved performance prediction for oscillating water column model test experiments". In: *International Journal of Marine Energy* 17 (2017), pp. 147–155.

[162] ISO. *5167-1: 1991/A1: 1998: Orifice plates, nozzles and Venturi tubes inserted in circular cross section conduits running full.* 1998.

[163] ITTC. "ITTC Recommended Guidelines: Uncertainty Analysis, Instrument Calibration (7.5-01-03-01)". In: *Proceedings of the 28th International Towing Tank Conference (Recommended Procedures and Guidelines register)* (2017).

[164] Saishuai Dai, Sandy Day, Zhiming Yuan, and Haibin Wang. "Investigation on the hydrodynamic scaling effect of an OWC type wave energy device using experiment and CFD simulation". In: *Renewable Energy* (2019).

[165] Mads Røge Eldrup and Thomas Lykke Andersen. "Applicability of Nonlinear Wavemaker Theory". In: *Journal of Marine Science and Engineering* 7.1 (2019), p. 14.

[166] I. Zabala, J. C. C. Henriques, J. M. Blanco, A. Gomez, L. M. C. Gato, I. Bidaguren, A. F. O. Falcão, A. Amezaga, and R. P. F. Gomes. "Wave-induced real-fluid effects in marine energy converters: Review and application to OWC devices". In: *Renewable and Sustainable Energy Reviews* 111 (2019), pp. 535–549. DOI: 10.1016/j.rser.2019.05.025. URL: https://dx.doi.org/10.1016/j.rser.2019.05.025.

[167] AJNA Sarmento. "Model-test optimization of an OWC wave power plant". In: *International Journal of Offshore and Polar Engineering* 3.01 (1993).

[168] Antonino Viviano, Stefania Naty, and Enrico Foti. "Scale effects in physical modelling of a generalized OWC". In: *Ocean Engineering* 162 (2018). experimental scale effects owc m2c (method to copy) i2c (introduction to copy), pp. 248–258. DOI: https://doi.org/10.1016/j.oceaneng.2018.05.019. URL: https://www.sciencedirect.com/science/article/pii/S0029801818307777.

[169] Damon Howe, Jean-Roch Nader, and G MacFarlance. "Experimental analysis into the effects of air compressibility in OWC model testing". In: *Proceedings of the Asian Wave and Tidal Energy Conference (AWTEC)* (2018), p. 449.

[170] TJT Whittaker, D Langston, N Fletcher, M Shaw, and AF de O Falcão. *Islay LIMPET wave power plant.* Tech. rep. The Queen's University of Belfast, 2002.

[171] Richard Jefferys and Trevor Whittaker. "Latching control of an oscillating water column device with air compressibility". In: Hydrodynamics of Ocean Wave-Energy Utilization, 1986, pp. 281–291.

[172] Herve Martins-Rivas and Chiang C Mei. "Wave power extraction from an oscillating water column at the tip of a breakwater". In: *Journal of fluid Mechanics* 626 (2009), pp. 395–414.

[173] Paulo RF Teixeira, Djavan P Davyt, Eric Didier, and Rubén Ramalhais. "Numerical simulation of an oscillating water column device using a code based on Navier–Stokes equations". In: *Energy* 61 (2013), pp. 513–530.

[174] Wanan Sheng, Raymond Alcorn, and Anthony Lewis. "On thermodynamics in the primary power conversion of oscillating water column wave energy converters". In: *Journal of Renewable and Sustainable Energy* 5.2 (2013), p. 023105.

[175] Arun Kamath, Hans Bihs, and Øivind A Arntsen. "Numerical modeling of power take-off damping in an oscillating water column device". In: *International Journal of Marine Energy* 10 (2015), pp. 1–16.

[176] Wanan Sheng and Anthony Lewis. "Wave energy conversion of oscillating water column devices including air compressibility". In: *Journal of Renewable and Sustainable Energy* 8.5 (2016), p. 054501.

[177] Aggelos S. Dimakopoulos, Mark J. Cooker, and Tom Bruce. "The influence of scale on the air flow and pressure in the modelling of Oscillating Water Column Wave Energy Converters". In: *International Journal of Marine Energy* 19.Supplement C (2017), pp. 272–291. DOI: `https://doi.org/10.1016/j.ijome.2017.08.004`. URL: `http://www.sciencedirect.com/science/article/pii/S2214166917300693`.

[178] I Simonetti, L Cappietti, H Elsafti, and H Oumeraci. "Evaluation of air compressibility effects on the performance of fixed OWC wave energy converters using CFD modelling". In: *Renewable energy* 119 (2018), pp. 741–753.

[179] E. Medina-López, A. Moñino Ferrando, M. Clavero Gilabert, C. Del Pino, and M. Losada Rodríguez. "Note on a real gas model for OWC performance". In: *Rewewable Energy* 85 (2016), pp. 588–597. DOI: `10.1016/j.renene.2015.07.017`. URL: `https://dx.doi.org/10.1016/j.renene.2015.07.017`.

[180] Robert G Dean and Robert A Dalrymple. *Water wave mechanics for engineers and scientists*. Vol. 2. World Scientific Publishing Company, 1991.

[181] I López, B Pereiras, F Castro, and Gregorio Iglesias. "Performance of OWC wave energy converters: influence of turbine damping and tidal variability". In: *International Journal of Energy Research* 39.4 (2015), pp. 472–483.

[182] A. Babarit, J. Hals, M. J. Muliawan, A. Kurniawan, T. Moan, and J. Krokstad. "Numerical benchmarking study of a selection of wave energy converters". In: *Renewable Energy* 41 (2012), pp. 44–63. DOI: `10.1016/j.renene.2011.10.002`.

[183] Ahmed Elhanafi, Gregor Macfarlane, Alan Fleming, and Zhi Leong. "Investigations on 3D effects and correlation between wave height and lip submergence of an offshore stationary OWC wave energy converter". In: *Applied Ocean Research* 64 (2017), pp. 203–216.

[184] Ahmed Elhanafi and Chan Joo Kim. "Experimental and numerical investigation on wave height and power take–off damping effects on the hydrodynamic performance

of an offshore–stationary OWC wave energy converter”. In: *Renewable energy* 125 (2018), pp. 518–528.

[185] Oliver Büker, Peter Lau, and Karsten Tawackolian. “Reynolds number dependence of an orifice plate”. In: *Flow Measurement and Instrumentation* 30 (2013), pp. 123–132.

[186] T Sarpkaya. “M. and Isaacson”. In: *Mechanics of wave forces on offshore structures, Van Norstrand Reinhold* (1981).

[187] US DOE. “Technology readiness assessment guide”. In: *DOE G* 413 (2011), pp. 3–4.

[188] F Stern, K Agdrup, SY Kim, AC Hochbaum, KP Rhee, FHHA Quadvlieg, P Perdon, T Hino, R Broglia, and J Gorski. “Experience from SIMMAN 2008—the first workshop on verification and validation of ship maneuvering simulation methods”. In: *Journal of Ship Research* 55.2 (2011), pp. 135–147.

[189] Amos Tversky and Daniel Kahneman. “Judgment under Uncertainty: Heuristics and Biases”. In: *Science* 185.4157 (1974), pp. 1124–1131. DOI: 10.1126/science.185.4157.1124. URL: https://dx.doi.org/10.1126/science.185.4157.1124.

[190] Christian D Schunn and J Gregory Trafton. “The psychology of uncertainty in scientific data analysis”. In: *Handbook of the psychology of science* (2012), 461e483.

[191] A. F. de O. Falcão and P. A. P. Justino. “OWC wave energy devices with air flow control”. In: *Ocean Engineering* 26.12 (1999), pp. 1275–1295. DOI: https://doi.org/10.1016/S0029-8018(98)00075-4. URL: http://www.sciencedirect.com/science/article/pii/S0029801898000754.

[192] Wanan Sheng, Florent Thiebaut, Marie Babuchon, Joseph Brooks, Anthony Lewis, and Raymond Alcorn. “Investigation to air compressibility of oscillating water column wave energy converters”. In: *ASME 2013 32nd International Conference on Ocean, Offshore and Arctic Engineering* (2013), V008T09A005–V008T09A005.

[193] ITTC. “ITTC Recommended Guidelines: Fresh Water and Seawater Properties (7.5-02-01-03)”. In: *Proceedings of the 28th International Towing Tank Conference (Recommended Procedures and Guidelines register)* (2011).

[194] Ahmed Elhanafi, Alan Fleming, Gregor Macfarlane, and Zhi Leong. “Numerical energy balance analysis for an onshore oscillating water column–wave energy converter”. In: *Energy* 116 (2016), pp. 539–557.

[195] Jonathan Binns. “Extreme motions of modern sailing yachts”. PhD thesis. National Centre for Maritime Engineering and Hydrodynamics, Australian Maritie College, 2008.

[196] Dracos Vassalos. “Physical modelling and similitude of marine structures”. In: *Ocean Engineering* 26.2 (1998), pp. 111–123. DOI: https://doi.org/10.1016/S0029-8018(97)10004-X. URL: http://www.sciencedirect.com/science/article/pii/S002980189710004X.

[197] Nazanin Ansarifard, S. S. Kianejad, Alan Fleming, and Shuhong Chai. “A radial inflow air turbine design for a vented oscillating water column”. In: *Energy* 166 (2019), pp. 380–391. DOI: https://doi.org/10.1016/j.energy.2018.10.068. URL: http://www.sciencedirect.com/science/article/pii/S0360544218320589.

Appendix A

Chapter 3 Supplementary Information

A.1 Reference list from the diagram of uncertainty sources

References for Fig. A.1:

Table A.1 Reference list from the diagram of uncertainty sources Fig. A.1.

1	Hughes, 1993 [22]	21	De Andrés, 2015. [103]
2	IEC, 2019. [10]	22	Mérigaud and Ringwood, 2018. [110]
3	Sarmento and Falcão, 1985. [86]	23	Coleman and Steele, 2018. [60]
4	Jefferys and Whittaker, 1986. [171]	24	ITTC 7.5-02-07-03.12, 2017. [17]
5	Falcão and Justino, 1999. [191]	25	Beatty et. al., 2017. [85]
6	Weber, 2007. [88]	26	Qiu et. al., 2014. [153]
7	Martins-Rivas, et. al., 2009. [172]	27	EquiMar, 2010. [42]
8	Sheng et. al., 2013. [192]	28	ITTC 7.5-02-01-03. [193]
9	Teixeira et. al., 2013. [173]	29	Caska and Finnigan, 2008. [81]
10	Falcão et. al., 2014. [89]	30	Bhinder et al., 2012. [79]
11	Kamath et. al., 2015. [175]	31	Wei et al., 2015. [78]
12	Sheng and Lewis, 2016. [176]	32	Giorgi and Ringwood, 2017. [76]
13	Elhanafi, 2016. [194]	33	Pathak et al., 2017. [80]
14	Medina-López et. al., 2016. [179]	34	Schmitt and Elsäßer, 2017. [77]
15	Dimakopoulos et. al., 2017. [177]	35	Palm et al., 2018. [74]
16	Simonetti et. al., 2018. [178]	36	Jin et al., 2018. [75]
17	Viviano et. al., 2018. [168]	37	Tversky and Kahneman, 1974. [189]
18	Howe et. al., 2018. [169]	38	Schunn (2012). [190]
19	Noble et. al., 2017. [64]	39	ITTC 7.5-01-03-01, [163]
20	Catapult, 2015. [151]		

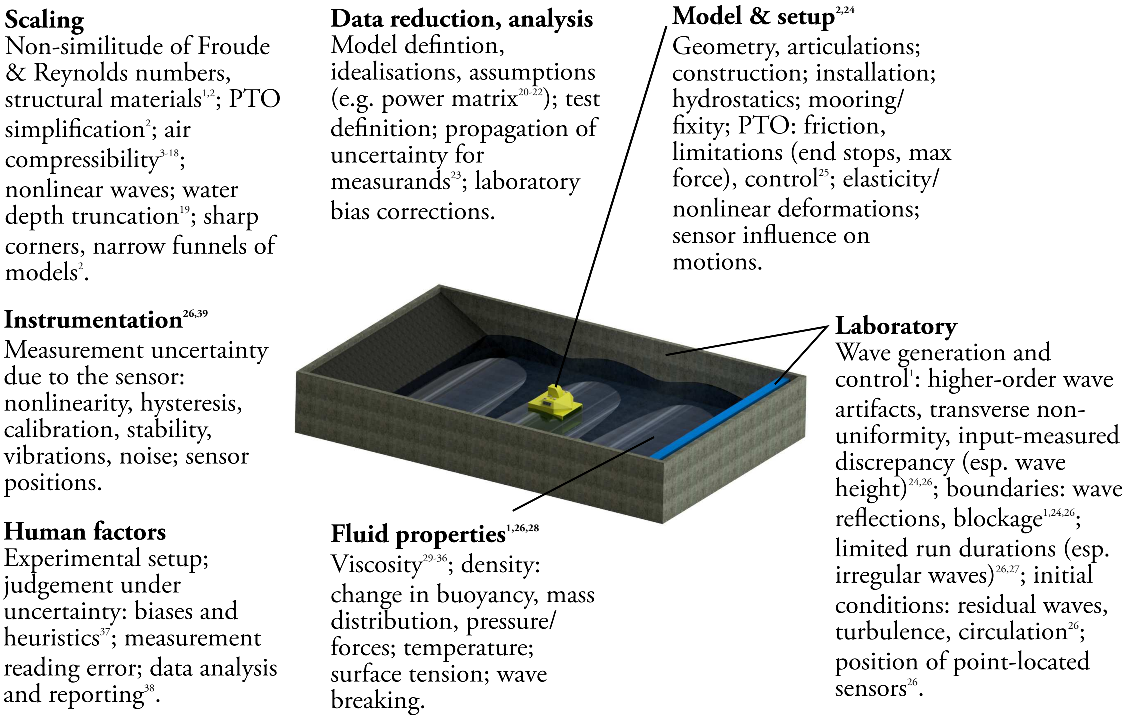

Figure A.1: Diagram of potential sources of uncertainty in a typical wave energy converter experiment.

A.2 Force balance: design and in-situ calibration

Details on the design of the force balance structure and load cell configuration can be found in [195]. A concise description follows. The force balance consists of a base structure, a measurement frame structure with a model mount within the base structure, and six load cells supporting the measurement frame structure. The load cells are configured to obtain force/moment measurement in six degrees of freedom. They are cantilever type load cells, connected with flexure rods that minimise cross talk. The total force applied to the model under wave action is decoupled into six components acting along each rod which are measured by the connected load cells. The measured forces can then be transformed into any desired coordinate system to obtain the forces/moments about the origin. Interactions between measured forces will occur due to slight deflections of the structure and load cells. These were minimised at the design stage through suitable choice of load cells, flexure design and optimised load cell arrangement using three dimensional beam finite element analysis. The small interactions that exist due to deflections and finite flexure stiffness are accounted for via a complete six component calibration, with the calibration method described below. The design summary specifies a maximum load of 220 kg; angular alignment better than 0.05°; a natural frequency response of 89 Hz, where it can measure up to 10 Hz signals with less than 1% error; the cross talks is under 0.15%, of which less than 1% is non-linear up to 65 kg loadings; and the linear portions of the cross talks will be calibrated out.

The materials and method of the in-situ calibrations were as follows. A bespoke calibration rig, constructed with T slot aluminium extrusion beams, was fixed to the circular stainless steel plate on top of the force balance (see Fig. A.2), where the model is connected when installed. It had eight loading points, from which the three force components and three moment components could be calibrated. The remaining two loading points provided two separate combined loading cases, useful in better resolving the calibration matrix. Wire cables were used to apply the known load to the calibration rig, which transfers the load directly to the force balance. The cables were connected between the calibration rig load points and stay points positioned a distance away in the positive X, Y and Z directions (the dominant force directions and moment rotations). The stay points consisted of T slot aluminium extrusion beams, bolted to the basin floor.

To apply the load, the cable was equipped with an inline turnbuckle and a pre-calibrated load cell (X-TRAN 250 kg). This load cell acted as the known load. The load cell was connected directly to the calibration rig load point, with the turnbuckle connected to the other end and then the wire connected to the stay point some distance away. The distance was sufficiently far away to minimise the effect of slight misalignment of the applied load. For the force component load cases, the applied load was configured such that it provided a pure force along the axes of the calibration coordinate system that is aligns with the body fixed coordinate system of the WEC model, where the origin is at the centre of gravity of the model, and based on a right hand system. For the moment component load cases, the applied load was configured such that a moment was generated about each respective principle axes by a horizontal or vertical force applied at a lever arm of a known distance. For the combined load cases, it was a similar configuration for the moment component load cases, except with a lever arm in two axes directions.

The loading schedule of each load case consisted of ten incremental set points each for loading to the maximum force and unloading back to zero, with the unloading set points shifted in order to reveal hysteresis effects (according to [163]). This process results in the calibration curve for each component, used to establish the calibration values of sensitivity, linearity, and hysteresis. The calibration range for each load case and each scale was estimated based on estimates of expected forces and moments in each respective degree of freedom, with these estimates informed from previous experiments. The calibration range was approximately 10% above the expected forces and moments. Before taking any calibration readings, the force balance was pre-loaded up to the maximum of each respective component and scale, and back to zero, to ensure any mechanical or electrical connection, offsets, or mismatches were allowed to 'settle-in". To evaluate repeatability of the calibration matrix, pre- and post-test calibrations were carried out for each of the three models tested, for a total of six calibrations.

A.2.1 Calibration procedure

Materials:

- Calibration rig (structure made of T slot aluminium extrusion)
- Calibrated single axis load cell (>250 kg rating) – external/applied/known load
- Calibration weights, to calibrate above load cell
- 6DoF load cells within force balance
- Calibration cables/wires, crimps, Turnbuckles, shackles, etc., for connecting external load cell to stay points
- DAQ

Calibration rig:

1. Calibration frame constructed, such that the structure provided capability to calibrate each of the pure components (X, Y, Z, Mx, My, Mz), as well as at least 2 combined loading points:

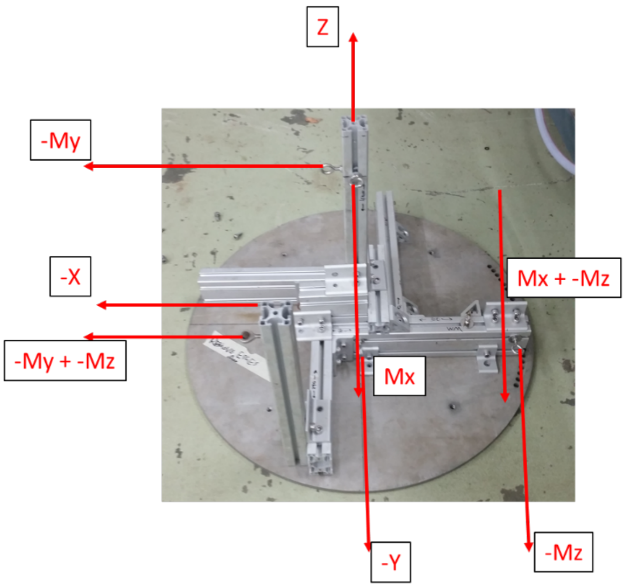

Figure A.2: force balance in-situ calibration rig with component loadings annotated (Noted, Mx + -Mz stay point not in photo)

2. Constructed stay points for calibrating each component, fixed to the basin floor using dynabolts or similar:

Figure A.3: Stay points, fixed to the basin floor (bottom of figure)

3. Cables assembled for each loading component, using crimps. Placed turnbuckle in line, with shackles to connect to single axis load cell, which connected to the calibration rig for each component:

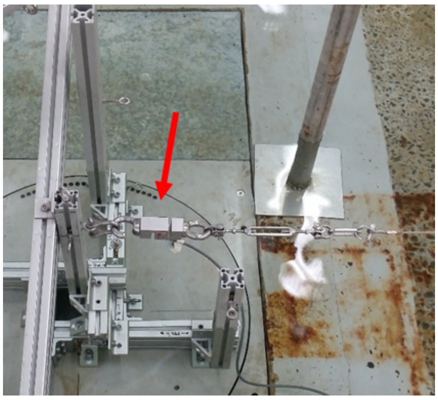

Figure A.4: Single axis load cell (known load) connected to calibration rig

External/applied load cell (known load):

1. Calibrated single axis load cell, as per ITTC guidelines [163].

DAQ

1. Used two separate data acquisition tasks: one for the 6 x force balance load cells, the other for the 1 x calibrated external load cell (used as the known load).

2. The force balance task shows volts; the external load cell task shows calibrated values (i.e. in kilogram, not volts)
3. To calibrate each component, readings in kilograms were copied from the calibrated load cell to the force balance cells, thus relating kilograms to volts. Such a reading was taken at 10+ increments for both loading and unloading, as per a normal load cell calibration.

Calibration

1. Set the voltage range for each component:
   (a) Apply maximum expected load
   (b) Adjust sensor range to maximum voltage range minus 15%, to avoid saturation for any larger than expected loads.
2. Load up component to maximum again to check the system is stable and rigid
3. Back to zero/no load
4. Load up the orientation to 0.5 kg or until all slack is taken up
5. Zero external load cell (using balance)
6. Set zeros at the start of each set (quick zeros)
7. Take first reading
8. Apply load using turnbuckle to first set point
9. Copy calibrated load value from external cell to force balance cells, in the appropriate component
10. Repeat process until maximum load, then increment back to zero, stopping at set points in between those for load up.
11. Remove load cell fully once complete
12. Repeat 4-11 steps for other load components

A.3 Example of results from the in-situ force balance calibration

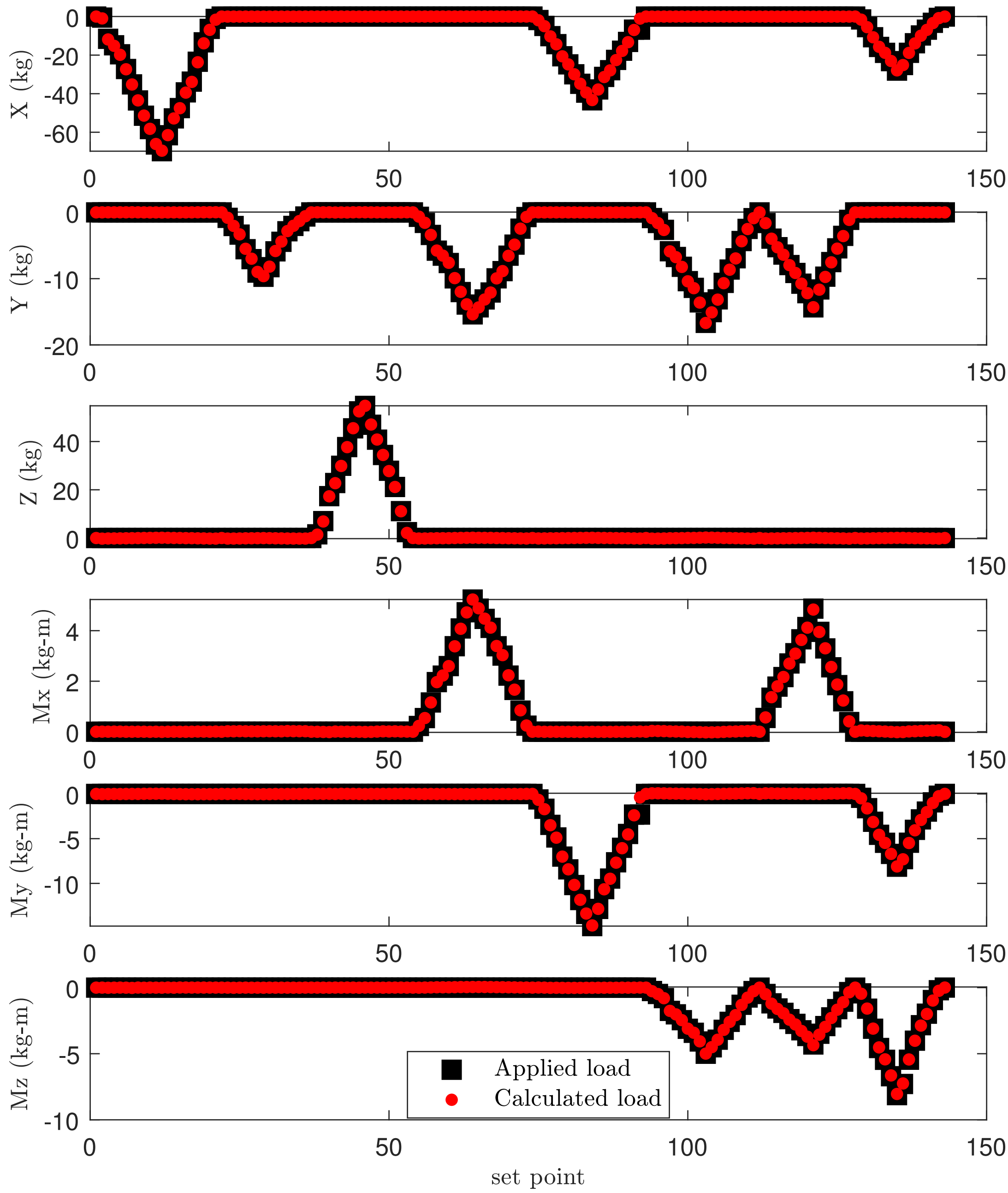

Figure A.5: Force balance calibration showing applied vs. calculated/fitted loads for 1:30 scale λ_{30}. It is apparent that the calculated load data points (red circles), calculated from the calibration matrix, lie on or very close to the centre of the applied load data points (black square), indicating high agreement between the applied and calculated load.

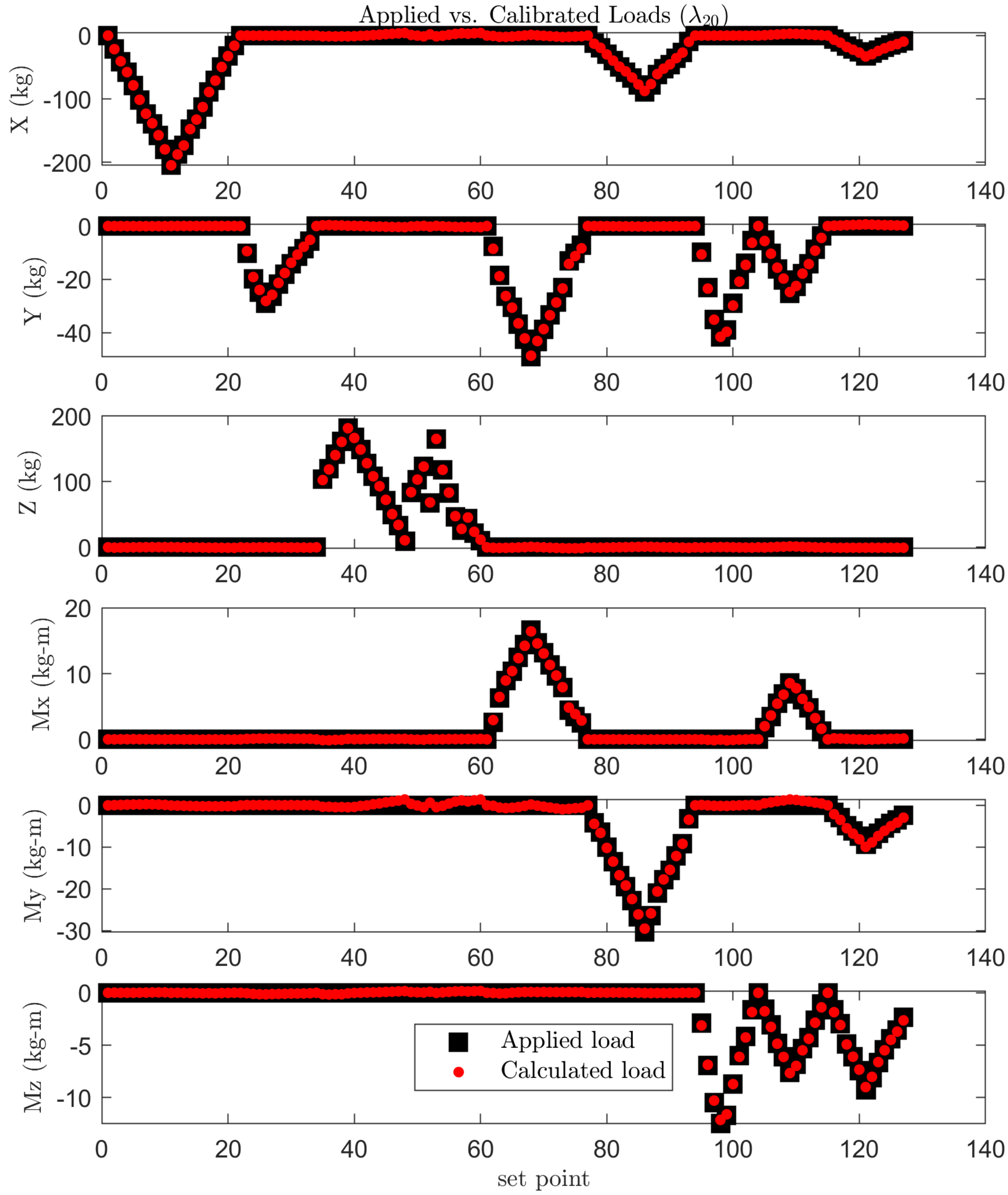

Figure A.6: Force balance calibration showing applied vs. calculated/fitted loads for 1:20 scale λ_{20}

Appendix B

Chapter 4 Supplementary Information

Here we present additional methods and results from Chapter 4. We briefly report the results and discuss their relevance with respect to scale effects of the WSE OWC WEC.

B.1 Dimensional analysis and similitude

This section describes dimensional analysis and the hydrodynamic and physical scale modelling considerations for this study. These efforts were carried out to develop a set of appropriate physical models, ones which were practically sound in terms of structure and components and which were likely to behave in a similar manner to the prototype.

Dimensional analysis can be used to identify relevant parameters and requirements of a model, inform the selection of an appropriate scaling law that assures the dominant forces of the problem are considered, and finally to evaluate potential violations of the selected scaling law by investigating whether the relevant physical phenomena scale correctly, or if corrections must be made [22]. The first step in the analysis requires acknowledging the fundamental problem at hand: assuring the model behaves in a similar manner to its prototype, i.e. model-prototype similarity [89]. This assumption, by definition, requires a general knowledge of the prototype behaviour – the physics at play. So, suppose we assume physical similarity between the model and the prototype, achieved when the ratio of corresponding magnitudes of physical quantities is the same between the two systems. This proposition assumes not only the domain of the system but also the system boundaries, inputs and outputs; that is, not only the physical model itself but also the laboratory, the environmental inputs, and the model response outputs [196]. Suppose, then, we assume the model is to be exact geometrical representation of the prototype. Similarly, suppose the wave basin laboratory, environmental effects, and model responses are all geometrically similar to the prototype (this assumption is clearly crude, given the prototype will be deployed in the uncontrolled open ocean, the model in the controlled enclosed laboratory). Building on these assumptions, we consider the environmental conditions of which the WEC will be subject to, and the physical quantities influencing the WECs behaviour, both the WEC body and the quantities associated with converting wave energy into usable power. That is, we determine the important quantities that enter into the physics of the wave-WEC interactions.

Following the description given by [89], we begin with unidirectional waves we assume a JONSWAP density spectrum $S_f(H_s, T_e; f)$, where $H_s = 4\sqrt{m_0}$ is the significant wave height, $T_e = m_{-1}/m_0$ is the energy period, and m_n is the nth moment of S_f with respect to the frequency f. For regular waves, H_s and T_e are simply wave height and period. We then define the parameters of the OWC model. For the geometry, we let L be the characteristic length ($L = \sqrt{4A_c/\pi}$, where A_c is the horizontal area of the OWC chamber). For the pressure in and out of the OWC chamber, we assume p_{at} to be atmospheric pressure and $p_{at} + p(t)$ the pressure in the OWC chamber. The pressure oscillation $p(t)$, which is driven by the oscillating column of water inside the OWC as waves pass, causes air flow inside the chamber, and in the prototype this air flow drives an air turbine and generator, comprising the power take-off (PTO) system. With respect to this PTO and the overall power performance of the WEC, the key performance indicator is the hydrodynamic efficiency of energy absorption from waves, often characterised by the capture width ratio $C_W = P/P_W B$ where P is the absorbed power by the OWC, P_W is the wave power, and B is the characteristic dimension of the WEC [99], defined here as the width of the OWC chamber W. Now we are ready to combine a set of physical quantities into dimensionless products that describe the interplay of forces and responses in and around the WEC.

We first consider a general dimensional quantity a as a function of n dimensional independent quantities $a = F(a_1, a_2, ..., a_n)$, where the function F represents a definite physical law. As said, the key performance indicator is C_W, however it is convenient to define the physical process in terms of P, such that

$$P = F(L, H_s, T_e, p, g, \rho, \nu) \tag{B.1}$$

where g is the acceleration of gravity (assumed as a physical constant), and ρ and ν are the density and kinematic viscosity of water. We neglect the surface tension of the water because the typical wave length is considerably larger than 0.1 m. Using Buckingham's theorem [22], we replace Eq. B.1 by

$$\Pi_1 = U(H_s/L, \mathrm{Fr}, \mathrm{Re}, \Pi_p) \tag{B.2}$$

where U is a function, Fr= $L^{1/2}g^{-1/2}T_e^{-1}$ is the Froude number, Re= $L^2\nu^{-1}T^{-1}$ is the Reynolds number, $\Pi_p = pL^{-1}\rho^{-1}g^{-1}$ is the dimensionless pressure and $\Pi_1 = PL^{-7/2}\rho^{-1}g^{-3/2}$ is the dimensionless power. Identical relationships could be established by replacing P1 by other dimensionless quantities. For example, this could be dimensionless volumetric flow rate $qL^{-5/2}g^{-1/2}$ where q is the flow rate displaced by the motion of the OWC free surface. If these four dimensionless quantities H_S/L, F_n, R_n, and Π_p are equal in the model and the full-scale prototype, the same will be true for $\Pi_1, \Pi_2, ...$

We can now use the above dimensional analysis to select the appropriate scaling law and, after, design the physical scale model. The relation between the model and prototype parameters is denoted by the *scale ratio* or simply the *scale*, defined as the ratio of a parameter X in the prototype (subscript p) to the value of the same parameter in the model (subscript m). That is

$$\lambda_X = \frac{L_p}{L_m} = \frac{\text{Value of L in the Protoype}}{\text{Value of L in the Model}} \tag{B.3}$$

where λ_L is the prototype-to-model scale ratio of the length parameter L. This definition of the scale ratio leads us to define the length scale ratio as $\lambda_L = L_p/L_m$.

Now we have obtained the above important quantities, we may choose which scaling law to use, by determining which two major forces dominate the physics of the wave-WEC interactions. For most WECs, inertial and gravitational forces dominate, so Froude scaling law is used to scale the hydrodynamics (wave and current) and the WEC body. Eq. (B.2) shows, however, that Reynolds number is also part of the process, and thus necessitates constancy to achieve full dynamic similarity. But Froude and Reynolds number cannot in practice be satisfied simultaneously, as this requires $\nu_m/\nu_F = \epsilon^{-3/2}$, a condition that is unachievable for small and even medium sized model scales, being tested in fresh or sea water. So in this case we are forced to keep Froude number constant and neglect Reynolds number. This problem is largely overcome by selecting a model scale large enough such that the fluid viscous effects are negligible and may be ignored. How large is large enough? There are various suggestions in the literature about keeping Reynolds number above a certain threshold to assure practical similitude; the current suggestion is Re $> 10^5$ [158], but this is a rough guide and further research is required in this area with regards to the main types of WECs.

Based on the above dimensional analysis considerations, we may turn our attention to the practical considerations of physical modelling. The expression of dimensionless power $\Pi_1 = PL^{-7/2}\rho^{-1}g^{-3/2}$ shows the scale ratio for power is $\lambda_L^{3/2}$ (neglecting ρ variation). Given model scale testing of WECs often occurs at length scales of $1:10 - 1:50$, the power ratio is likely far too disparate to model an exact dynamical PTO system. For example, if $\lambda_L = 20$ then the power ratio is ∼1:36,000, and if we assume a 1 MW rating at full-scale, then the maximum power we can expect the model to absorb would be ∼28 W. This scale is too small to, for example, simulate an air turbine/generator with an exact miniature system. Thus, the accepted procedure to simulate an OWC air turbine, to obtain acceptable dynamic similarity, is by either porous material or an orifice plate. If a Wells turbine is to be used in the prototype, which exhibits roughly linear pressure-flow characteristics, porous material is used. If an impulse type turbine is to be used in the prototype, whereby the pressure-flow relationship is quadratic, an orifice plate is used. Given subject technology of this study, the WSE technology, will use an impulse type turbine (see [197]), an orifice plate was used to model the OWC PTO system.

B.2 Orifice calibrations

Modelling the PTO system of OWC WECs using an orifice produces a quadratic relationship between pressure and volume flow rate inside the chamber, described as

$$p = \delta Q^2 \tag{B.4}$$

where δ is the damping coefficient and is a real number. This δ can be determined two ways. The first is by linearising the pressure-flow rate relationship to determine a straight line equation, based on least squares estimation, and from this obtain the gradient, m (Fig. C.5). The second method is to rearrange the C_d equation,

$$q_{C_d} = \frac{p}{|p|} C_d A_0 \sqrt{\frac{2|p|}{\rho_a}}, \tag{B.5}$$

in the form of Eq. (B.4):

$$p = \left(\frac{\rho_a}{2 C_d^2 A_o^2} \right) Q^2 \tag{B.6}$$

so that

$$\delta = \frac{\rho_a}{2 C_d^2 A_o^2} \tag{B.7}$$

By substituting the respective measured values of C_d and A_o for each scale, and Froude-scaling δ with λ^{-4}, δ may be obtained for the prototype scale. The results of determining δ with this method are presented in Table B.1.

Table B.1 Relationship between damping coefficient δ and discharge coefficient C_d.

Scale	$\boldsymbol{\rho_a}$	$\boldsymbol{A_o}$	$\boldsymbol{C_d}$	$\boldsymbol{\delta}$
-	kgm^{-3}	m^2	$kgs^{-2}Pa^{-1}$	Pas^2m^{-6}
λ_{40}	1.2	6.25e-4	0.80	0.94
λ_{30}	1.2	1.11e-3	0.74	1.10
λ_{20}	1.2	2.50e-3	0.67	1.34

Fig. C.5 shows the in-situ orifice damping results across scales, including plots of C_d and the linearised relationship between q' and p', denoted m. It is clear that C_d and m deviated across scales. As scale increased, C_d decreased and δ increased. C_d decreased approximately linearly across scales. $C_{d,\lambda_{30}}$ was 7.5% smaller than $C_{d,\lambda_{40}}$ and $C_{d,\lambda_{20}}$ 9.5% smaller than $C_{d,\lambda_{30}}$, resulting in a 16.3% relative difference between the smallest and largest scale. Similarly, m increased approximately linearly across scales. $m_{\lambda_{30}}$ was 9.3% larger than $m_{\lambda_{40}}$, and $m_{\lambda_{20}}$ 10.3% larger than $m_{\lambda_{30}}$, resulting in a 20.9% difference between the smallest and largest scale.

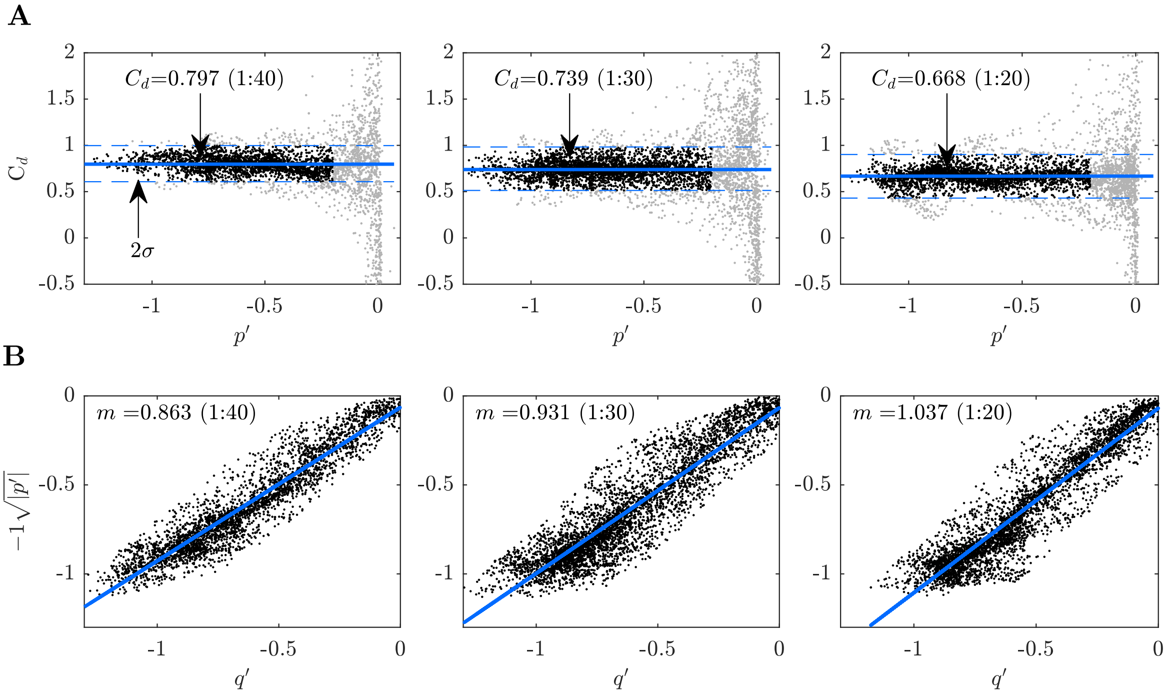

Figure B.1: (**A**) Orifice discharge coefficient C_d plotted against dimensionless pressure p' for the three scales, where C_d was calculated for $p' < -0.2$ and within 2 standard deviations σ of the mean (95%). (**B**) Plots of three scales showing pressure p' and dimensionless air volume flow rate q' relationship. This relationship is quadratic, i.e., q' is theoretically proportional to the square root of p', because an orifice was used as the PTO simulator. Outliers have been removed (points > 3 times the mean of Cook's Distance were omitted)

The trends of C_d and m are linked in that, referring to Eq. (B.5), a smaller q' value relative to the square root of p' causes m to increase positively and produces a commensurate reduction in C_d. This discrepancy between scales arises from the nonlinear relationship between p' and q', described by Eq. (B.5), where A_0 is scaled geometrically according to maintaining a 1:150 orifice ratio. If C_d were to be desired consistent across scales, one might have to violate geometrical similitude with a slightly different orifice ratio and in turn orifice diameter.

The trend of C_d against p' was similar across scales, with C_d data points spread sparsely towards zero pressure, and converging toward the mean value as pressure decreased further negatively, taking the shape of a wine glass stem and base on its side. When $p \rightarrow 0$, q' as derived was often wavy in its profile due to the numerical derivation based on η_{owc} which was affected by sloshing; in effect, C_d varied sporadically, explaining the exponential spread of data points for $p' < -0.25$. This justifies considering only C_d values for $p' > -0.25$ Pa in determining the mean of C_d.

B.3 Additional regular wave results

B.3.1 Wave elevation inside the OWC chamber

Fig. B.2 shows measured profiles of the free surface elevation inside the OWC chamber η_{owc} across scales and wave heights. The profiles shapes were similar to the respective profiles of incident waves η_{inc}. The η_{owc} profiles were more unstable than η_{inc}, noticeable as the small undulations in the profile shape, caused by sloshing, which tended to increase with increasing wave height. These η_{owc} profiles clearly show the deviating water column dynamics inside the OWC across scales. The water column induced similar deviating p and q, which in turn lead to deviating power and loads.

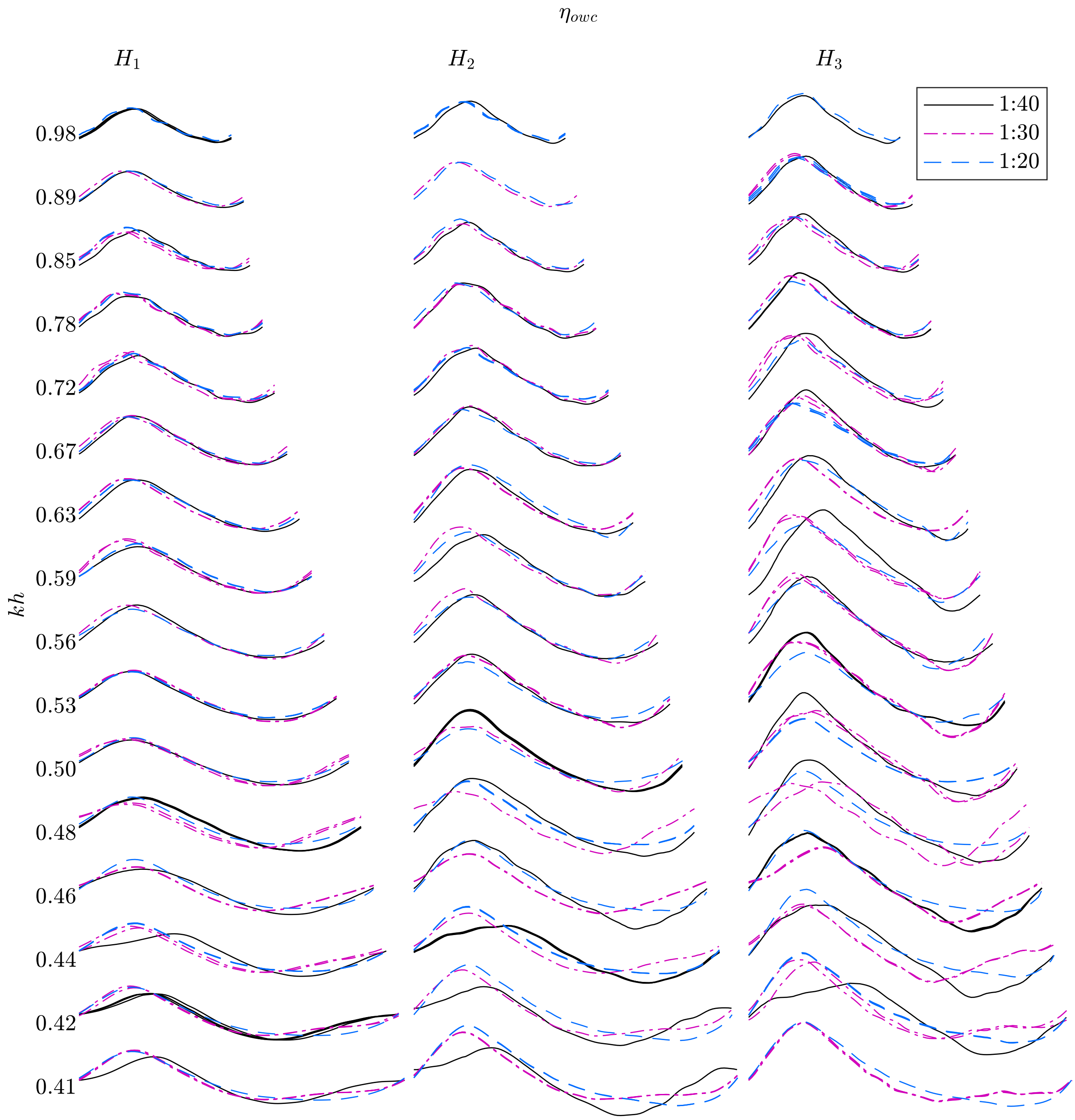

Figure B.2: Free surface elevation inside the OWC chamber η_{owc} across scales and wave heights.

B.3.2 Pressure inside the OWC chamber

Fig. B.3 shows profiles of pressure p measured inside the OWC chamber across scales and wave heights. p is (almost) always negative due to the vented unidrectional flow, where air only flows back into the chamber, hence negative pressure. Where p flattens out it is slightly positive due to the reaction of the passive flaps ($<\sim$5 Pa at model scale). Along with η_{owc}, p is coupled to the forcing of η_{inc}, so deviations in η_{inc} induces similar deviations in p. In general, $p_{\lambda_{20}}$ was largest, and $p_{\lambda_{40}}$ smallest. Another key contributor to this result was the relatively higher PTO damping for larger scales (Fig. C.5), thereby inducing relatively larger pressures in the OWC.

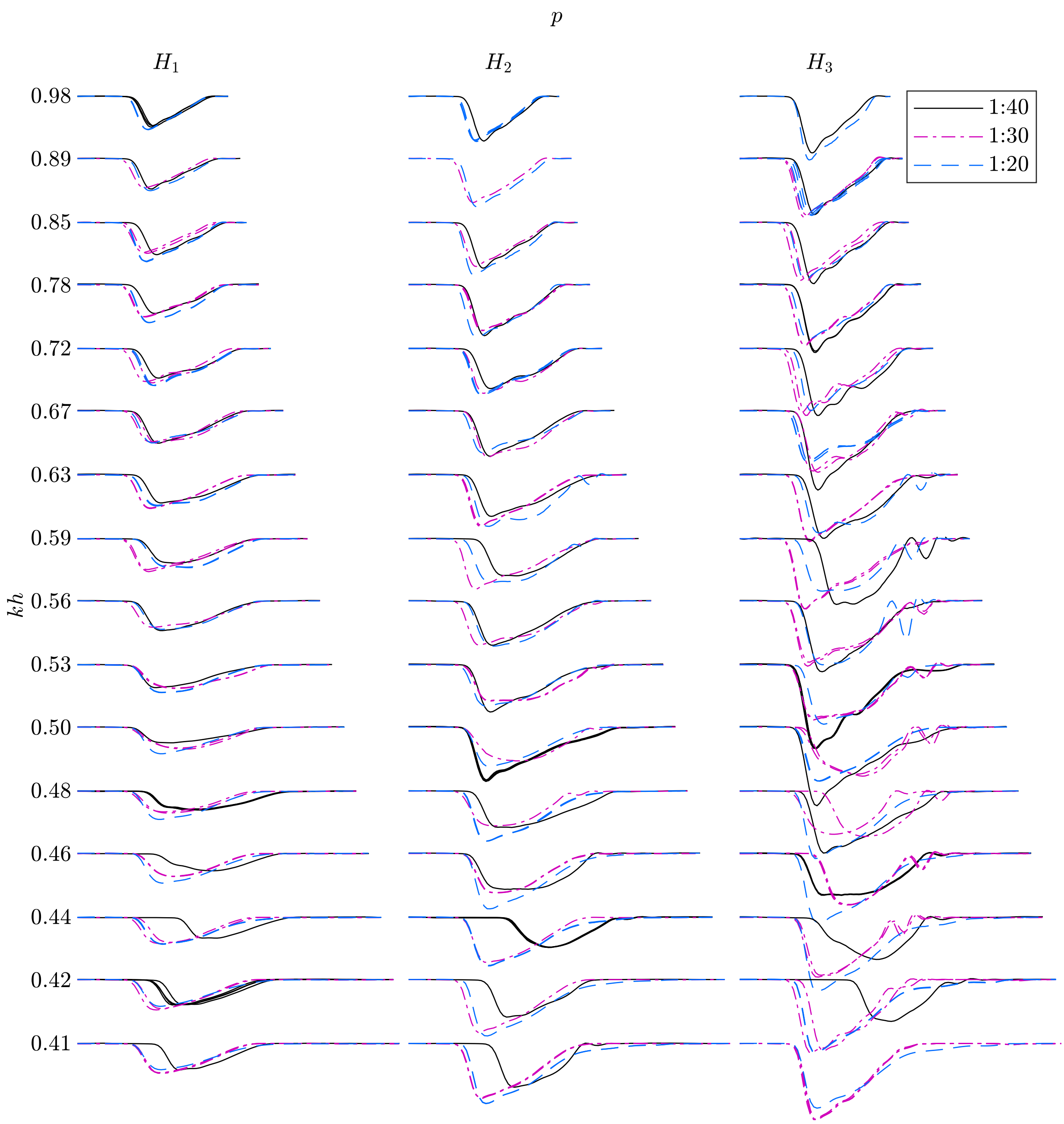

Figure B.3: Pressure inside the OWC chamber p across scales and wave heights.

B.4 Experimental waves compared to wave theories

Fig. B.4 shows the regular waves tested in the experiments, where it is seen that about half of the waves were shallow water, half intermediate.

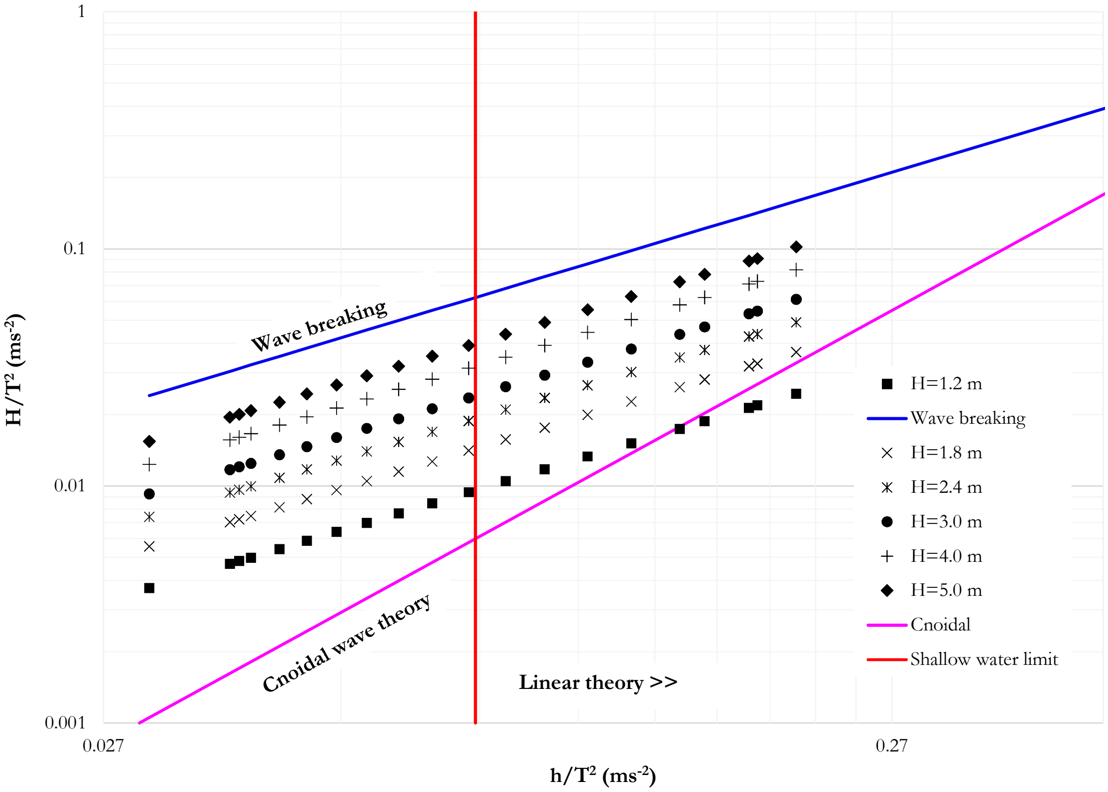

Figure B.4: Ranges of validity for various wave theories with actual experimental waves run.

B.5 Uncertainty analysis results

Figs. B.5 and B.6 shows the uncertainty analysis results in regular waves for λ_{40}, λ_{30}, and λ_{20} respectively. It is seen that the Type A, Type B, and expanded uncertainty results are similar across scales. This suggest measurement uncertainty had a negligible influence on the differences in results across scales.

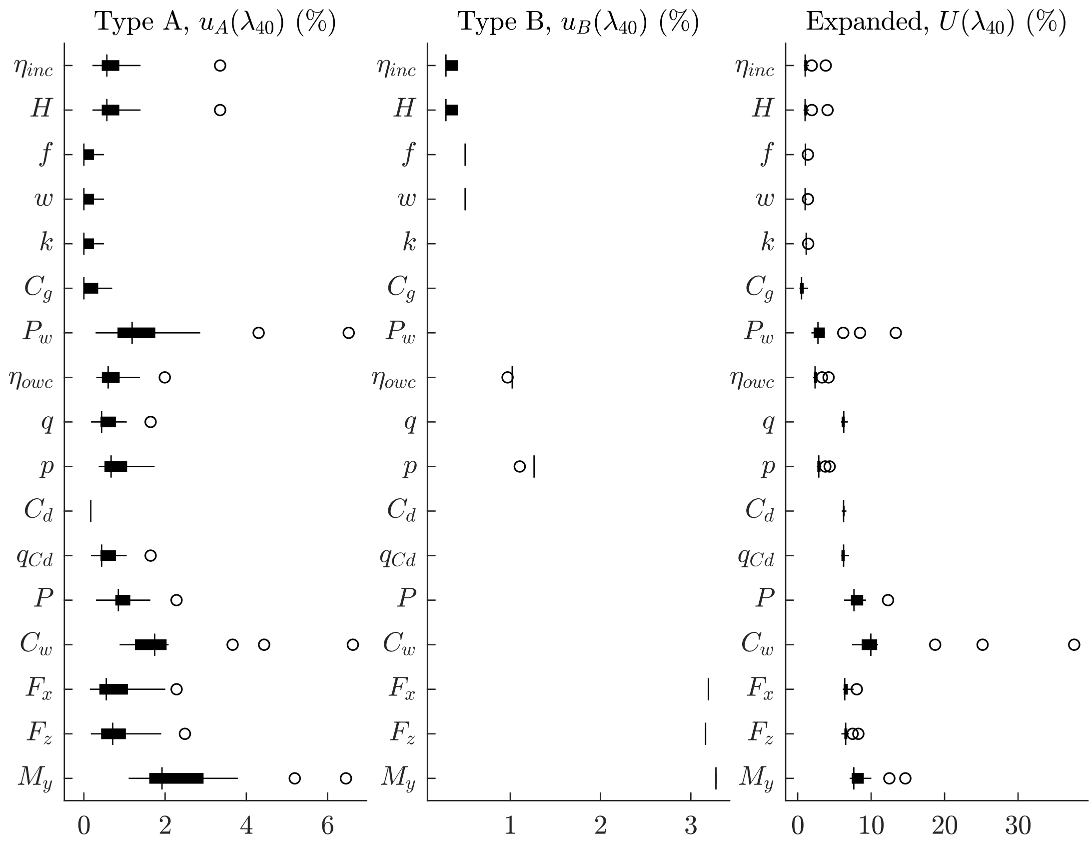

Figure B.5: Uncertainty of experimental quantities and measurands for λ_{40}, shown as box and whisker plots (distributions). For u_A, the distribution captures all wave frequencies and heights. For u_B, the distribution captures all the calibrations carried out throughout the experiment, as well as including other sources of u_B. The distributions of expanded uncertainty U captures everything, and was determined by the Monte Carlo Method.

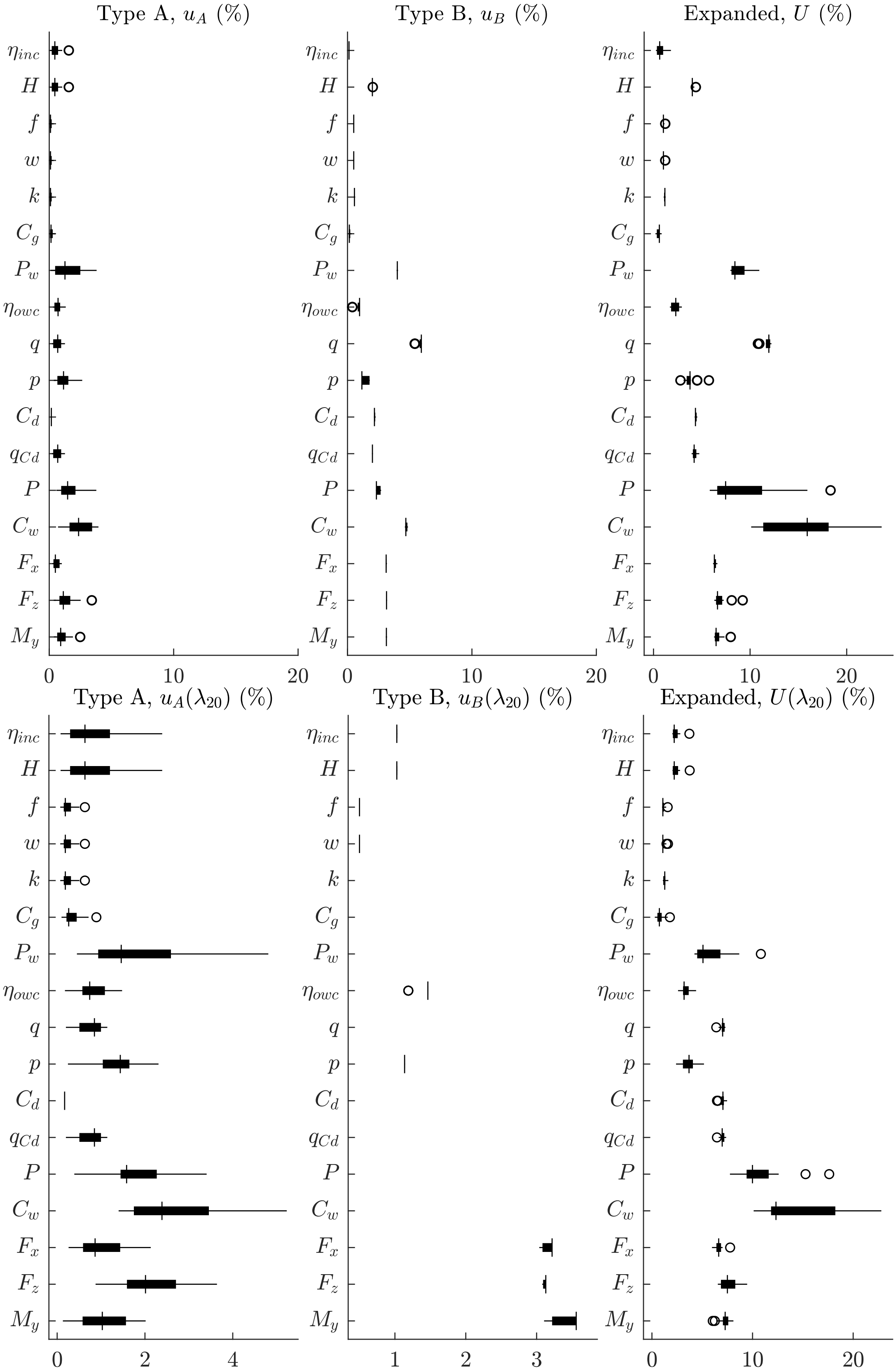

Figure B.6: Uncertainty of experimental quantities and measurands for λ_{30}

B.6 Issues with load measurements for 1:40 scale

Fig. B.7 shows phase-averaged timeseries' of forces/moments for three kh values and H_1. These results show why we omitted all the load components from the λ_{40} experiment except the surge force component (X). It is clear that λ_{40} profiles deviate significantly for main load components of heave force (Z) and pitch moment (M_y) compared to the other two scales. It is assumed that these differences were mostly due to the λ_{40} loads measurement range being very small compared to other scales. This situation likely lead to the relatively larger differences in the pre- and post-test calibration matrices for λ_{40} compared to the larger scales. In hindsight, the in-situ calibration was probably not ideal for the λ_{40}.

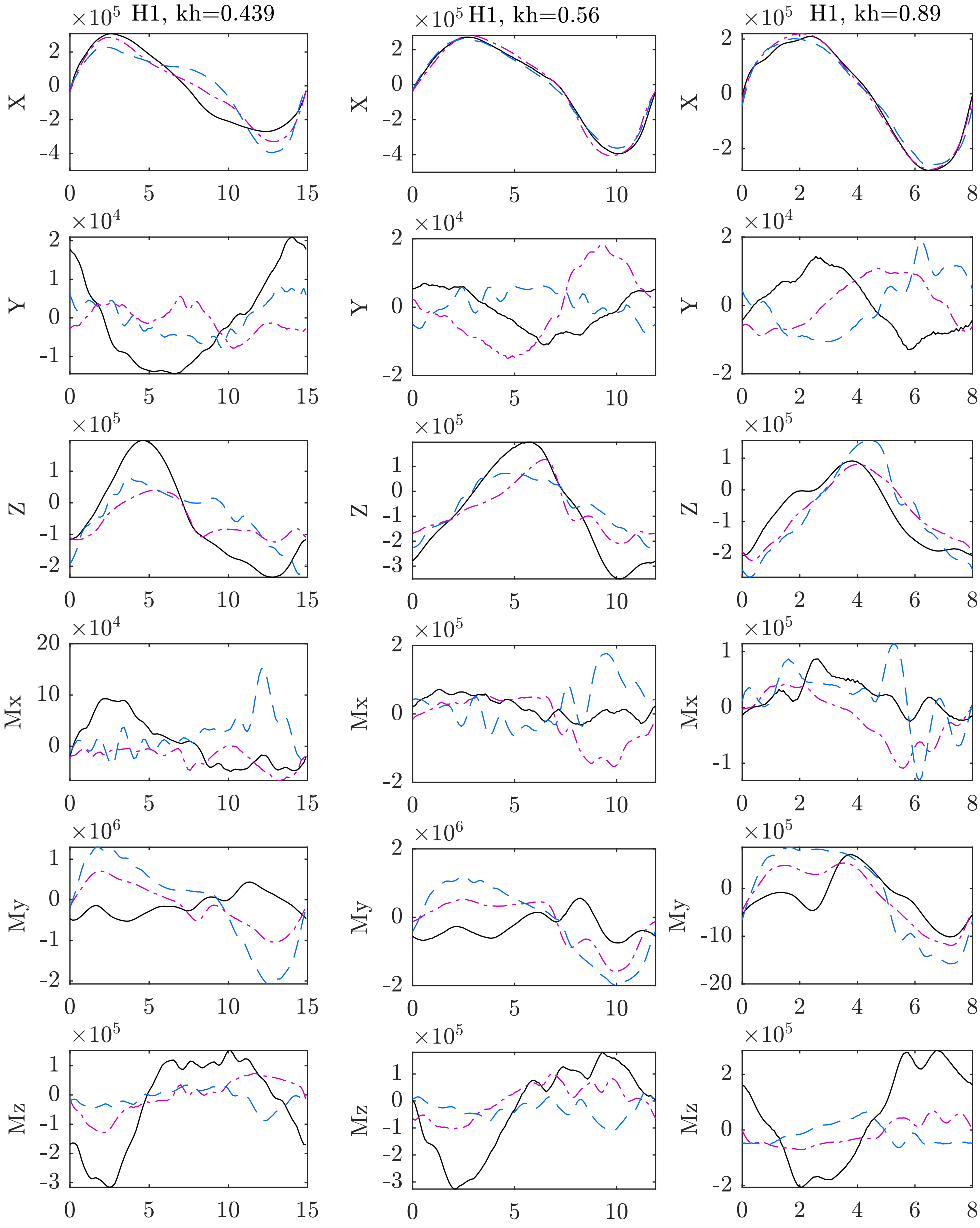

Figure B.7: Phase-averaged timeseries' of forces/moments for three kh values and H_1 (refer to Fig. B.3 above for legend of colours/lines).

Appendix C

Chapter 5 Supplementary Information

Here we present additional results from Chapter 5. We briefly report the results and discuss their relevance with respect to laboratory effects of the WSE OWC WEC.

C.1 Additional results for 1:30 scale model

C.1.1 Wave elevation inside the OWC chamber

Fig. C.1 shows a comparison of measured profiles of the free surface elevation inside the OWC chamber η_{owc} for two wave heights at λ_{30} scale. These η_{owc} profiles clearly show the deviating water column dynamics inside the OWC between laboratories. The water column dynamics were strongly influenced by the incident wave profiles and their deviations between laboratories. These wave-water column interactions induced similar deviating air pressure and flow, which in turn lead to deviating absorbed power. Slightly different PTO damping between laboratories also contributed to the differences in results.

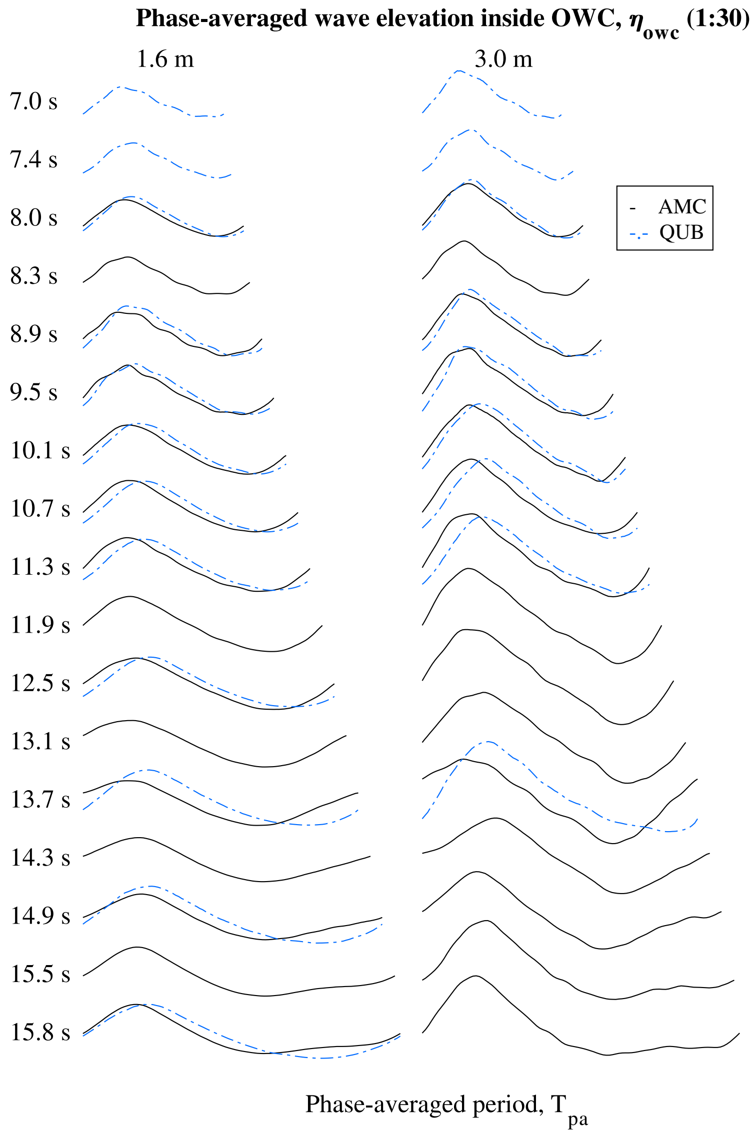

Figure C.1: Free surface elevation inside the OWC chamber η_{owc} across scales and wave heights. Results are for λ_{30} scale.

C.1.2 Pressure inside the OWC chamber

Fig. C.2 shows a comparison of profiles of pressure p measured inside the OWC chamber for two wave heights at λ_{30} scale. p_{QUB} tended to be relatively larger, which contributed to E_{QUB} showing better power performance results overall.

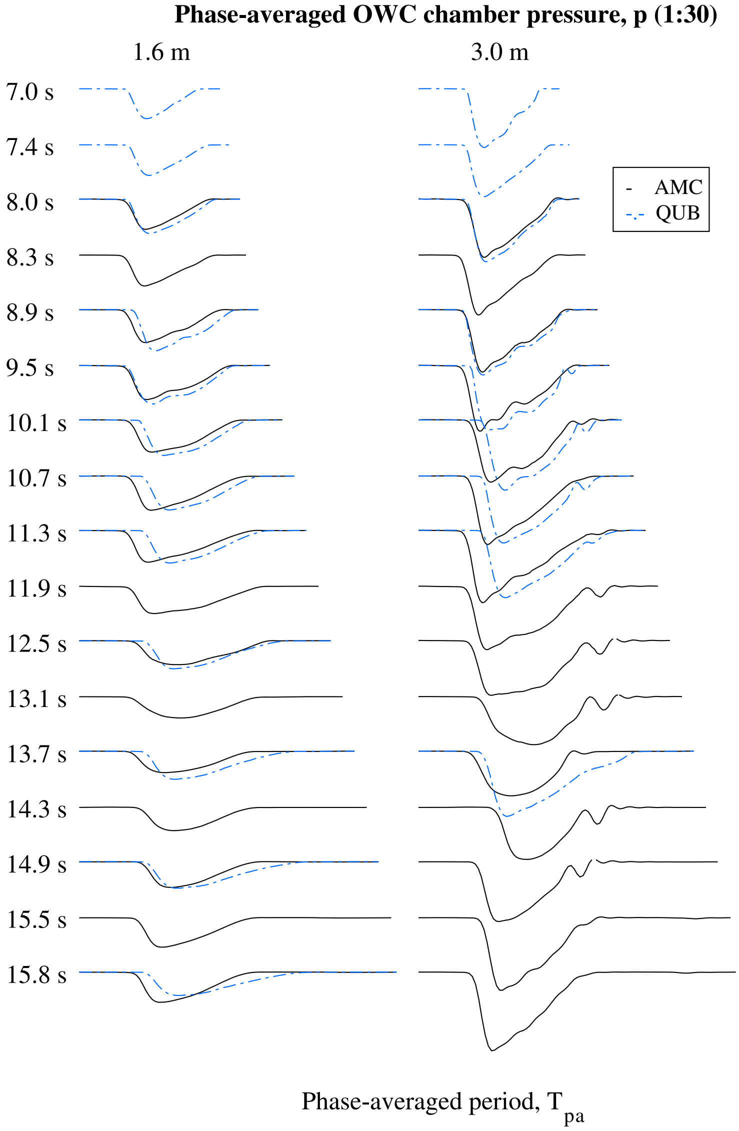

Figure C.2: Pressure inside the OWC chamber p across scales and wave heights. Results are for λ_{30} scale.

C.1.3 OWC hydrodynamics and power RAOs

Fig. C.3 shows a comparison of RAOs of key power measurands across two wave heights at λ_{30} scale. The agreement between experiments was marginally better for H_3, however E_{QUB} still showed consistently larger values, therefore better power performance.

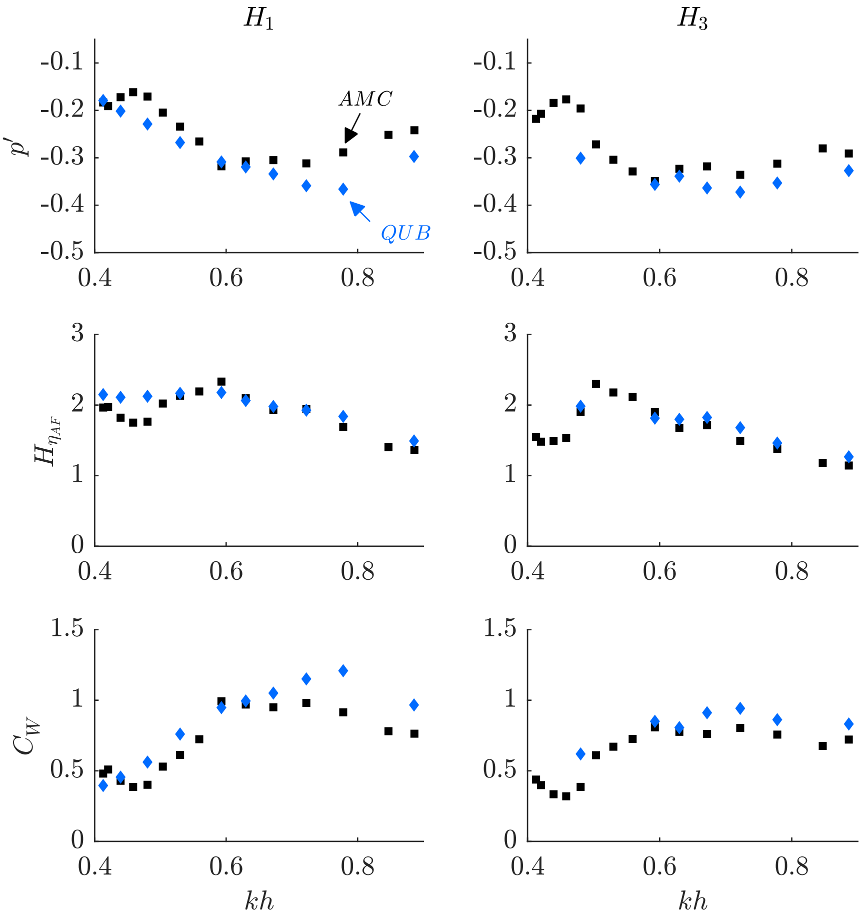

Figure C.3: Effect of wave height on RAOs on dimensionless pressure p', amplification factor $H_{\eta_{AF}}$, and capture width ratio C_W. Results are for λ_{30} scale.

C.2 Results for 1:20 scale model

C.2.1 Regular waves

C.2.1.1 Incident waves

Fig. C.4 shows a comparison of the phase-averaged incident wave elevation profiles at λ_{20} scale. These profiles deviated between laboratories similarly to the λ_{30} results.

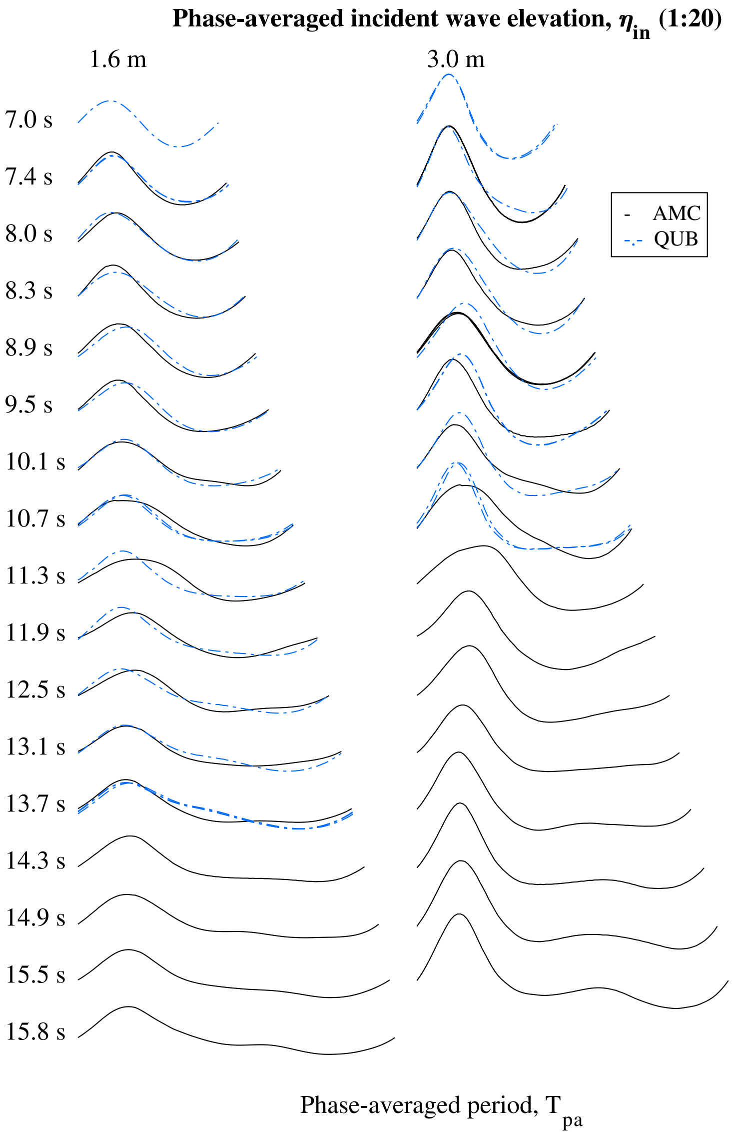

Figure C.4: Incident regular wave profiles η_{inc}. Profiles shown as wave period for axis ticks.

C.2.1.2 Orifice calibrations

Fig. C.5 shows a comparison of the orifice calibration results for λ_{20}. $C_{d,QUB}$ was just over 1% RD larger than $C_{d,AMC}$. While for λ_{30} the $C_{d,QUB}$ was smaller, it is clear that there are far fewer $C_{d,QUB}$ data points due to the limited waves that could be generated in E_{QUB}, which means the average value is not as well resolved.

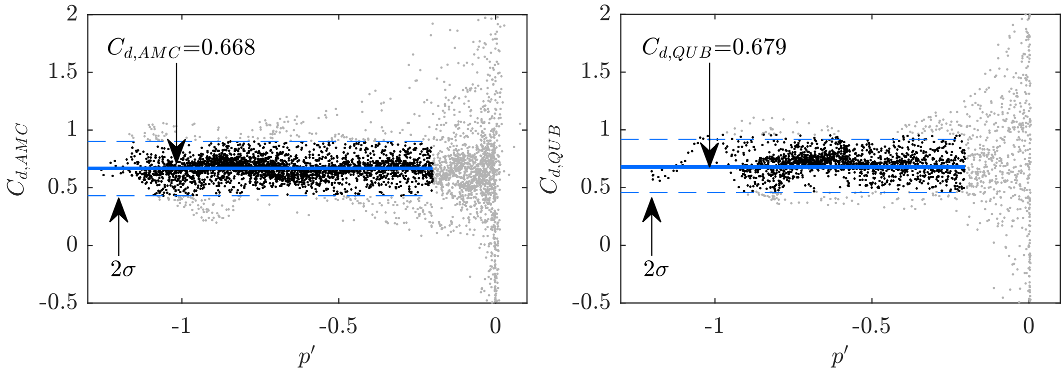

Figure C.5: Orifice discharge coefficient C_d. C_d was determined from in-situ orifice calibrations (method described in Chapter 3). Mean C_d was calculated for dimensionless chamber pressure $p < -0.2$.

C.2.1.3 Wave elevation inside the OWC chamber

Fig. C.6 shows a comparison of measured profiles of the free surface elevation inside the OWC chamber η_{owc} for two wave heights at λ_{20} scale. These profiles deviated between laboratories similarly to the λ_{30} results.

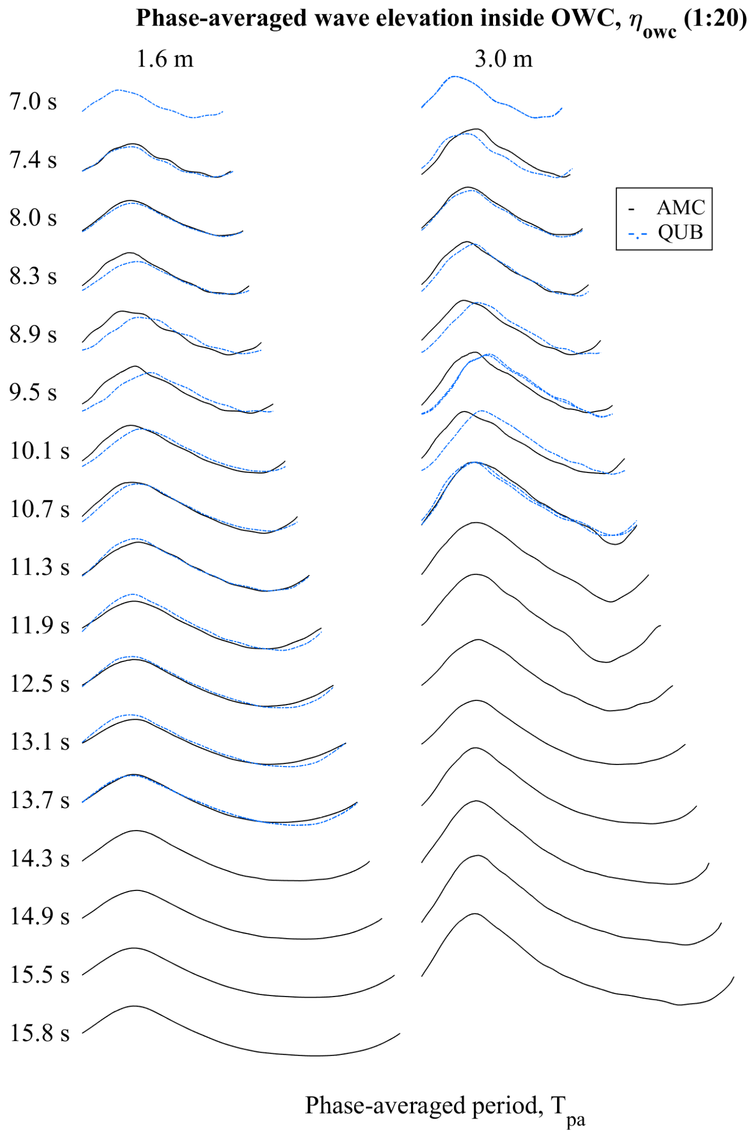

Figure C.6: Free surface elevation inside the OWC chamber η_{owc} across scales and wave heights.

C.2.1.4 Pressure inside the OWC chamber

Fig. B.3 shows a comparison of measured profiles of pressure p inside the OWC chamber for two wave heights at λ_{20} scale. These profiles deviated between laboratories similarly to the λ_{30} results.

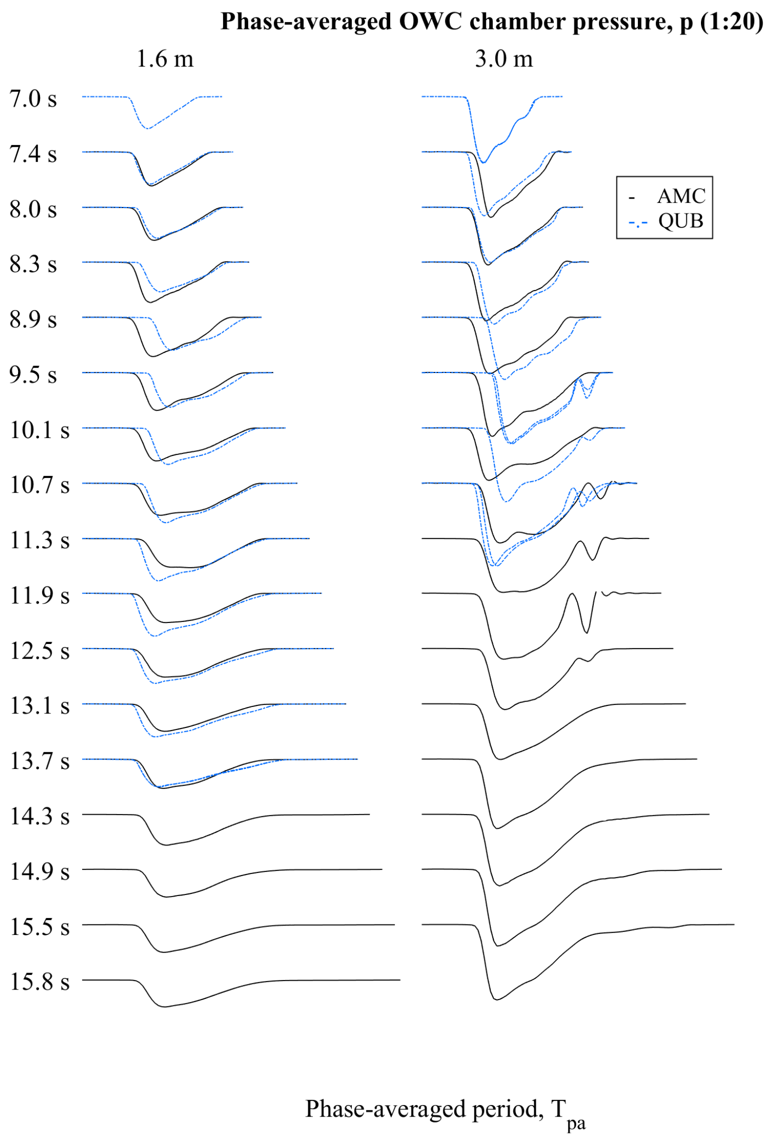

Figure C.7: Pressure inside the OWC chamber p across scales and wave heights.

C.2.1.5 OWC hydrodynamics and power

Fig. C.8 shows a comparison of RAOs of key power measurands across two wave heights at λ_{30} scale. The agreement between experiments was marginally better for H_3, however E_{QUB} still showed consistently larger values, therefore better power performance.

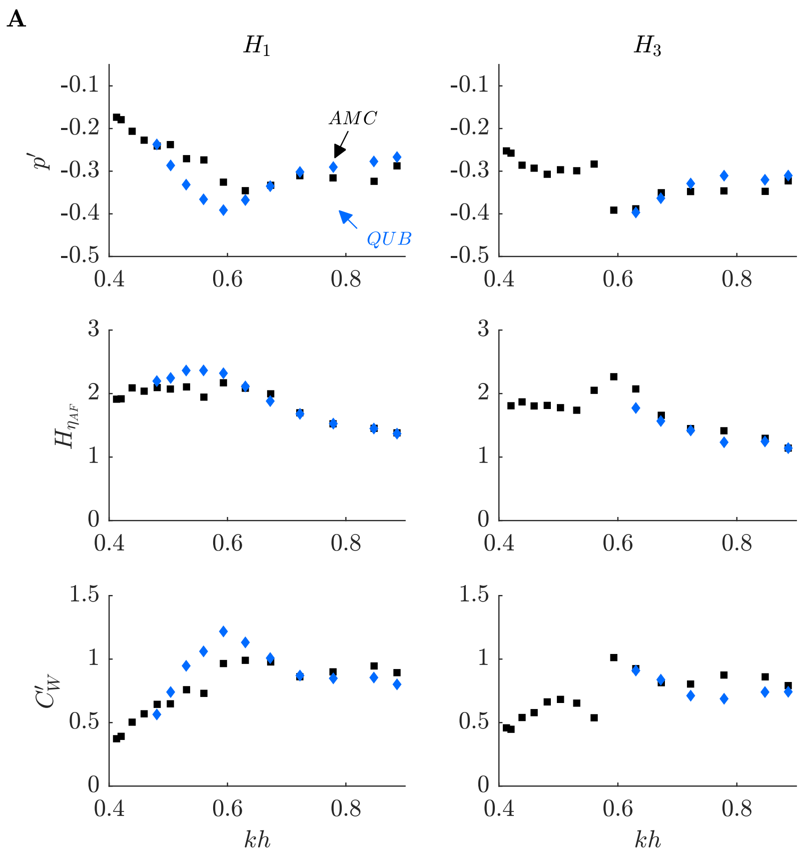

Figure C.8: Effect of wave height on RAOs on dimensionless pressure p', amplification factor $H_{\eta_{AF}}$, and capture width ratio C_W.

C.2.2 Irregular waves

C.2.2.1 Incident waves

Fig. C.9 shows irregular wave sea states, showing the energy spectra density S. Despite a careful and extensive calibration procedure of the incident waves, $S_{E_{QUB}}$ and associated statistics tended to be moderately smaller than $S_{E_{AMC}}$. However, while $S_{E_{QUB}}$ was relatively smaller leading to relatively smaller P_W and p', $H_{m0,\eta_{AF}}$ and C_W were relatively larger in E_{QUB} (Fig. C.10). These results were similar to λ_{30}, which were described in Chapter 5.

C.2.2.2 OWC hydrodynamics and power

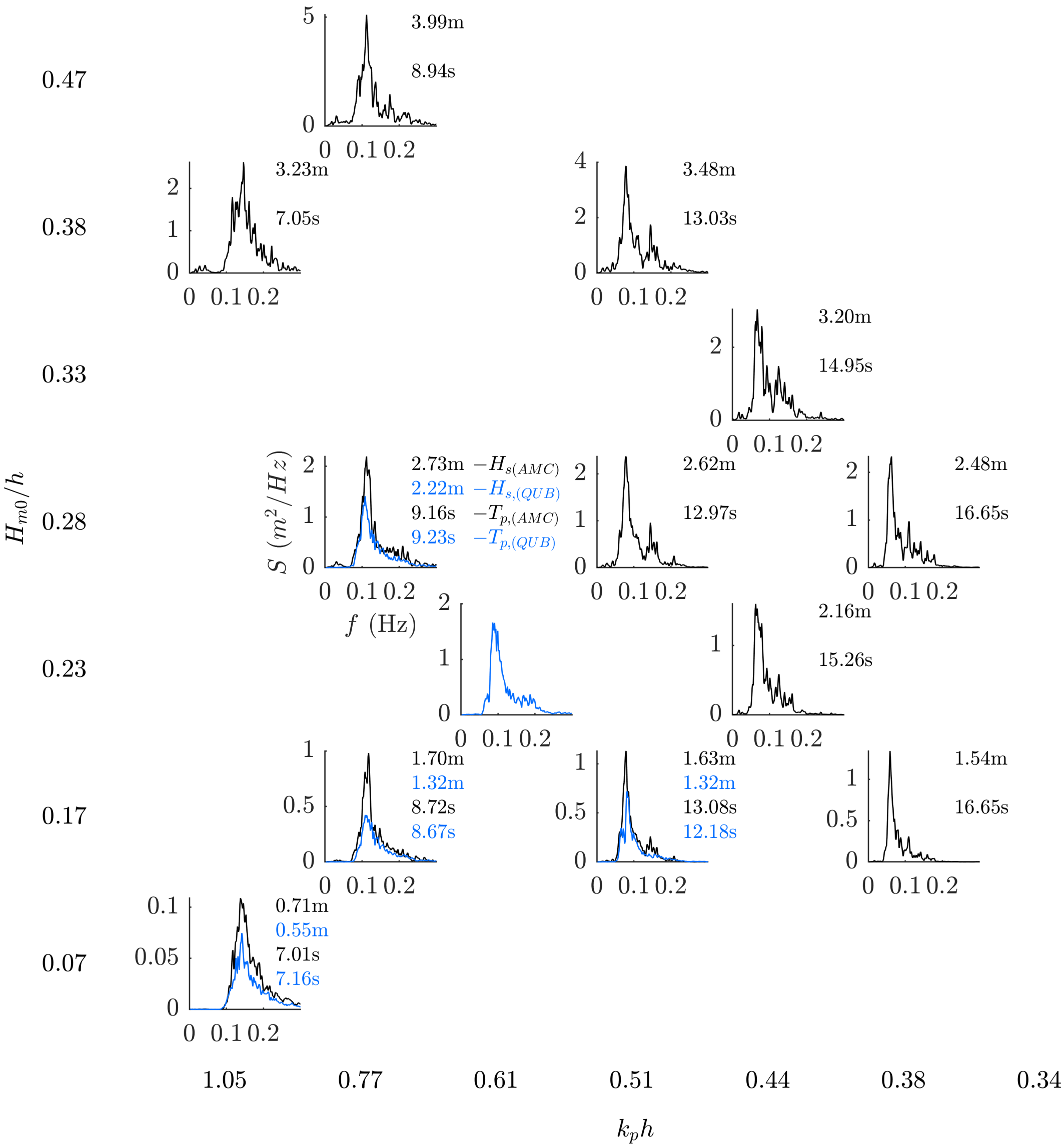

Figure C.9: Incident irregular wave spectra energy density S for E_{AMC} and E_{QUB} across the range of tested sea states (see middle subplot for axes labels and legend). The significant wave height H_{m0} and peak period (shown as peak wavenumber k_ph) matrix also shows the statistics obtained for H_{m0} and peak period T_p to the right of each subplot for reference.

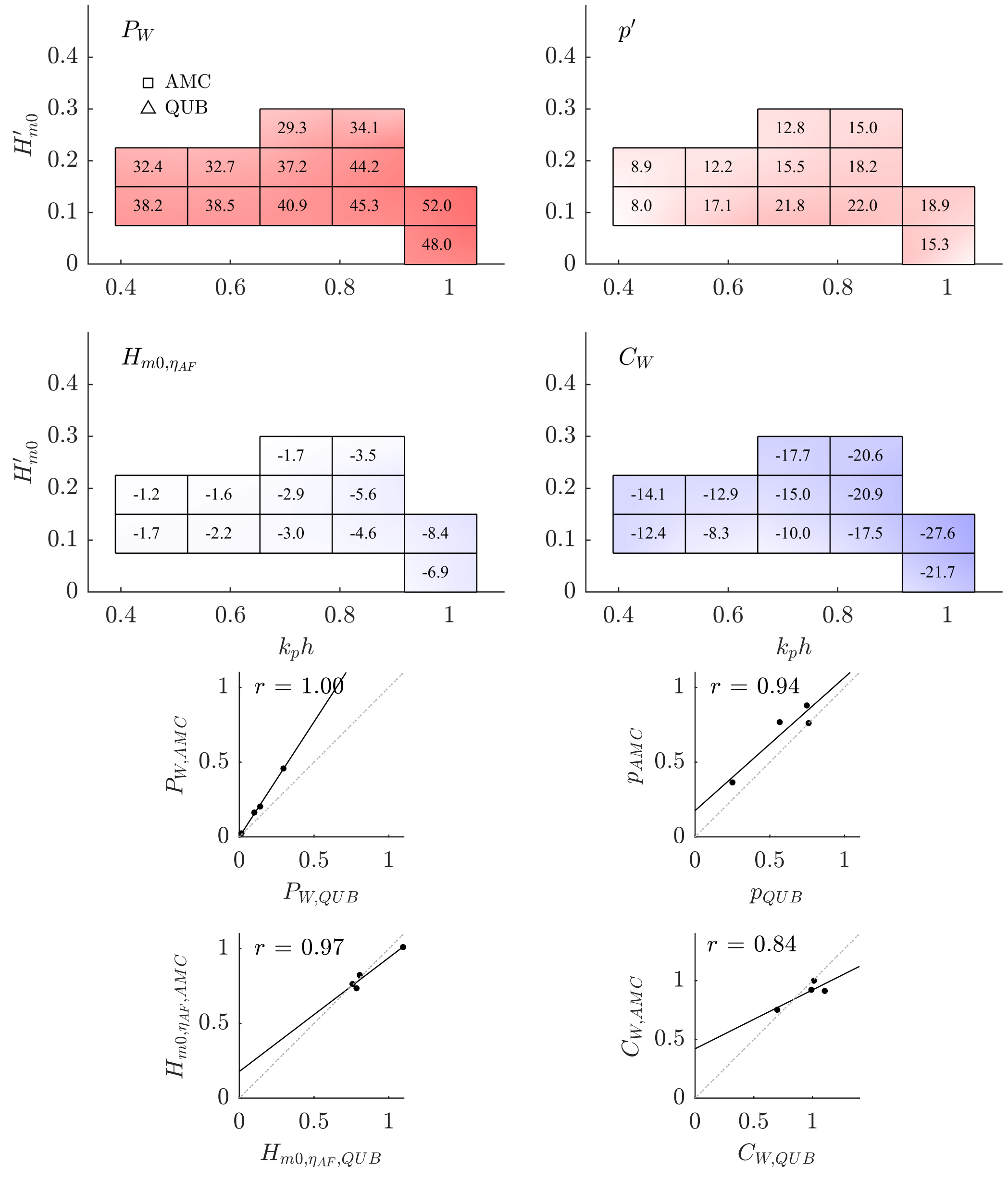

Figure C.10: Matrices for key measurands showing the relative percentage difference (RD) between E_{AMC} and E_{QUB}, where a positive/red RD value corresponds to E_{AMC} being larger than E_{QUB}, and vice-versa for negative/blue.

Appendix D

Conference Paper 1

This article has been removed for copyright or proprietary reasons.

It is the following published article: Orphin, J. J. , Nader, J.-R., Penesis, I. Howe, D. P., 2017. Experimental uncertainty analysis of an OWC wave energy converter, in Proceedings of the 12th European Wave and Tidal Energy Conference (EWTEC) 2017, EWTEC, United Kingdom, pp. 1096-1

Appendix E

Conference Paper 2

This article has been removed for copyright or proprietary reasons.

It is the following published article: Orphin, J. J., Penesis, I., Nader, J.-R., 2018. Uncertainty analysis for a wave energy converter: the Monte Carlo method, paper presented at the The 4th Asian Wave and Tidal Energy Conference (AWTEC 2018), 09-13 September 2018, Taipei, Taiwan.